STUDIES DIRECTED TOWARDS THE SYNTHESIS OF CHROMONE CARBALDEHYDE–DERIVED HIV-1 PROTEASE INHIBITORS

THESIS

Submitted in fulfilment of the requirements
for the degree of

DOCTOR OF PHILOSOPHY

of

RHODES UNIVERSITY

By

DUDUZILE MABEL MOLEFE
BSc. (Natal), BSc. Honours (Rhodes)

June 2007

ABSTRACT

A series of chromone-3-carbaldehydes have been prepared using Vilsmeier-Haack methodology while a corresponding series of chromone-2-carbaldeydes have been synthesized *via* the Kostanecki–Robinson reaction. Baylis-Hillman reactions have been conducted on both series of chromone carbaldehydes using three different catalysts, *viz.*, 1,4-diazabicyclo[2.2.2]octane (DABCO), 1,8-diazabicyclo[5.4.0]-undec-7-ene (DBU) and 3-hydroxyquinuclidine (3HQ), and acrylonitrile, methyl acrylate and methyl vinyl ketone as the activated alkenes. These reactions have typically (but not always!) afforded both normal Baylis-Hillman and dimeric products. Attention has also been given to the use of 1-methyl-2-pyrrolidine (1-NMP), an ionic liquid, to replace normal organic solvents, and it has been found that, in the presence of DABCO, chromone-3-carbaldehydes afford the dimeric products alone. Reactions of chromone-3-carbaldehydes with methyl vinyl ketone have yielded unexpected, novel adducts, which appear to arise from preferential attack at C(2) in the chromone nucleus. Research on chromone-2-carbaldeydes under Baylis-Hillman conditions has also resulted in the formation of some interesting products instead of the expected Baylis-Hillman adducts.

The Baylis-Hillman products have been explored as substrates for aza-Michael reactions using various amino derivatives including protected amino acids in the presence of the tetrabutylammonium bromide (TBAB) and the ionic liquid, 3-butyl-1-methylimidazoleboranetetrafluoride ($BmimBF_4$), as catalysts. The aza-Michael products have been targeted as truncated ritonavir analogues for investigation as potential HIV-1 protease inhibitors, and representative compounds have been subjected to enzyme inhibition assays to explore the extent and type of inhibition. Lineweaver-Burk and Dixon plots have indicated competitive inhibition in one case as well as non-competitive inhibition in another, and the inhibition constants (K_i) have been compared with that of the ritonavir.

Computer modelling studies have also been conducted on selected chromone-containing derivatives, using the ACCELRYS Cerius^2 platform. Interactive docking of the chromone-containing ligands into the HIV-1 protease receptor site, using the

Ligandfit module, has indicated the importance of hydrogen-bonding interactions mediated by bridging water molecules situated in the receptor cavity.

NMR spectroscopy has been used to elucidate complex and competing mechanistic pathways involved in the Baylis-Hillman reactions of selected 2-nitrobenzaldehydes with MVK in the presence of DABCO – reactions which afford the normal Baylis-Hillman product, the MVK dimer and *syn*- and *anti*-Baylis-Hillman type diadducts. The kinetic data confirm the concomitant operation of two pathways and reveal that, in the initial stage of the reaction, the product distribution is kinetically controlled, whereas in the latter stage, thermodynamic control results in the consumption of the normal Baylis-Hillman product and predominance of the *anti*-diadduct.

ACKNOWLEDGEMENTS

I would first and foremost like to thank God for giving me the strength to be tenacious when pursuing this project and also not to be despondent even when things are not going accordingly, but instead He just provided some incentives which will make me look beyond the obstacles.

To my supervisor, Prof. P.T. Kaye, thank you so much for your support, guidance, availability which has become an inspiration and a motivation to me during this project. It was an honour and a privilege for me to be part of your research group. I also wish to thank Prof. Brown and Dr Bradley for their co-supervision and input in this project.

To Mr A. Soper, Mr K. Lobb, Mr Soneman, Mr Dondashe and Mr Ntebe, thank you for your contribution.

To the contribution from other universities: Tommy van der Merwe (Witwatersrand University) and Prof. L. Fourie (Potchefstroom University), thank you for running the high resolution mass spectrometer.

To MRC and DAAD, thank you for financial support.

To my family: my mom and dad, Christine and Norman Molefe ngiyabonga ngezimfundiso zenu ezingenze ngafika kulelizinga, without those words of encouragement I couldn't have made it, your understanding even when I sacrifice our quality time for the sake of completing this project. To my sisters (Ntombifuthi and Philile) and my brother (Thabo), your support has been astounding, ngiyabonga zingane zakwethu. To Mr and Mrs Bhengu, angazi ngingaqala ngakuphi, ngiyabonga, you have been a good example and a blessing empilweni yami, may God richly bless you. To my niece, Buhle, and my nephew, S'ya, your messages has kept me going and thank you so much for being a blessing in my life, just watch the space since the sky is the limit as my vision is about to be fulfilled.

To my handsome darling, thank you for being a friend, a brother and a shoulder to lean on at all times. You have really changed my attitude of perceiving some other aspects of life. I know it was not easy but thank you for empathizing with me and become my incentive at all times. Ubeyindvodza emadvodzene emphilweni yami.

To all my friends, Babs kuzolunga, Prue, Pumla, Hlombe, Nozuko, Zama, Smarties and Sindi, thanks for those words of encouragement, you are really friends indeed.

CONTENTS

1. INTRODUCTION

1.1 The Human Immunodeficiency Virus

Human immunodeficiency virus subtypes 1 and 2 (HIV-1 and HIV-2) are the two forms of HIV that are recognized as the cause of the pandemic called Acquired Immunodeficiency Syndrome (AIDS).[1-4] However, since the HIV-2 pathogen has a longer latent period prior to the development of the disease and the virus is not easily transmitted, the AIDS infections found in humans is typically caused by HIV-1.[3] These two subtypes were found to originate from two African monkeys; the chimpanzee (*Pan troglodytes troglodytes*) for HIV-1 and the sooty mangabay (*Cercocebus atys*) for HIV-2.[5-6] HIV-1 was first isolated from a patient with multiple lymphadenopathies, a condition associated with AIDS.[7] Initially, various names were given to the virus isolated from AIDS patients, *viz.*, human T lymphotropic virus III (HTLV-III), immunodeficiency associated virus (IDAV), lymphadenopathy-associated virus (LAV), and AIDS-associated retrovirus (ARV).[8-12] However, in 1986, human immunodeficiency virus, HIV, was the name approved for this type of virus.[9] HIV belongs to the *Retroviridae* family, in which genetic information flows from RNA to DNA;[13-14] it also belongs to the *Lentivirus* subfamily,[15-16] members of which are able to infect non-dividing cells.[17] In this review the focus will be on HIV-1.

1.1.1 HIV-1 Structure and function

HIV-1 is composed of nine known genes with the ends being flanked by long terminal repeat sequences (LTR), which are crucial for the initiation of viral gene expression (Figure 1).[18-19] These genes are classified into three major coding domains:- (i) the three standard core genes: *gag*, a gene coding for a protein which forms the viral core and which is also involved in the assembly of the virion in the host cell membrane; *pol*, which codes for the enzymatic proteins, *viz.*, protease (PR), reverse transcriptase (RT), and integrase (IN); and *env*, which directs the formation of the surface envelope, glycoproteins gp120 and gp41;[4, 17-18] (ii) the two regulatory genes (*tat*, *rev*); and (iii)

four accessory genes (*vpr*, *vpu*, *nef*, *vif*) which are essential for viral replication and host pathogenesis.[4, 18, 20-21]

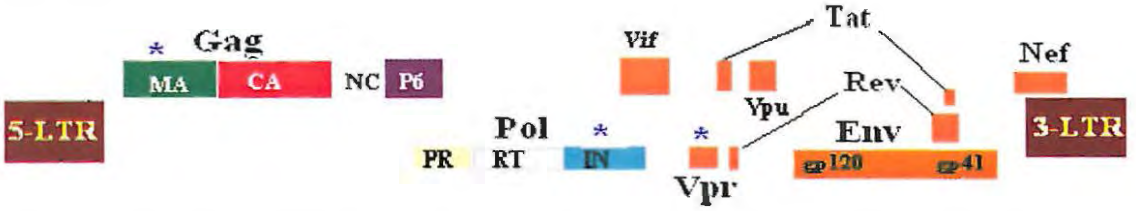

Figure 1. Genetic organisation of HIV-1. The asterisked genes together with the central DNA flap are involved in HIV-1 nuclear import. [Adapted from ref. 18]

The HIV-1 virion (Figure 2) is enveloped by a lipid bilayer membrane with two types of glycoprotein attached to the surface, *viz.*, the surface (SU) envelope protein (gp120), located on the external face, and the transmembrane (TM) envelope protein (gp41).[22-23] In mature virions, the matrix (MA) proteins line the inner surface of the membrane, while the capsid (CA) protein forms a cone-shaped core which contains two copies of identical, single-stranded RNA (diploid genomic RNA) complexed with nucleocapsids (NC), and the replicative enzymes: reverse transcriptase (RT), protease (PR) and integrase (IN).[18,21,23-25] Immature virions have a spherical capsid which collapses to a conical shape during replication and maturation to the virion.[23-24, 26-27]

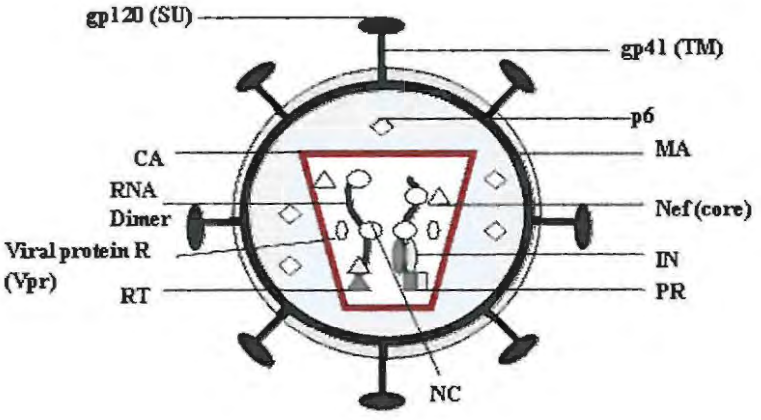

Figure 2. Organisation of the matured HIV-1 virion. [Adapted from ref. 25]

1.1.2 Replication cycle of HIV-1

The HIV-1 life cycle illustrated in Figure 3, begins when the envelope glycoprotein (gp120) of the virus binds with a surface CD4 receptor of the host cell (**Stage 1**).[28] This interaction results in the conformational change of gp120 which activates the envelope protein (gp41) to mediate fusion of the viral and cellular membrane resulting in the "microinjection" of the capsid contents (**Stage 2**). The capsid (**Stage 3**) undergoes uncoating followed by reverse transcription in **Stage 4**, where the viral single-stranded RNA is transcribed into viral DNA. **Stage 4** also involves the pre-integration complex (PIC) which comprises viral RNA/DNA, reverse transcriptase (RT), integrase (IN), matrix (MA) and viral protein R (Vpr). However, various core proteins are lost during the formation of the PIC.[29-30]

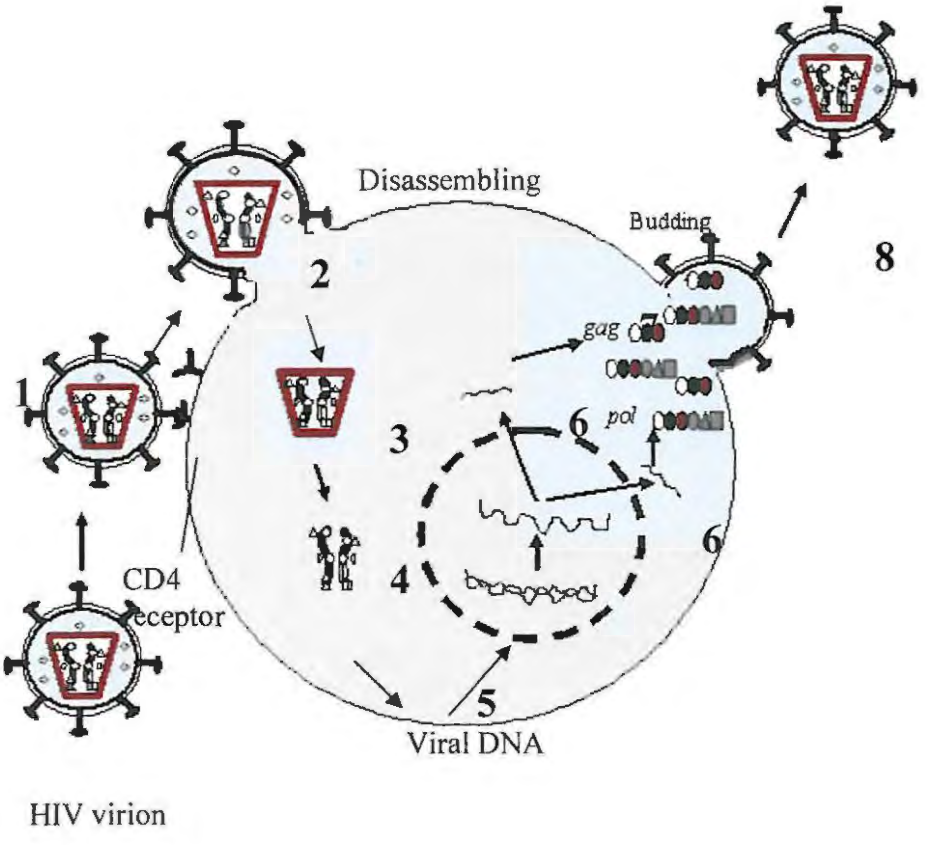

Figure 3. HIV-1 life cycle. [Adapted from ref. 29]

The PIC crosses through the lipid bilayer of the nuclear membrane where the viral DNA is integrated into the host cell DNA (**Stage 5**). The viral RNA synthesized from the integrated DNA is then transported back to the cell cytoplasm for translation to polypeptides and further protein synthesis (**Stage 6**).[4,29] Newly synthesized viral proteins, the intermediate gag-pol polypeptide and two strands of viral RNA migrate to the cell membrane where assembly of the virion occurs (**Stage 7**).[31] As the immature virion buds off from the host cell taking cell membrane with it, HIV-1 PR cleaves the gag-pol polypeptide into major structural proteins thus producing infectious and mature HIV-1 virions (**Stage 8**).[26, 32,33-34]

1.1.3 The HIV-1 Protease Enzyme

1.1.3.1 HIV Protease structure

HIV-1 PR, an aspartic protease, is a 22 kDa homodimeric endopeptidase comprising two identical 99 amino acid polypeptides.[35-39] The active site of HIV-1 PR is a hydrophobic cavity of about 10Å in diameter.[40] Inside the cavity, Asp-Thr/Ser-Gly triad sequence residues and an aspartate from each monomer, together with structural water molecules are involved in the cleavage of substrate amide bonds.[41-44] The X-ray crystal structure of HIV-1 PR (Figure 4) reveals a symmetric structure with each monomer contributing an extended glycine-rich β-sheet region known as the flap. Each monomer has a hydrophobic core consisting of two loops, one of which includes the active site aspartic acid. The enzyme-binding cavity is capable of accommodating a minimum of seven consecutive amino acid residues in the substrate.[46,47] The amino acid residues found in the binding pockets (or subsites) of HIV-1 PR are specified in Table 1.

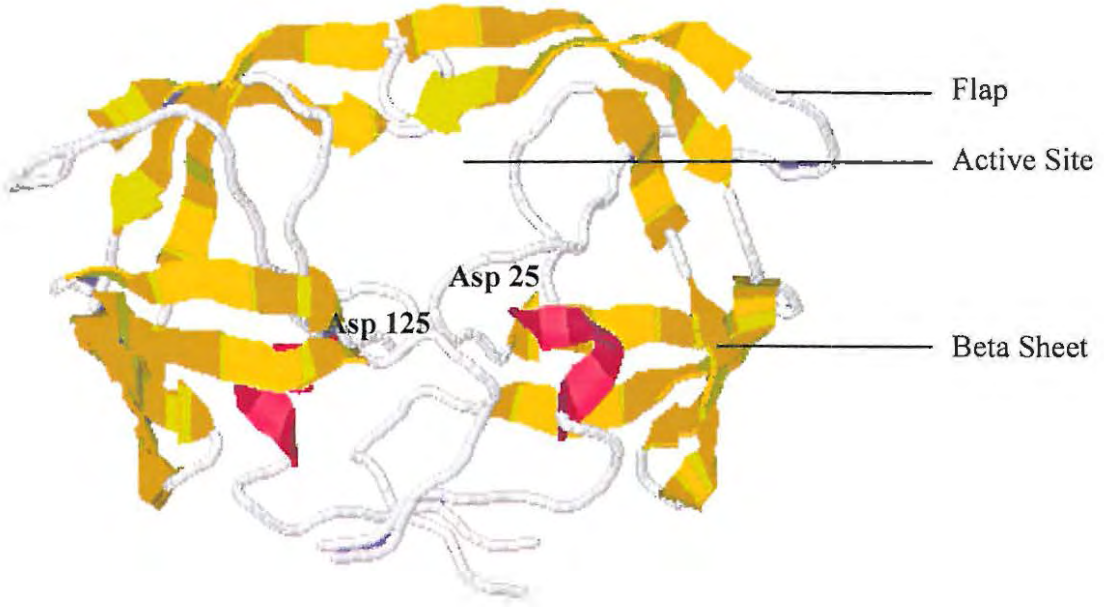

Figure 4. X-ray crystal structure of HIV-1 PR dimer. [Adapted from ref. 46]

Table 1. Amino acid sequences forming the HIV-1 protease subsites.[41]

Subsite	HIV-1 PR
S_4	$Asp^{30'}$ $Ile^{50'}$ $Ile^{54'}$
S_3	Arg^{8} $Asp^{29'}$ Leu^{23} Val^{82} $Arg^{87'}$
S_2	Ala^{28} Val^{82} $Phe^{53'}$ $Ile^{54'}$ $Leu^{76'}$ $Thr^{80'}$ $Ile^{84'}$
S_1	Leu^{23} Asp^{25}* Phe^{53} Pro^{81} Val^{82} Ile^{84}
$S_{1'}$	$Leu^{23'}$ $Asp^{25'}$* $Phe^{53'}$ $Ile^{84'}$
$S_{2'}$	Ala^{28} Asp^{30} Val^{32} Phe^{53} Ile^{54} Leu^{76} Ile^{84}
$S_{3'}$	Arg^{8} Asp^{29} Ile^{50} $Pro^{81'}$ Arg^{87}

Primes (') distinguish the residues from the two subunits in the dimer of HIV-1 PR.
* Catalytic Asp residue.

1.1.3.2 HIV-1 Protease Function

HIV-1 PR is one of the viral enzymes essential for the HIV-1 life cycle,[39,48-49] selectively cleaving viral polyproteins at specific peptide bonds.[50-51] Figure 5 depicts how HIV-1 PR functions as a "molecular pair of scissors", by hydrolyzing the viral gag-pol precursor proteins to produce structural proteins.[16] Hydrolysis of the amide carbonyl group, by a water molecule accommodated between the side-chains of the aspartic acid residues 25 and 125, is believed to involve a tetrahedral intermediate.[16,44]

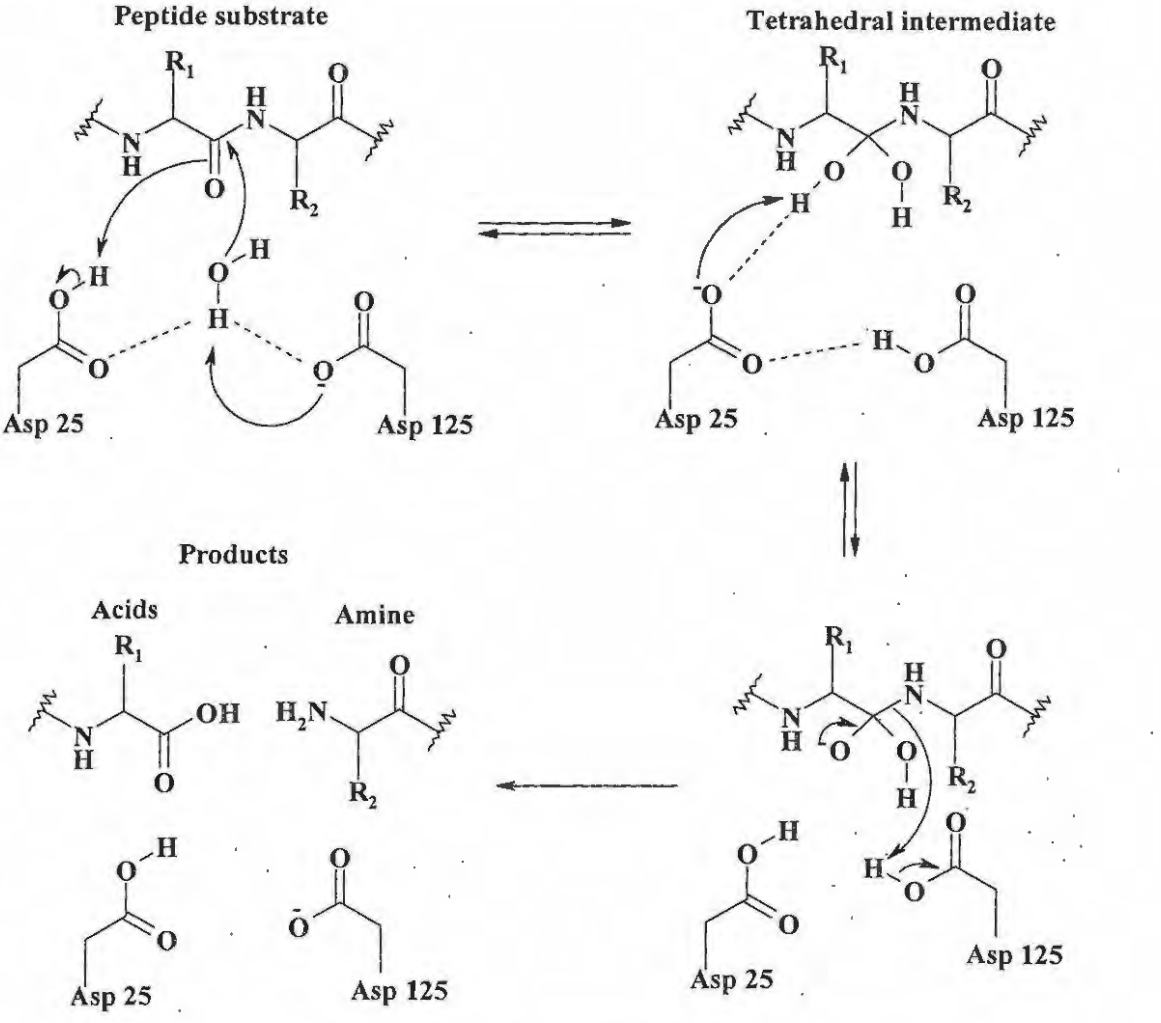

Figure 5. Catalytic mechanism of HIV-1 Protease.[Adapted from ref. 16]

1.1.4 HIV-1 Protease Substrates

HIV-1 PR polypeptide substrates contain various amino acid sequences, which may dictate cleavage at different substrate sites (Table 2).[31] Such sequences comprise approximately seven amino acids.[26,31]

Table 2. Amino acid sequences forming the substrate sites cleaved by HIV Protease.[31]

Site	Amino acid sequences at cleavage site
1	Ser.Gln.Asn.Tyr*Pro.Ile.Val.Gln
2	Ala.Arg.Val.Leu*Ala.Glu.Ala.Met
3	Ala.Thr.Ile.Met*Met.Gln.Arg.Gly
4	Pro.Gly.Asn.Phe*Leu.Gln.Arg.Gly
5	Ser.Phe.Asn.Phe*Pro.Gln.Ile.Thr
6	The.Leu.Asn.Phe*Pro.Ile.Ser.Pro
7	Ala.Glu.Thr.Phe*Tyr.Val.Asp.Gly
8	Arg.Lys.Ile.Leu*Pro.Leu.Asp.Gly

* Signifies the scissile bond location

In 1967, Schechter and Berger[47] developed the nomenclature now used for the HIV-1 protease- substrate complex and which is illustrated in Figure 6, where S_1, S_2,.....,S_n and S_1', S_2',.....,S_n' denote the amino acid residues constituting the subsites in the enzyme active site. The corresponding groups in the substrate are denoted by P_1, P_2,.....,P_n and P_1',P_2',.....,P_n' with the scissile bond being situated between P_1 and P_1'.[31,47] The amino acid residues found in the binding pockets of HIV-1 PR are specified in Table 1.[41] Preliminary studies have shown that the S_1 and S_1' (S_2 and S_2' etc.) sites are structurally equivalent.[47] Furthermore, the two S_1 and S_2 subsites are more hydrophobic than S_3.[41,47] Mutagenesis of the active site Asp to Asn in PR hinders the processing of polyprotein, and results in the formation of immature, non-infectious virions thereby preventing the spread of the virus to other cells.[48,49,50-51]

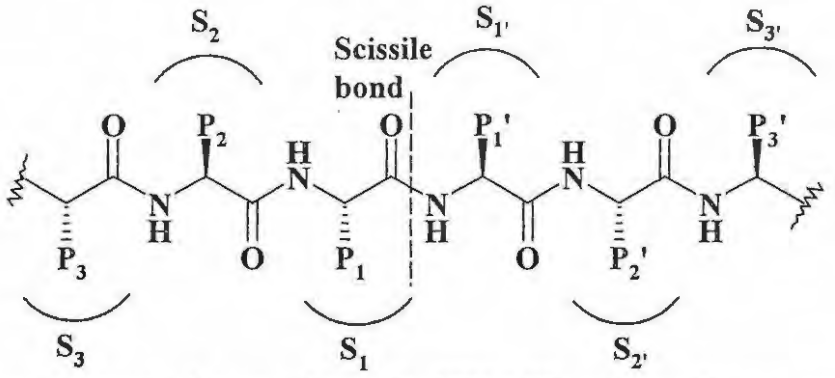

Figure 6. Standard nomenclature for HIV-1 PR and the substrate complex. [Adapted from ref. 47]

1.1.5 Acquired Immuno Deficiency Syndrome (AIDS)

AIDS is the severe immunosuppressive condition which is caused by the increase of HIV replication.[3,31,52] This results in the depletion of $CD4^+$ T-cells, with symptoms beginning to appear when the $CD4^+$ T-cell concentration falls below 500/μL; full-blown AIDS is indicated when the $CD4^+$ T-cell concentration falls below 200/μL (Figure 7).[3] The time for progression to AIDS following HIV infection is variable but averages approximately 10 years. Apparently, the first documented case of AIDS occurred in Central Africa in 1959.[53]

AIDS has become a pandemic which is escalating at an alarming rate.[54] At the end of 2006, about 39.5 million people, globally, were found to be living with HIV/AIDS; of these, 4.3 million people were newly infected, and more than 2.9 million had died in that year from the disease (Figure 8).[55] In some countries the AIDS epidemic statistics are very low, but that does not mean they are not affected. Some recent studies have suggested that by the end of 2010 another 45 million people will have been infected with HIV if no effective preventive measures are taken globally.[28]

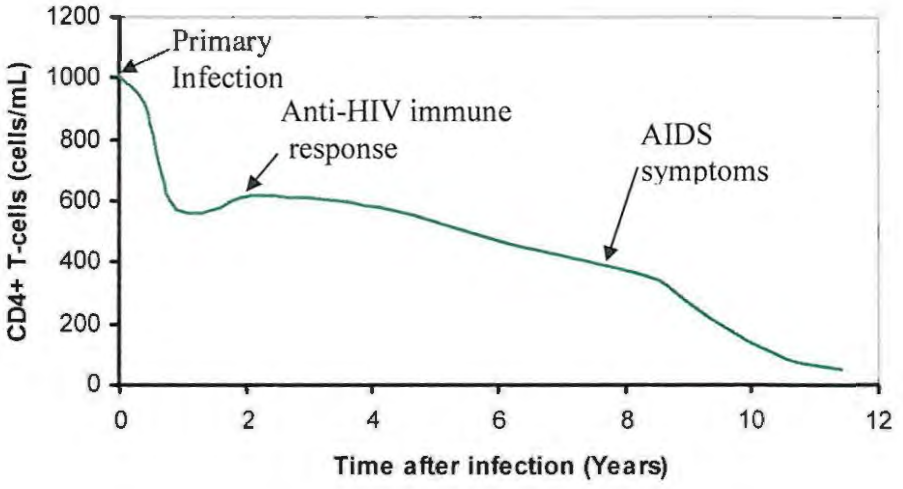

Figure 7. Progression of HIV to AIDS over time.[Adapted from ref. 3]

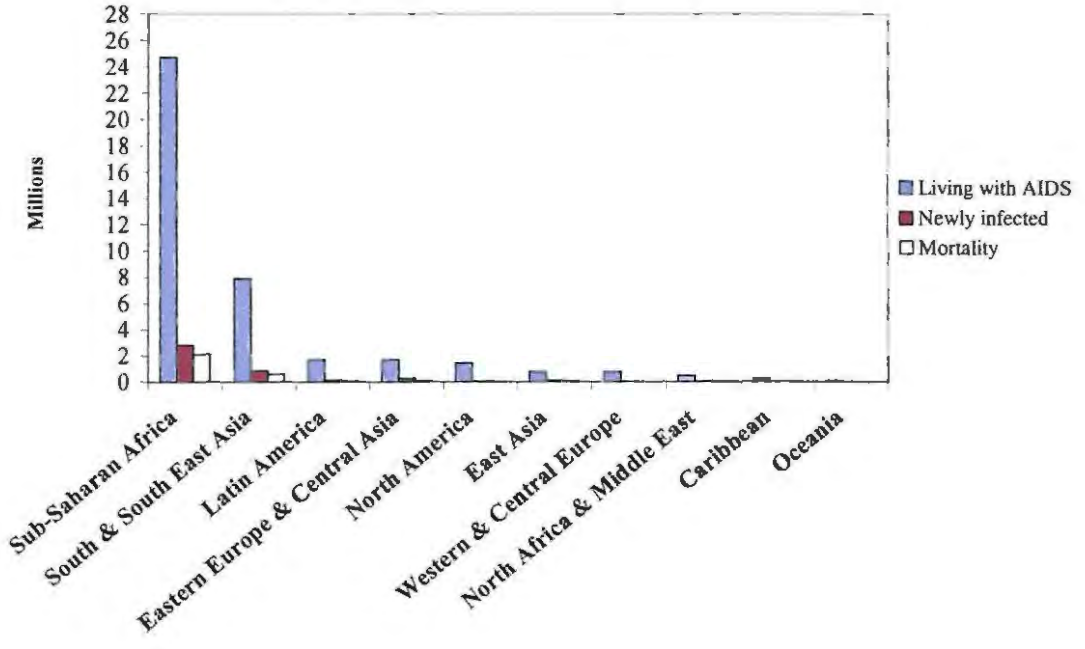

Figure 8. Global HIV/AIDS pandemic statistics for 2006. [Adapted from ref. 55]

1.1.6 Designing HIV-1 Protease Inhibitors

Computational studies have been used to design HIV-1 PR inhibitors (PIs). This approach explores structural compatibility between the inhibitor and the HIV PR active site.[13,56-57] The conformation of both the HIV PR active site and the substrate are critical factors in the biocatalytic process, and it is therefore crucial to understand the role of each specific amino acid within the active site in the presence of the substrate or inhibitor.[58] Enzyme kinetic studies are crucial in identifying what type of enzyme inhibition occurs, and this can be described in terms of competitive inhibition, non-competitive inhibition or uncompetitive inhibition.[59]

When designing HIV-1 PR inhibitors (PIs) various characteristics need to be considered. They should: (i) be effective against various HIV clinical isolates; (ii) be specific for HIV-1 PR (compared with other mammalian aspartic acid proteases) to minimize possible adverse effects; (iii) have good oral bioavailability and duration in humans; (iv) be more effective in the suppression of the wild-type virus through increased efficacy and higher plasma levels; (v) be active against PI-resistant variances of HIV-1; and (vi) and be safe to use and well tolerated.[60-62]

There are currently nine HIV PR inhibitors clinically approved for use in the treatment of AIDS; they may be classified as peptidomimetic or non-peptidomimetic inhibitors.[55,63] These PIs are usually administered as one or two drugs in combination with two nucleoside reverse transcriptase inhibitors.[64-70] The peptidomimetic PIs are:[16,62-69] Invirase® [Saquinavir, Hoffman-La Roche, Dec. 1995] (**1**); Norvir® [Ritonavir, Abbott Laboratories, March 1996] (**2**); Crixivan® [Indinavir, Merck, March 1996] (**3**); Viracept® [Nelfinavir, Pfizer, March 1997] (**4**); Agenerase® [Amprenavir, GlaxoSmithKline, May 1999] (**5**); Kaletra® [Lopinavir, Abbott Laboratories, September 2000] (**6**); Reyataz® [Atazanavir, Bristol-Myers Squibb, June 2003] (**7**); Lexiva®

[Fosamprenavir, GlaxoSmithKline, October 2003] (**8**). The non-peptidomimetic PI is: Aptivus® [Tipranavir, Boehringer Ingelheim, June 2005] (**9**).[63, 70]

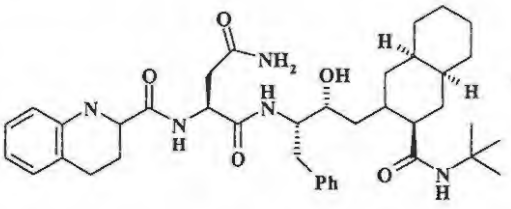

1

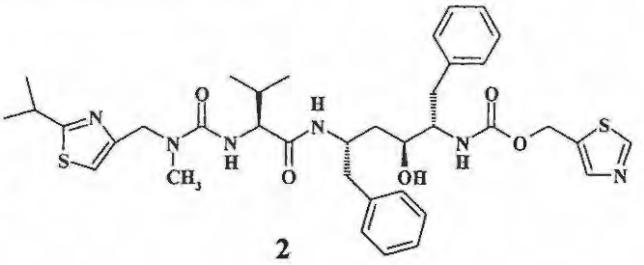

2

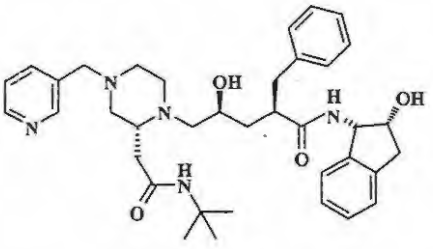

3

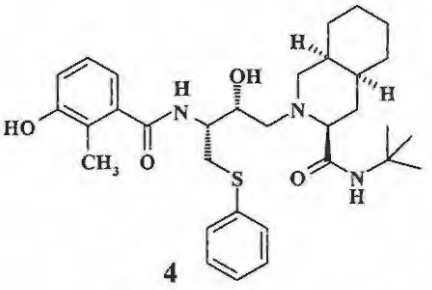

4

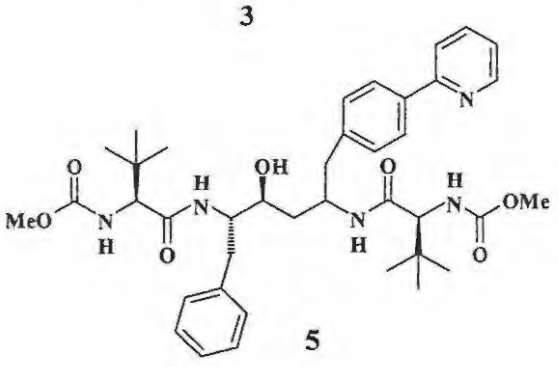

5

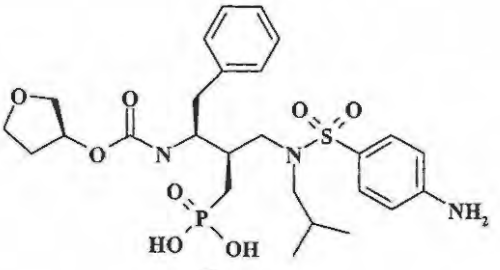

6

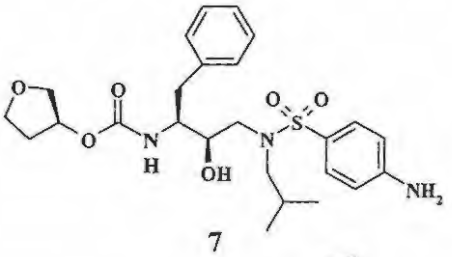

7

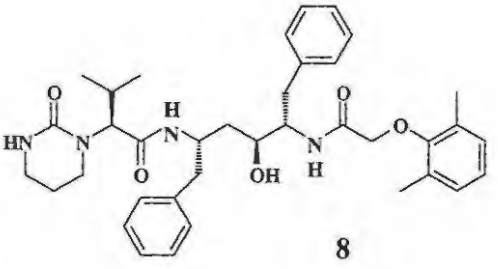

8

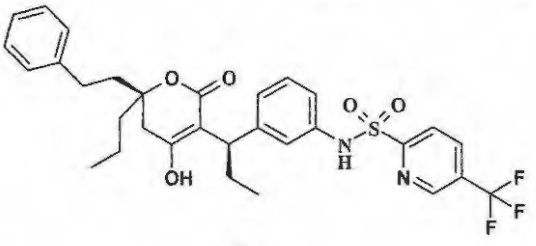

9

Most clinically approved HIV-1 PR inhibitors (PI) contain a non-hydrolyzable hydroxyethylamine (**10**) or hydroxyethylene dipeptide (**11**) isostere at would otherwise be the scissile site. These inhibitors have a particular configuration at the hydroxyl-bearing asymmetric centre, which is crucial for their inhibitory activity.[71] Hydroxyethylene dipeptide isosteres (**11**) have an *S*-configuration, at the hydroxyl bearing centre,[71-74] while hydroxyethylamine isosteres (**10**) show a preference for an *R*-configuration.[74-75] The hydroxyl group concerned participates in hydrogen bonding interactions with the catalytic aspartic acid residues in the HIV PR active site, and its orientation plays a crucial role in the binding.[76]

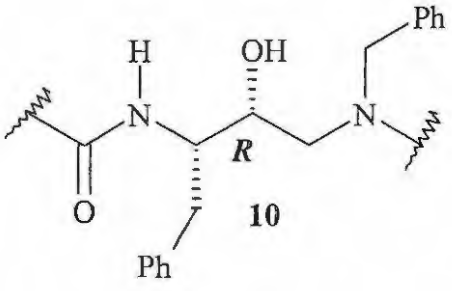

Hydroxyethylamine isostere

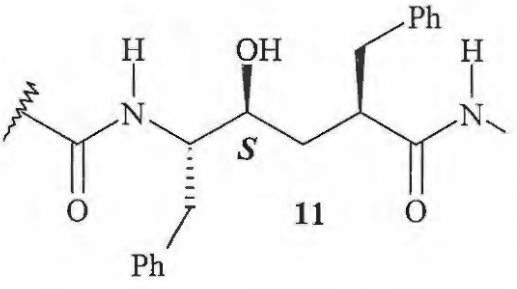

Hydroxyethylene dipeptide isostere

1.2 Enzyme Kinetics and Inhibition

Enzyme kinetic studies are crucial for discovering the kinetic parameters involved during the reversible interaction of the free enzyme (E) with the substrate (S) to form an enzyme-substrate complex (ES), which then decomposes to form the enzyme and the reaction product (P). These studies provide an understanding of the rate and specificity of biological processes.[77] This can be described in terms of the steady state mechanism for a one-substrate reaction,[78]

$$[E] + [S] \underset{k_{-1}}{\overset{k_1}{\rightleftharpoons}} [ES] \xrightarrow{k_2} [E] + [P] \qquad \text{..... (1)}$$

where k_1, k_{-1} are the forward and reverse rate constants which describe the enzymatic process for the formation of ES, while k_2 is the rate constant for the decomposition of ES to form product, the assumption being that second step is irreversible.[79] The rate can be expressed in terms of the kinetic parameter known as the Michaelis constant, K_m:

$$K_m = \frac{(k_{-1} + k_2)}{k_1}$$

The Michaelis constant (K_m) measures the binding affinity between the substrate and enzyme and also determines the substrate concentration at which the reaction rate is half of its maximum value (V_{max}), which occurs at a sufficiently high substrate concentration such that the enzyme is saturated.[77-79]

However, when the inhibitor is introduced in the enzymatic reaction, it affects the binding of the substrate to the enzyme and this effect can be described in terms of competitive, non-competitive or uncompetitive inhibition.[80-82] In competitive inhibition, the inhibitor is assumed to bind to the active site of the free enzyme without forming any product thus reducing the concentration of free enzyme available to bind with the substrate. Competitive inhibition can be expressed by the following model.[80,82]

$$\begin{array}{l} [E] + [S] \underset{k_{-1}}{\overset{k_1}{\rightleftharpoons}} [ES] \xrightarrow{k_2} [E] + [P] \\ + \\ [I] \\ \Big\| \; K_i \\ [EI] + [S] \longrightarrow \text{NO REACTION} \end{array} \qquad \text{..... (2)}$$

In the case of non-competitive inhibition, the inhibitor is presumed to bind at a site distinct from the substrate active site in either the free enzyme or the enzyme-substrate (ES) complex. Such inhibition can be represented as follows.[80,82]

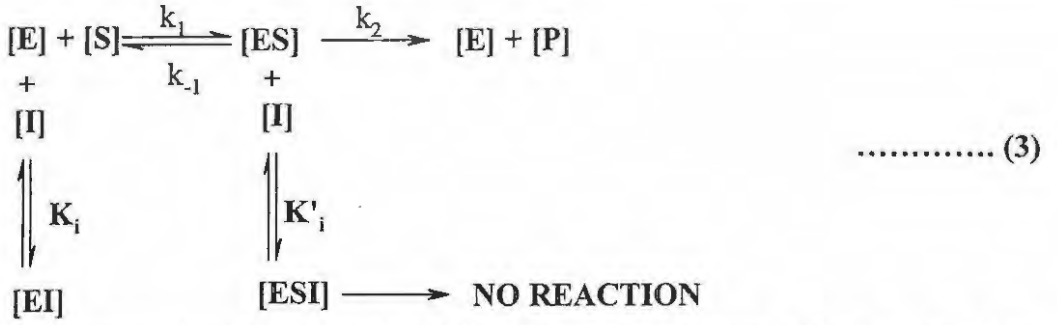

..... (3)

In uncompetitive inhibition, the inhibitor is presumed to only bind to the ES complex at a site distinct from the substrate active site and this can be represented by the following model.[80,82]

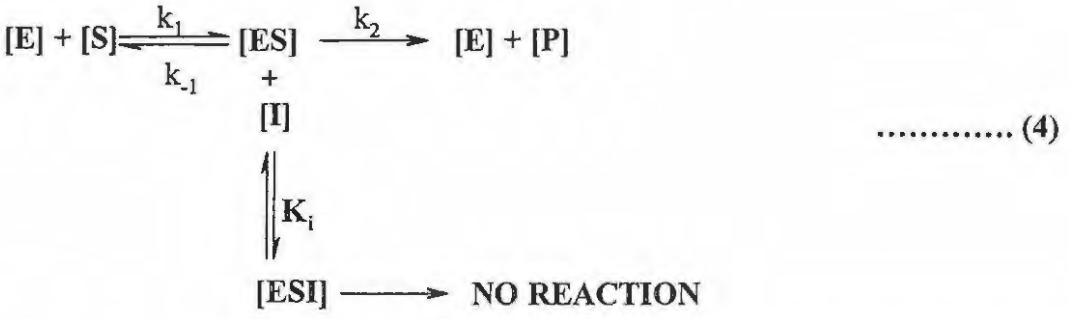

..... (4)

The K_m, V_{max} values and the inhibition constant (K_i), which measures the binding affinity between the enzyme and the inhibitor, are the kinetic parameters which determine the effect of an inhibitor on a catalytic reaction between an enzyme and a substrate.[81-83]

1.3 Chromones

Chromone **12** is the parent structure for the benzannulated oxygen-containing heterocyclic compounds which contain a γ-pyrone ring **13**.[84,85] Bloch and Kostanecki[86] used the name "chromone" when describing several coloured, naturally occurring compounds which contain the benzopyran-4-one moiety. Xanthone **14**, a chromone derivative, is doubly benzannulated, while other common derivatives include flavones **15** (2-phenylchromones), and isoflavones **16** (3-phenylchromones).[87] Chromone

derivatives are widely distributed in plants, and their biological activity and pharmacological properties have prompted research into their chemical properties.[88,89] The pyran analogues **17** and **18** have no carbonyl group, while coumarin **19** is isomeric with chromone, differing only in the location of the carbonyl group.[87, 90]

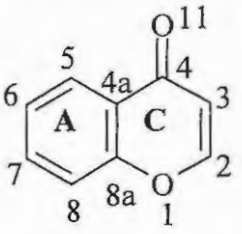

12

chromone
(benzo-γ-pyrone)
(4*H*-1-benzopyran-4-one)
(4-oxo-4*H*-benzopyran)
(4-oxo-4*H*-chromene)

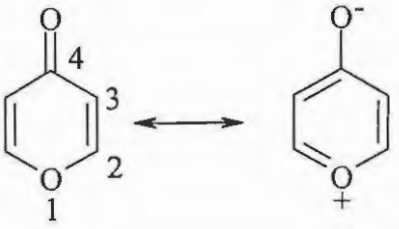

13a **13b**

γ-pyrone
(pyran-4-one)

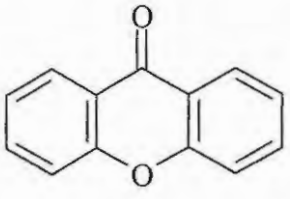

14

xanthone
(9*H*-xanthen-9-one)

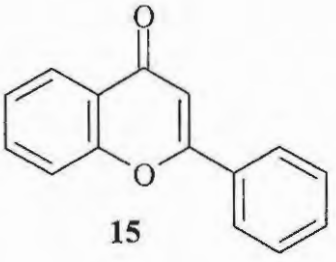

15

flavone
(2-phenlychromone)
(2-phenyl-4*H*-1-benzopyran-4-one)

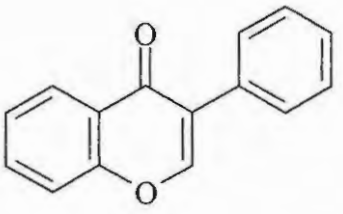

16

isoflavone
(3-phenylchromone)
(2-phenyl-4*H*-1-benzopyran-4-one)

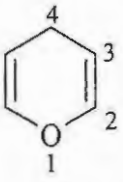

17

4*H*-pyran

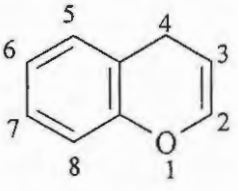

18

γ-chromene
(4*H*-chromene)
(4*H*-1-benzopyran)

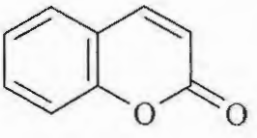

19

coumarin
(2*H*-1-benzopyran-2-one)

1.3.1 Structure and Spectroscopic Properties of chromone systems

The π-electronic structure has been used to rationalize general chromone properties,[87] with the γ-pyrone ring assuming the aliphatic dienone structure **13a** rather than the pyrylium betaine structure **13b**. However, certain properties, such as lack of normal ketonic behavior and the tendency to form salts with acids, has been attributed to a contribution by the pyrylium betaine structure **13b**.[91] These properties are consistent with Arndt's[92] suggestion, made in 1924, that the γ-pyrone ether oxygen could interact electronically with the carbonyl group, thus modifying the properties of the latter. The "aromaticity" of the γ-pyrone is evidenced by the failure to form a Diels–Alder adduct when 2,3-dimethylbuta-1,3-diene is treated with γ-pyrone.[93] The aromaticity of the γ-pyrone ring is also supported by the results of semi-empirical calculations (*ab initio* and DFT).[85]

While molecular orbital delocalization energy (M.O.D.E), dipole moment and ^{1}H- and ^{13}C-NMR data also indicate that the γ-pyrone ring in chromone possesses a significance degree of aromaticity,[91,94] some spectroscopic properties of chromone derivatives are better explained in terms of the aliphatic dienone structure **13a**. For example, the IR carbonyl stretching frequency for chromone **12** ($\nu_{C=O} \approx 1660$ cm^{-1}) is higher than for γ-pyrone ($\nu_{C=O} \approx 1650$ cm^{-1}), but lower than for the isomeric coumarin **19** ($\nu_{C=O} \approx 1710$ cm^{-1}).[95-97]

The ^{1}H-NMR spectrum of chromone **12** in $CDCl_3$ reveals that the 2-H and 3-H nuclei resonate at δ 7.88 and 6.34 ppm, respectively.[95] These values are almost the same as those found for γ-pyrone **13a** (δ 7.88 and 6.38 ppm respectively),[98] which implies that benzannulation has relatively little effect on the ring current of the heterocyclic ring. In the ^{13}C-NMR spectra of chromones, the carbonyl carbon (C-4) signal always resonates at low field (δ 177 ppm) and is relatively unaffected by substitution in the system. Substitution at C-2 or C-3 of the chromone nucleus, on the other hand, has a major effect

on the chemical shifts of these carbon atoms. For example, substitution with either methyl or phenyl groups induces a downfield shift for the carbon to which they are attached, but an upfield shift for the adjacent carbon atom.[98]

In electron-impact mass spectrometry, chromone **12** fragments *via* two main pathways, which involve either elimination of carbon monoxide or ring cleavage by a *retro*-Diels-Alder (RDA) reaction as depicted in **Scheme 1**.[90] While these transformations appear to be general in chromone systems, **A**-ring substitution may divert the fragmentation pattern.[90]

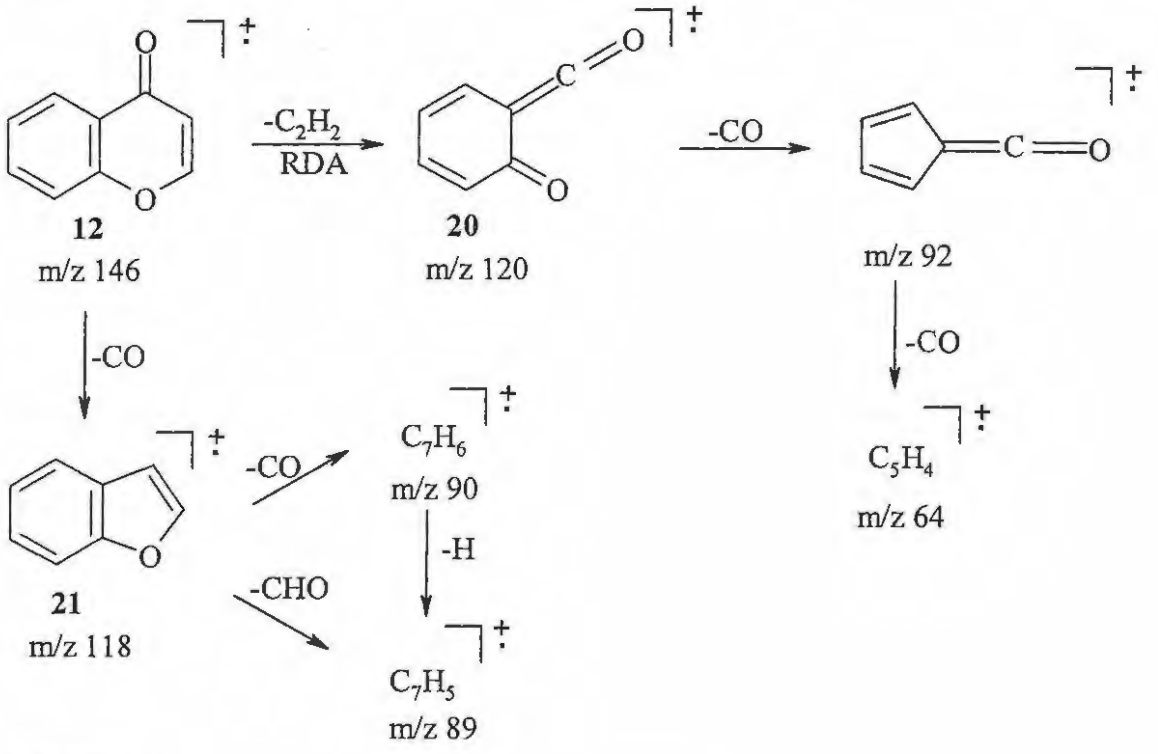

Scheme 1

1.3.2 Biological activity of chromone systems

Since the chemistry of chromones has been comprehensively studied,[87] this review focuses mainly on the more recent literature (since 1980) on synthetic and naturally occurring chromone derivatives, which exhibit pharmacological activity. The collective term chromones will also be used in reference to chromone derivatives.

Many naturally occurring chromones contain a methyl group at C-2, a phenyl group at C-2 or C-3 and a hydroxyl group at C-5 and/or C-7.[87] These features are exemplified by the polyoxygenated chromones, 5,7-dihydroxy-2-methylchromone **22** and 5,6-dihydroxy-7-methoxy-2-methylchromone **23**, both of which were isolated from the bulb of *Pancratium biflorum* Roxb. when the plant still had flowers,[99] by quercategetin **24**, a flavone isolated from *Sculletaria baicarensis* and by the isoflavone **25**, isolated from the roots of *Salsola somalensis* (synonyms: *Halotamnus somalensis* and *S. bottae*).[100-102]

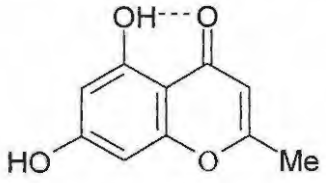

22

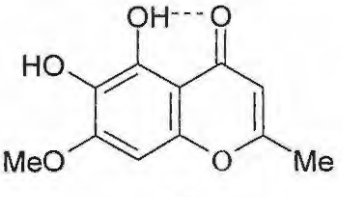

23

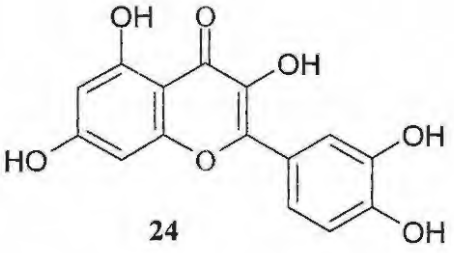

24

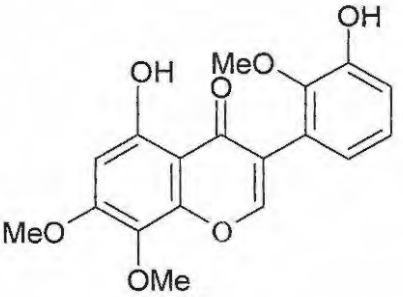

25

The chromone moiety constitutes an important component of the pharmacophore of a number of biologically active molecules. For example, the extracts of the bulb and the flowers of *P. biflorum* are used for the treatment of ear-ache, chest ailments and fungal diseases. [102] Compound **24** is known as the most potent HIV-1 integrase (IN) inhibitor, with the activity being attributed to the numerous hydroxyl groups.[100,103] The extract of the root of *S. somalensis* is used for the treatment of tapeworm infestations, while root parts are utilised as tooth sticks; the fibrous roots slowly disintegrate in the mouth and the juice is swallowed resulting, it is claimed, in the expulsion of parasites.[102]

The synthetic 3'*R*,4'*R*-di-*O*-(-)-camphanoyl-2',2'-dimethyldihydropyrano[2,3-*f*]chromone (DCP) analogues **26** and **27** have been found to exhibit extremely high anti-HIV activity.[104] A hydrophobic moiety, either aliphatic or phenyl, at position 2 appears

to be significant for anti-HIV activity by increasing binding to a putative hydrophobic cleft on the surface of the target thereby increasing affinity and the desired pharmacogical response. The extremely high anti-HIV activity of **27** indicates that C-2 ethyl group probably fits well into the putative hydrophobic cleft. Substitution at position 3 with methyl group, as in compound **26**, also appears to increase activity against the multi-RT inhibitor resistant strain while decreasing cytotoxicity.[104]

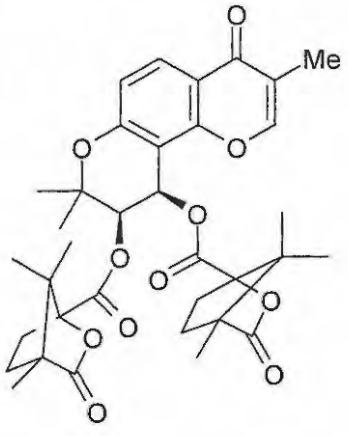

26

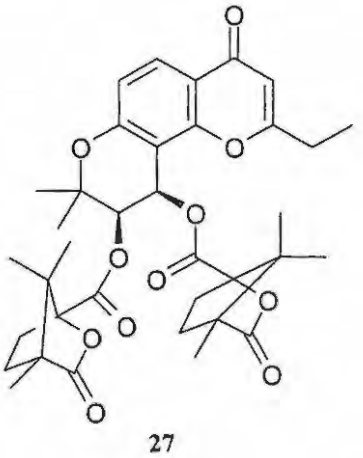

27

The synthetic chromone derivatives **28-31** have also shown some anti-HIV-1 protease (PR) activity with inhibition efficiencies of 93.6%, 93,3%, 92.2% and 92.02%, respectively.[105] Docking studies of these compounds has revealed that the bulky 3-benzoyl and 2-phenyl substituents interact with the hydrophobic S1 subsite, whereas the 7- or 8-hydroxyl groups interact with Asp 25 and Asp 25' in the receptor cavity. The hydroxyl groups act as hydrogen-bond donor moieties, forming hydrogen bonds with the carbonyl oxygen of Asp 25 and Asp 25'.[105] The chromone xanthone derivatives **32** and **33** are found in *Penicillium glabrum* (Wehmer) Westling extract. These compounds exhibit CD4 binding activity in an enzyme-linked immunosorbent assay (ELISA) on the

binding of the monoclonal antibody, anti Leu 3a, to soluble recombinant CD4.[106] CD4 is a glycoprotein expressed on the surface of mature helper/inducer T-lymphocytes; it has a crucial role in many immune responses and functions as a cellular receptor for HIV. Anti Leu 3a blocks both CD4 dependent T-cell responses and the binding of HIV to the T-cells. These compounds thus have potential as immunosuppressive and anti-HIV agents.[106]

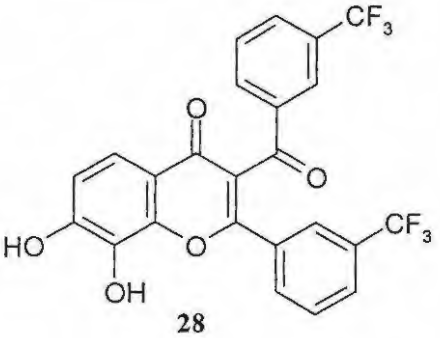

28

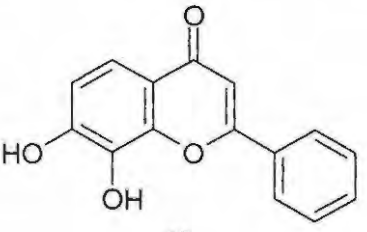

29

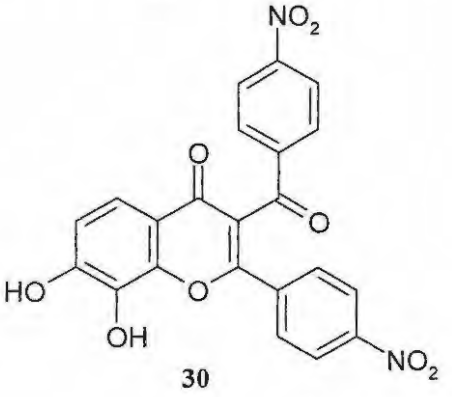

30

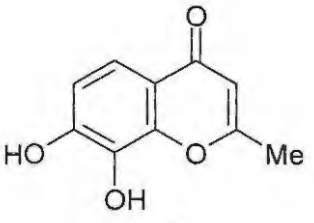

31

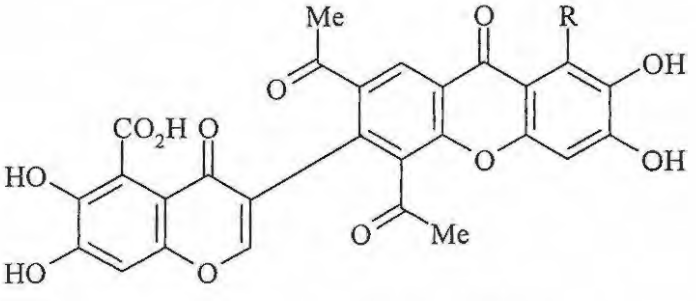

32 R = COOH
33 R = H

Biflorin **34**, a polyoxygenated chromone-*C*-glucoside isolated from the roots of *P. biflorum*, has been found to inhibit phosphodiesterase. This property of biflorin reflects its general ability to activate phosphokinase enzymes which are important for active

growth of the producer organism.[107] 6-β-*C*-Glucopyranosyl-5,7-dihydroxy-2-isopropylchromone **35** is a chromone derivative isolated from *Baeckea frutescens* L. (Myrtaceae) the leaves of which are used as a medicinal tea for fever diseases in China.[108] Aloesin **36** is a chromone derivative isolated from the dried leaves of *Aloe excelsa* A. Berger, which is widely distributed in Southern Africa. These leaves are commonly used in traditional medicine to treat venereal sores, asthma and abdominal pains.[109] Schumanniofioside A **37** and Schumanniofioside B **38** are chromone glycosides isolated from the root bark of *Schumanniophyton magnificum*, a small tree that grows in the tropical zone of West and Central Africa. In Cameroon, the bark decoction is used as a remedy for dysentery and also as an enema, while other tribes use it after circumcision.[110]

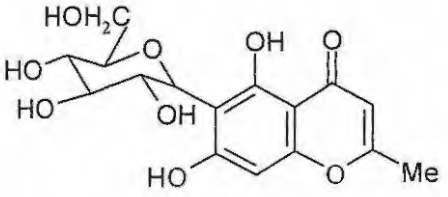

34

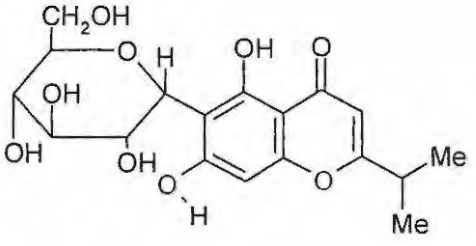

35

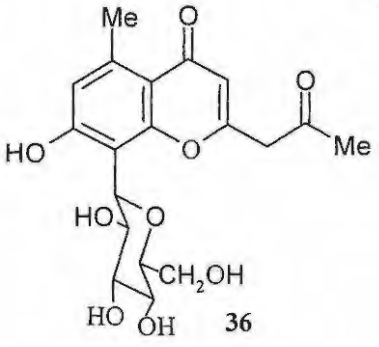

36

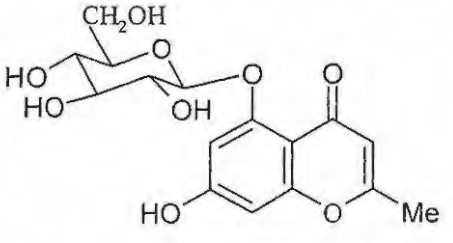

37

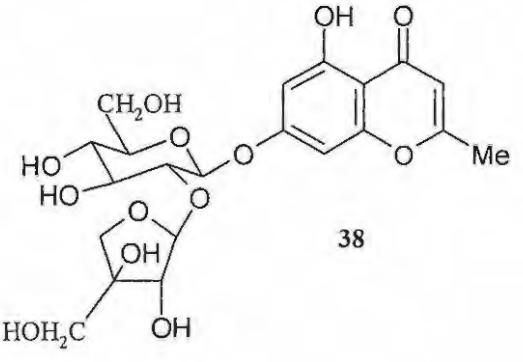

38

Ginkgetin **39** is a biflavone extracted from *Selaginella moellendorffii* Hieron (Selaginellaceae), which has been found to possess an inhibitory effect on the growth of the cancer cell line, human ovarian adenocarcinoma (OVCAR-3). This plant, *S. moellendorffii*, has been used as a remedy for jaundice, gonorrhea, bleeding and acute hepatitis.[111] Cromoglycic acid **40**, the first drug to have the ability to prevent asthmatic attacks has stimulated medicinal chemical research on anti-asthmatic drugs.[112, 113]

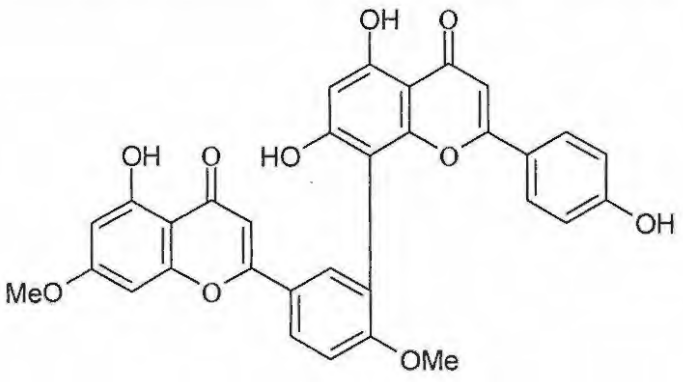

39

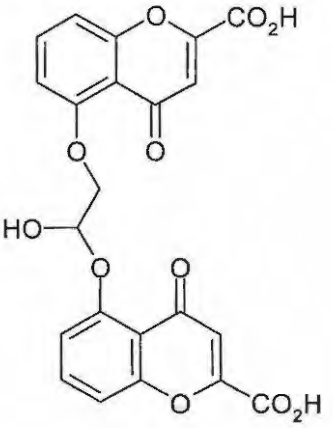

40

Robustaflavone 4'-methyl ether **41** is a new biflavone, which was isolated from *Selaginella delicatula* Desv. Alston (Selaginellaceae), a perennial herb found in a Taiwanese mountain forest. This compound **41** was found to possess cytotoxic activity on various human tumor cell lines where it suppresses the growth of Raji and Calu-1 tumor cell lines.[114] Variabiloside B **42**, a quercetin found in the leaves of *Strychnos variabilis* Wildem, appears to alleviate the symptoms of cerebrovascular insufficiency and poor arterial circulation.[115]

The chromone derivatives, 5-hydroxy-6-methoxy-2-(2-phenylethyl)chromone **43** and 6-hydroxy-2-(2-hydroxy-2-phenylethyl)chromone **44,** were isolated from an extract of withered wood of *Aquilaria senensis* (Thymelaeaceae).[116] The decay or injury of A. *senensis* results in the formation of resinous agarwood, a famous incense which is used as a sedative, analgesic and digestive in Kampo.[116] Eryvarins F **45** and G **46** are 3-phenoxychromones isolated from the roots of *Erythrina variegate* L. (Leguminosae).

This plant is found in many tropical and subtropical regions and is used as an antibacterial, anti-inflammatory, antipyretic and antiseptic agent; however, in China it is used as a collyrium.[117]

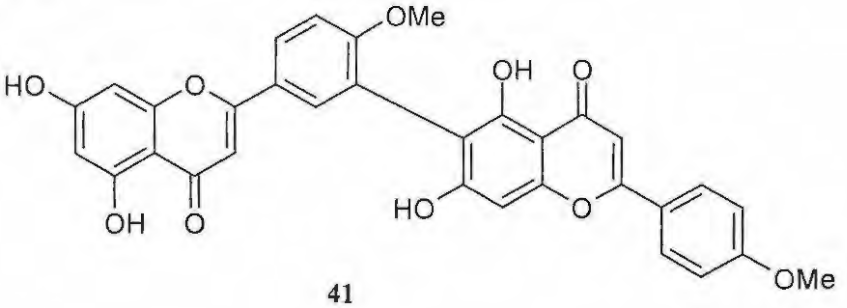

41

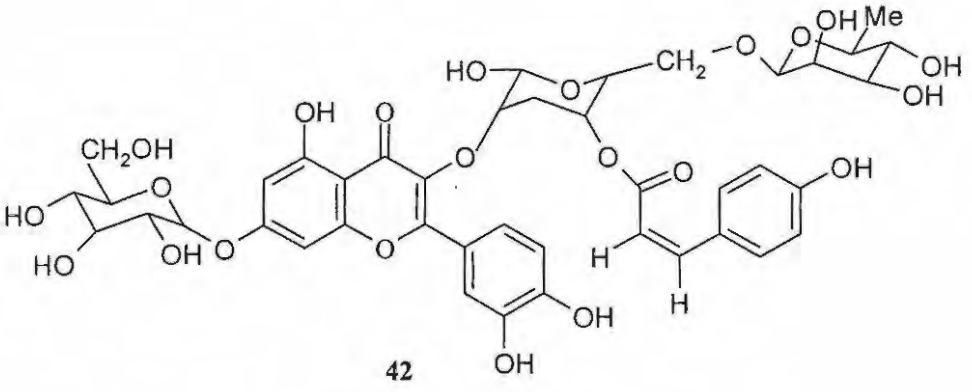

42

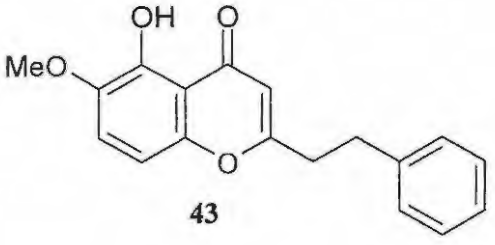

43

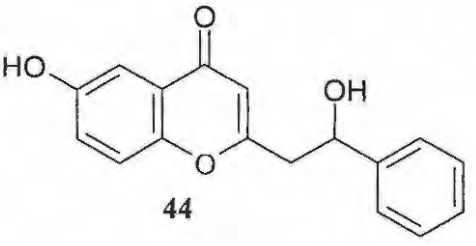

44

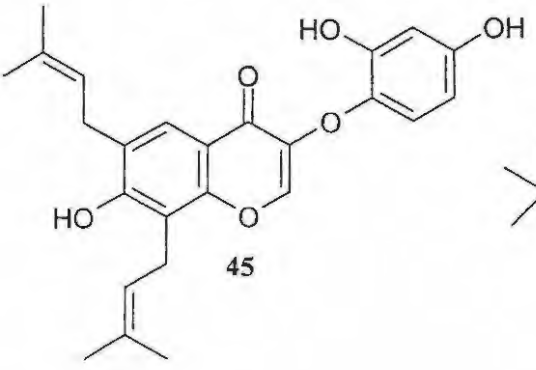

45

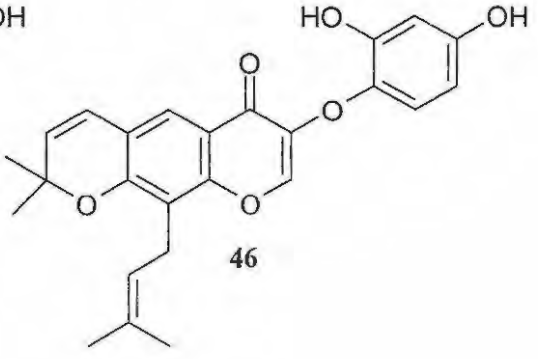

46

Hormothamnione **47** was the first naturally occurring styrylchromone to be isolated from the marine cryptophyte, *Chrysophaeum taylori*. Hormothamnione **47** has been found to be potent cytotoxin to several human leukemia cell lines; it appears to operate *via* selective inhibition of RNA synthesis,[118] but lacks the catechol moiety characteristic of other flavone derivatives which cleave the DNA material. The isoflavones **48-50** were isolated from the roots of *Salsola somalensis* found in drier parts of Asia, Europe and Africa and, as indicated earlier, *S. somalensis* is used in local medicine. [102]

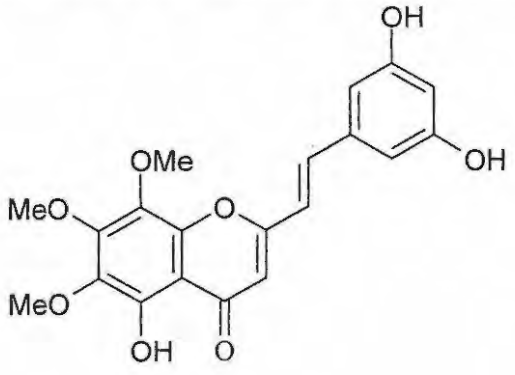

47

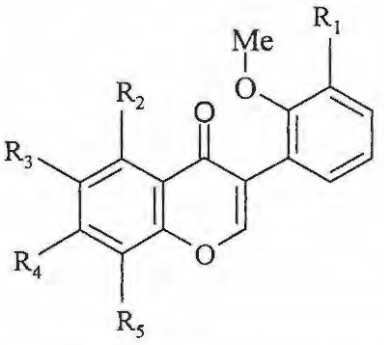

48 $R_1 = R_2 = OH$; $R_3 = H$; $R_4 = R_5 = OMe$
49 $R_1 = R_2 = OH$; $R_3 = R_4 = OCH_2O$; $R_5 = H$
50 $R_1 = R_2 = OH$; $R_3 = R_4 = R_5 = OMe$

1.3.3 Synthesis of chromone derivatives

There are two commonly used methods for preparing chromone derivatives. The first, which is more preferable, is known as the Kostanecki–Robinson[86] reaction, and involves the condensation of *o*-hydroxyacetophenone **51** with an acylating agent to form a β-diketone derivative **52**, which on acidification spontaneously cyclises to the chromone derivative **53 (Scheme 2).** This reaction is actually the reverse of chromone hydrolysis. The second method is the Simonis reaction,[86] which involves the acid-catalysed condensation of a phenol **54** with a β-ketoester to give a chromone **53 (Scheme 3).** The formation of a coumarin **55** under these conditions is known as the Pechmann condensation. Chromone formation is favoured provided the phenol contains a

deactivating group, such as chlorine, the β-ketoester is α-substituted and phosphorus pentoxide is used as the condensing agent.[92]

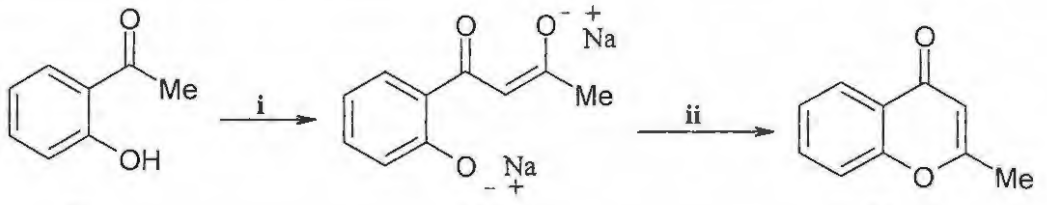

51 **52** **53**

Scheme 2
Reagents: i) NaOEt, CH_3CO_2Et; ii) H^+.

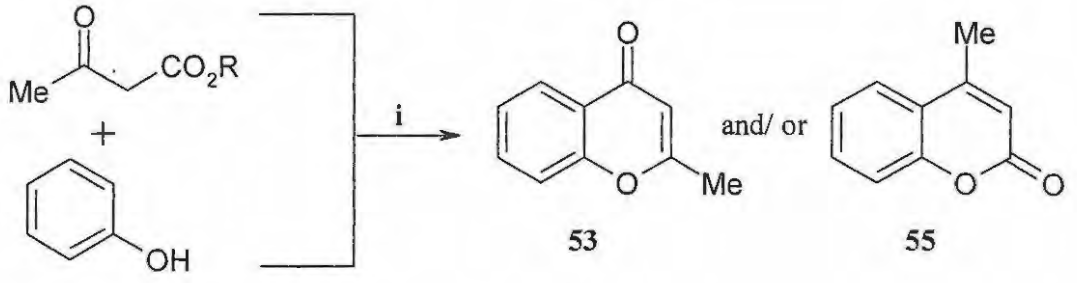

54 **53** **55**

Scheme 3
Reagents: i) Condensing agent (H_2SO_4 or P_2O_5).

Recently, it has been discovered that chromones **58** can be synthesized by reacting substituted phenols **56** with Meldrum's acid **57** in the presence of the catalyst, $Yb(OTf)_3$, **(Scheme 4)**. During the reaction, two distinct multibond-forming reactions, known as Friedel-Crafts *C*-alkylation/*O*-acylation and Friedel-Crafts *C*-acylation/*O*-alkylation, are involved and the degree of substitution on the alkylidene moiety **57** controls the regioselectivity of the annulation reaction.[118]

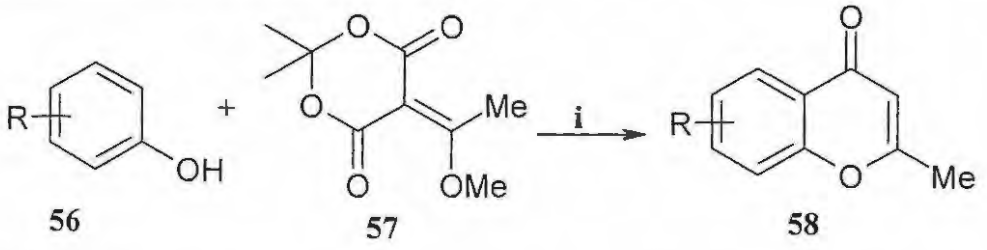

56 **57** **58**

Scheme 4
Reagents: (i) $Yb(OTf)_3$, CH_3NO_2, 100°C, 1.5h.

5-Hydroxy-2-isopropyl-7-methoxychromone **64** has been synthesized *via* the Konstanecki-Robinson method **(Scheme 5)**. Thus, methylation of 2'4'6'-trihydroxyacetophenone **59** with dimethyl sulfate affords 2'-hydroxy-4',6'-dimethoxyacetophenone **60,** which undergoes acylation to form an enolate which reacts with a carboxylate ester to give a mixture of compounds **61** and **62.** Treatment of this mixture with acetic and sulfuric acids gives the 5,7-dimethoxychomone derivative **63**, which undergoes selective demethylation at the C-5 position to afford 5-hydroxy-2-isopropyl-7-methoxychromone **64**.[119]

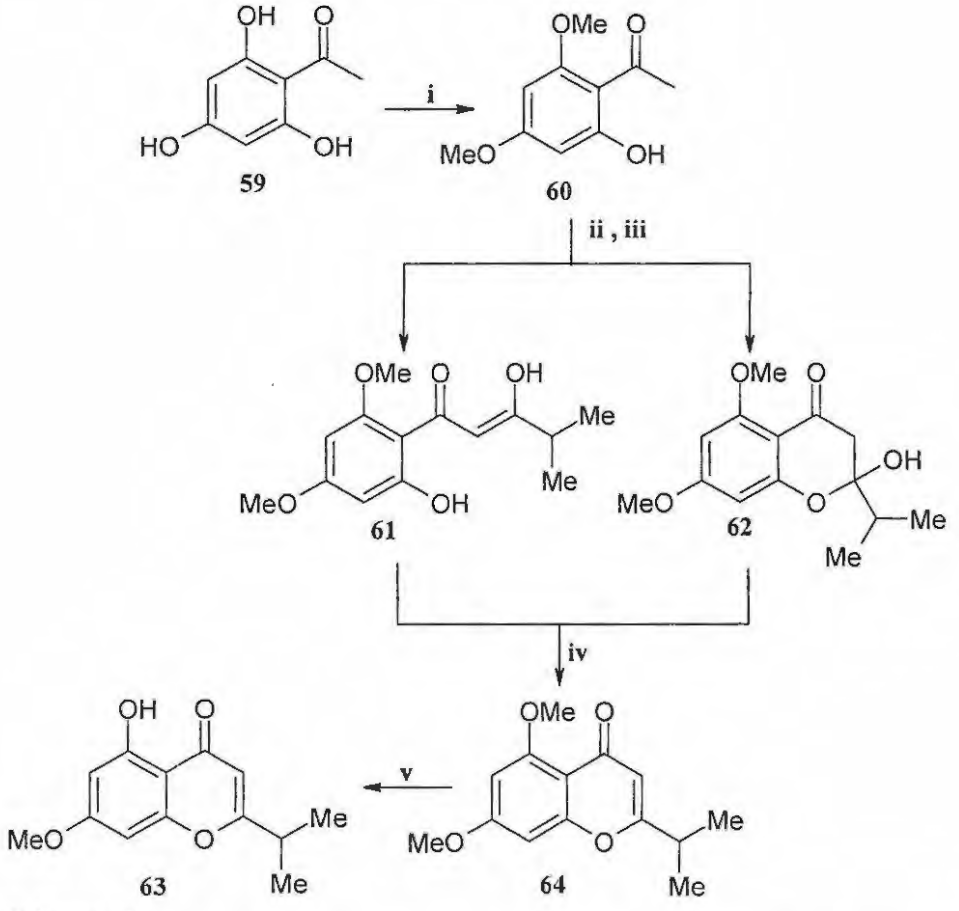

Scheme 5

Reagents: (i) Me_2SO_4 (2eq.), K_2CO_3 (2eq.), acetone; (ii) NaOEt, EtOH;
(iii) Me_2CHCO_2Et; (iv) AcOH, H_2SO_4; (v) Ac_2O, HI, 115°C, 30min.

2-Methyl-3-nitrochromone **67**, which is used for preparation of analgesics, has been obtained in a one-pot reaction *via* nitration of *o*-hydroxybenzoylacetone **65** with acetic

anhydride, which permits direct cyclization of the β-diketone **66** as depicted in **Scheme 6**.[120] Kaye *et al.* have reported another method for the synthesis of 2-(dimethlamino)chromone **70**, which involves the reaction of 2-ethylsulfinylchromone **69** obtained, in turn, from the thiolactone **68 (Scheme 7)**.[121]

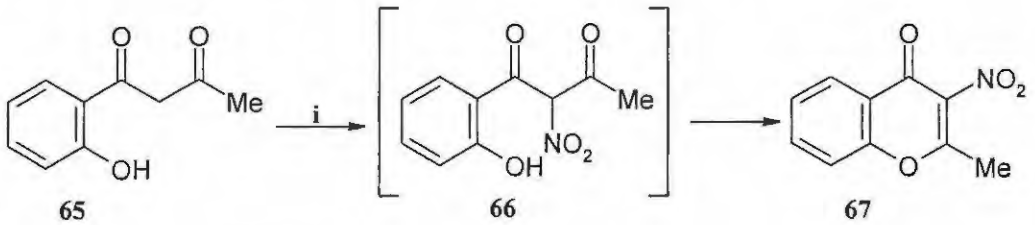

65 66 67

Scheme 6

Reagents: (i) HNO_3, $(Me\text{-}CO)_2O$.

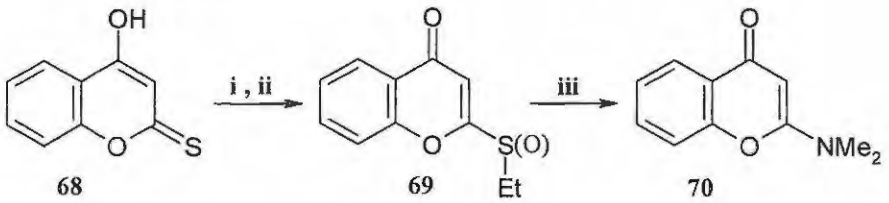

68 69 70

Scheme 7

Reagents: (i) K_2CO_3, EtI, $(CH_3)_2CO$; (ii) MCPBA, $Cl(CH_2)_2Cl$; $(Me)_2NH$.

5,7-Dihydroxychromone **72**, has been prepared by condensation of 2',4',6'-trihydroxyacetophenone monohydrate **71** with ethyl oxalyl chloride, followed by hydrolysis, acidification and decarboxylation **(Scheme 8)**.[122] Treatment of 2',4'-dihydroxyacetophenone **73** or 2',4'-dihydroxypropiophenone **74** with triethyl orthoformate and 70% perchloric acid, followed by hydrolysis in boiling water afforded 7-hydroxychromone **75a** or 7-hydroxy-3-methylchromone **75b**, respectively **(Scheme 9)**.[123] Nishinaga *et al.*[124] published a convenient method for synthesizing 2,3-dialkylchromones. This approach involves the base-catalyzed rearrangement of *o*-acetoxypropiophenone **76** to give the diketone **77** which undergoes cyclisation to afford 2,3-dimethylchromone **78 (Scheme 10)**.[124] Recently, a modified Baker-Venkataraman reaction for the synthesis of 3-acyl chromones and flavones has been published by Ganguly *et al.*[125] This involves the reaction of 2',4',6'-trihydroxyacetophenone **79** with

acyl chlorides **80** in the presence of DBU and pyridine to afford 3-acyl chromone derivatives **81 (Scheme 11)**.[125] 3-Acyl chromones have been shown to be useful precursors for the formation of other chromone derivatives.

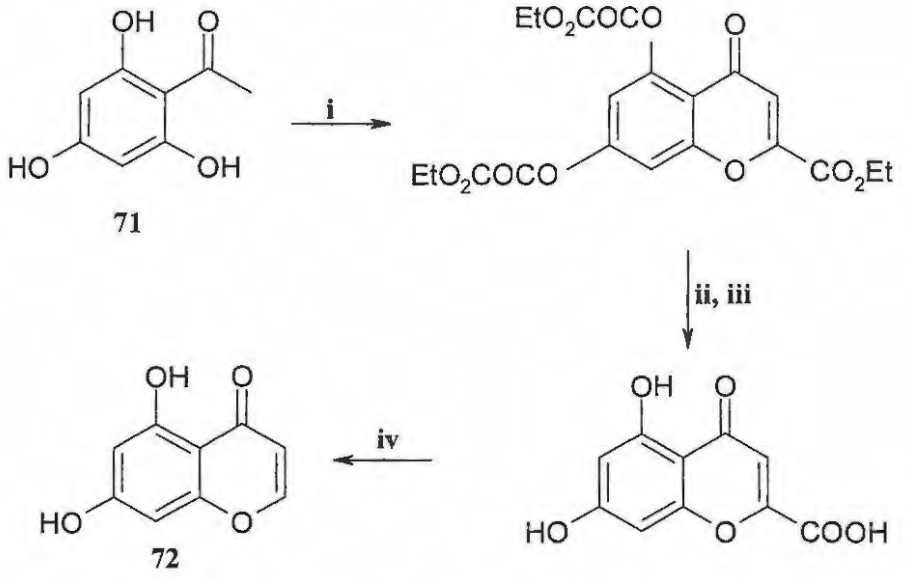

Scheme 8
Reagents: (i)EtOOCCOCl, pyridine; (ii) OH^-; (iii) H^+; (iv) heat.

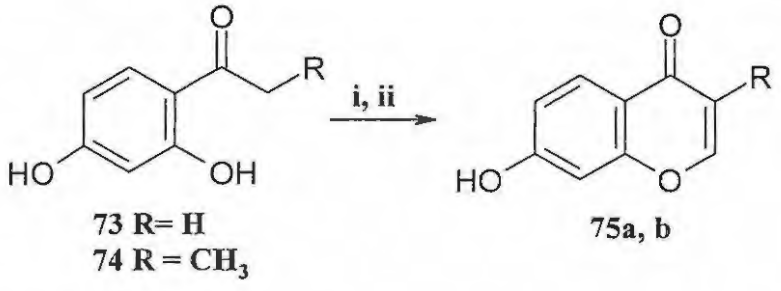

73 R= H
74 R = CH_3

75a, b

Scheme 9
Reagents: (i) 70% perchloric acid, triethyl orthoformate, 40min; (ii) H_2O, reflux, 40min.

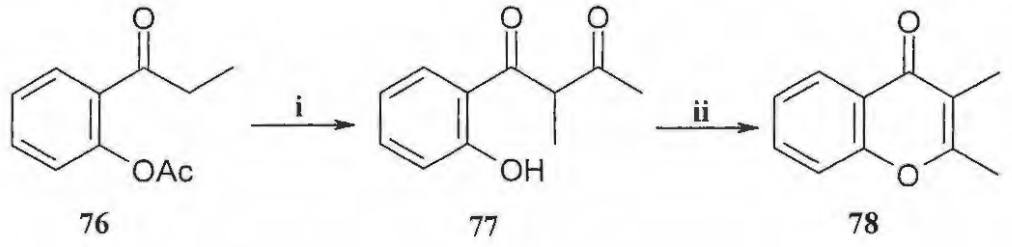

76 77 78

Scheme 10
Reagents: (i) $KOBu^t$, DMF, r.t.; (ii) $Co^{III}(salpr)(OH)$, CF_3CH_2OH, 60°C.

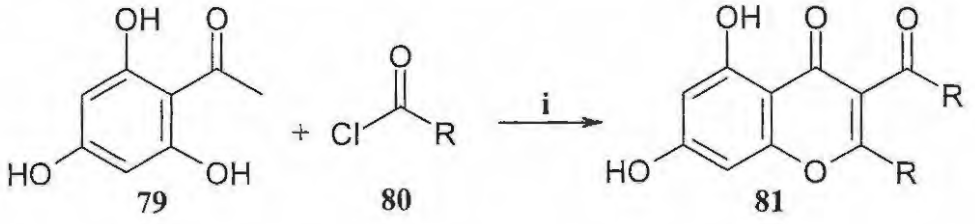

79 80 81

Scheme 11
Reagents: (i) DBU, Pyridine.

Chromone-3-carbaldehyde **83** was first synthesized in relatively low yield (≤ 30%) by the reaction of the ketoaldehyde **82** with ethyl formate or acetic acid **(Scheme 12)**.[126] However, application of Vilsmeier-Haack methodology has permitted significant improvement in this yield. A one-pot synthesis, in which *o*-hydroxyacetophenone **84** is treated with phosphorus oxychloride in dimethylformamide has been reported to afford chromone-3-carbaldehyde **83** in 61-85% yields **(Scheme 13)**.[127]

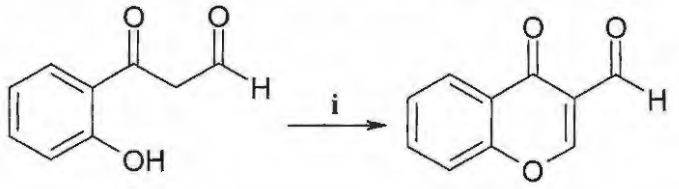

82 83

Scheme 12
Reagents: (i) HCO_2Et or HCO_2CH_3.

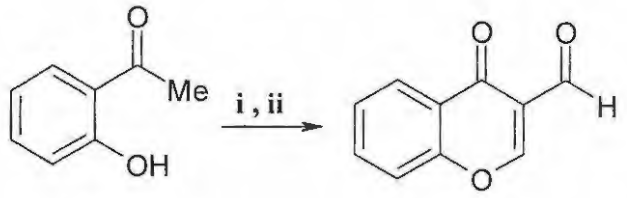

84 **83**

Scheme 13
Reagents: (i) DMF, $POCl_3$; (ii) H_2O.

Treatment of the 2,4-dihydroxyphenyl ketone **85** with methanesulfonyl chloride in dry DMF has been shown to afford 7-hydroxy-3-phenylchromone **86 (Scheme 14)**,[128] while Dawood *et al.*[129] have recently reported that heating chromanone **87** with 4-chlorobenzaldehyde **88** in the presence of a catalytic quantity of piperidine resulted in the formation of 3-(4-chlorobenzyl)chromone **89** as depicted in **Scheme 15**[129] Selenium dioxide has been recognized as an effective reagent for the incorporation of an oxygen functionality at allylic positions and, recently, chromone-2-carbaldehydes **91** have been synthesized by selenium dioxide oxidation of 2-methylchromones **90 (Scheme 16)**.[130-131]

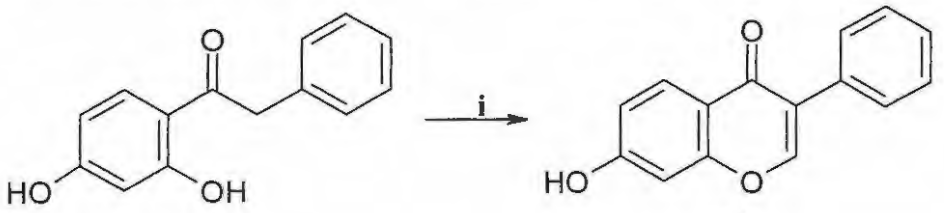

85 **86**

Scheme 14
Reagents: (i) methanesulfonylchloride, dry DMF.

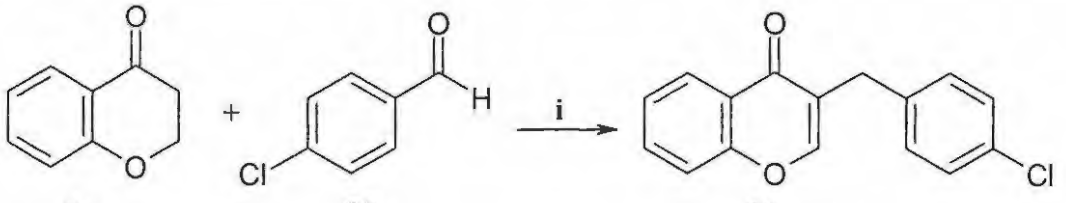

87 **88** **89**

Scheme 15
Reagents: (i) Piperidine, 170°C.

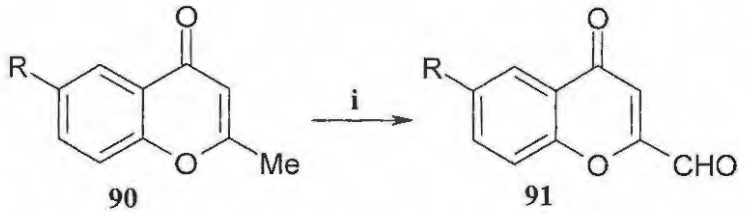

90 **91**

Scheme 16
Reagents: (i) SeO_2, xylene.

Hormothamnione **97**, which is a potent cytotoxin for several types of human leukemia cells, has been synthesized by treating 2,3,4,5-tetramethoxyphenol **92** with 2-butynoic acid and Eaton's reagent (phosphorus pentoxide in methanesulfonic acid) to afford the alkynyl ketone **93**, which undergoes cyclization to form the 5,6,7,8-tetramethoxychromone **94**. Condensation of the chromone **94** with 3,5-bis(benzyloxy)benzaldehyde yields the styrylchromone **95**, which undergoes C-3 methylation to afford 3-methyl-2-[3,5-bis(benzyloxy)styryl]-5,6,7,8-tetramethoxychromone **96**. Selective demethylation of the methyl ether at C-5 and debenzylation leads to the styrylchromone, hormothamnione **97** (**Scheme 17**).[132]

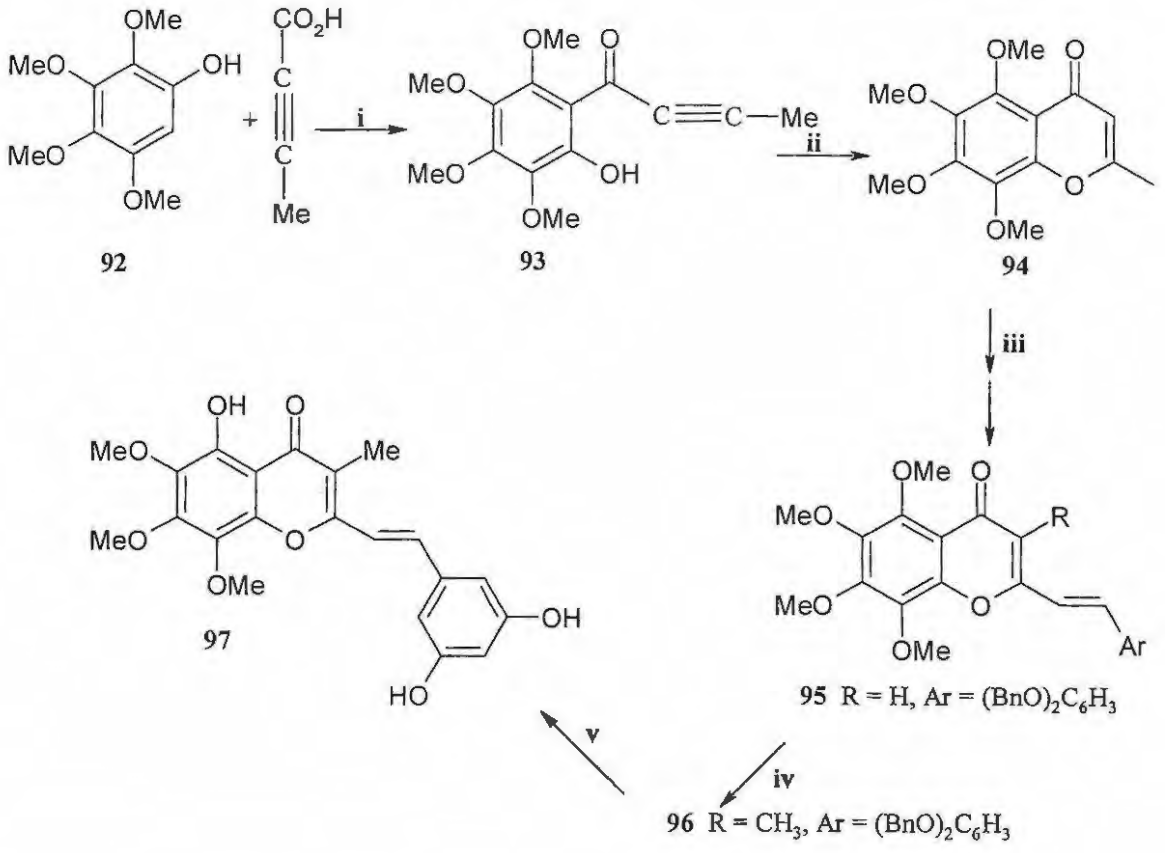

Scheme 17
Reagents: (i) P_2O_5/CH_3SO_3H, 0^oC, 4h, Ar; (ii) K_2CO_3, Acetone; (iii) 3,5-bis(benzyloxy)benzaldehyde, EtONa, EtOH; (iv) THF, LDA, $CF_3SO_3CH_3$ $-78\ ^oC$; (v) CH_2Cl_2, BCl_3

1.3.4 Reactivity of chromone derivatives

Chromones have intrigued many researchers due to the spectrum of reactivity with nucleophiles, electrophiles and other reagents to give various derivatives, examples of which are provided below.

1.3.4.1 Reactions with Nucleophiles

Chromones normally undergo nucleophilic attack at the C-2 and C-4 positions of the heterocyclic ring.[133] However, nucleophilic attack at C-2 in chromone derivatives has been found to result in either pyrone ring opening or loss of the C-(2)-C-(3) π-bond.[134]

Thus, reaction of chromone-3-carboxylic acid **98** with piperidine, a nitrogen nucleophile, affords an enamino ketone **100**. In this reaction, the chromone substrate **98** undergoes 1,4-addition to form β-keto-β'-amino acid **99**, which then undergoes decarboxylative ring opening to afford the enamine derivative **100 (Scheme 18)**.[135] In this reaction the *o*-carbonylphenoxy group behaves as nucleofugal group.[133] It has been noted that similar reactions occur with chromone-3-carbaldehyde **83**.

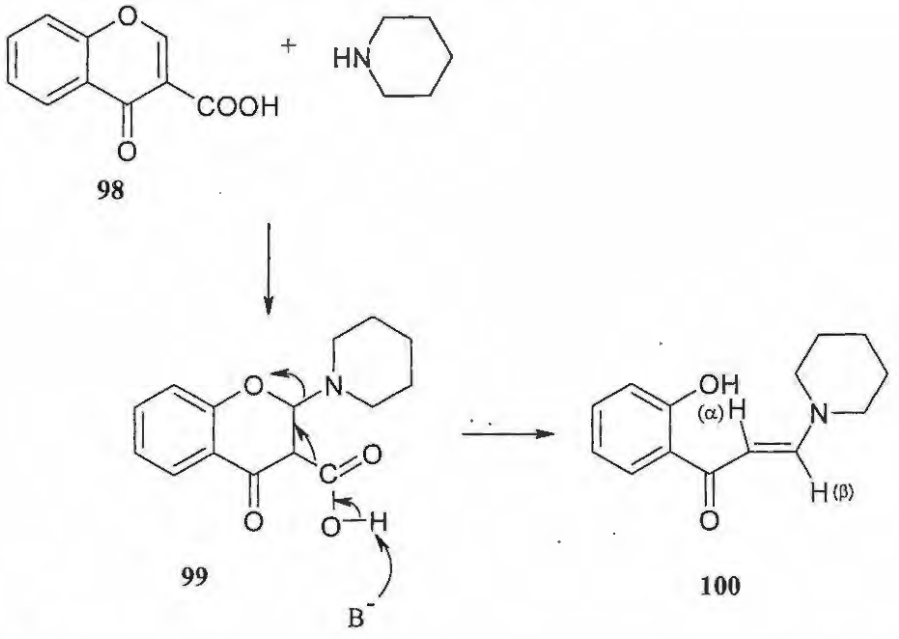

Scheme 18

With tertiary amines, 1,4-addition to the chromone-3-carboxylic acid **98** affords a reactive zwitterionic substrate **101**, which then undergoes spontaneous decarboxylative Hofmann elimination, instead of ring opening, to form chromone **12**. This is attributed to the greater nucleofugality of the positively charged quaternary ammonium cation **(Scheme 19)**.[135]

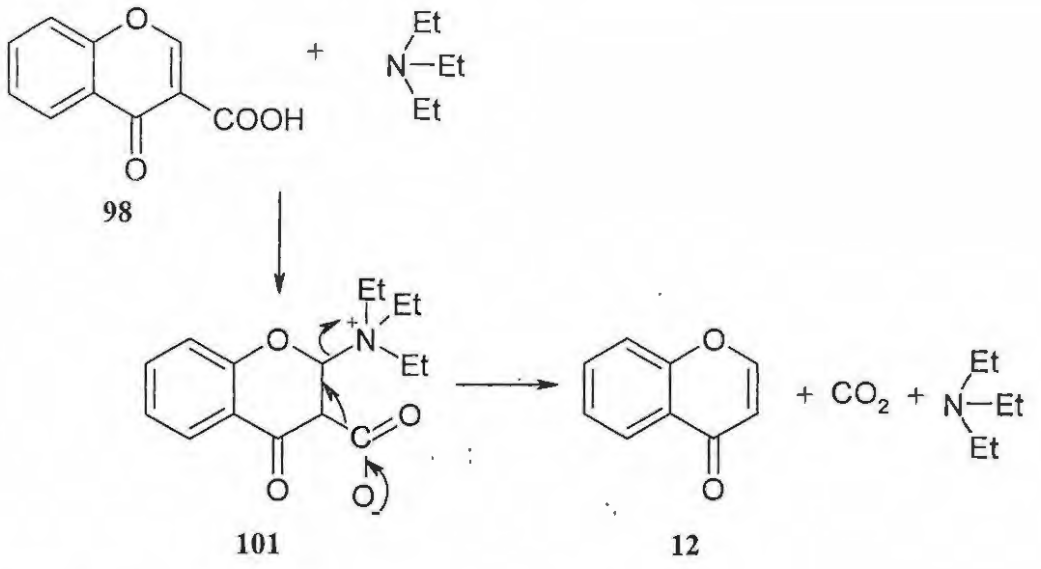

Scheme 19
Reagents: (i) Triethylamine, EtOH, reflux, 2-3h.

Reaction of chromone-3-carbaldehyde **83** with aminopyrazole **102** has been shown to afford pyrazolo[1,5-*a*]pyrimidine **103**. This reaction occurrs *via* a conjugate addition of the endocyclic nucleophilic nitrogen of the aminopyrazole **102**, followed by the ring-opening of the resulting adduct **(Scheme 20)**.[136] It has also been shown that refluxing chromone-3-carbaldehyde **83** with ethyl glycinate hydrochloride **104** in aqueous acetonitrile, in the presence of triethylamine, affords the C-2 substituted product **105**. Further heating in aqueous acetonitrile, in the presence of potassium carbonate, gave the tricyclic compound **106 (Scheme 21).**[137]

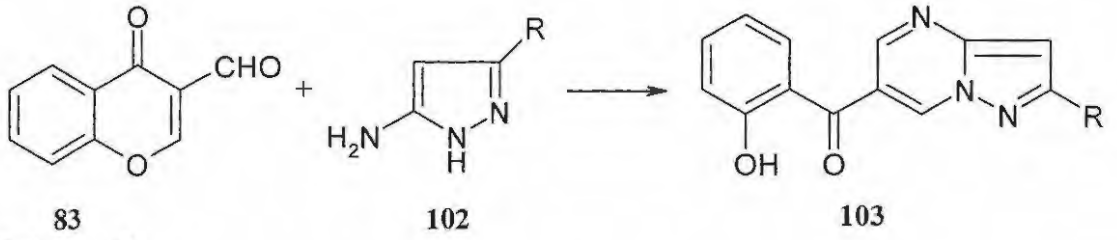

Scheme 20
Reagents: (i) Refluxing absolute EtOH, 2-3h, R =H, CH_3.

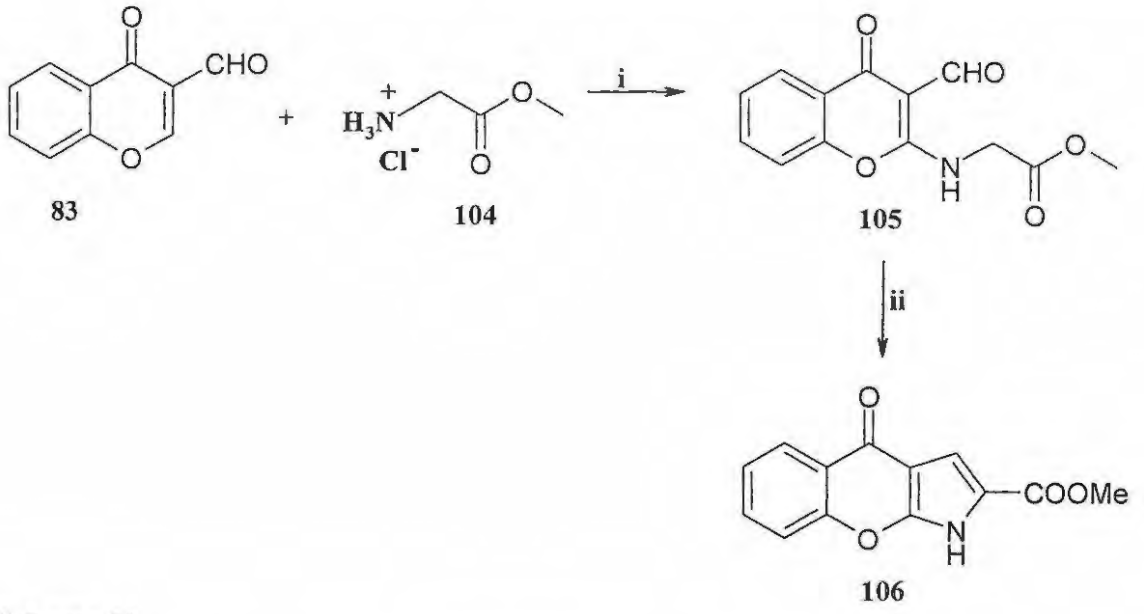

83 **104** **105** **106**

Scheme 21
Reagents: (i) Aq. acetonitrile, TEA; (ii) Aq. acetonitrile, K_2CO_3.

It is interesting to note that the reaction of chromone-3-carbaldehyde **83** with 6-aminopyrimidin-4-ones **107** by heating in absolute ethanol or by microwave irradiation in the absence of solvent resulted in the unexpected pyrido[2,3-*d*]pyrimidines **112** instead of the expected pyridopyrimidines **108**. This was attributed to the regiospecific cyclocondensation of amine **107** with the aldehyde **83**, to give the pyrido[2,3-*d*]pyrimidine **109**. The intermediate derivative **109** can either be converted into the aromatic pyrylium species **110** or, alternatively, undergo nucleophilic attack by water, released in the previous step to afford the dihydroxy species **111**. Either of the intermediates **110** or **111** afford compound **112**, *via* nucleophilic addition of hydroxide ion or elimination of water, respectively (**Scheme 22**).[136]

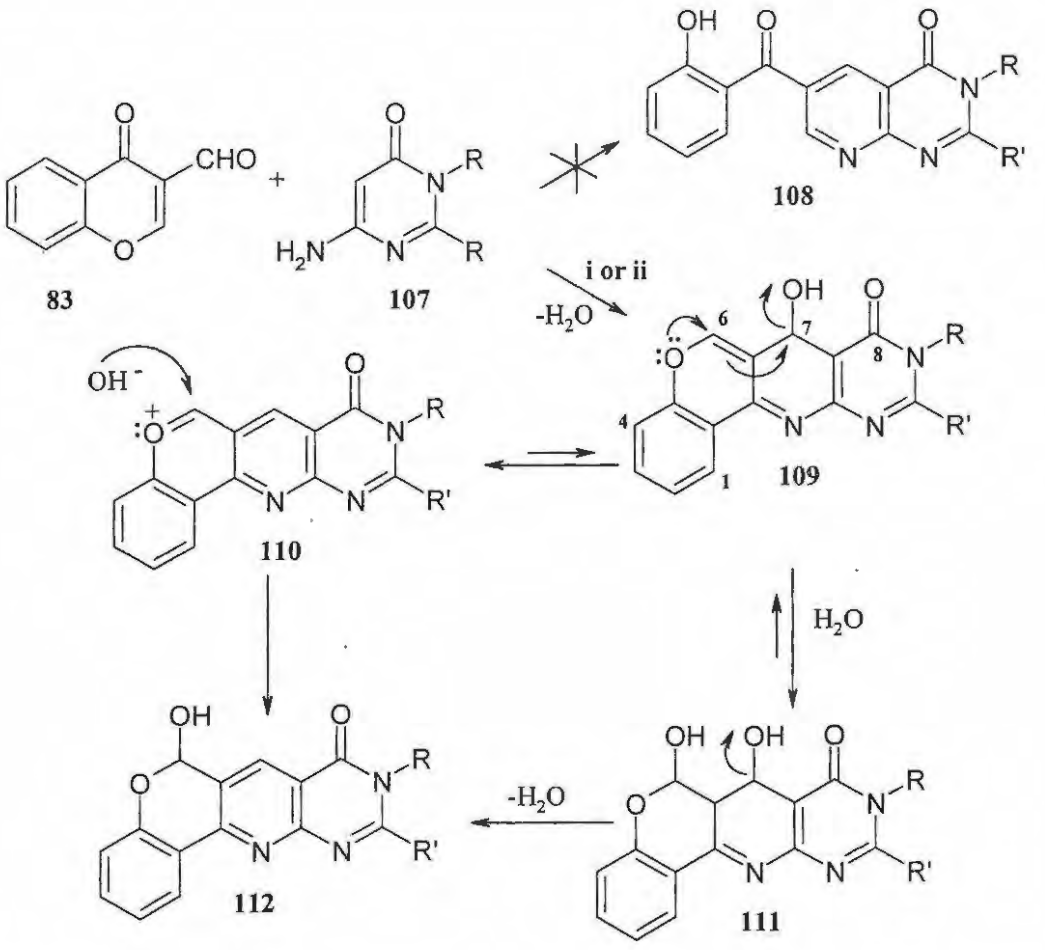

Scheme 22
Reagents: (i) Microwave irradiation, 2-3 min, solvent free conditions; (ii) EtOH, reflux, 2-3h. (R = H, CH_3; R' = CH_3O, CH_3S, NH_2, OH, SH)

Reaction of chromone-3-carbaldehyde **83** with the 1,3-bis-(silyl enol ether) derivative **113**, in the presence of TMSOTf, has been reported to afford the benzoyl substituted benzophenone **118** as shown in **Scheme 23.** The formation of **115** can be explained by the TMSOTf-catalysed domino 'Michael-*retro*-Michael-aldol' reaction, outlined in **Scheme 23**.[138]

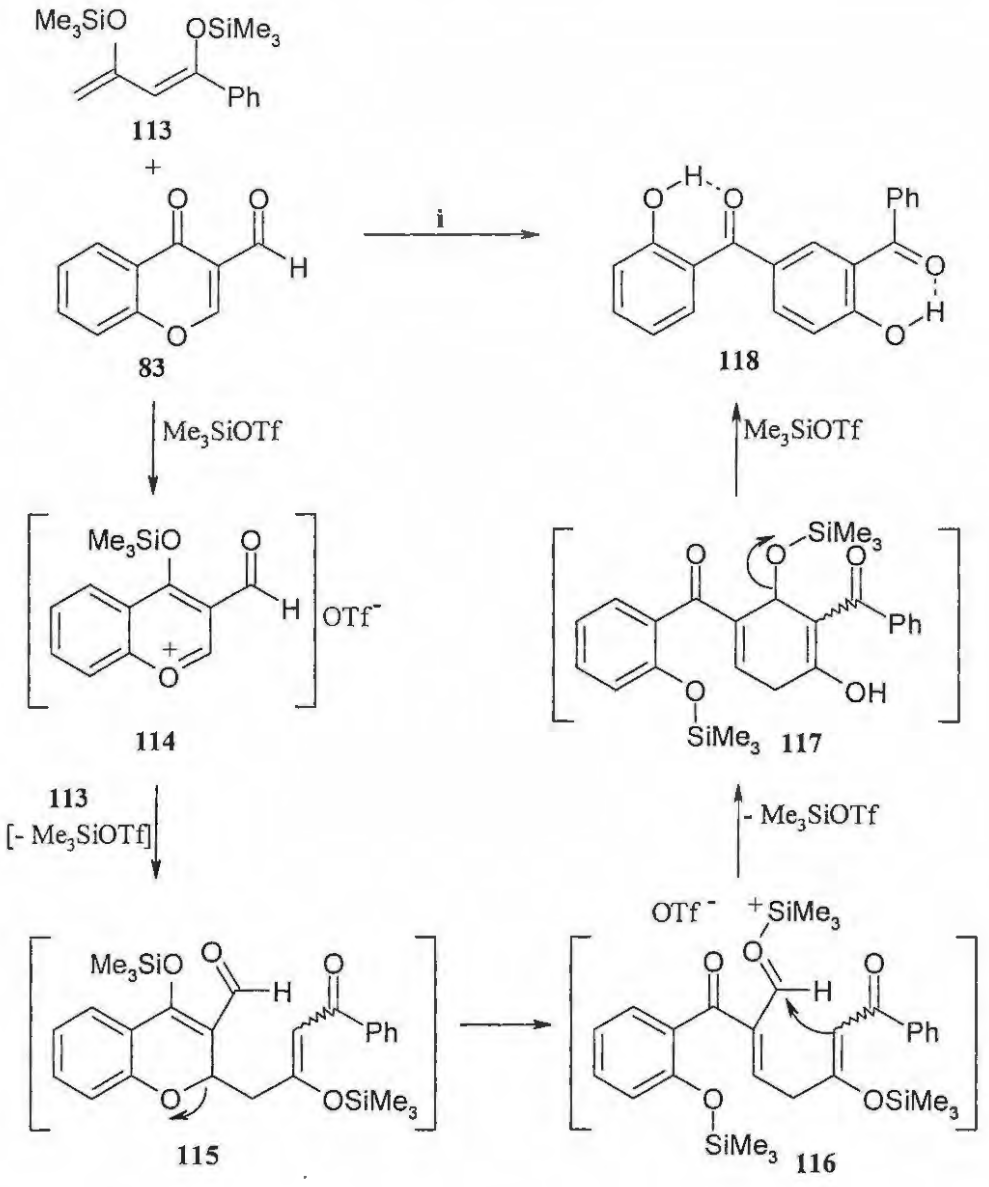

Scheme 23
Reagents: (i) Me_3SiOTf, CH_2Cl_2, 0-20°C.

Chromones typically undergo ring-opening when treated with aqueous alkali. The nucleophilic hydroxide ion attacks C-2 in a rate-determining step, the rate constant of which varies with the ground state electron density at that centre.[133] Thus, chromone **12** in aqueous alkali undergoes the nucleophilic addition of hydroxide ion at C-2 resulting in the formation of the enolate **119,** which can undergo fission of the γ-prone ring to give

a mixture of enolate species **120a-c (Scheme 24)**.[139] The chromone-2-carboxylate derivative **121** similarly undergoes ring-opening when treated with aqueous sodium hydroxide under reflux, affording 2,4-dibromo-3,6-dihydroxyacetophenone derivative **122** as depicted in **Scheme 25**.[140]

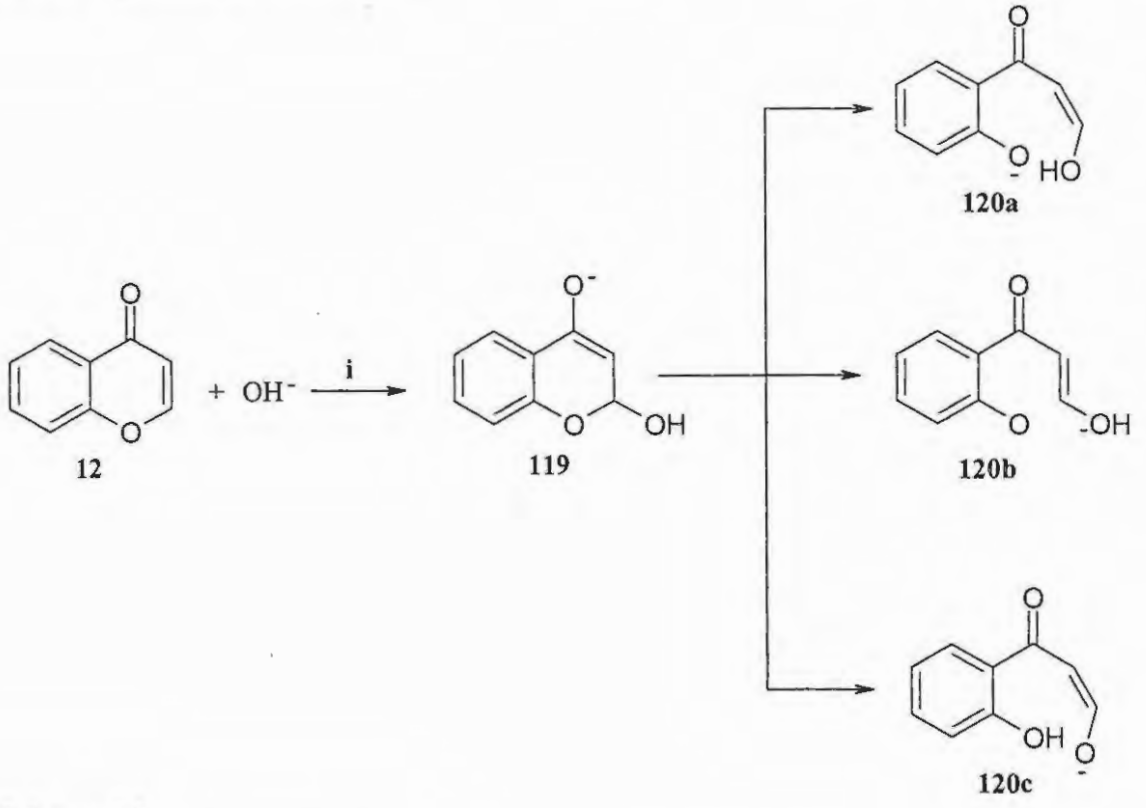

Scheme 24
Reagents: (i) alkaline medium.

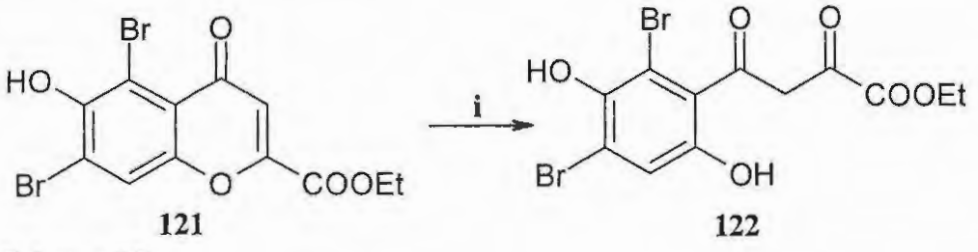

Scheme 25
Reagents: (i) aqueous NaOH.

However, if a substituent attached to the chromone is more electrophilic than C-2 or C-4, then the nucleophile will attack at that position. Acrylic acid derivates **123**, for example, have been synthesized, in high yield, by reacting chromone-3-carbaldehydes **122** with

malonic acid (**Scheme 26**).[141] Reaction of 3-nitrochromone **124** with diazomethane, a carbon nucleophile, under mild conditions affords cyclopropabenzopyrans **125** (**Scheme 27**), reflecting ring-forming rather than ring-opening.[142]

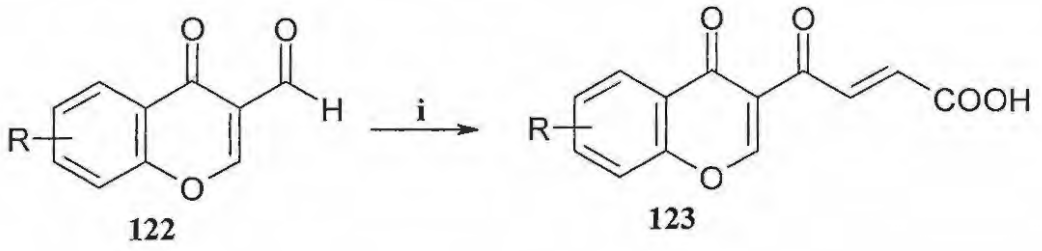

122 **123**

Scheme 26
Reagents: (i) $CH_2(CO_2H)_2$, pyridine

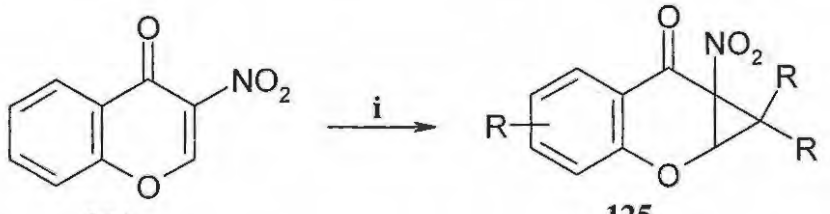

124 **125**

Scheme 27
Reagents: (i) R_2CN_2

Reaction of chromone-3-carbaldehyde **83** with a binucleophile (Nu_1-Nu_2) may result in the formation of a new heterocyclic ring. The first nucleophile attacks the formyl carbon (C-1'), to give an intermediate **126**, which then undergoes intramolecular attack by the second nucleophile (*e.g.* NH_2) at the reactive C-2 position, leading to ring-closure and concomitant ring-opening of the pyrone system. This method has been used to prepare products such as 4-(2-hydroxybenzoyl)pyrazole **127a** (**Scheme 28**).[143]

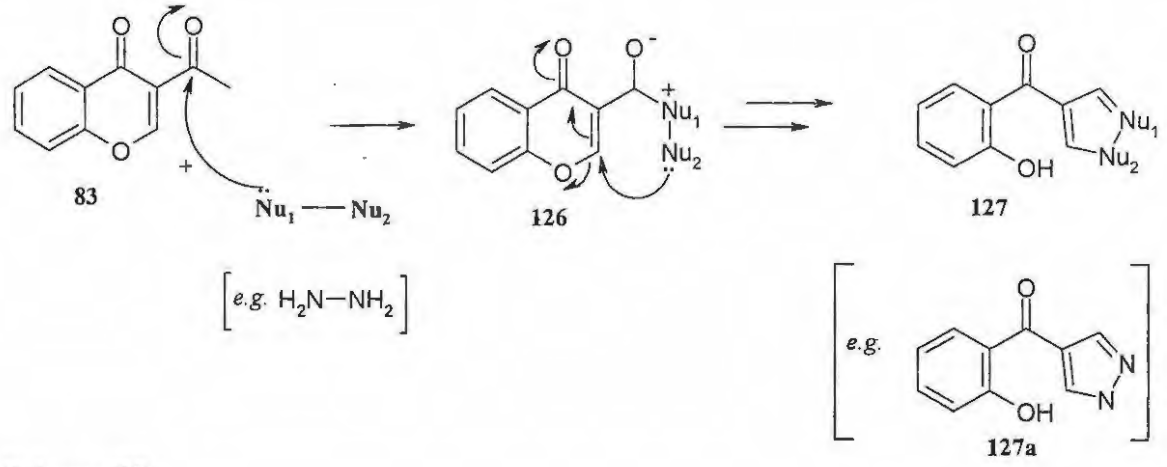

Scheme 28

Reaction of 3-substituted chromones **83** with the allene-derived 1,3-dipolar species **128** gave 3a,9a-dihydro-1-ethoxycarbonyl-1-cyclopenteno[5,4-*b*]benzopyran-4-one **129** (**Scheme 29**).[144] During the reaction, the dipolar species **128** adds regioselectively to the C2-C3 π-bond and deformylation results in the formation of the product **129** in good yield.[144]

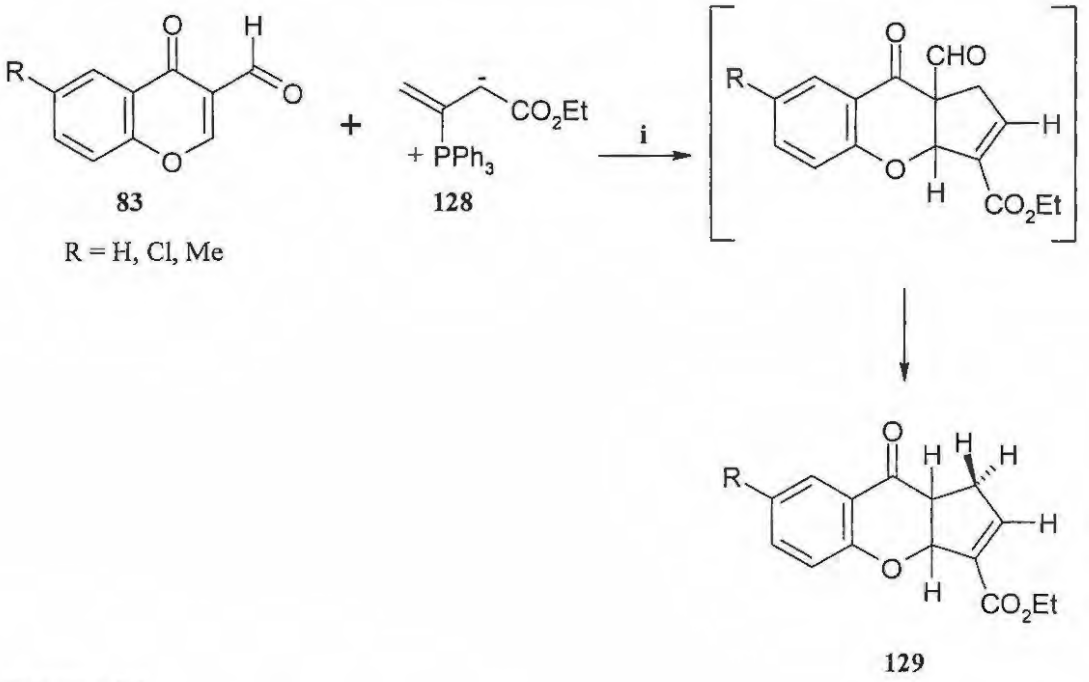

Scheme 29
Reagents: (i) Dry benzene, reflux

The direct nucleophilic introduction of perfluoroalkyl and especially, trifluoromethyl moieties is very important for synthesizing compounds with applications in the pharmaceutical industry. Treatment of the chromone derivative **12** with (trifluoromethyl)trimethylsilane and a three-fold excess of the nucleophilic initiator, Me_4NF, afforded a mixture of the 1,4-addition product **130** and the 1,2-addition product **131 (Scheme 30)**. [145]

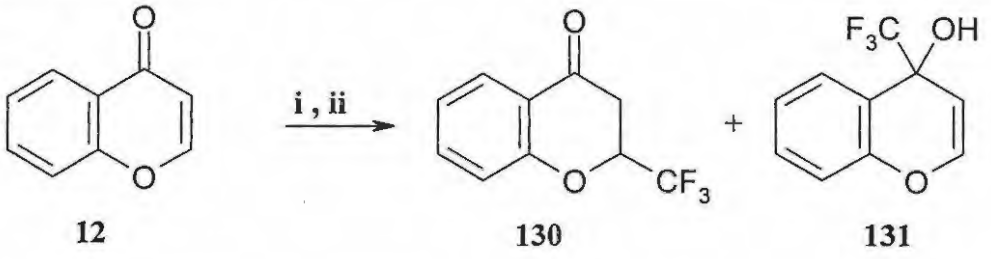

12 **130** **131**

Scheme 30
Reagents: (i) CF_3SiMe/Nu; (ii) H^+

Reaction of 3-(dimethoxyphosphoryl)-2-methylchromone **132a** or 3-(methoxycarbonyl)-2-methylchromone **132b** with *N*-methylhydrazine resulted in the formation of isomeric, highly substituted pyrazole derivatives **133** and **134**, the former as the major product in each case. Intramolecular transesterification of **133a,b** and **134a,b** under basic conditions afforded the corresponding tricyclic derivatives **135** and **136,** respectively, as shown in **Scheme 31**.[146]

Chromone-3-carbaldehyde **83** possess a highly polarized C2-C3 π-bond and annulation across this bond can be anticipated, and reaction of 3-(*N*-aryliminomethyl)chromones **137**, which resemble chromone-3-carbaldehyde **83**, with the 1,3-dipolar allenic ester **128** gave the cyclopentanochromones **144**.[144] During the reaction, the dipolar species **128** adds regioselectively to the C2-C3 π-bond resulting in the intermediates **140**. Subsequent thermal opening of the chromone ring affords the phenoxide species **141**, internal rotation, recyclization and a 1,5-hydride shift then leads to the tricyclic products **144 (Scheme 32).** Reaction of 3-methylchromone **145** with vinyl magnesium bromide resulted in the direct formation of the open-chain product **146 (Scheme 33)**.[147]

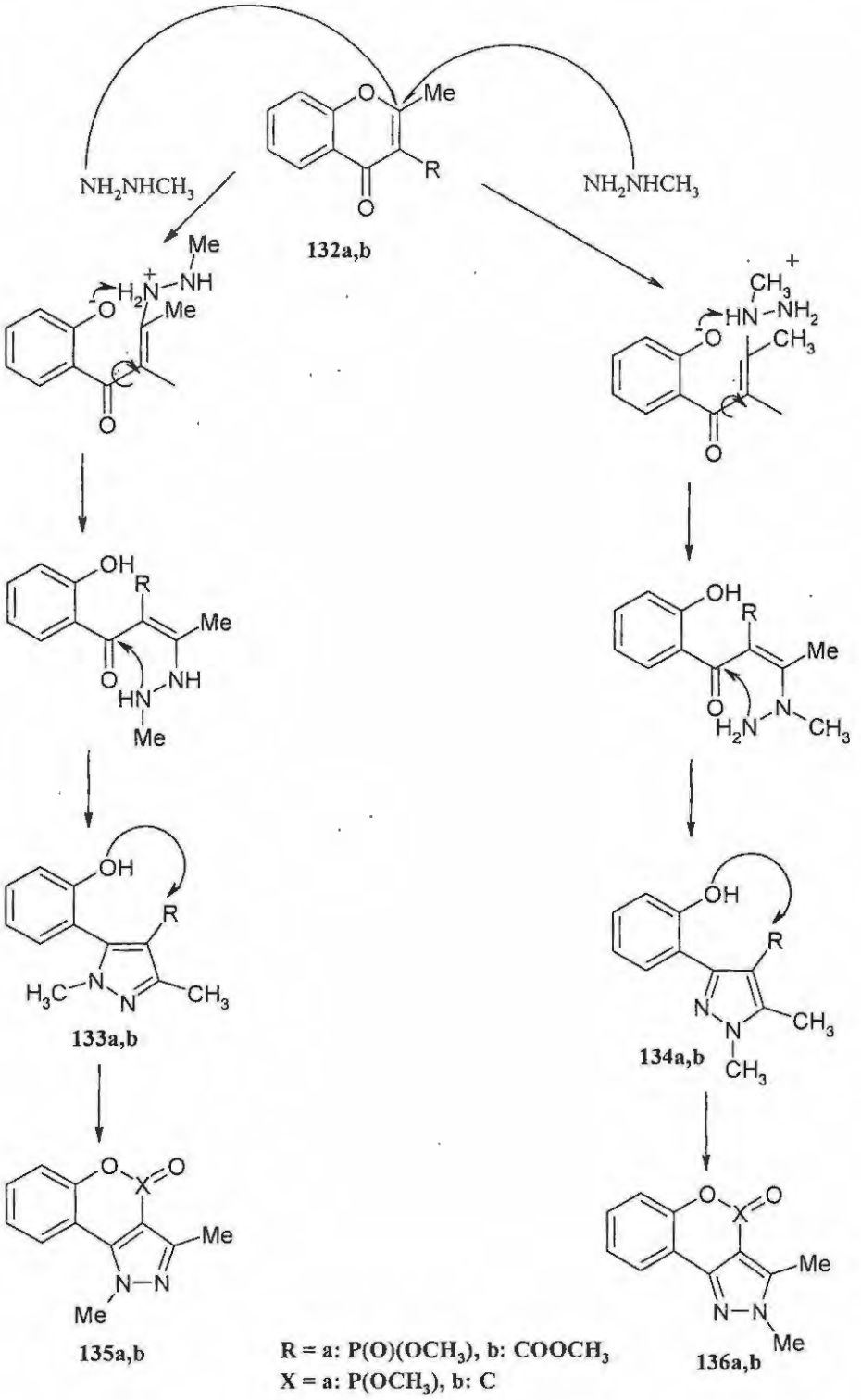
NH2NHCH3
Me
R
O
132a,b
NH2NHCH3
OH
133a,b
134a,b
135a,b
136a,b
R = a: P(O)(OCH3), b: COOCH3
X = a: P(OCH3), b: C

Scheme 31

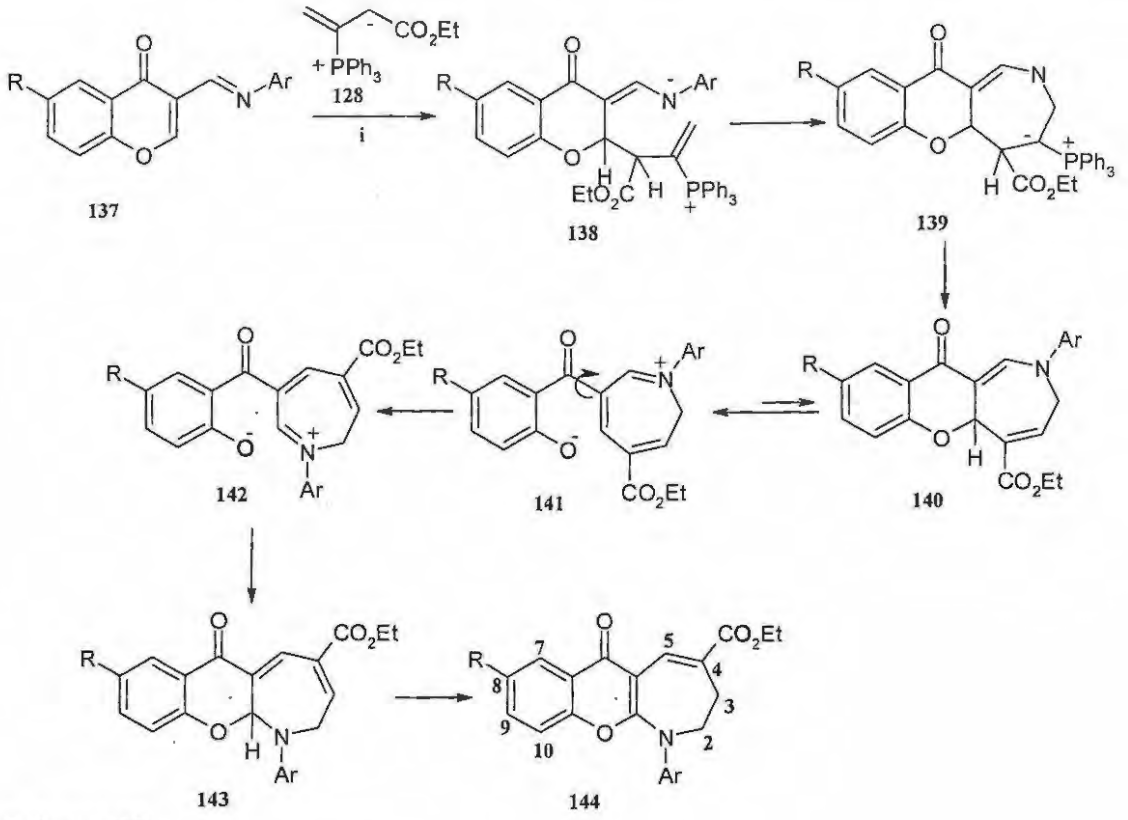

Scheme 32
Reagents: (i) Benzene, reflux.

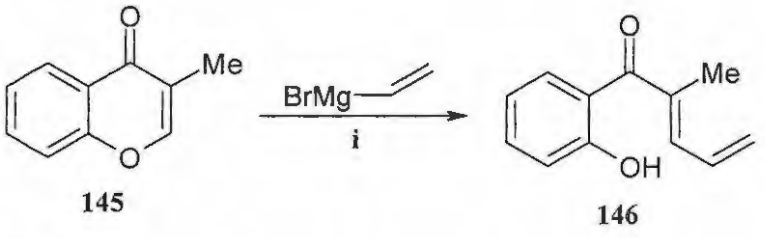

Scheme 33

1.3.4.2 Reactions with Electrophiles

Chromones are slightly basic and form salts with strong acids, with protonation normally occurring at O-1, C-3 or the carbonyl oxygen.[134] Although the pyran ring in chromone derivatives is relatively unreactive towards electrophiles, an electron-releasing substituent at C-2 or C-3 activates the adjacent vacant position.[148] Vilsmeier formylation

of 2-(dimethylamino)-8-isopropyl-5-methylchromone **147**, for example, furnishes the 2-formylchromone derivative **148 (Scheme 34)**.[144]

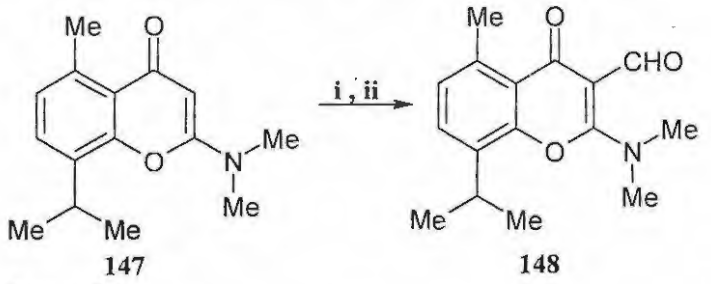

Scheme 34
Reagents: (i) $POCl_3$, DMF; (ii) H_2O.

The elements of hypobromous acid are added across the 2,3-double bond when chromone **12** is treated with NBS in aqueous DMSO to form 3-bromo-2-hydroxychromanone **149 (Scheme 35)**.[142]

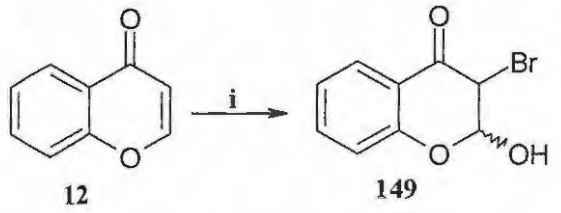

Scheme 35
Reagents: (i) NBS, aq. DMSO.

When the electrophilic reagents are either strong acids or produce strong acids during the reaction, protonation of the pyran ring may be expected to inhibit further attack by the electrophile.[142] However, aminomethylation under Mannich reaction conditions is often achieved under less acidic conditions, resulting, for example, in the formation of 3-aminodimethylchromone **151** from 8-methoxychromone **150 (Scheme 36)**.[142]

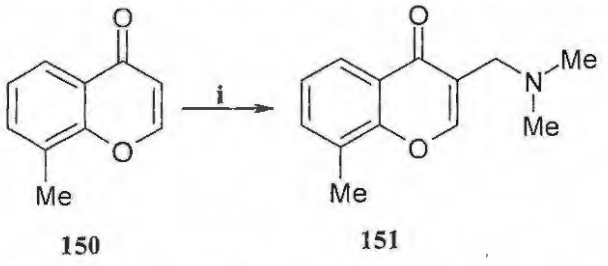

Scheme 36
Reagents: (i) HCHO, $NHMe_2$, AcOH.

1.3.4.3 Other reactions

While the enone moiety of the parent chromone system does not function as dienophile in cycloaddition reactions, an electron-withdrawing substituent at C-3 enhances the dienophilicity of the 2,3-double bond, permitting such reaction to occur. Cycloaddition of chromone-3-carbaldehyde **83**, reacting as the dienophile, and *ortho*-benzoquinodimethane **152**, a highly reactive diene, resulted in the expected adduct **153** which is susceptible to deformylation under the reaction conditions to afford a mixture of the diastereomeric cycloadducts **154** and **155**. Oxidation of these diastereomeric cycloadducts with dimethyl sulfoxide in the presence of iodine afforded the novel benzo[*b*]xanthones **156 (Scheme 37)**.[149]

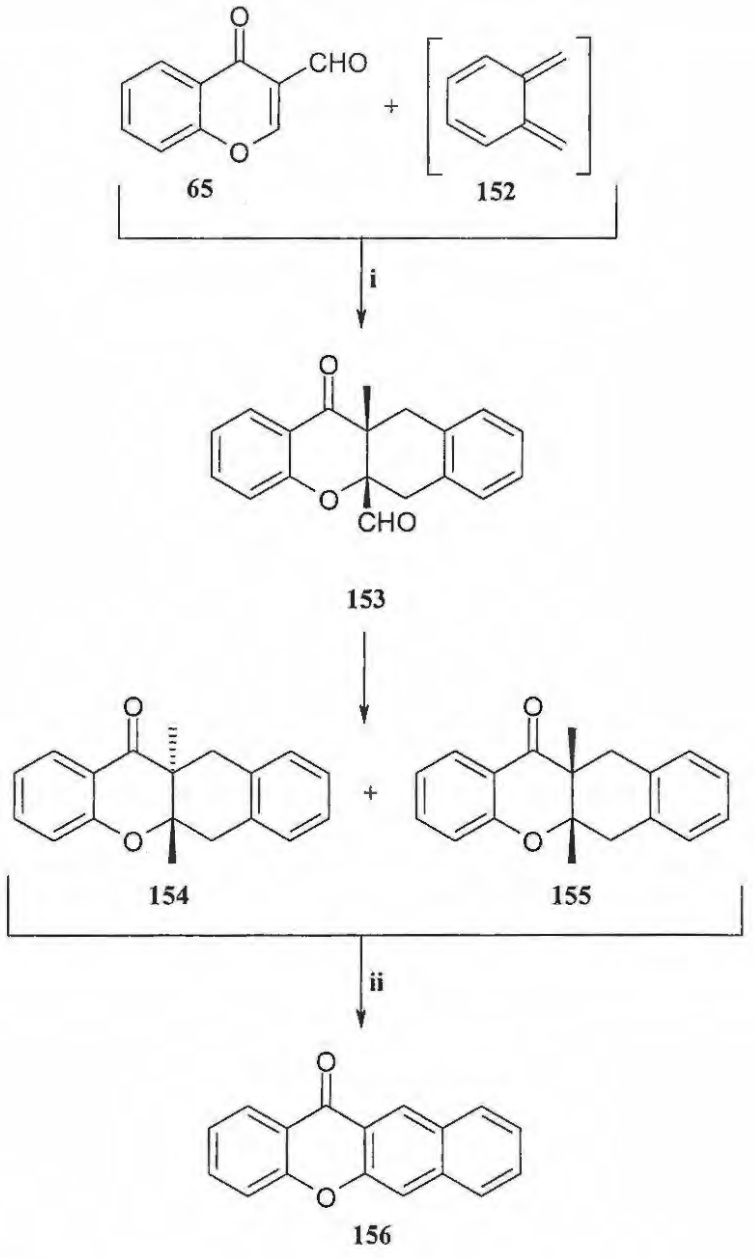

Scheme 37
Reagents: (i) 1,2,4-Trichlorobenzene, 250°C; (ii) Me_2SO, I_2.

Reaction of chromone-3-carbonitrile **157** with *o*-phenylenediamine **158** (an aromatic 1,2-diamine) under reflux, resulted in the amidine derivative **159**, which also exists as the tautomeric form **160**. Further heating in glacial acetic acid afforded a fused diazepine derivative **162 (Scheme 38)**.[150] During this reaction the aromatic 1,2-diamine

nucleophile **158** adds 1,2 to the nitrile function of compound **157** to afford the amidine **159**, which undergoes cyclisation and air oxidation to furnish compound **162**.

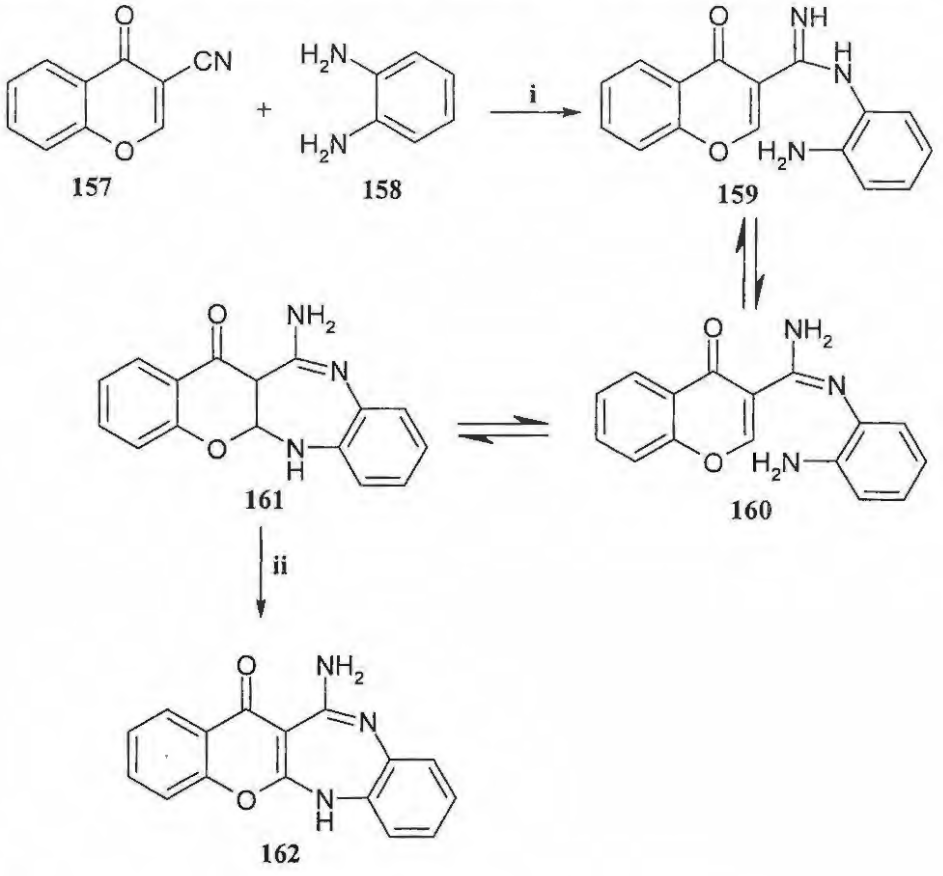

Scheme 38
Reagents: (i) Ethanol, reflux; (ii) glacial acetic acid, reflux, air.

However, when chromone-3-carbonitrile **157** was heated under reflux with ethylenediamine **163** (an aliphatic 1,2-diamine) in ethanol, 2-amino-3-formylchromone **169** was obtained together with a minor product **170** (**Scheme 39**).[150] The mechanism for the formation of the products **169** and **170** involves 1,4-addition by the nucleophile which results in the intermediate adducts **164-166**. The intermediate **165** cyclizes to the aldimino derivative **167**, which undergoes hydrolysis to afford the aminochromone **169**. This hydrolysis occurs partially in ethanolic medium and is completed during crystallization from acetic acid. The intermediate **166**, on the other hand, loses a molecule of hydrogen cyanide, and the resultant intermediate **168** undergoes

intramolecular 1,4-addition with concomitant opening of the pyrone ring to form the tetrahydroimidazole **170**.

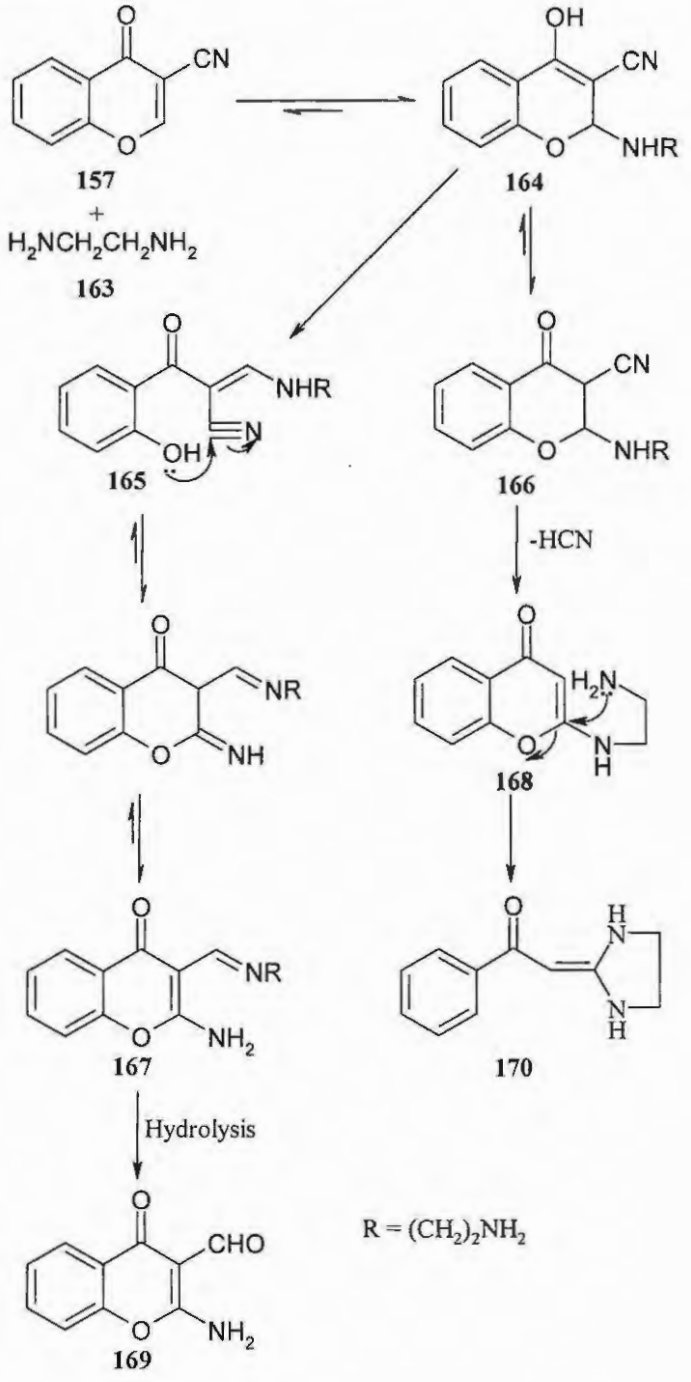

Scheme 39
Reagents: (i) Ethanol, reflux; (ii) glacial acetic acid, reflux, air.

The acetal **171** can be metalated with lithium 2,2,6,6-tetramethylpiperidine (LTMP) at the electrophilic centre C-2. The 2-lithiated derivative can then be trapped with acetaldehyde to give furan derivative **172**. The unmasking of the acetal moiety proceeds rapidly when a trace of TsOH in warm toluene is used, as illustrated in **Scheme 40**.[151]

2-Carboxamido chromones **176-179** have been synthesized from ethyl chromone-2-carboxylate **175**, by reacting the ester **175** with alkyl amines, as shown in **Scheme 41**. These chromone derivatives are used in hair-conditioning agents, as they bind to human hair and protect it from UV-radiation which damages hair fibre.[84]

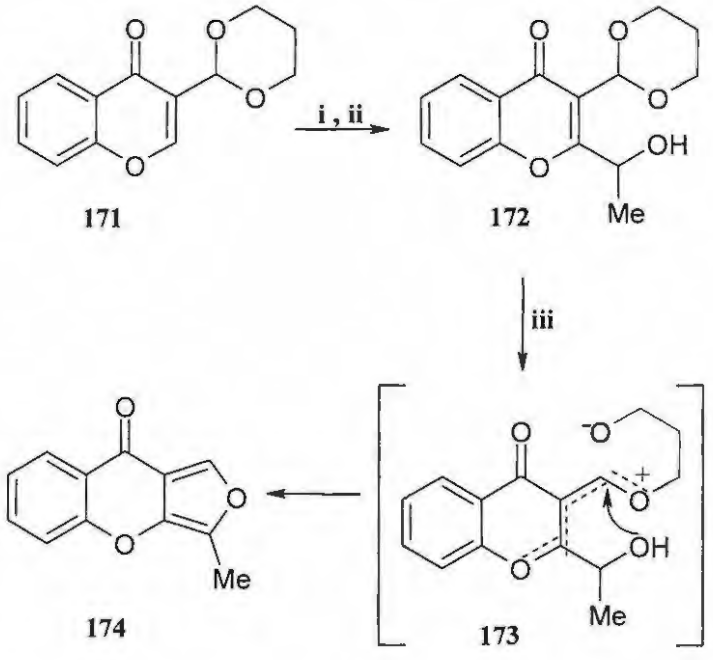

Scheme 40
Reagents: (i) LTMP, THF, -78°C; (ii) MeCHO; (iii) TsOH (cat.), PhMe, ca. 50°C.

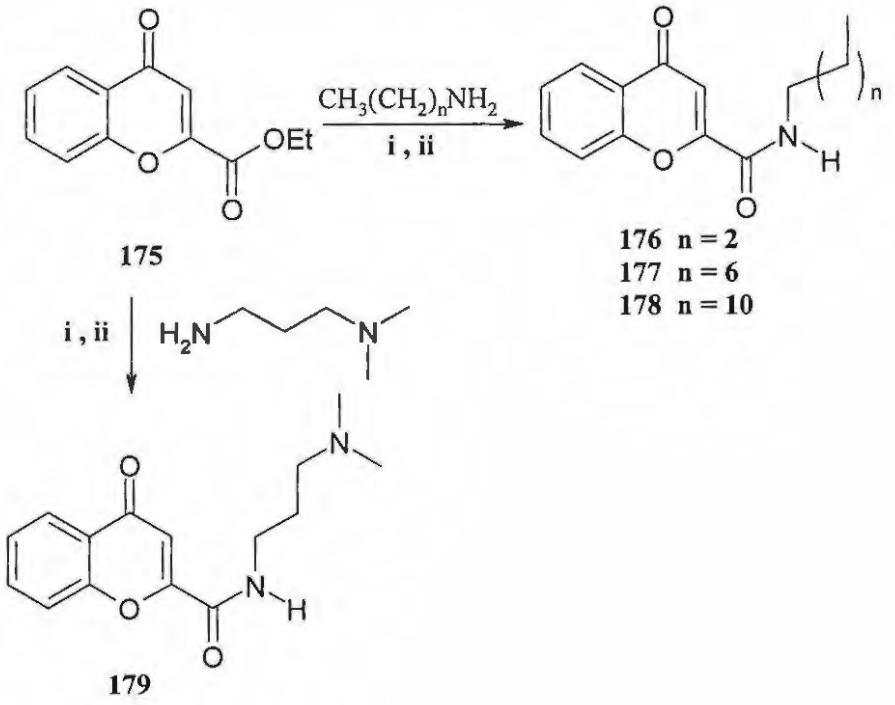

Scheme 41
Reagents: (i) Na, EtOH; (ii) HCl.

1.4 Previous work done in the group

Chromone chemistry has been the subject of investigation in our research group for many years, and this investigation has provided a context for the present study.

In previous years, infrared carbonyl band doubling exhibited by substituted chromone-2-carboxylate ester was observed to be solvent-, substituent- and temperature dependent and was explained in terms of rotameric equilibria between *syn-s-trans* and *anti-s-trans* forms.[152] A synthesis of *N,N*-dimethylchromone-2-carboxamides has been developed,[153] and dynamic NMR studies of such compounds revealed a temperature dependent splitting of the *N*-alkyl ^{1}H and ^{13}C NMR signals, which was attributed to internal rotation of the amide group.[154]

The amine-mediated ring-opening of substituted chromone-2-carboxamides has been explored to clarify the susceptibility of chromone derivatives to ring-opening *via* nucleophilic attack at C-2,[155] and kinetic mechanistic studies have illustrated the influence of substituents on the ring-opening process.[156] Mass spectrometric analysis of the ring-opened, polyfunctional acrylamide derivatives permitted elucidation of their major fragmentation patterns,[157] while dynamic NMR analysis of rotational isomerism in these systems permitted the calculation of internal rotational barriers.[158]

Dynamic ^{1}H NMR spectroscopic methods were also used to study the effect of substituents on the internal rotation of the amino group in 2-(*N*,*N*-dialkylamino)chromones;[159] delocalisation of the nitrogen lone pair was presumed to inhibit rotation about the N-C(O) bond - a property which influences the basicity of these compounds. The effect of various substituents on the electron density at C-2 and, hence, on the acidity of a series of chromone-2-carboxylic acids has also been investigated.[160] Chromone systems have also been used in the construction of ritanovir analogues as potential HIV-1 protease inhibitors.[161]

Research in our group has also focused on applications of the Morita-Baylis-Hillman reaction, in the synthesis of 2-substituted indolizines,[162] quinoline derivatives,[163] chromenes,[164] thiochromenes[165] and coumarins,[166] while chromone-3-carbaldehydes have been employed as Baylis-Hillman substrates, affording unprecedented dimeric products.[167]

1.5 Aims of the current investigation

The present investigation has been focused on the application of Baylis-Hillman methodology to chromone systems with a view to preparing compounds with HIV-1 protease inhibition potential. The inhibitors currently in clinical use (see p. 11) are relatively large and structurally complex molecules. The intention in our approach was

to prepare and elaborate truncated analogues which are not only structurally simpler but also synthetically more accessible. The research has included the following specific objectives:

1. The synthesis of substituted chromone-3-carbaldehydes and chromone-2-carbaldehydes and their use as substrates in Morita-Baylis-Hillman reactions using acrylonitrile, methyl acrylate and methyl vinyl ketone as activated alkenes.

2. Exploring the effect of varying the catalyst and solvent system on reaction efficiency and product selectivity.

3. Aza-Michael reactions of the Baylis-Hillman products using various amino derivatives with a view to generating readily accessible derivatives as potential HIV-1 protease inhibitors.

4. Enzyme kinetic studies of representative derivatives to investigate their inhibition capabilities.

5. Computer-modelling studies of representative derivatives using an interactive docking programme to explore their binding to the HIV-1 protease active site.

6. Kinetic mechanistic studies of the DABCO-catalysed Baylis-Hillman reaction of a series of substituted 2-nitrobenzaldehyde derivatives with MVK using NMR methods.

2. RESULTS AND DISCUSSION

In line with the identified aims, the discussion covers:- the preparation of chromone carbaldehydes (Section 2.1); their use as substrates in Baylis-Hillman reactions (Section 2.2); aza-Michael reactions of the Baylis-Hillman products (Section 2.3); HIV-1 protease enzyme inhibition assays (Section 2.4); computer modelling studies of the aza-Michael products and the chromone dimers (Section 2.5); and finally kinetic-mechanistic study of the Baylis-Hillman reaction involving selected 2-nitrobenzaldehydes with MVK (Section 2.6).

Ritanovir **2**, a drug in clinical use, was used as a template in the design of potential HIV-1 protease inhibitors, with the intension of developing chromone derivatives as scaffolds for the construction of HIV-1 protease inhibitors. It was hoped that chromone dimers of type **222** could be elaborated to afford products which, like ritonavir **2**, contain termini linked by a peptidomimetic chain. (In the event, time did not permit such elaborations of the dimeric products). Monochromone derivatives, on the other hand, would be elaborated to afford truncated analogues of ritonavir **2** such as compound **260** (See below) .

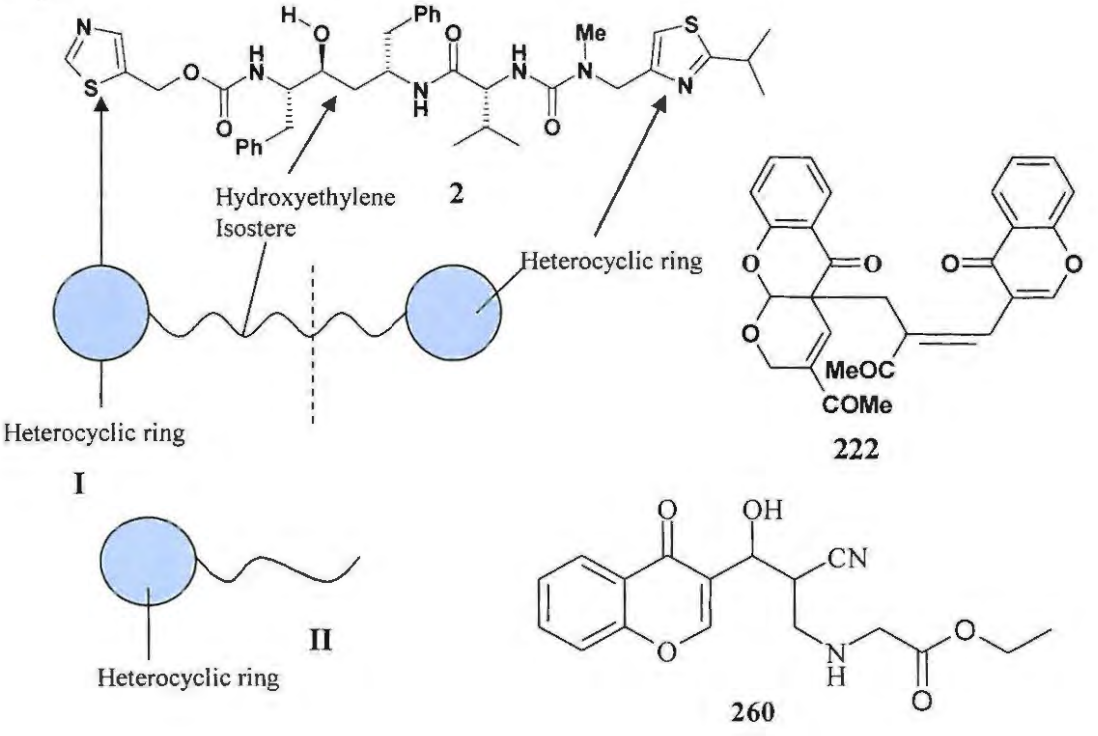

2.1 Preparation of chromone carbaldehydes

2.1.1 Synthesis of chromone-3-carbaldehydes using the Vilsmeier-Haack reaction

A series of substituted chromone-3-carbaldehydes **83** and **184-187** were prepared as Baylis-Hillman precursors using the Vilsmeier-Haack reaction in which the corresponding *o*-hydroxyacetophenones **84** and **180-183** were treated with phosphorus oxychloride ($POCl_3$) in dry DMF at -20°C **(Scheme 42)**.[127] The mechanism of the Vilsmeier-Haack reaction involves double formylation of the acetophenone enolate **189** by the Vilsmeier-Haack "complex" **188a-c** with structures **b** and **c** being the predominant tautomers **(Scheme 43)**.[168] Subsequent hydrolysis gave the desired chromone-3-carbaldehydes **83** and **184-187 (Scheme 44)**. The approach thus provides a one-pot conversion of *o*-hydroxyacetophenones to chromone-3-carbaldehydes.

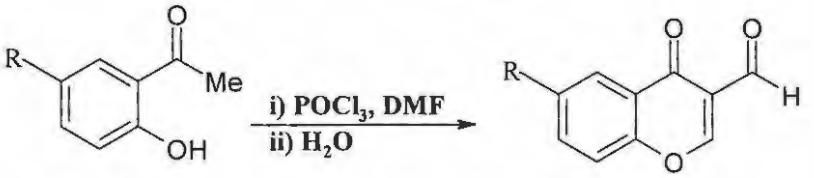

	R
84	H
180	Cl
181	Br
182	F
183	OMe

	R
83	H
184	Cl
185	Br
186	F
187	OMe

Scheme 42

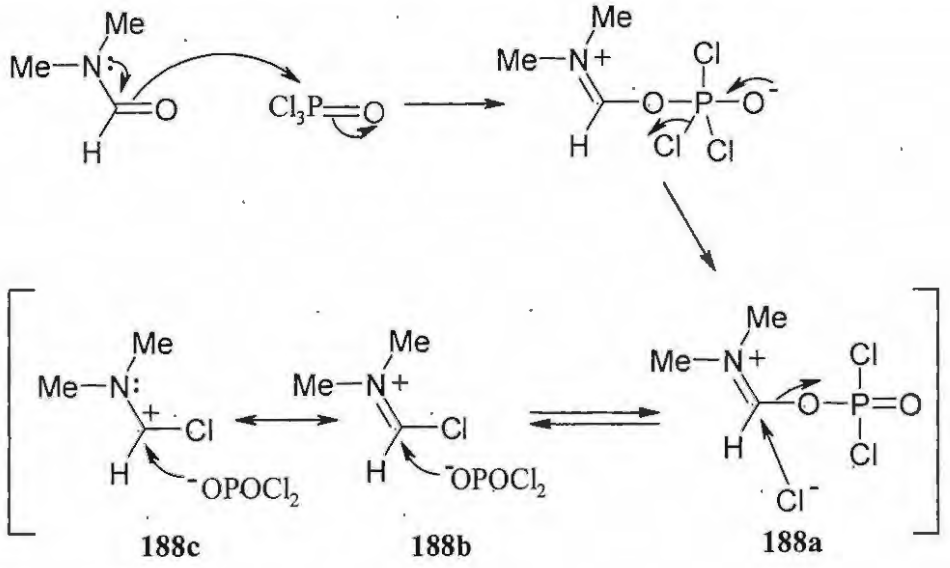

Scheme 43

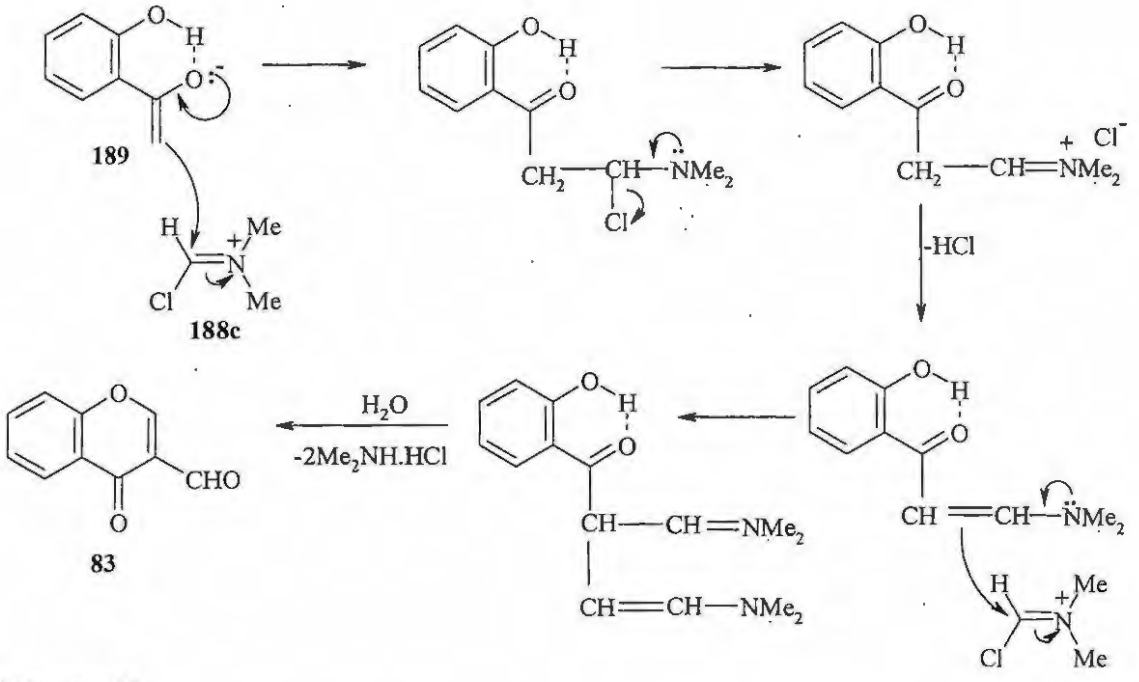

Scheme 44

Recrystallisation of the crude chromone-3-carbaldehydes from acetone afforded the pure products **83** and **184-187** in yields of 43-85% (Table 3). The products were fully characterized by spectroscopic (IR, ^{1}H and ^{13}C NMR) and elemental (HREIMS) analysis.

Table 3. Comparative yields for chromone-3-carbaldehydes **83** and **184-187**.

R	Compound No.	Yield (%)
H	**83**	71
Cl	**184**	81
Br	**185**	83
F	**186**	85
OMe	**187**	43

The ^{1}H NMR spectrum (Figure 9) of the parent system **83** reveals an overlapping triplet and doublet at *ca.* 7.50 ppm corresponding to the 6-methine and 8-methine protons, respectively, a singlet at 8.54 ppm corresponding to the 2-methine proton, and a singlet corresponding to the formyl proton at 10.38 ppm. The ^{13}C NMR spectrum (Figure 10) shows the expected 10 carbon signals, with the 2-methine carbon resonating at 160.6 ppm and the carbonyl carbon signals at 176.0 and 188.6 ppm.

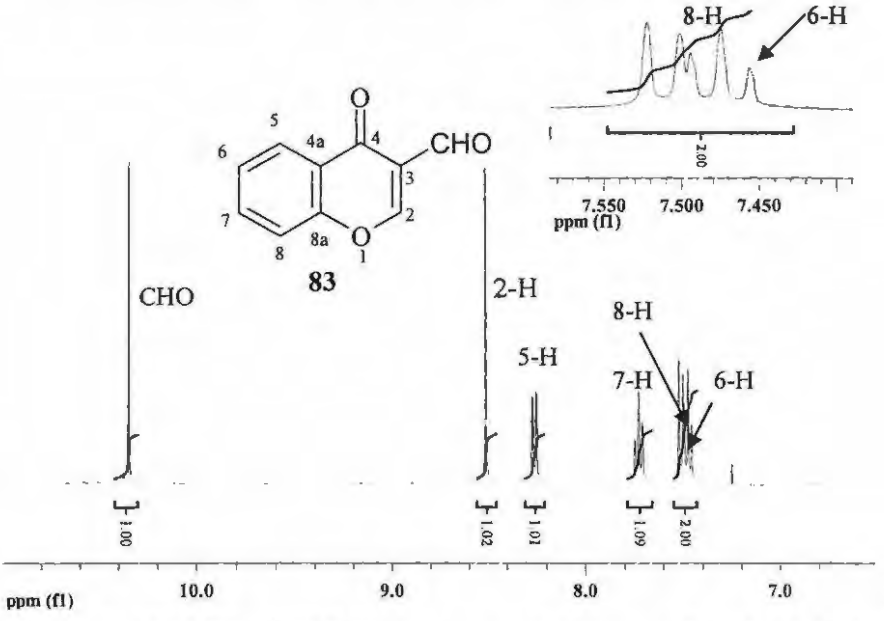

Figure 9. 400 MHz ^{1}H NMR spectrum of chromone-3-carbaldehyde **83** in $CDCl_3$.

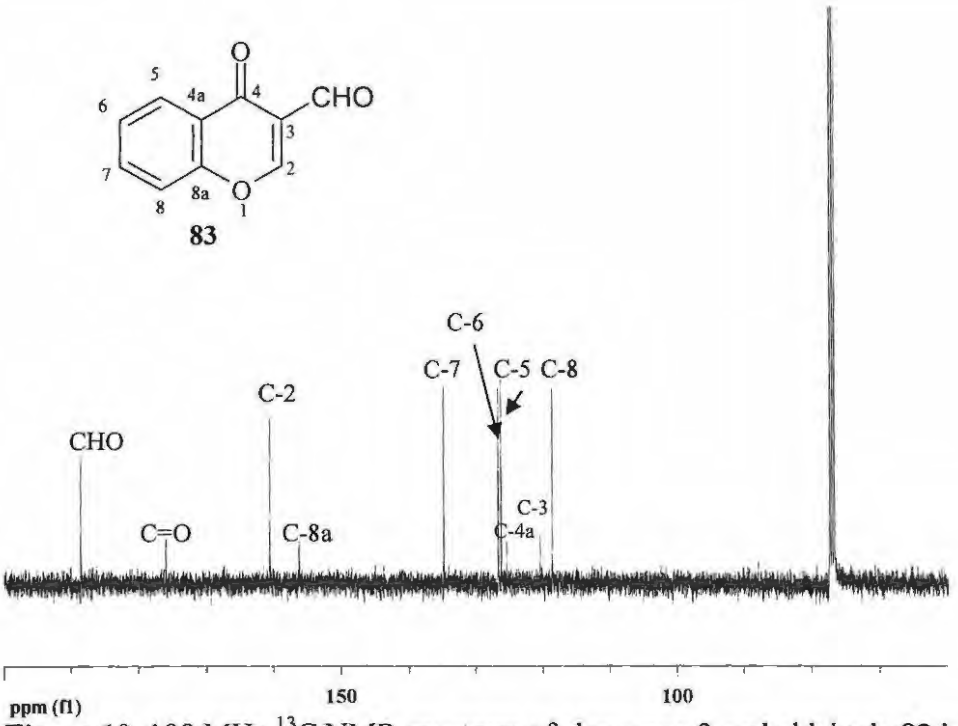

Figure 10. 100 MHz ^{13}C NMR spectrum of chromone-3-carbaldehyde **83** in $CDCl_3$.

2.1.2. Synthesis of chromone-2-carbaldehydes

Due to the reactivity of the 2-formyl group, chromone-2-carbaldehydes are well known intermediates in the synthesis of a variety of interesting products.[130-131] A series of chromone-2-carbaldehydes were prepared in order to explore their behaviour under Morita-Baylis-Hillman conditions and their elaboration to potential HIV-1 inhibitors.

The chromone-2-carbaldehydes **91** and **201-204** were synthesized *via* selenium dioxide (SeO_2) oxidation of the appropriate 2-methylchromones **90** and **197-200**, which were obtained using the Kostanecki-Robinson method.[86,129-131] This approach involves the condensation of suitable *o*-hydroxyacetophenone **84, 188-191** with ethyl acetate to form the corresponding β-diketo derivatives **192-196**. On acidification these intermediates cyclised spontaneously to the 2-methylchromones **90** and **197-200 (Scheme 45)**. The mechanism **(Scheme 46)** for SeO_2 oxidation of the 2-methylchromones is considered to involve deprotonation of the methyl group to form a resonance stabilized enolate (step

a), which undergoes selenation at C-3 (step b). A [2,3]-sigmatropic rearrangement (step c) followed by deselenation affords the chromone-2-carbaldehydes **91** and **201-204**.[169-176] The selenium oxidation reaction has been reported to proceed in poor yield (*ca.* 40%), but in this case, the yields ranged from 45-65% (Table 4). Optimization was achieved by washing the selenium residue thoroughly with hot xylene after observing that some of the expected products remained in the selenium residues. It was also noticed that extending the reaction time from 12hrs to 20 hours enhanced the product yields as shown in Table 4. Further optimization was attempted by using 1-chloronaphthalene or dioxane instead of xylene. However, use of 1-chloronaphthalene and dioxane gave compound **91** in yields of 36% and 7.5%, respectively, much lower than the 65% obtained using xylene. These results confirmed that xylene was the best of the solvents used in these reactions.

Recrystallisation of the crude 2-methylchromones **90** and **197-200** from hexane afforded the pure products in yields ranging from 43 to 86% (Table 4). These products were fully characterized by spectroscopic (IR, ^{1}H and ^{13}C NMR) and elemental (HREIMS) analysis. The ^{1}H NMR spectrum (Figure 11) of compound **198** reveals a singlet at 2.38 ppm corresponding to the 2-methyl protons, while the 3-methine proton resonates as singlet at 6.17 ppm. The ^{13}C NMR spectrum (Figure 12) shows the expected 10 carbon signals, with the 2-methyl carbon resonating at 20.6 ppm and the carbonyl carbon signal at 178.0 ppm.

Purification of crude chromone-2-carbaldehydes **91** and **201-204** using flash chromatography on silica gel afforded yields ranging from 46 to 65% and 50 to 70%, depending on the reaction period (Table 4). The ^{1}H NMR spectrum (Figure 13) of compound **202** reveals a singlet at 6.91 ppm corresponding to 3-methine proton, while the singlet corresponding to the aldehyde proton resonates at 9.78 ppm. The ^{13}C NMR spectrum (Figure 14) shows the expected 10 carbon signals, with the aldehydic carbonyl carbon (CHO) resonating at 185.0 ppm.

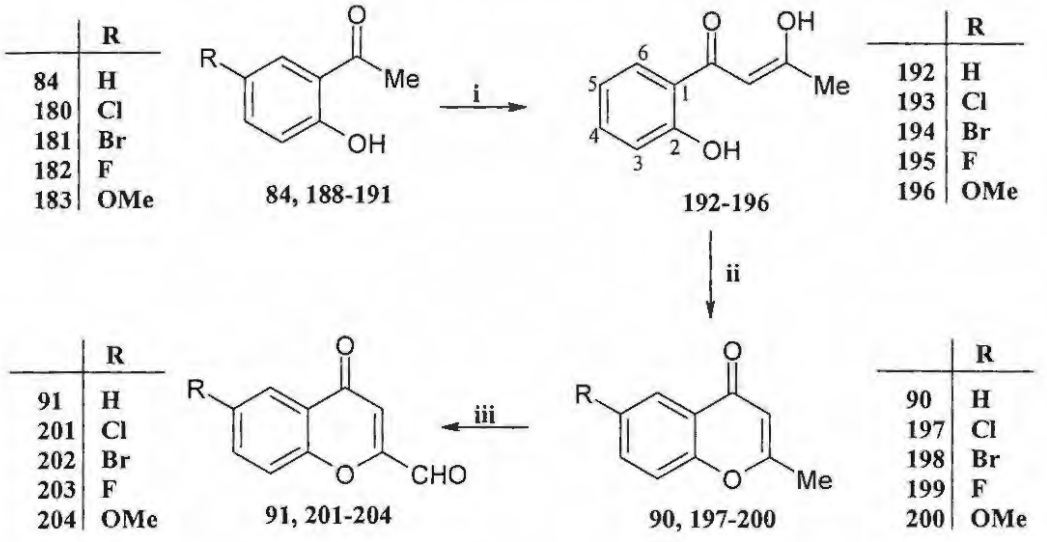

Scheme 45

Reagents: (i) NaOEt, dry EtOH, dry CH_3CO_2Et; (ii) AcOH, conc.H_2SO_4;
(iii) SeO_2, xylene/ naphthalene/ dioxane, reflux.

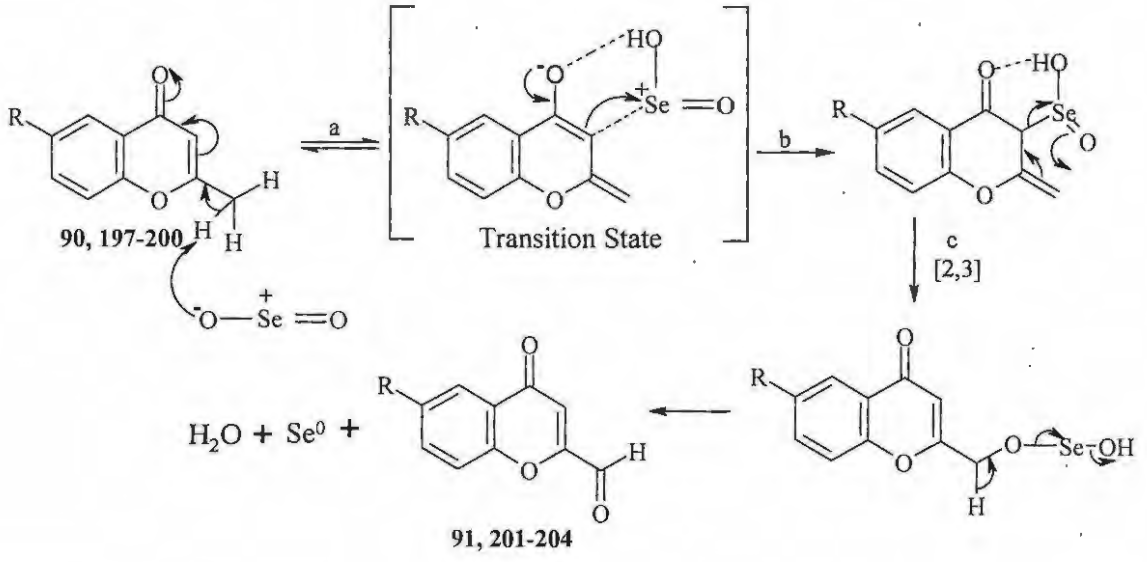

Scheme 46

Table 4. Isolated yields (%) of the 2-methylchromones **90** and **197-200** and the chromone-2-carbaldehyde **91** and **201-204**.

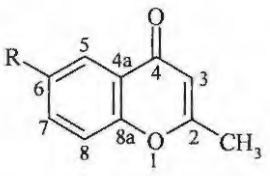

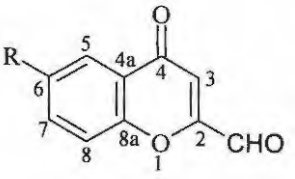

R	Compound	Yields	Compound	After 12 hours	After 20 hours
H	**90**	65	**91**	65	70
Cl	**197**	86	**201**	46	50
Br	**198**	69	**202**	47	51
F	**199**	45	**203**	52	54
MeO	**200**	43	**204**	64	68

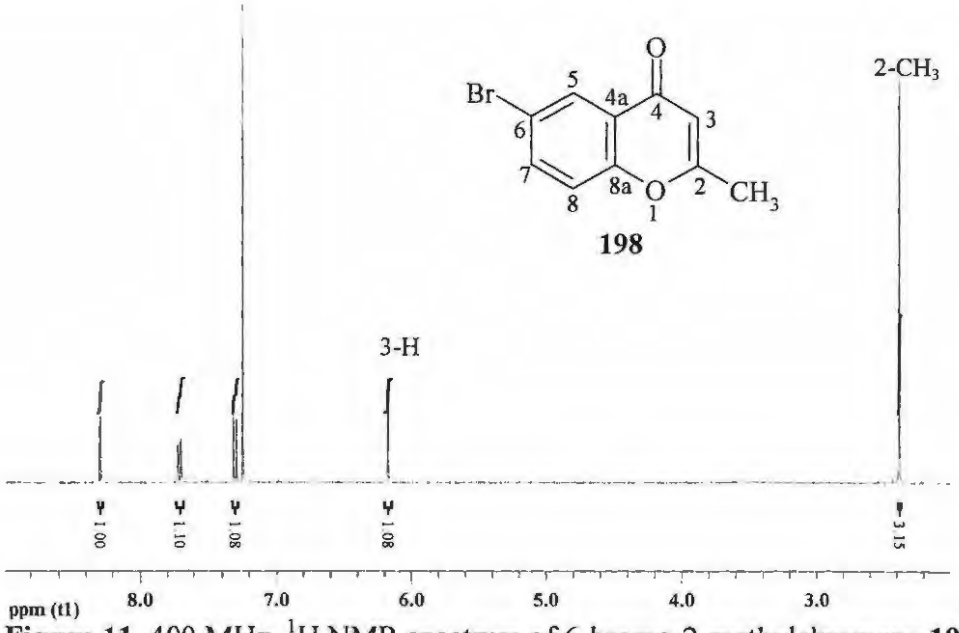

Figure 11. 400 MHz ^{1}H NMR spectrum of 6-bromo-2-methylchromone **198** in $CDCl_3$.

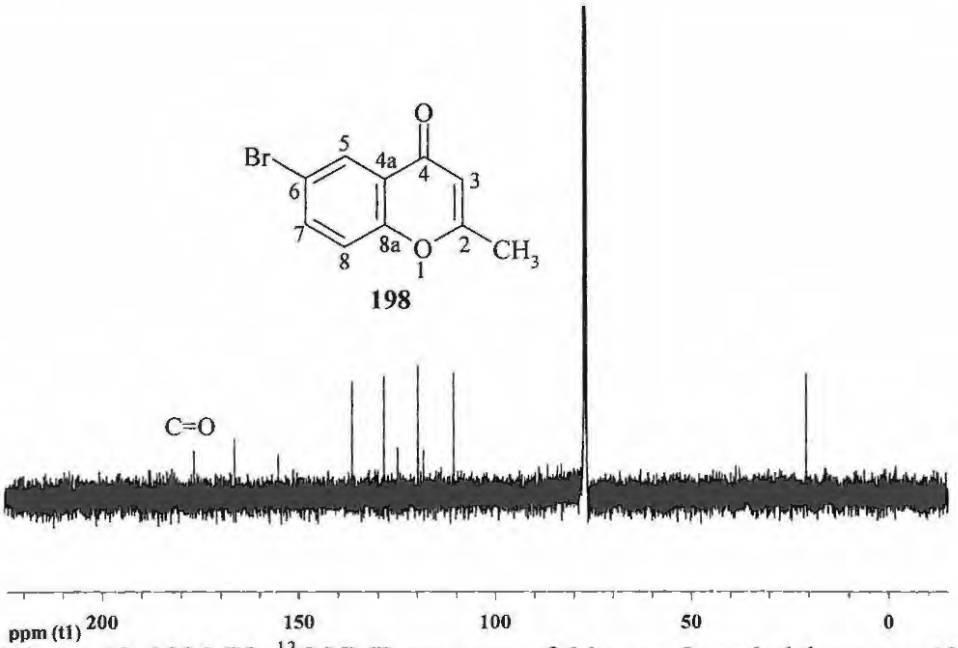

Figure 12. 100 MHz ^{13}C NMR spectrum of 6-bromo-2-methylchromone **198** in $CDCl_3$.

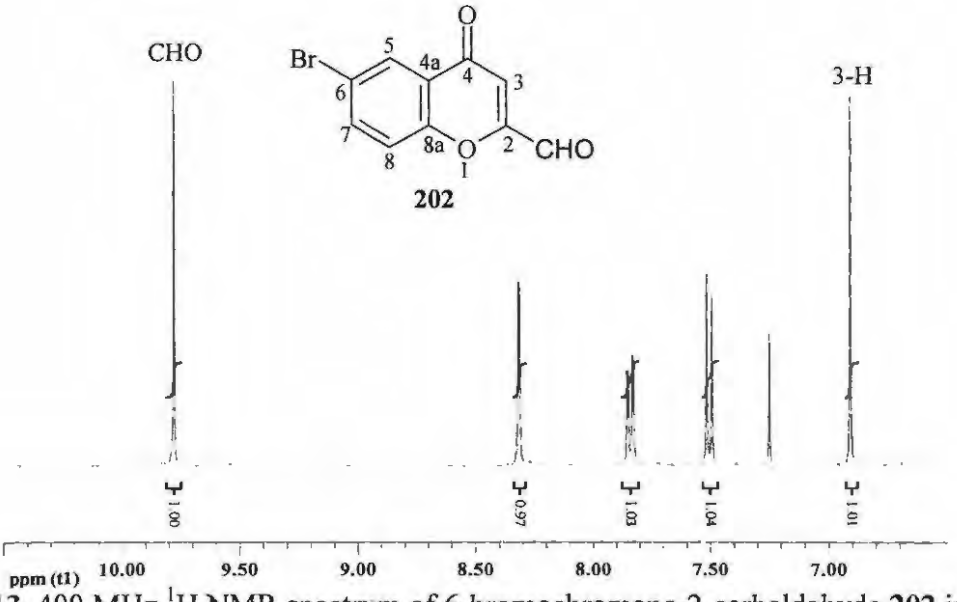

Figure 13. 400 MHz ^{1}H NMR spectrum of 6-bromochromone-2-carbaldehyde **202** in $CDCl_3$.

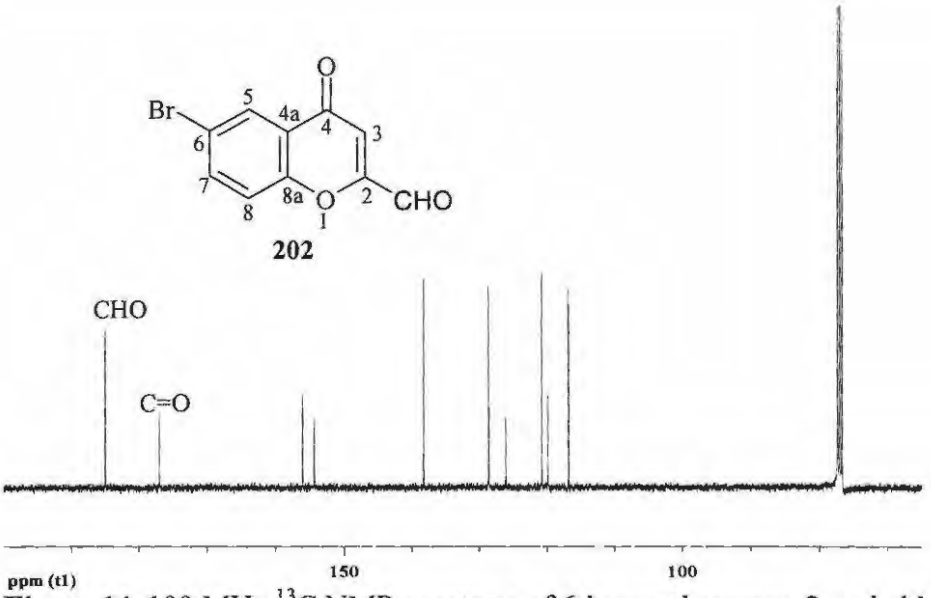

Figure 14. 100 MHz ^{13}C NMR spectrum of 6-bromochromone-2-carbaldehyde **202** in $CDCl_3$.

2.2 Morita-Baylis-Hillman reactions

The Morita-Baylis-Hillman reaction, or more simply, the Baylis-Hillman reaction, is a very useful method for carbon-carbon bond formation between an activated alkene and an aldehyde in the presence of a tertiary amine catalyst. [177-179] The reaction typically results in polyfunctional products with a new chiral centre.[177-182] The rate of reaction has often been found to be sluggish when 1,4-diazabicyclo[2.2.2]octane (DABCO) is used as the catalyst. This was confirmed by preliminary studies performed in our laboratory by Sabbagh[166] on Baylis-Hillman reactions between chromone-3-carbaldehydes and the activated alkenes, methyl acrylate, acrylonitrile and methyl vinyl ketone. In the presence of DABCO, reactions took several weeks to afford the expected Baylis-Hillman products together with unexpected chromone dimers in very low yields ranging from 8 to 17% and 2 to 15%, respectively. 3-Hydroxyquinuclidine (3-HQ), a nucleophilic catalyst, and 1,8-diazabicyclo[5.4.0]undec-7-ene (DBU), a non-nucleophilic catalyst, have, however, been shown to be very efficient catalysts in some cases.[179,183-185] The generally accepted mechanism[186] is illustrated for the 3-hydroxyquinuclidine-catalyzed reaction of acrylate esters with pyridine-4-carboxaldehyde **208** in **(Scheme 47).** The reaction is initiated by

the nucleophilic addition of the tertiary amine catalyst, *e.g.* 3-hydroxyquinuclidine **205**, to the activated alkene, *e.g.* methyl acrylate **206** to form a zwitterionic enolate intermediate **207** that subsequently attacks the electrophilic aldehyde **208** to form a second zwitterionic intermediate **209 (Scheme 47).**[186-187] Proton transfer then results in the resonance-stabilized species **210**, which collapses to the product **211** *via* an E1cB elimination, releasing the catalyst.[186-187]

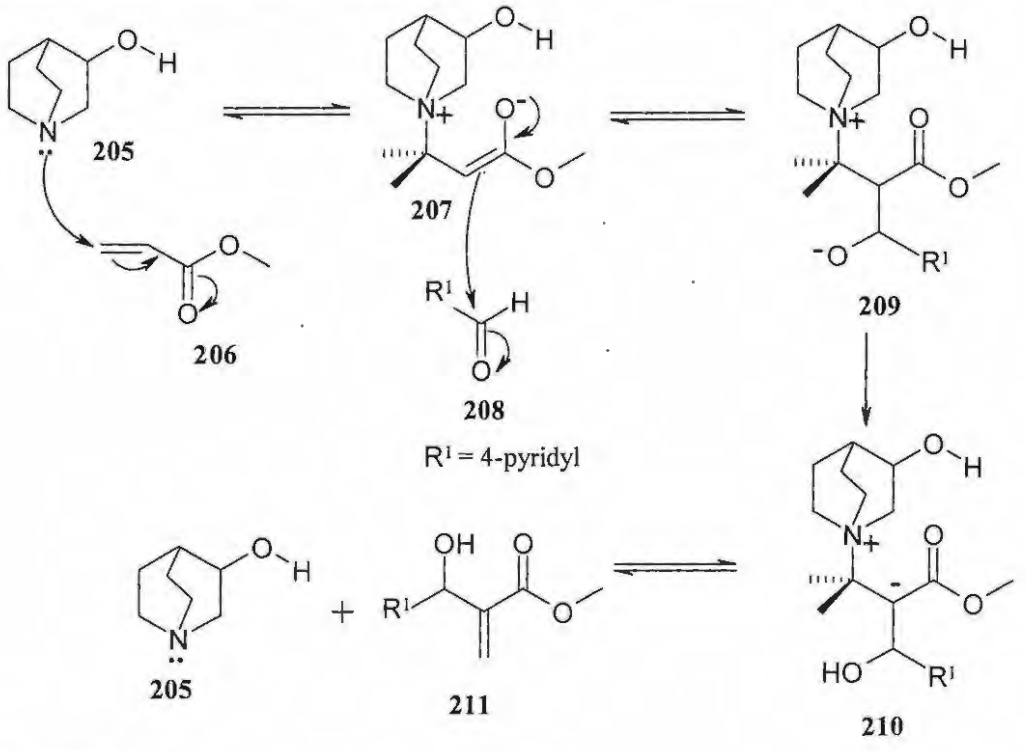

Scheme 47

2.2.1. Reaction of chromone-3-carbaldeydes under Baylis-Hillman conditions

2.2.1.1. Reaction of chromone-3-carbaldehydes with acrylonitrile

The series of chromone-3-carbaldehydes **83** and **184-187** were reacted with acrylonitrile using 3-hydroxyquinuclidine as a nucleophilic catalyst, in a minimal volume of chloroform at 25°C for 24hours **(Scheme 48)**. Purification of the crude products using flash chromatography afforded the desired Baylis-Hillman products **212-216** in yields

ranging from 60 to 98% (Table 5), *i.e.* significantly higher than the yields previously obtained by Nchinda 53-67%.[166] The chromatographic purification was optimized by increasing the polarity of the mobile phase (hexane:EtOAc: 2:3) and adding a few drops of dichloromethane immediately after loading the sample on to the silica column. Use of DBU as the catalyst gave the corresponding Baylis-Hillman products **212-216** in yields ranging from 50 to 60% and 63 to 80% in 6 and 24 hours, respectively (Table 5). It was also observed that when DABCO was used as catalyst in the presence of the ionic liquid, 1-methyl-2-pyrrolidine (1-NMP), the Baylis-Hillman products were obtained in yields ranging from 45 to 60% in 24 hours (Table.5). When DABCO is used alone, such yields are normally only obtained after several weeks. These results indicate that DBU is a very acceptable catalyst, in terms of reaction rate, when composed with 3-hydroxyquinuclidine, the previously favoured catalyst.[185] The structures of these catalysts are shown in Table 5. The products were fully characterized by spectroscopic (IR, 1- and 2-dimensional NMR) and elemental (HREIMS) analysis.

The ^{1}H NMR spectrum (Figure 15) of the Baylis-Hillman product **216** reveals a singlet at 3.89 ppm corresponding to the methoxy group, broad signals at 4.41 ppm and at 5.28 ppm corresponding to the 3'-hydroxyl group (OH) and 3'-H respectively, and two distinct singlets at 6.14 and 6.34 ppm corresponding to the diastereotopic 1'-methylene protons. The ^{13}C NMR spectrum (Figure 16) reveals 14 carbon signals as expected. The methoxy carbon resonates at 55.9 ppm, the 3'-methine carbon at 69.6 ppm, the 1'-methylene carbon at 130.0 ppm and the carbonyl carbon at 177.6 ppm. The DEPT 135 spectrum (Figure 17) confirms assignment of the methylene carbon to the signal at 130.0 ppm. Data from the 2-D spectra (COSY, HMQC and HMBC) were used to facilitate assignment of the signals.

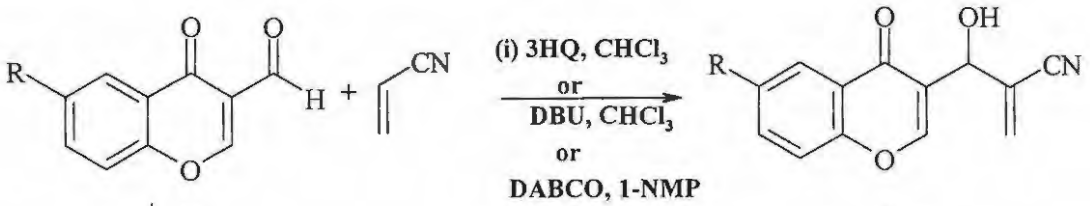

	R
83	**H**
184	**Cl**
185	**Br**
186	**F**
187	**OMe**

	R
212	**H**
213	**Cl**
214	**Br**
215	**F**
216	**OMe**

Scheme 48

Table 5. Isolated yields (%) of Baylis-Hillman products **212-215** using various catalysts.

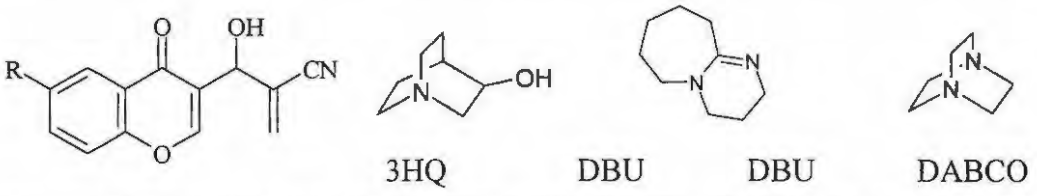

3HQ DBU DBU DABCO

R	Compound	After 24 hours	After 6 hours	After 24 hours	After 24 hours
H	**212**	98	60	80	60
Cl	**213**	85	56	71	50
Br	**214**	73	52	63	55
F	**215**	60	50	60	48
MeO	**216**	71	55	77	45

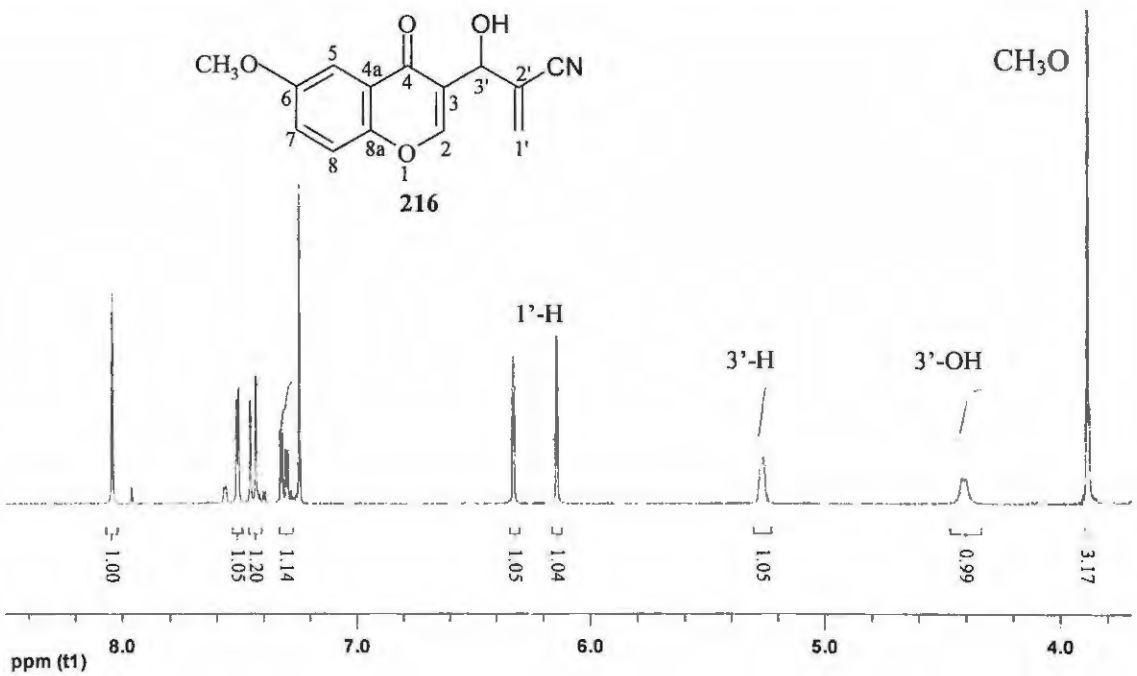

Figure 15. 400 MHz ^{1}H NMR spectrum of the Baylis-Hillman product **216** in $CDCl_3$.

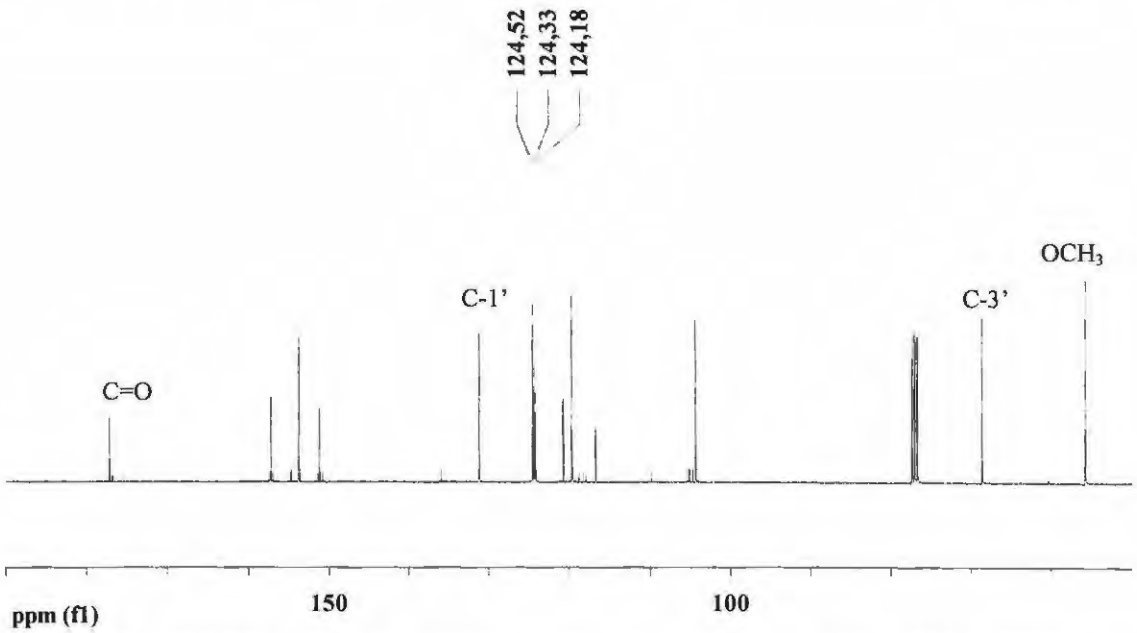

Figure 16. 100 MHz ^{13}C NMR spectrum of the Baylis-Hillman product **216** in $CDCl_3$.

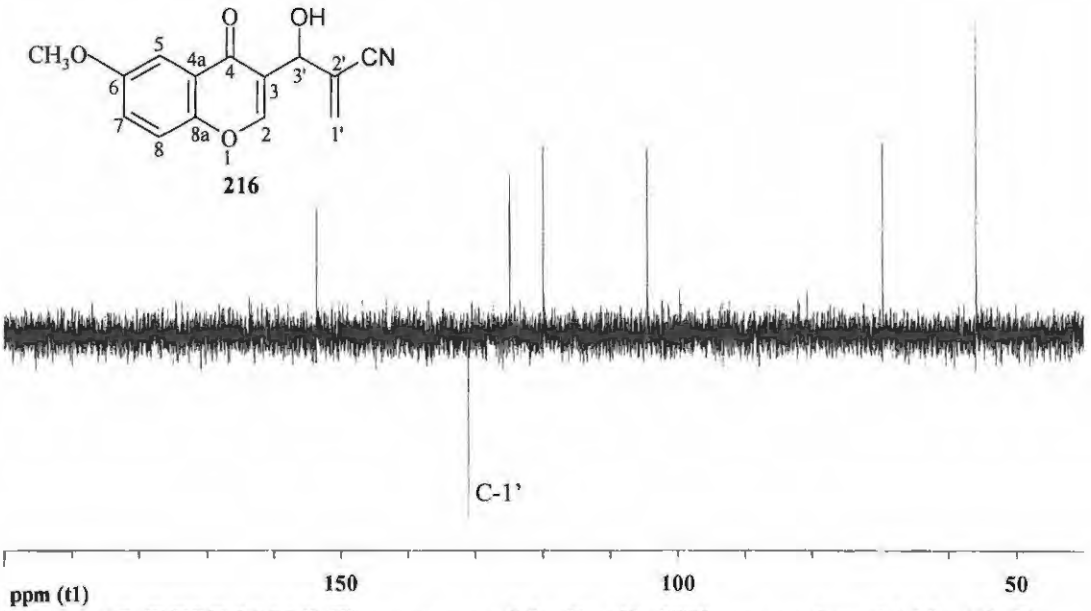

216

Figure 17. DEPT 135 NMR spectrum of the Baylis-Hillman product **216** in $CDCl_3$.

2.2.1.2. Reaction of chromone-3-carbaldehydes with methyl acrylate

The series of chromone-3-carbaldehyde **83** and **184-187** were reacted with methyl acrylate using 3-hydroxyquinuclidine as the catalyst in chloroform for 24hours (**Scheme 49**). Purification of the crude products using flash chromatography afforded the desired Baylis-Hillman products **217-221** and the corresponding chromone dimers **222-226** in yields ranging from 63 to 80% and 5-25%, respectively (Table 6). When DBU was used as the catalyst, the Baylis-Hillman products **217-221** were obtained alone in yields ranging from 50 to 65% (Table 6). Furthermore, when DABCO was used in the presence of the ionic liquid, 1-methylpyrrolidine (1-NMP), the Baylis-Hillman products **217-221** were again obtained as the sole products in yields ranging from 30 to 50% (Table 6). These products were fully characterized by spectroscopic (IR, 1- and 2-dimensional NMR) and elemental (HREIMS) analysis. NMR data are illustrated for the Baylis-Hillman product **218** in Figures 18-20 and for the dimeric products **222** in the Figures 21-23.

	R
83	**H**
184	**Cl**
185	**Br**
186	**F**
187	**OMe**

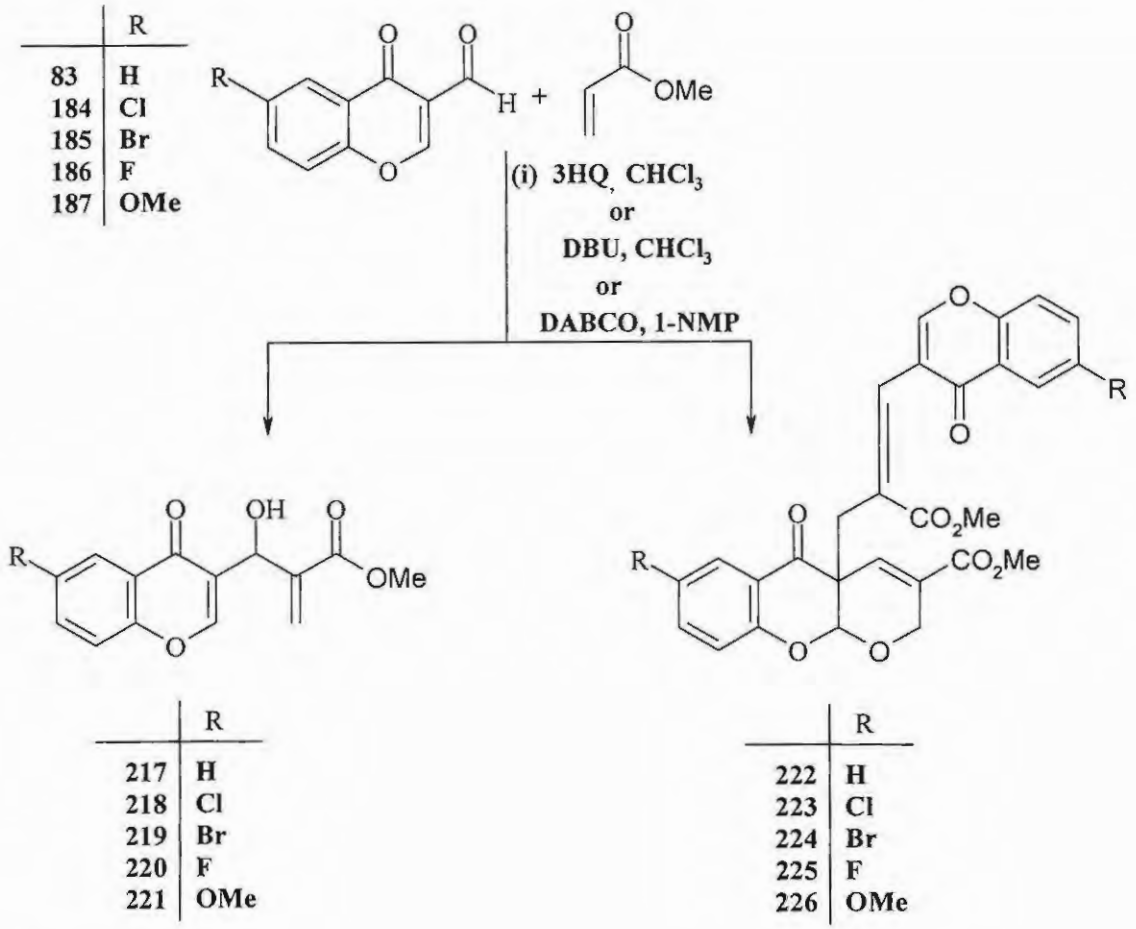

	R
217	**H**
218	**Cl**
219	**Br**
220	**F**
221	**OMe**

	R
222	**H**
223	**Cl**
224	**Br**
225	**F**
226	**OMe**

Scheme 49

Table 6. Isolated yields (%) of the Baylis-Hillman products **217-221** and chromone dimers **222-226** obtained using various catalysts.

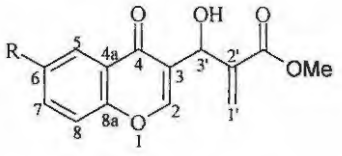

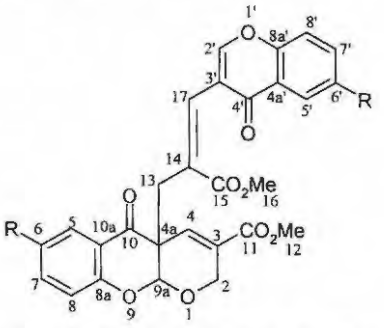

R	B-H product	3HQ	DBU	DABCO	Chromone Dimer	3HQ
H	**217**	80	65	50	**222**	25
Cl	**218**	68	63	47	**223**	22
Br	**219**	70	57	38	**224**	18
F	**220**	63	50	30	**225**	5
Meo	**221**	75	61	44	**226**	15

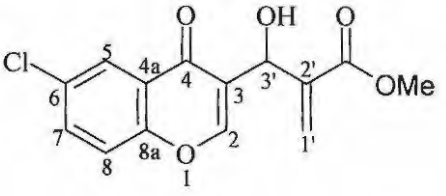

218

Figure 18. 400 MHz ^{1}H NMR spectrum of the Baylis-Hillman product **218** in $CDCl_3$.

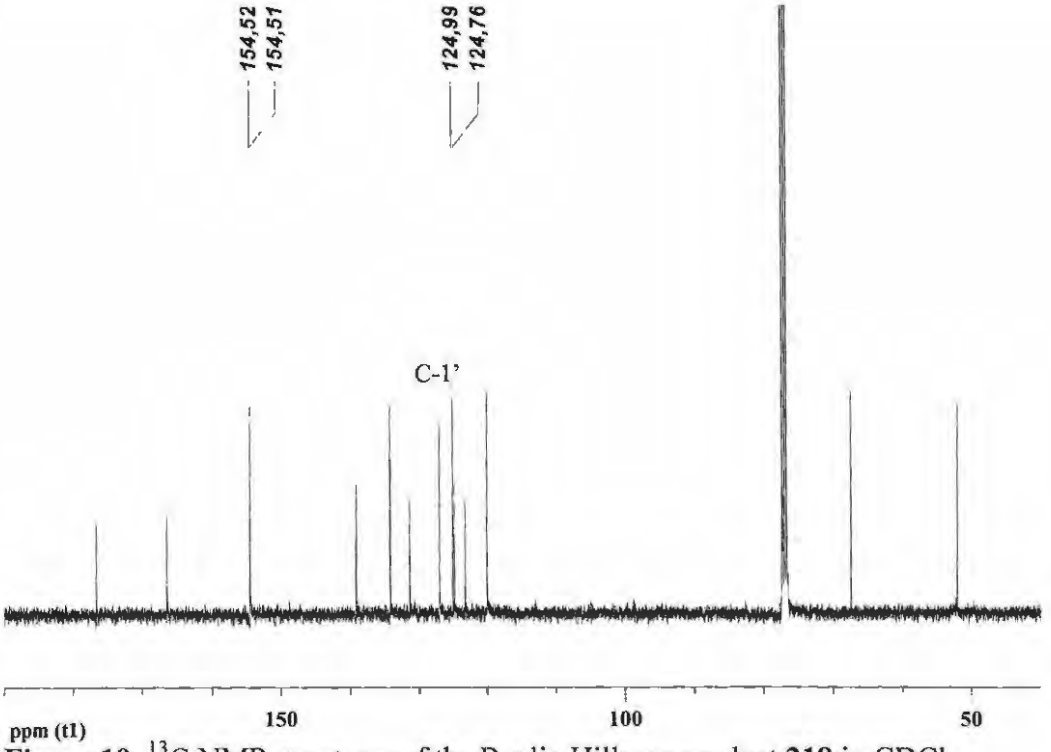

Figure 19. ^{13}C NMR spectrum of the Baylis-Hillman product **218** in $CDCl_3$.

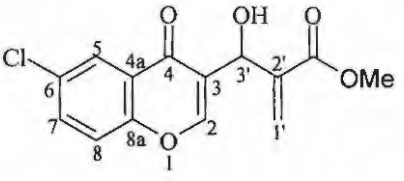

218

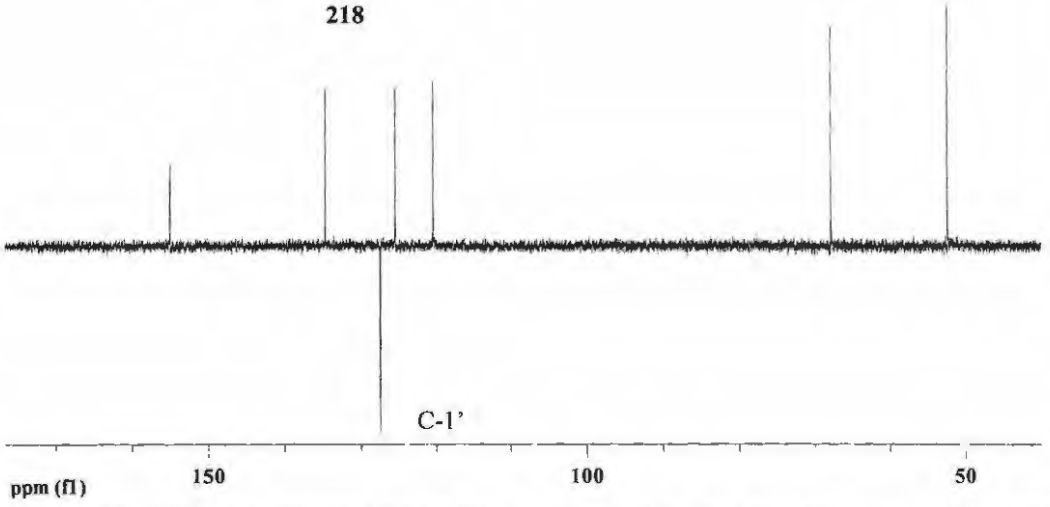

Figure 20. 400 MHz DEPT 135 NMR spectrum of the Baylis-Hillman product **218** in $CDCl_3$.

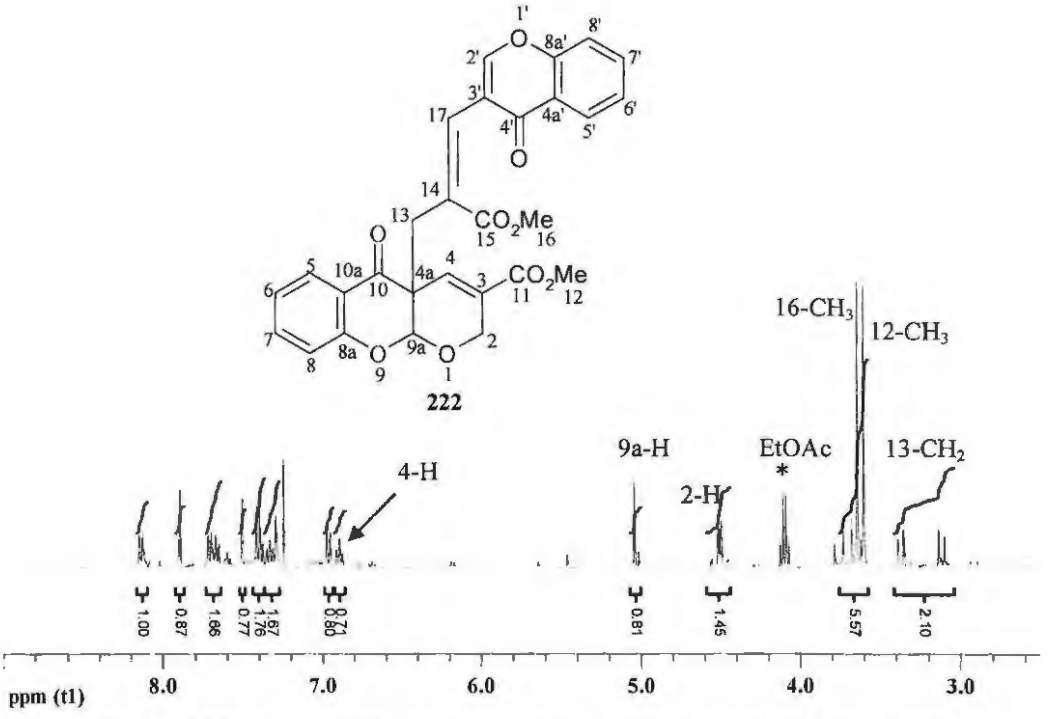

Figure 21. 400 MHz ^{1}H NMR spectrum of the dimeric product **222** in $CDCl_3$.

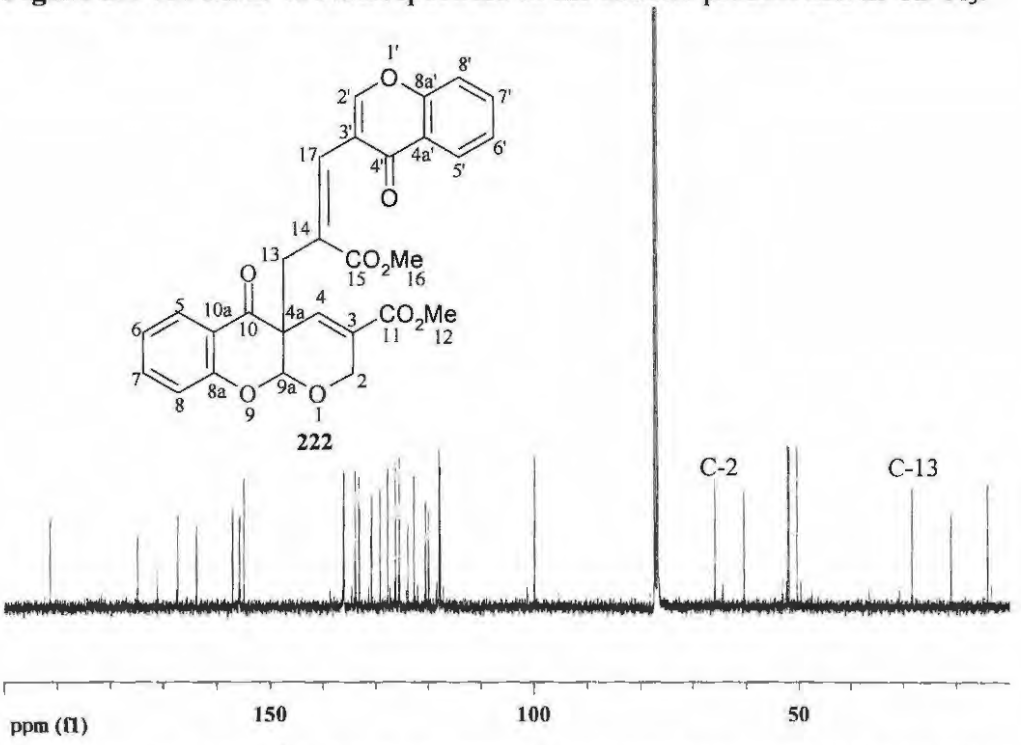

Figure 22. 100 MHz ^{13}C NMR spectrum of the dimeric product **222** in $CDCl_3$.

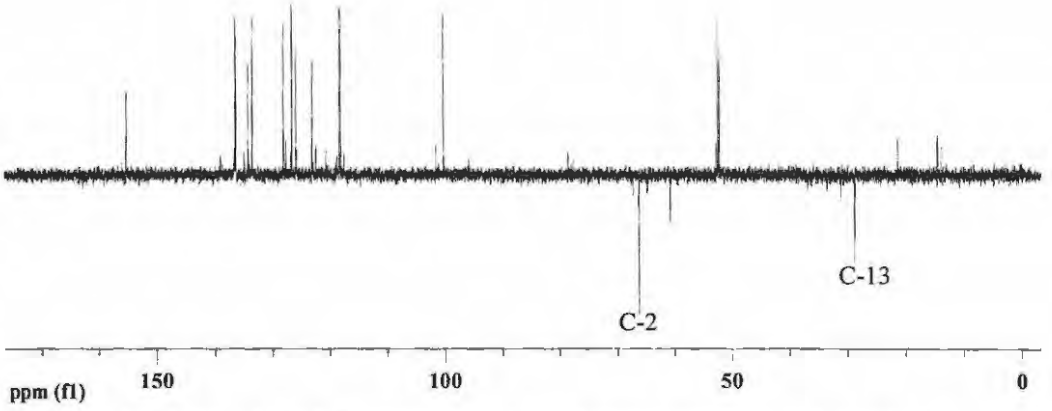

Figure 23. DEPT 135 NMR spectrum of the dimeric product **222** in $CDCl_3$.

The ^1H NMR spectrum (Figure 18) of the Baylis-Hillman product **218** reveals a very broad signal at 2.90 ppm corresponding to the 3'-hydroxyl proton, a singlet at 3.74 ppm corresponding to the methoxy group, a singlet at 5.60 ppm corresponding to 3'-methine proton and two distinct singlets at 6.14 and 6.44 ppm corresponding to the diastereotopic 1'-methylene protons. The ^{13}C NMR spectrum (Figure 19) reveals 14 carbon signals as expected. The methoxy carbon resonates at 52.0 ppm, the C-3' methine carbon at 67.4 ppm, the C-1' methylene carbon at 127.0 ppm and the two carbonyl carbons at 166.5 and 176.6 ppm. The DEPT 135 spectrum (Figure 20) confirms assignment of the methylene carbon at 127.0 ppm, while the data from the COSY, HMQC and HMBC spectra were also used to assign the signals.

The ^1H NMR spectrum (Figure 21) of the chromone dimer **222** reveals two distinct doublets at 3.12 and 3.37 ppm corresponding to the diastereotopic 13-methylene protons, two singlets at 3.61 and 3.65 ppm corresponding to the two methoxy groups, a doublet of doublets at 4.51 ppm corresponding to the 2-methylene protons, a singlet at 5.05 ppm

corresponding to the 9a proton and a triplet at 6.69 ppm corresponding to the 4-methine proton reflecting coupling with the 13-methylene protons. The ^{13}C NMR spectrum (Figure 22) reveals the expected 28 carbon signals and 3 additional signals due to residual ethyl acetate. The C-13 and C-2 methylene carbons resonate at 28.4 and 65.8 ppm, respectively, while the C-9a methine carbon resonates at 99.8 ppm. The DEPT 135 spectrum (Figure 23) confirms the assignment of the C-13 and C-2 methylene carbons to the signals at 28.4 and 65.8 ppm, respectively, while the data from COSY, HMQC and HMBC spectra were also used to facilitate the assignment of the signals.

It was interesting to discover that the highest rates for Baylis-Hillman reactions using DABCO can be achieved at lower temperature.[177,187-188] Consequently, a series of chromone-3-carbaldehydes **83** and **184-185** were reacted with methyl acrylate in the presence of DABCO using a minimal volume of solvent (either $CHCl_3$ or CH_2Cl_2 or THF or DMF) at 0°C for 12hours (**Scheme 50**). Purification of the crude products using flash chromatography did not afford the dioxanone derivatives **227-229** as expected but afforded the chromone dimer **222-224** in yields ranging from 5 to 45% (Table 7). While no Baylis-Hillman products **217-219** were observed after 12hours, however it is presumed that, in fact, they may well have been formed from dioxanone derivatives **227-229** and then converted to chromone dimers **222-224**. The dimeric products **222-224**, first isolated by Sabbagh,[166] are presumed to form *via* the mechanistic sequence outlined in **Scheme 51**.[166] This involves the intermolecular reaction between two molecules of the Baylis-Hillman product **217** which results in intermediate **230**. Attack of the hemi-acetal hydroxyl oxygen on the α, β-unsaturated carbonyl moiety results in intramolecular cyclisation *via* an S_N2' or conjugate addition-elimination process (as illustrated in structure **230a**), to produce the dimeric product **222**. These products **222-224** were fully characterized by spectroscopic (IR, 1- and 2-dimensional NMR) and elemental (HREIMS) analysis.

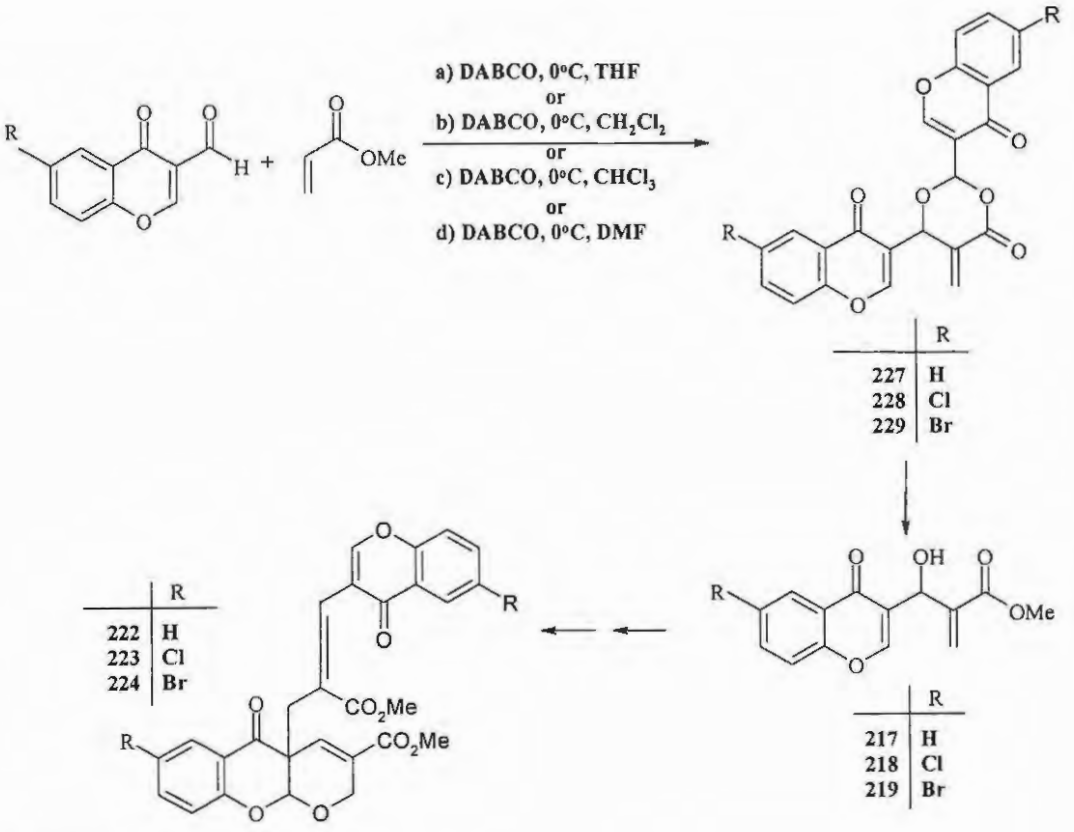

Scheme 50

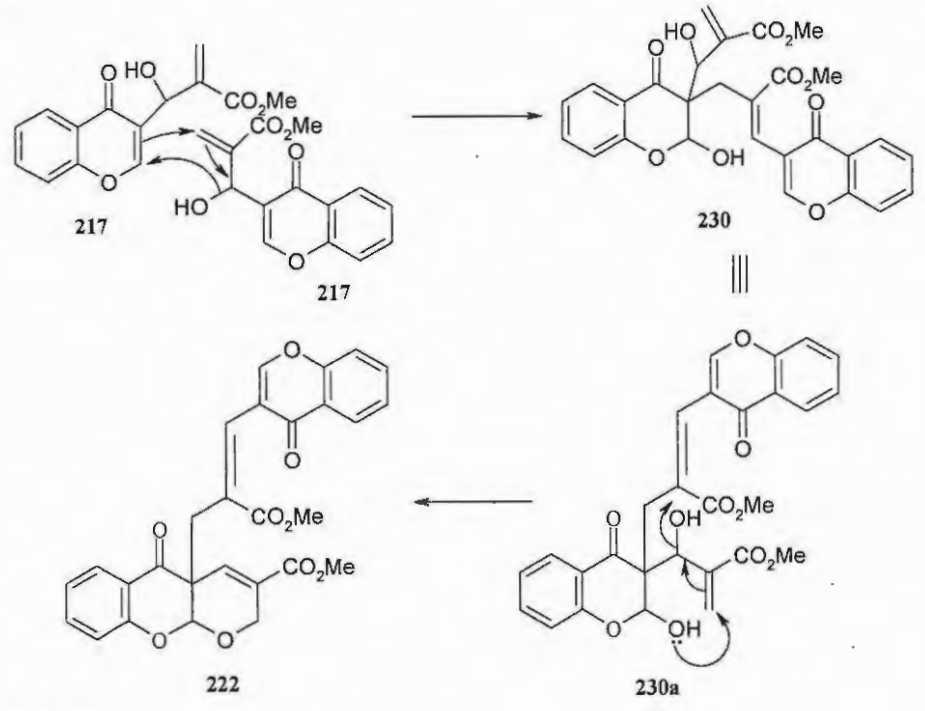

Scheme 51

Table 7. Isolated yields (%) of chromone dimer **222-224.**

R	Chromone Dimer	Using THF	Using CH_2Cl_2	Using $CHCl_3$	Using DMF
H	**222**	5	22	45	15
Cl	**223**	12	35	25	20
Br	**224**	17	37	30	27

2.2.1.3. Reaction of chromone-3-carbaldehydes with methyl vinyl ketone

The series of chromone-3-carbaldehydes **83** and **184-187** were reacted with methyl vinyl ketone using of 3-hydroxyquinuclidine as catalyst in chloroform for 24hours (**Scheme 52**). Purification of the crude products afforded the novel tricyclic adducts **231-235** and the chromone dimers **241-245** in yields ranging from 60 to 80% and 20 to 35%, respectively (Table 8). When DABCO was used as the catalyst and 1-methylpyrrolidine was employed as an ionic solvent, the adducts **231-235** were isolated alone in lower yield ranging from 30 to 45%. There were no Baylis-Hillman products **236-240** observed in these reactions after 24 hours but it is assumed that they had been to be converted into the corresponding chromone dimers **241-245**. When DBU was employed as catalyst, however, the reaction did not take place, confirming the observation by Aggarwal *et al.* that MVK is not reactive in the presence of DBU.[185] The formation of the new tricyclic adducts **231-235** can be rationalized as indicated in **Scheme 53**. The zwitterionic enolate **D**, formed from reaction of the catalyst and MVK, attacks the chromone-3-carbaldehyde **83** at position 2 to afford intermediate **246**. Proton transfer, followed by elimination of the catalyst, yields the intermediate **247**. Cyclisation *via* an intramolecular conjugate addition and a tandem intermolecular Michael reaction then provide access to the novel tricyclic system **231**. These tricyclic products **231-235** were fully characterized by spectroscopic (IR, 1 and 2-dimension NMR) and elemental (HREIMS) analysis.

Table 8. Comparative yields (%) of novel chromone adducts **231-235** and chromone dimer **241-245** obtained using 3-hydroxyquinuclidine and DABCO as catalyst.

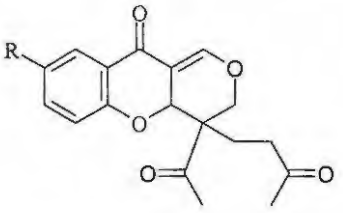

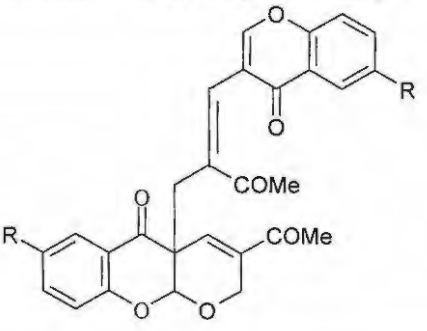

R	Compound	Using 3HQ	Using DABCO	Chromone dimer	Using 3HQ
H	**231**	69	45	**241**	25
Cl	**232**	80	40	**242**	18
Br	**233**	63	33	**243**	28
F	**234**	60	30	**244**	23
MeO	**235**	73	37	**245**	20

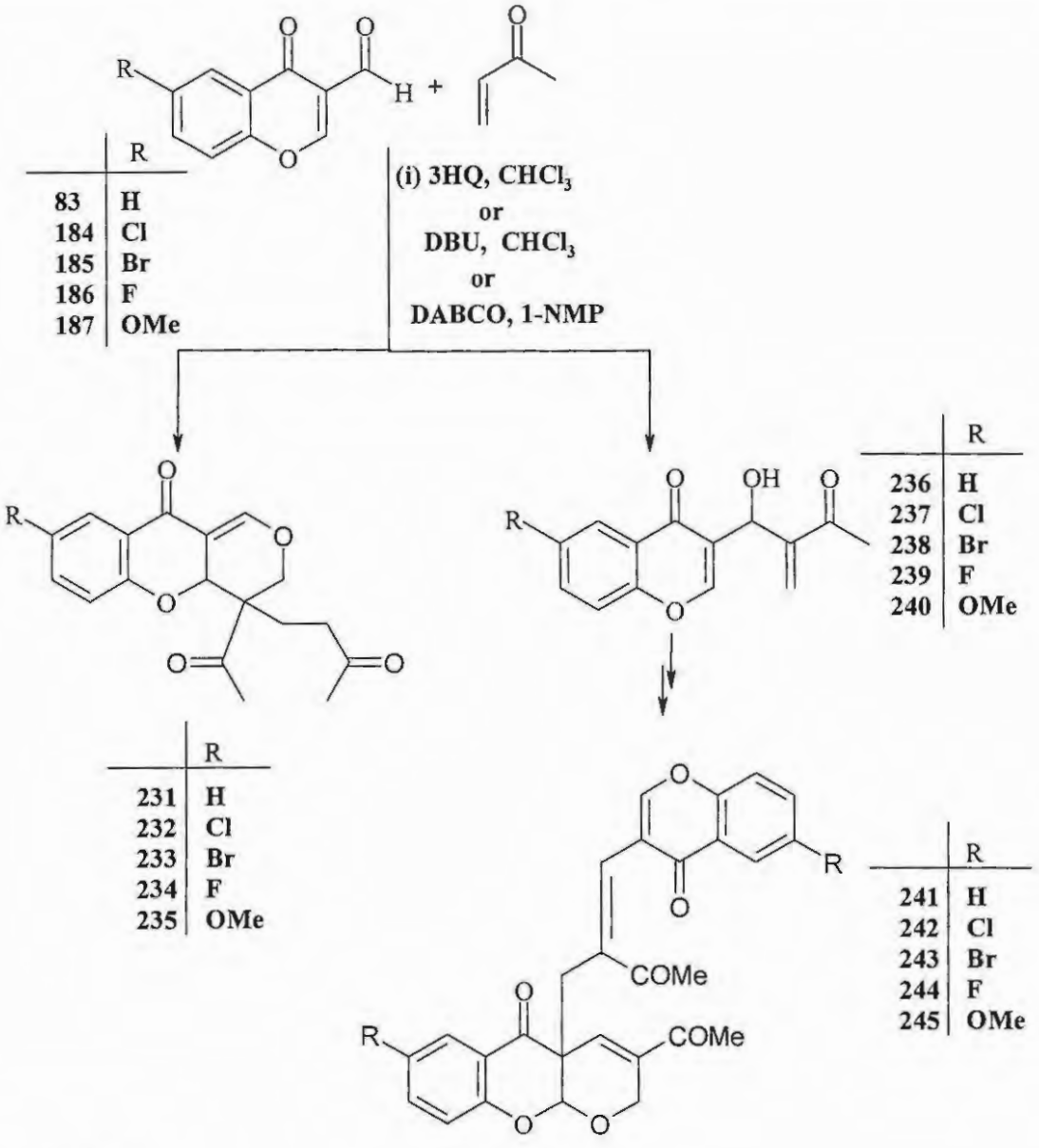

	R
83	H
184	Cl
185	Br
186	F
187	OMe

	R
231	H
232	Cl
233	Br
234	F
235	OMe

	R
236	H
237	Cl
238	Br
239	F
240	OMe

	R
241	H
242	Cl
243	Br
244	F
245	OMe

Scheme 52

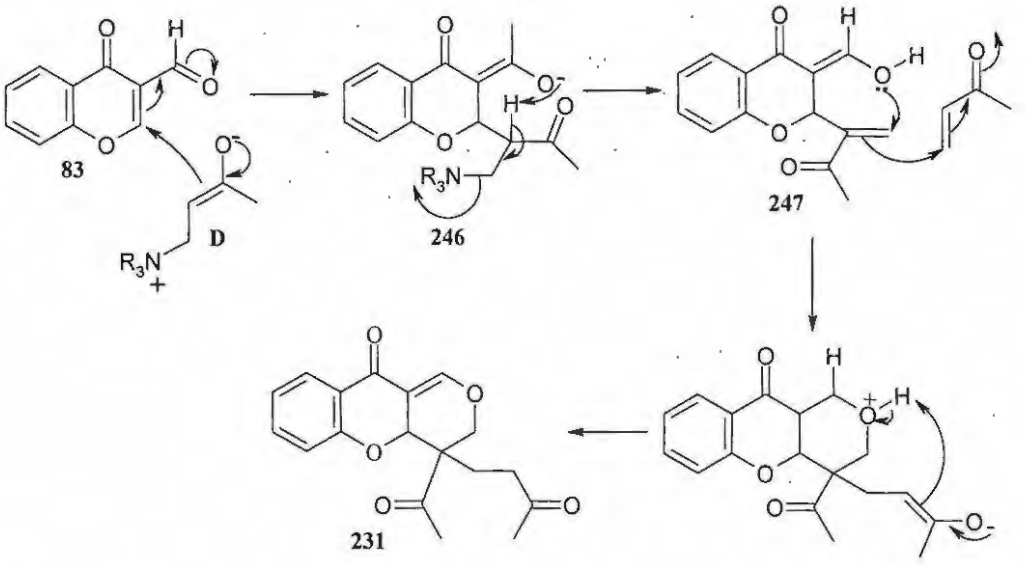

Scheme 53

The ^{1}H NMR spectrum (Figure 24) of the tricyclic adduct **231** reveals two multiplets at 1.98 and 2.25 ppm corresponding to the diastereotopic 13-methylene protons, two singlets at 2.07 and 2.39 ppm corresponding to the 16- and 12-methyl groups, two multiplets at 2.40 and 2.60 ppm corresponding to the diastereotopic 14-methylene protons, a doublet of doublets at *ca.* 4.7 ppm corresponding to 10-methylene protons, a singlet at 5.13 ppm corresponding to the 8a-methine proton and a triplet at 7.30 ppm corresponding to the 2-methine proton which couples with the 10-methylene protons. The ^{13}C NMR spectrum (Figure 25) reveals 18 carbon signals. The C-13 methylene nucleus resonates at 24.9 ppm, the C-12 and C-16 methyl nucleus at 25.5 and 30.0 ppm, the C-14 methylene nucleus at 37.8 ppm, the quaternary carbon C-9 at 49.1 ppm, the C-10 methylene nucleus at 65.9 ppm, the C-8a methine at 99.9 ppm, the vinylic carbon C-2 at 135.4 ppm and the three carbonyl carbons at 192.6, 196.6 and 206.7 ppm. The DEPT 90 spectrum (Figure 26) confirms that there are only 6 methine carbon signals as expected. The DEPT 135 spectrum (Figure 27) confirms the presence of three methylene carbons, C-13, C-14 and C-10, which resonate at 55.9, 37.8 and 65.9 ppm, respectively; the absence of the C-9 signal, which resonates at 49.1 ppm, confirms that it is a quaternary carbon. The COSY spectrum (Figure 28) reveals long range couplings (**A**) between the 2-methine proton and the diastereotopic 10-methylene protons. The HMQC

and HMBC spectra (Figures 29 and 30) were used to assign the aromatic signal and also to confirm the other signal assignments.

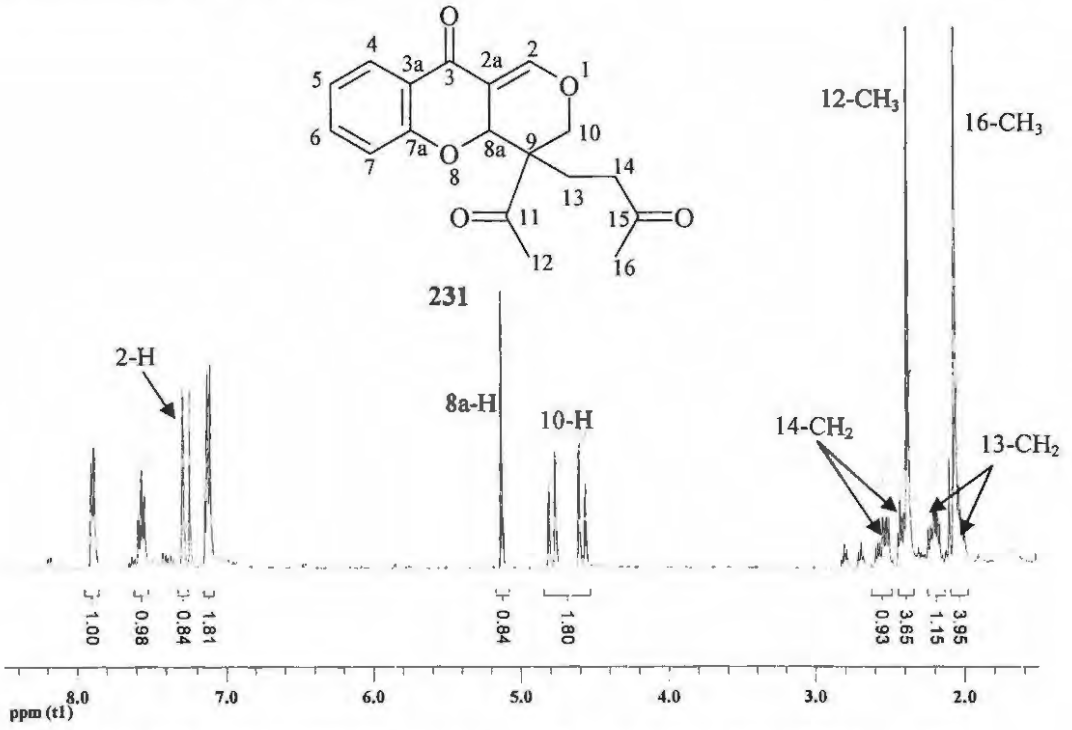

Figure 24. 400 MHz ^{1}H NMR spectrum of the tricyclic adduct **231** in $CDCl_3$.

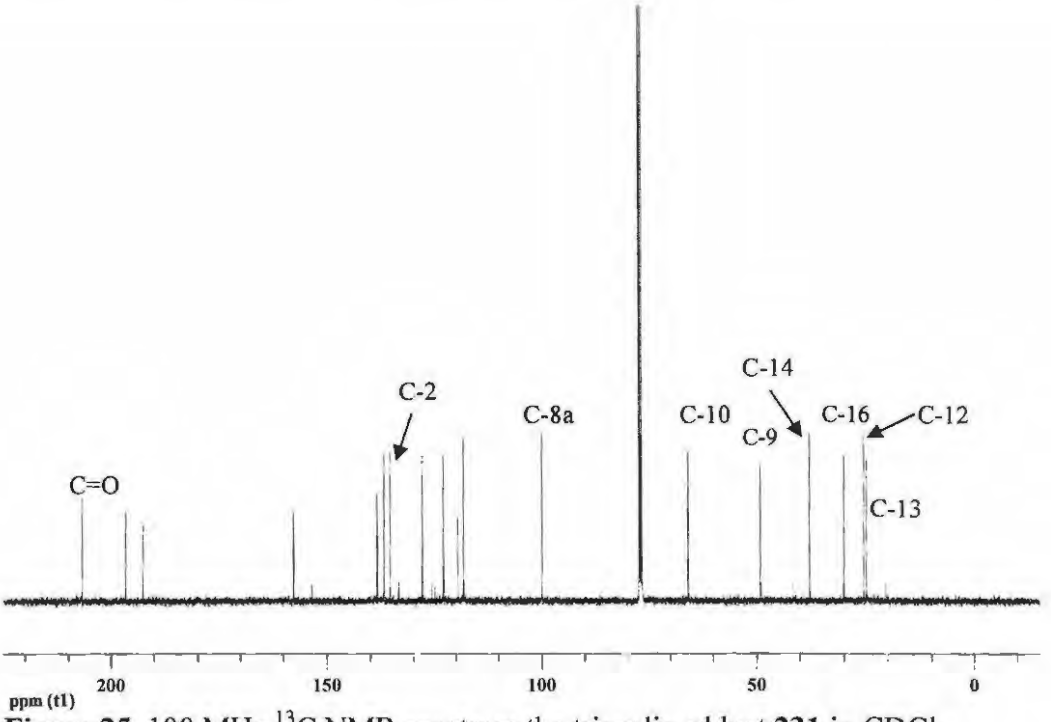

Figure 25. 100 MHz ^{13}C NMR spectrum the tricyclic adduct **231** in $CDCl_3$.

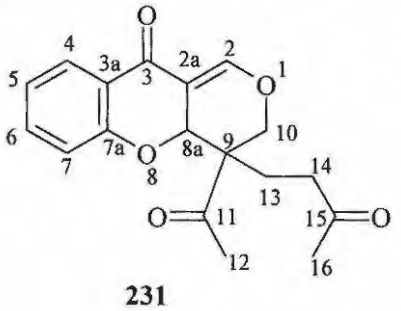

231

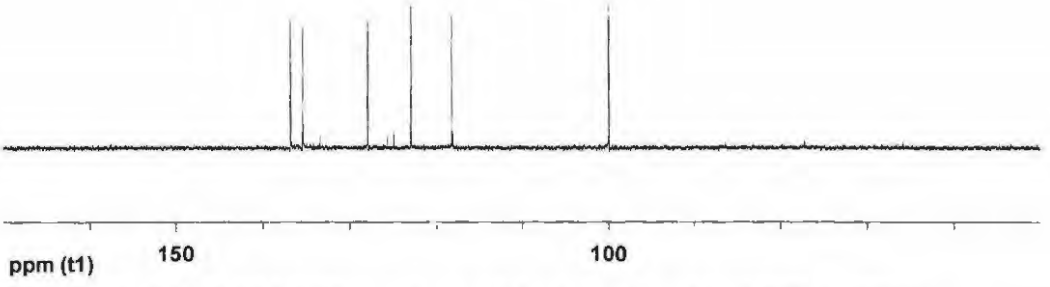

Figure 26. DEPT 90 NMR spectrum of the tricyclic adduct **231** in $CDCl_3$.

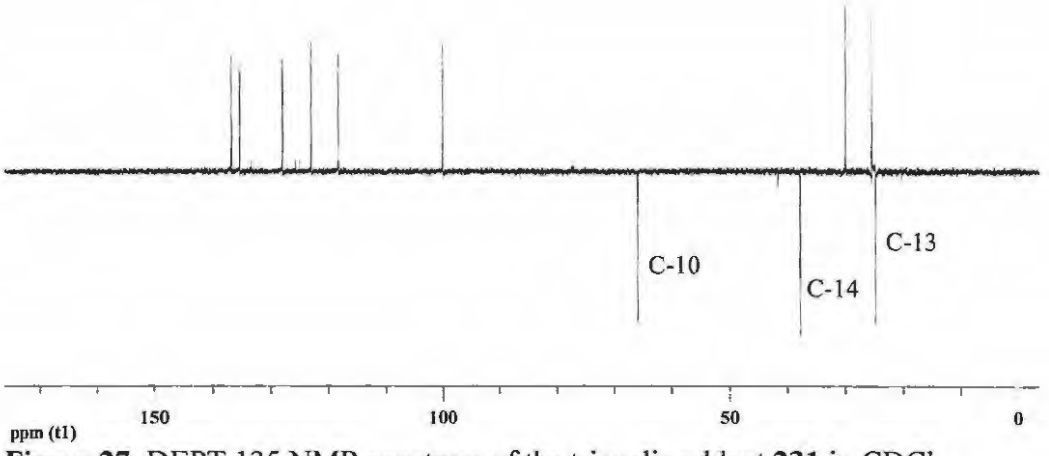

Figure 27. DEPT 135 NMR spectrum of the tricyclic adduct **231** in $CDCl_3$.

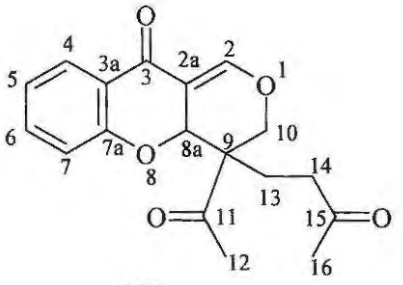

231

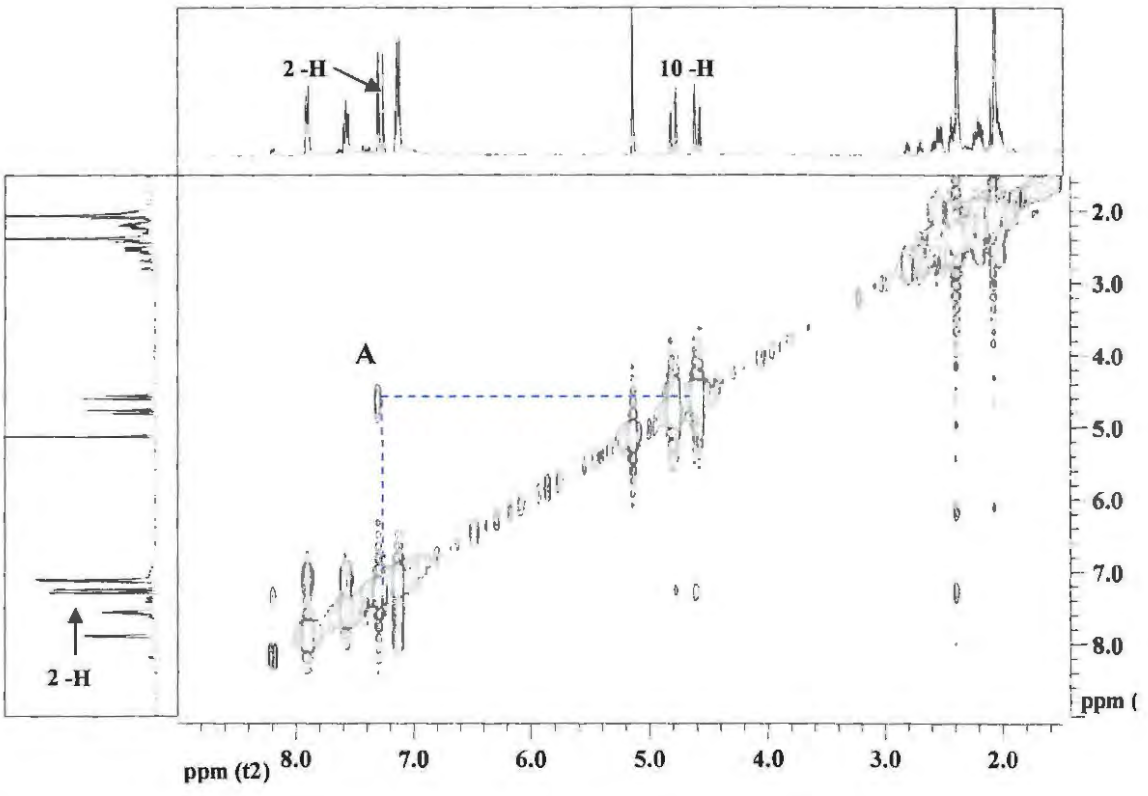

Figure 28. 400 MHz COSY NMR spectrum of the tricyclic adduct **231** in $CDCl_3$.

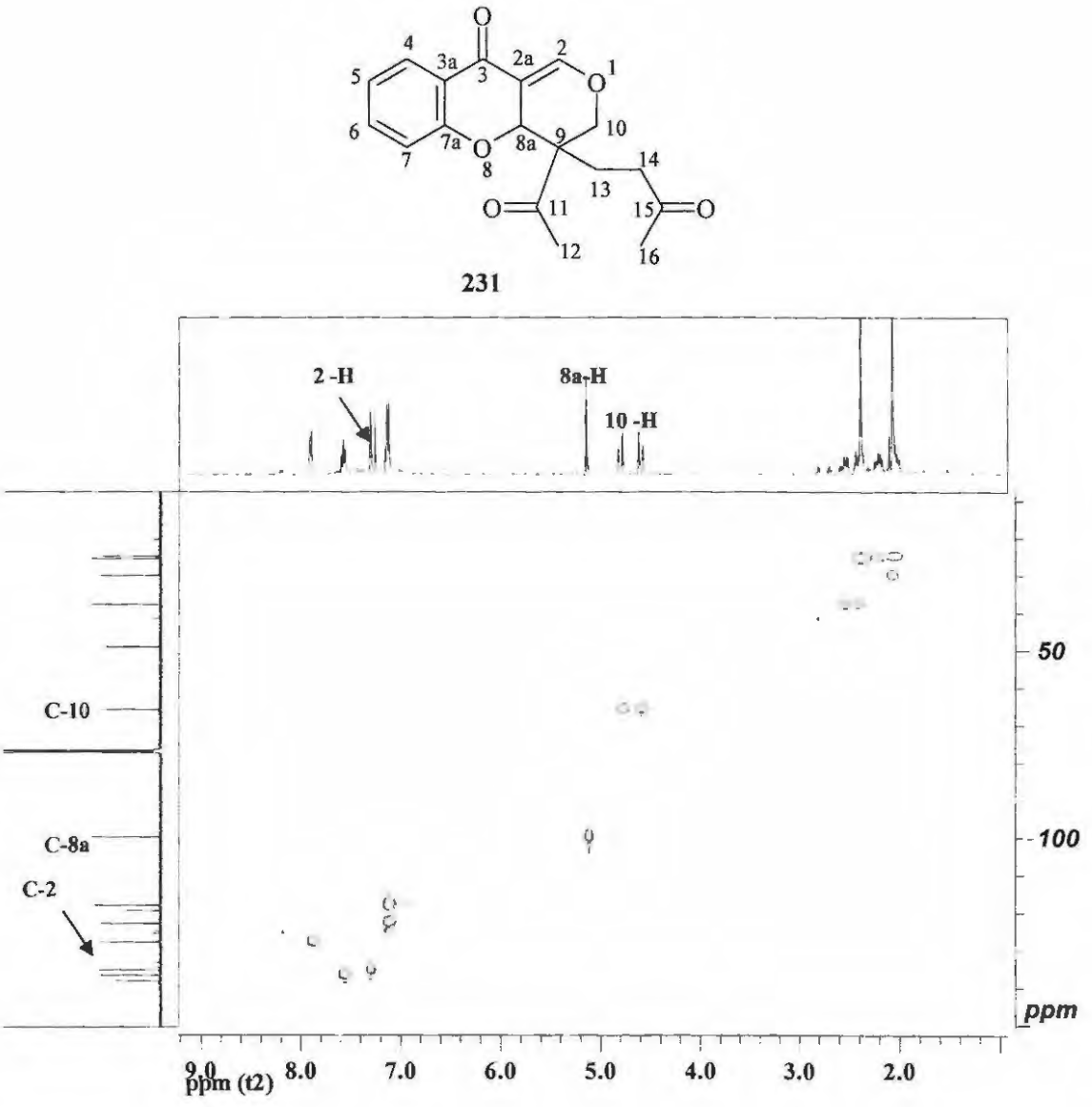

Figure 29. 400 MHz HMQC NMR spectrum of the tricyclic adduct **231** in $CDCl_3$.

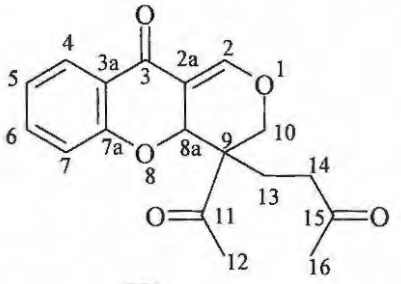

231

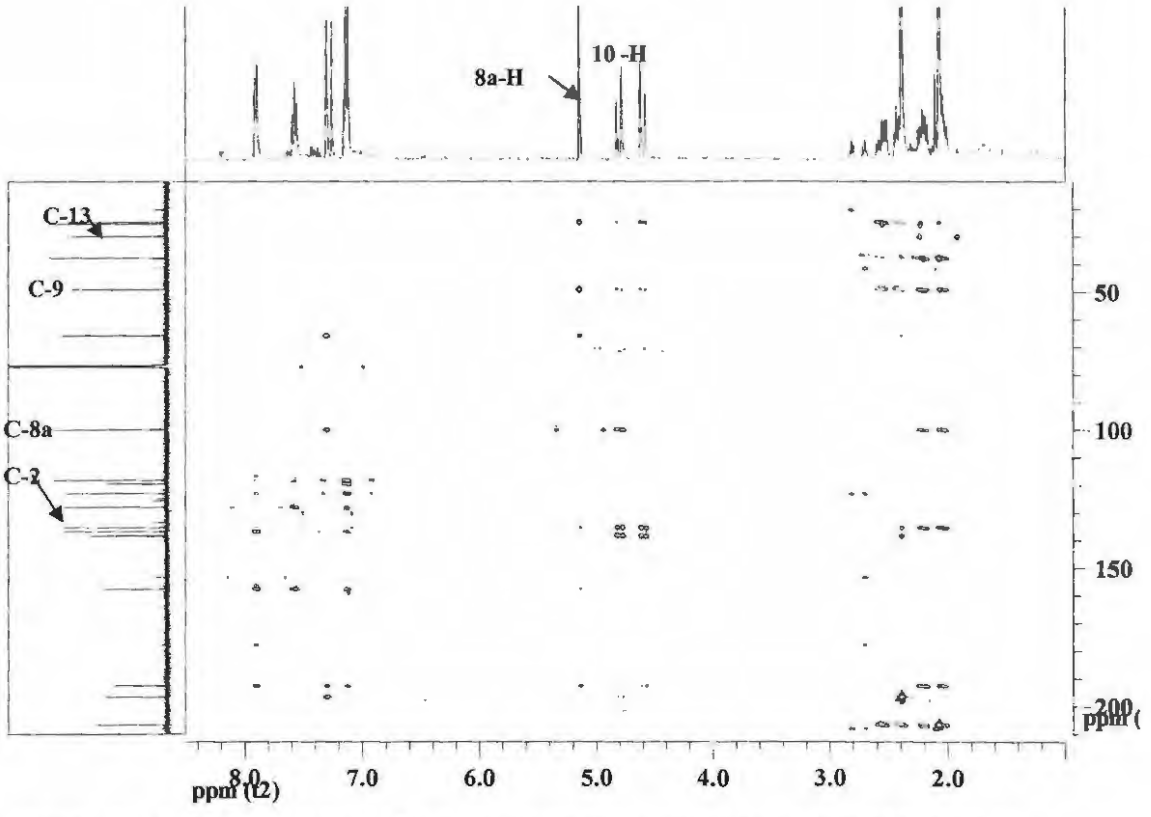

Figure 30. 400 MHz HMBC NMR spectrum of the tricyclic adduct **231** in $CDCl_3$.

The ^{1}H NMR spectrum (Figure 31) of the chromone dimer **241** reveals two singlets at 2.29 and 2.42 ppm corresponding to the 12- and 16-methyl groups, a singlet at 3.23 ppm corresponding to the 13-methylene protons, a doublet of doublets at 4.52 ppm corresponding to the 2-methylene protons, a singlet at 5.00 ppm corresponding to the 9a proton and a singlet at 7.17 ppm corresponding to the 4-methine proton. The ^{13}C NMR spectrum (Figure 32) reveals the expected 28 carbon signals. The C-13 and C-2 methylene carbons resonate at 30.9 and 65.9 ppm, respectively, the C-4a quaternary carbon at 50.1 ppm and the C-9a methine carbon at 99.8 ppm. The data from DEPT 135, COSY, HMQC and HMBC spectra were also used to facilitate the assignment of the signals.

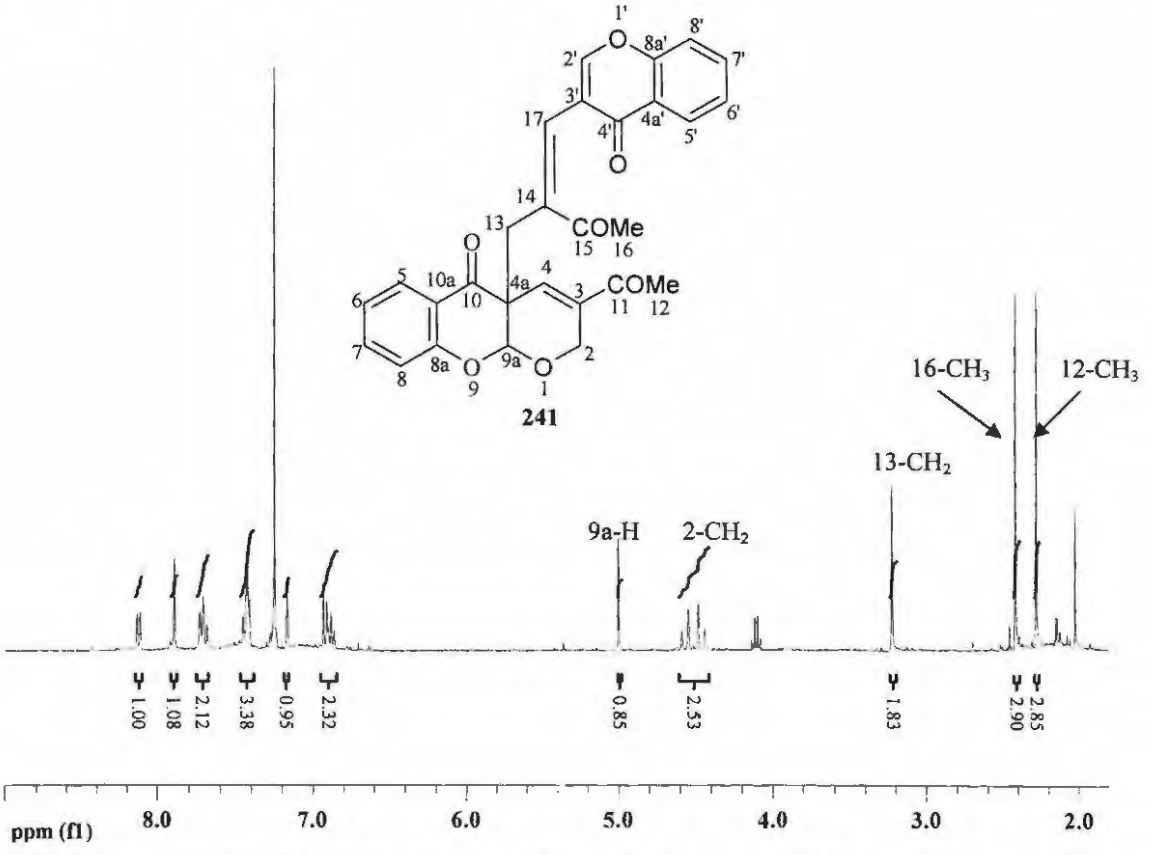

Figure 31. 400 MHz ^{1}H NMR spectrum of the dimeric product **241** in $CDCl_3$.

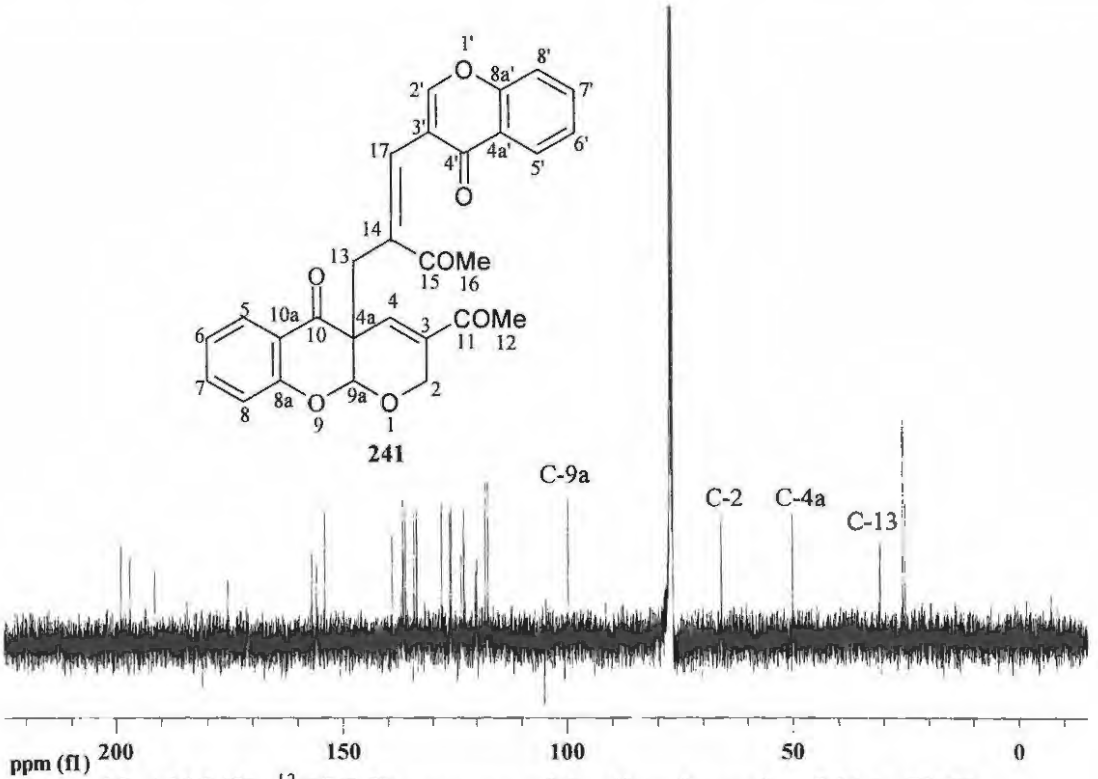

Figure 32. 100 MHz ^{13}C NMR spectrum of the dimeric product **241** in $CDCl_3$.

2.2.2 Reaction of chromone-2-carbaldehydes with Michael acceptors

2.2.2.1. Reaction of chromone-2-carbaldehydes with methyl vinyl ketone

The chromone-2-carbaldehydes **91, 202** and **204** were reacted with methyl vinyl ketone using 3-hydroxyquinuclidine, as catalyst, in chloroform at room temperature for 24hours **(Scheme 54).** Purification of the crude products using flash chromatography afforded the MVK dimer **246** and the new adducts **247-249** in *ca.* 2:3 mixtures of *syn-* and *anti-* diastereomers in yields of 23-40% and 55-70%, respectively (Table 9a and b) and similar adducts have been reported for Baylis-Hillman reactions involving benzaldehyde substrates (see Section 2.7, p 157). None of the normal Baylis-Hillman product was found in the reaction mixtures after 24 hours. The mechanism for the formation of the adducts **247-249** has yet to be fully established, but it is likely that the normal Baylis-Hillman product **250** is formed first (see **Scheme 46**, p 63), and then undergoes the conjugate addition by the MVK zwitterion **D** (Path I; **Scheme 55)** to form the

intermediate zwitterion **251**; elimination of the catalyst then results in the adduct **247**. Since there is an excess of MVK in the reaction mixture, dimerization occurs to form the dimer **246** (path II).[190-195] When these reactions were repeated using DABCO as catalyst, the MVK dimer **246** and the adducts **247-249** were obtained in yields of 25-35% and 40-55%, respectively. When dichloromethane was used as the solvent and 3HQ as the catalyst, the MVK dimer **246** and adducts **247-249** were obtained in lower yields (15-27% and 50-65%, respectively). Furthermore, when DABCO was used as the catalyst but dichloromethane was used as the solvent, instead of chloroform, the MVK dimer **246** and the adducts **247-249** were obtained in even lower yields (15-23% and 30-45%, respectively). However, when DBU was employed as catalyst, in either chloroform or dichloromethane, there was no reaction at all, confirming that MVK is not a good substrate for DBU.[185] Its appears that the excess MVK favours the formation of Baylis-Hillman adducts **247-249** as the Baylis-Hillman product **250**, once formed, acts as an electrophile and reacts with the zwitterionic enolate **D** as depicted in **Scheme 55**.

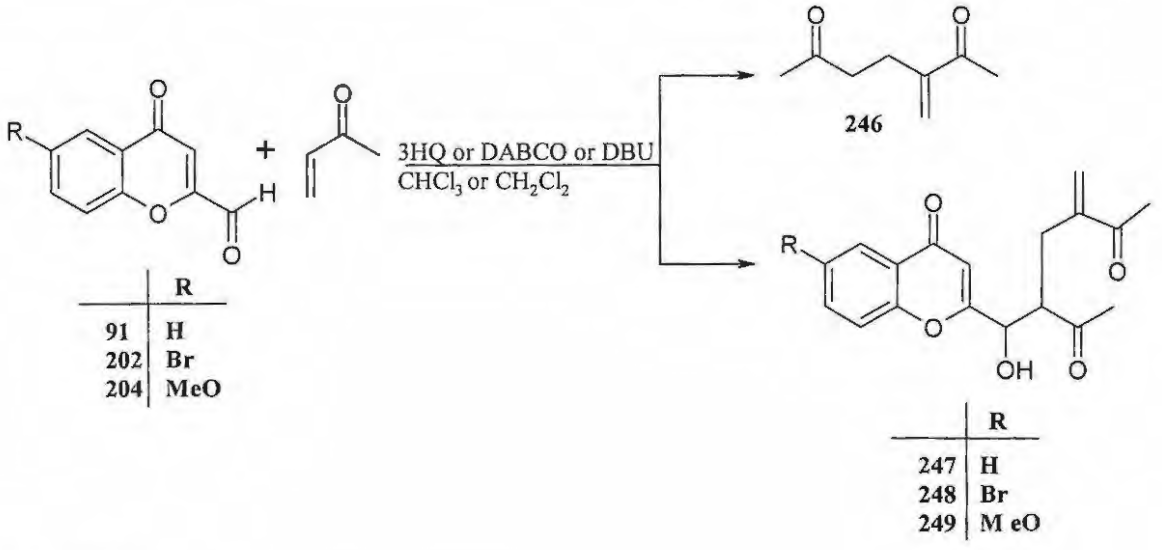

Scheme 54

The diastereomeric adducts **247-249** appeared as single spots on thin layer chromatography plates and even when HPLC was applied following flash chromatography, the *syn* and *anti*-diastereomers could not be separated. These products

were, however, characterized by spectroscopic (IR, 1- and 2-dimensional NMR) and elemental (HREIMS) analysis. The signal assignments in the representative ^{1}H- and ^{13}C-NMR spectrum (Figures 34 and 35) of the parent system **247** were based on a careful analysis of the DEPT 135, HSQC and HMBC spectra.

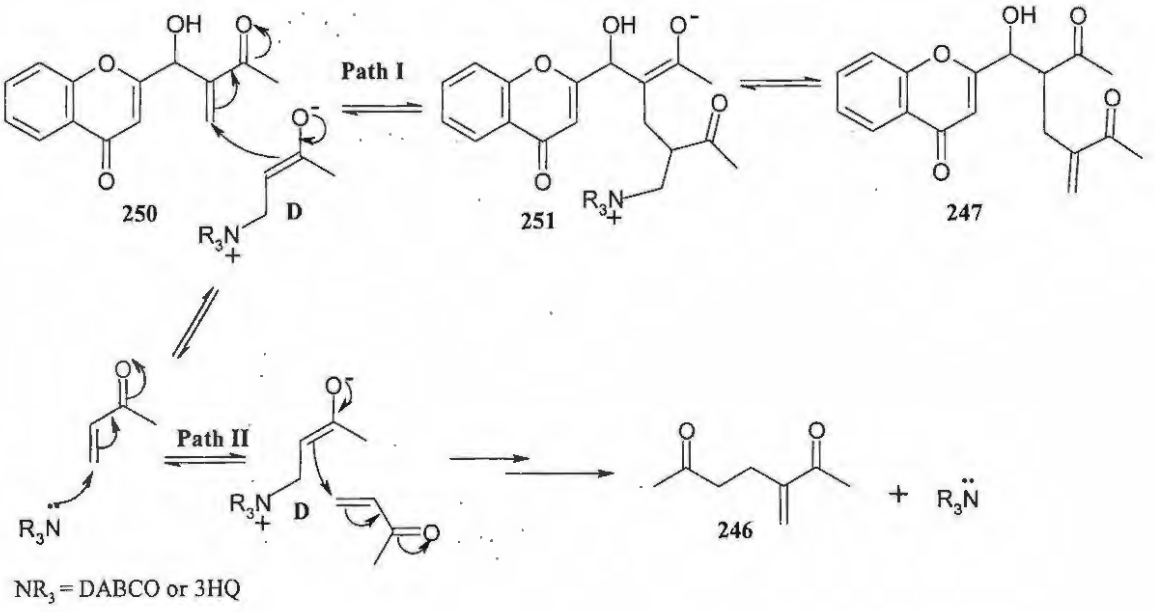

Scheme 55

Table 9a. Isolated yields (%) of MVK the dimer **246** at different solvents and catalysts.

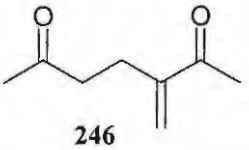

246

3HQ Catalysis		DABCO Catalysis	
$CHCl_3$	CH_2Cl_2	$CHCl_3$	CH_2Cl_2
40	35	27	23
37	28	19	17
23	25	15	15

Table 9b. Isolated yields (%) of the adducts **247-249** using different solvents and catalysts.

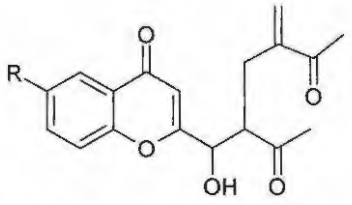

R	Product	3HQ Catalysis		DABCO Catalysis	
		$CHCl_3$	CH_2Cl_2	$CHCl_3$	CH_2Cl_2
H	**247**	70	65	55	45
Br	**248**	63	50	47	35
MeO	**249**	55	57	40	30

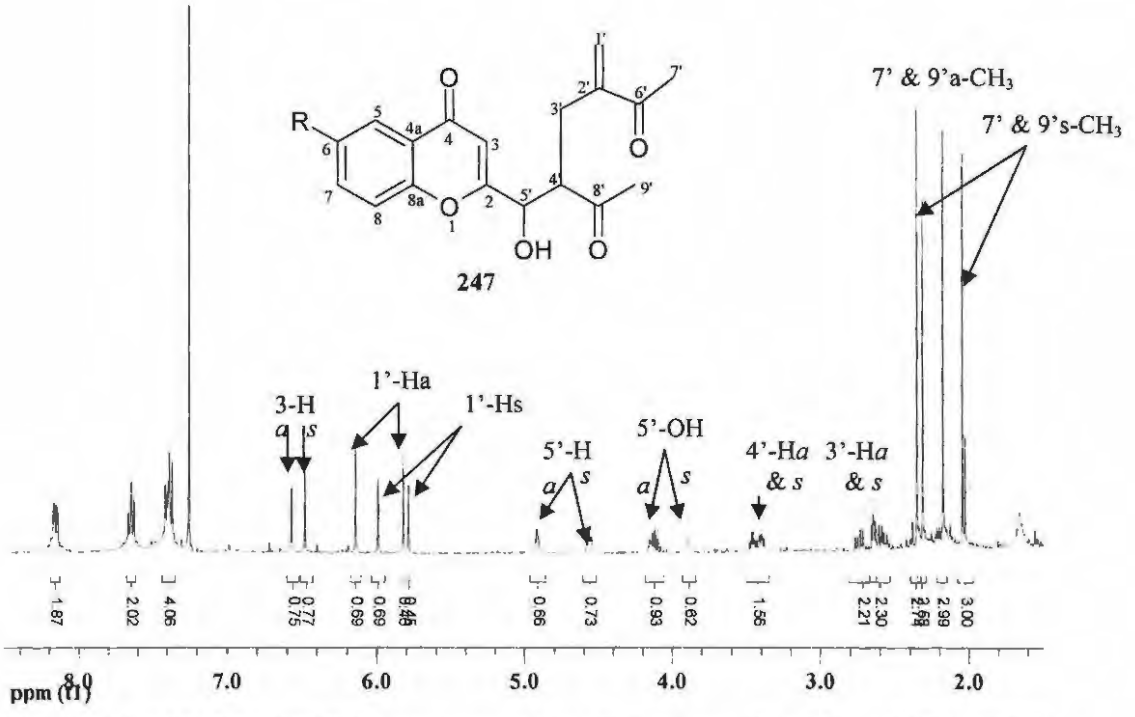

Figure 34. 400MHz ^{1}H NMR spectrum of the diastereomeric adducts **247** in $CDCl_3$, with signals due to *syn* isomer denoted by (*s*) and the signals due to *anti* by (*a*).

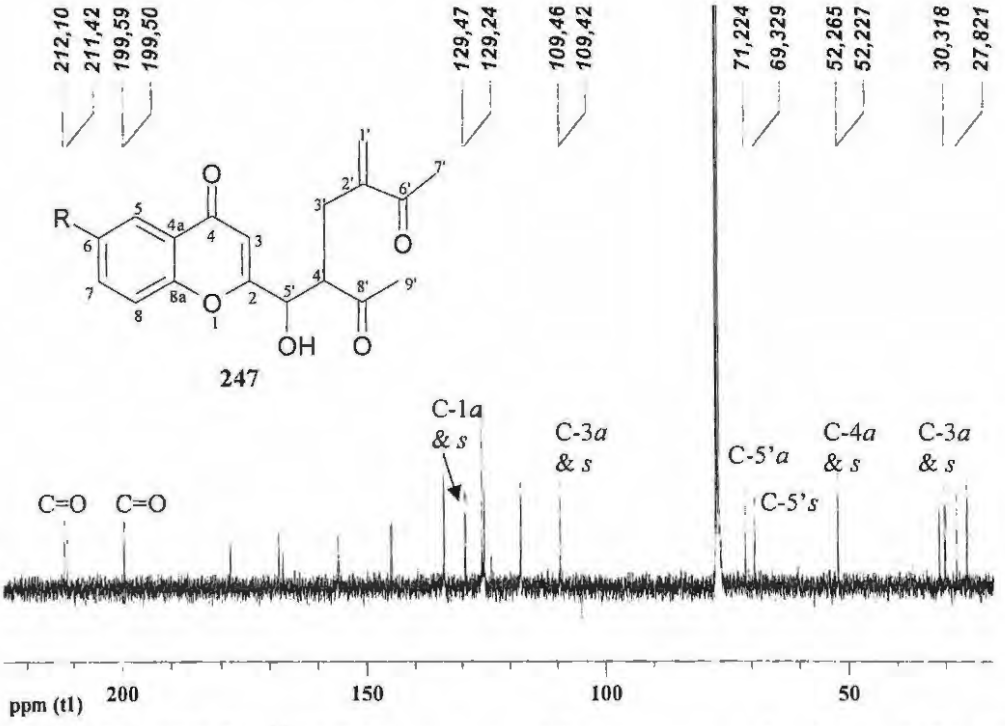

Figure 35. 100MHz ^{13}C NMR spectrum of the diastereomeric adducts **247** in $CDCl_3$, with signals due to *syn* isomer denoted by (*s*) and the signals due to *anti* by (*a*).

The ^{1}H NMR spectrum (Figure 34) of the diastereomeric *syn* and *anti*- Baylis-Hillman adducts **247** reveals two singlets at 2.05 and 2.31 ppm, which correspond to the 7'- and 9'-methyl protons, respectively, of the *anti*-isomer, and another two singlets at 2.18 and 2.35 ppm which correspond to the 7' and 9'-methyl protons, respectively, of the *syn*-isomer. The overlapping multiplets between 2.51 and 2.78 ppm correspond to the diastereotopic 3'-methylene protons of both *syn*- and *anti*-isomers, the remaining signals maybe similarly assigned to the *syn* (*s*)- and *anti* (*a*)–diastereomers as indicated in Figure 34. The ^{13}C NMR spectrum (Figure 35) reveals 36 carbon signals as expected with the *anti*- and *syn*-isomers each containing 18 different carbon atoms. The remaining ^{13}C signals have been assigned (*s*) or (*a*) in Figure 35, the assignments being based on careful examination of the 2-D NMR data.

2.2.2.2. Reaction of chromone-2-carbaldehyde with methyl acrylate

The chromone-2-carbaldehyde **204** was reacted with methyl acrylate using 3-hydroxyquinuclidine as catalyst in a minimal volume of chloroform at room temperature for 24hours **(Scheme 56)**. Purification of the crude product using flash chromatography afforded the interesting product **250** in 45% yield, but none of the expected Baylis-Hillman product **251**. When dichloromethane was used as solvent this interesting product **250** was obtained in lower yield of 12%. The proposed mechanism for the formation of this product is in **Scheme 57**, and involves the displacement of the aldehyde group at position 2. It is apparent that instead of attacking the aldehydic carbonyl carbon, the zwitterionic enolate attacks electrophilic C-2 centre on the chromone system. Furthermore, when either DABCO or DBU were used, the reaction did not take place. Increasing the reaction time to 5 days and monitoring the progress every 24 hours failed to provide any evidence of the formation of the Baylis-Hillman product. The product **250** was fully characterized by spectroscopic (IR, 1- and 2-dimensional NMR) and elemental (HREIMS) analysis. The ^{1}H NMR spectrum (Figure 36) of compound **250** reveals a doublet at 1.51 ppm corresponding to the 3'-methyl protons, a singlet at 3.93 ppm corresponding to the 1'-methoxy protons, a quartet at 4.26 ppm corresponding to the 2'-methine proton, and a singlet at 7.00 ppm corresponding to the 3-methine proton. The ^{13}C NMR spectrum (Figure 37) reveals 14 carbon signals as expected. The 3'-methyl carbon resonates at 12.6 ppm, the 2'-methine carbon signal at 48.0 ppm, the 3-methine carbon at 111.1 ppm, and the ester carbonyl carbon at 190.4 ppm. The DEPT 135 spectrum (Figure 38) confirms the assignment of the 3'-methyl carbon to the signal at 12.6 ppm, the 2'-methine carbon to the signal at 48.0 ppm; the two methoxy carbons C-1' and C-6 resonate at 52.8 and 56.0 ppm, respectively. The COSY, HMBC (Figures 39-40) and elemental (HREIMS) analysis confirmed these results.

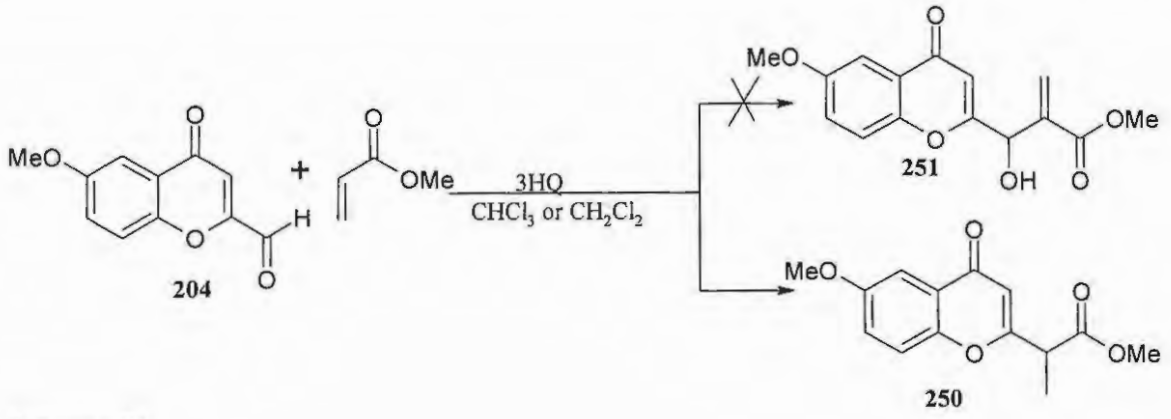

Scheme 56

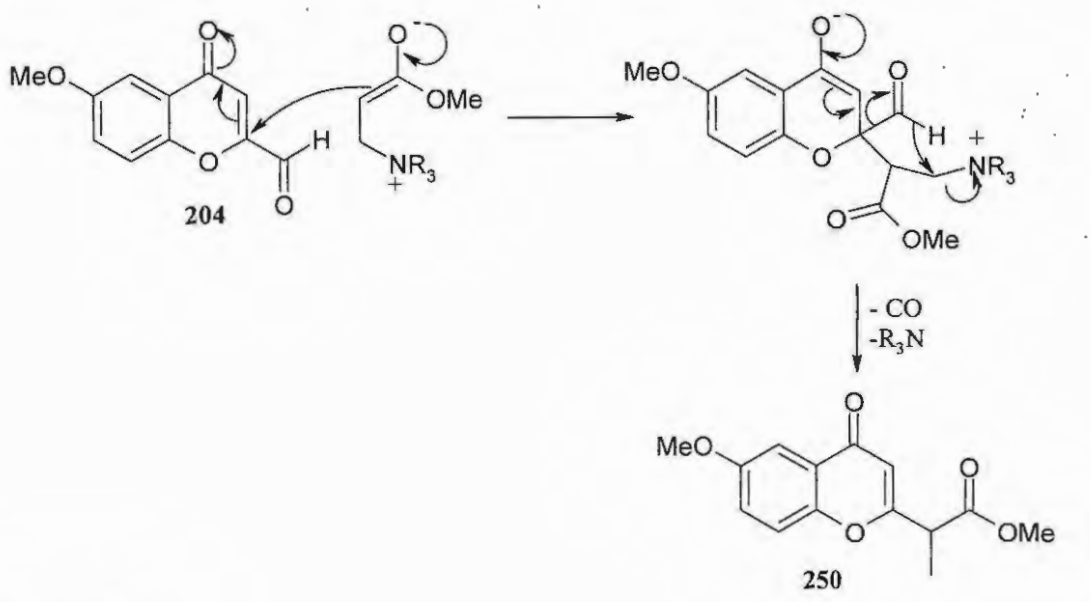

Scheme 57

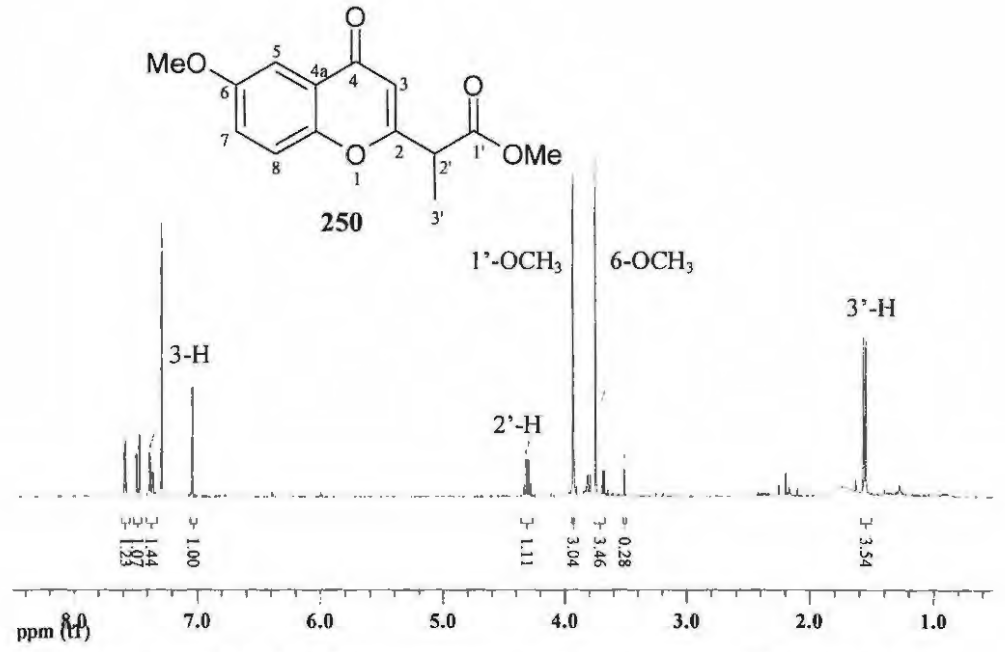

Figure 36. 400 MHz ^{1}H NMR spectrum of the compound **250** in $CDCl_3$.

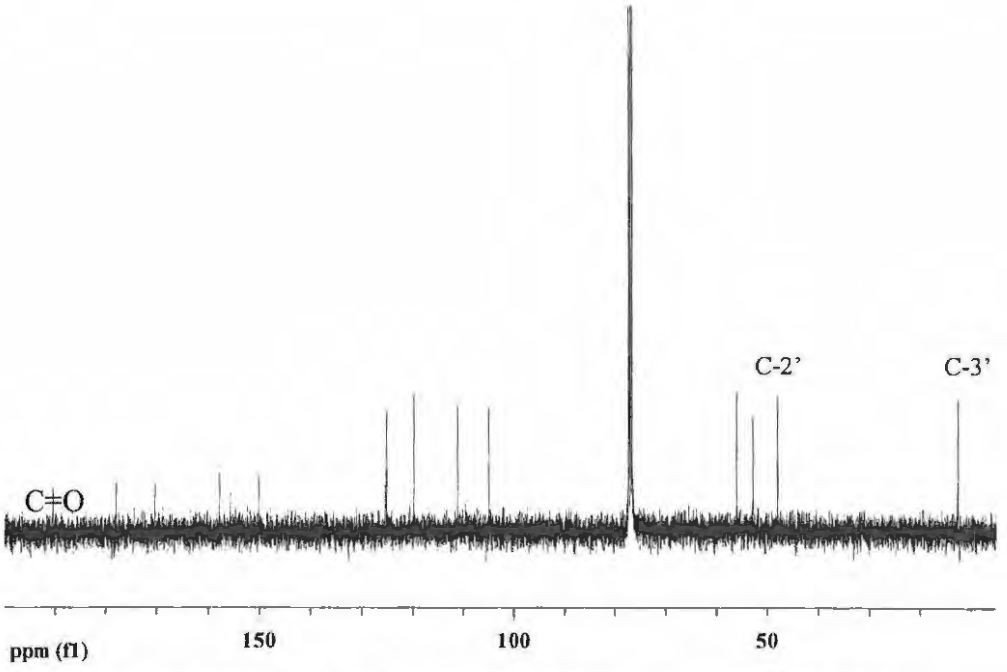

Figure 37. 100 MHz ^{13}C NMR spectrum of the compound **250** in $CDCl_3$.

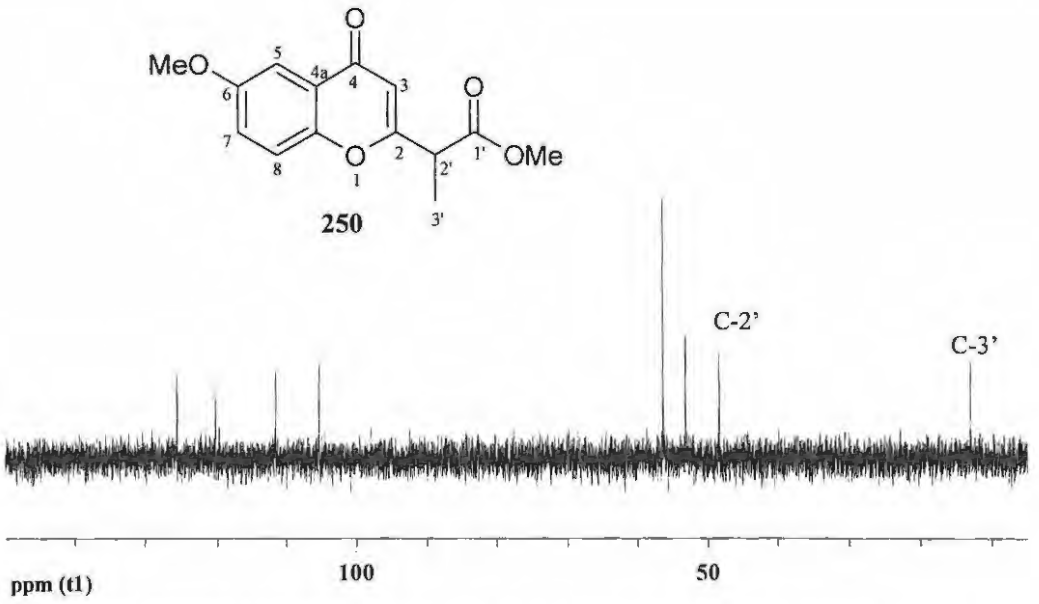

Figure 38. DEPT 135 NMR spectrum of the compound **250** in $CDCl_3$.

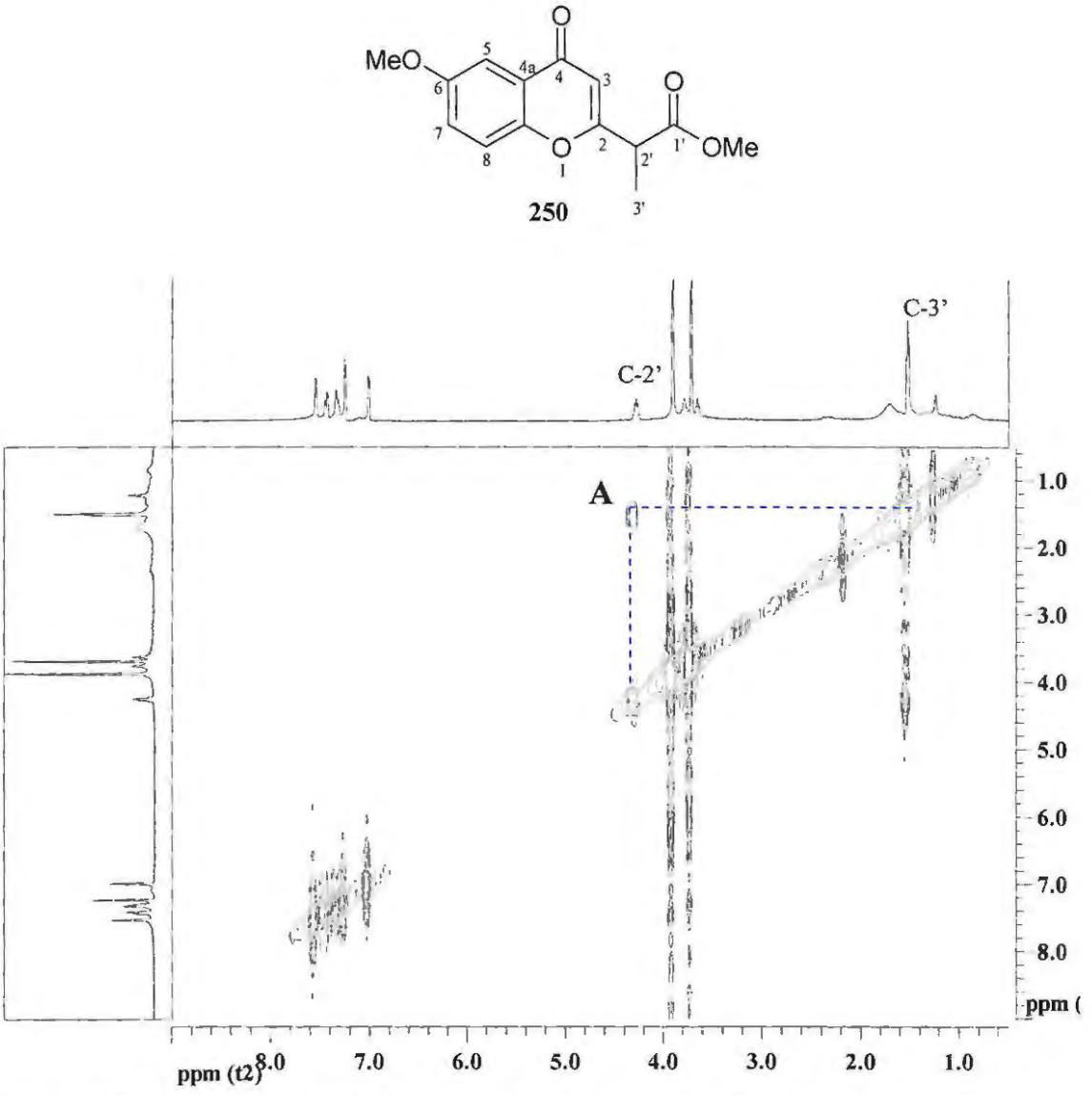

Figure 39. 400 MHz COSY NMR spectrum of the compound **250** in $CDCl_3$.

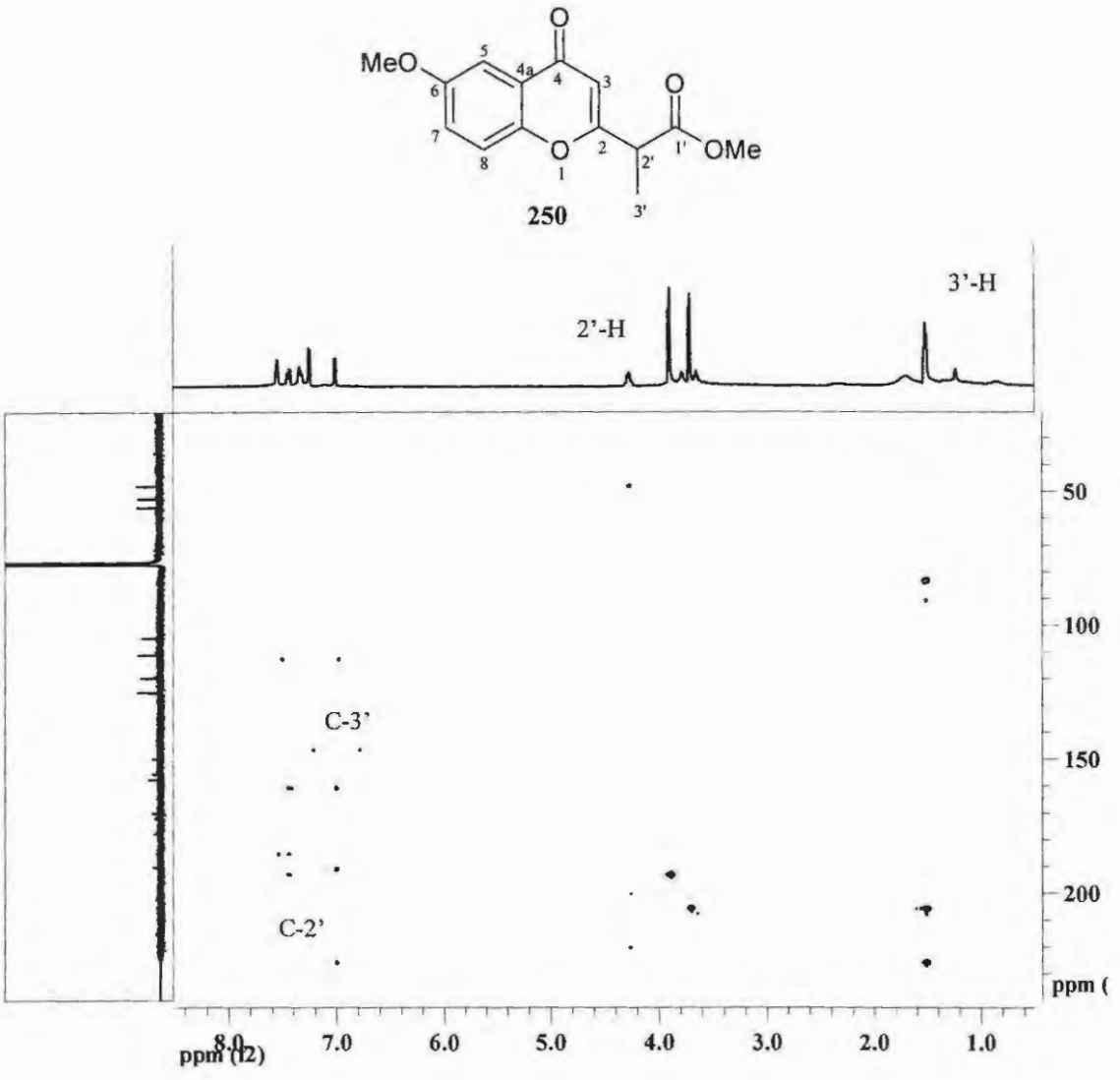

Figure 40. 400 MHz HMBC NMR spectrum of the compound **250** in $CDCl_3$.

2.2.2.3. Reaction of chromone-2-carbaldehydes with acrylonitrile

The chromone-2-carbaldehydes **91**, **202** and **204** were also reacted with acrylonitrile using 3-hydroxyquinuclidine as catalyst in a minimal volume of chloroform at room temperature for 24 hours **(Scheme 58)**. Purification of the crude products using flash chromatography failed to produce the expected Baylis-Hillman products **251-253** but, instead, afforded the interesting products **255-257** in yields ranging from 40 to 55% (Table 10). The proposed mechanism (**Scheme 59**) for the formation of these products **255-257** involves nucleophilic attack of the cyanide nitrogen in the zwitterionic enolate at the electrophilic C(2) centre instead of the aldehydic carbonyl carbon, followed by the cyclisation to yield product **254a** which tautomerises to **254b**. Hydration then affords product **254**. When either DABCO or DBU was used as the catalyst, the reaction did not take place, and when dichloromethane was used as solvent these interesting products (**255-257**) were obtained in lower yields ranging from 15 to 25%, but when either THF or DMF was used as solvent, the reaction did not take place at all. The reactions were repeated and monitored for 5 days but still did not afford the expected Baylis-Hillman products **251-253**. The isolated products **255-257** were characterized by spectroscopic (IR, 1- and 2-dimensional NMR) and elemental (HREIMS) analysis.

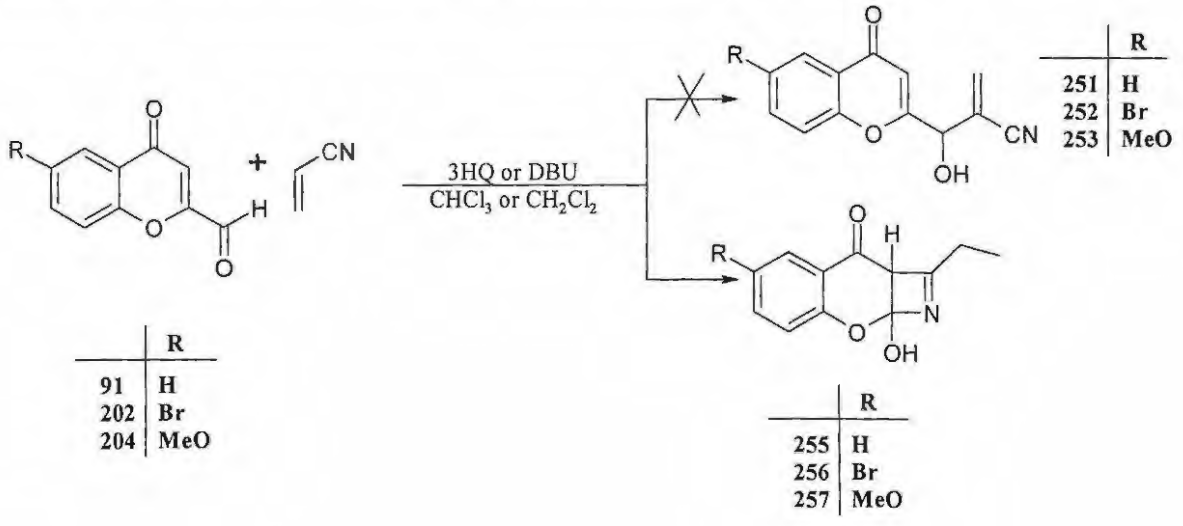

	R
91	H
202	Br
204	MeO

	R
251	H
252	Br
253	MeO

	R
255	H
256	Br
257	MeO

Scheme 58

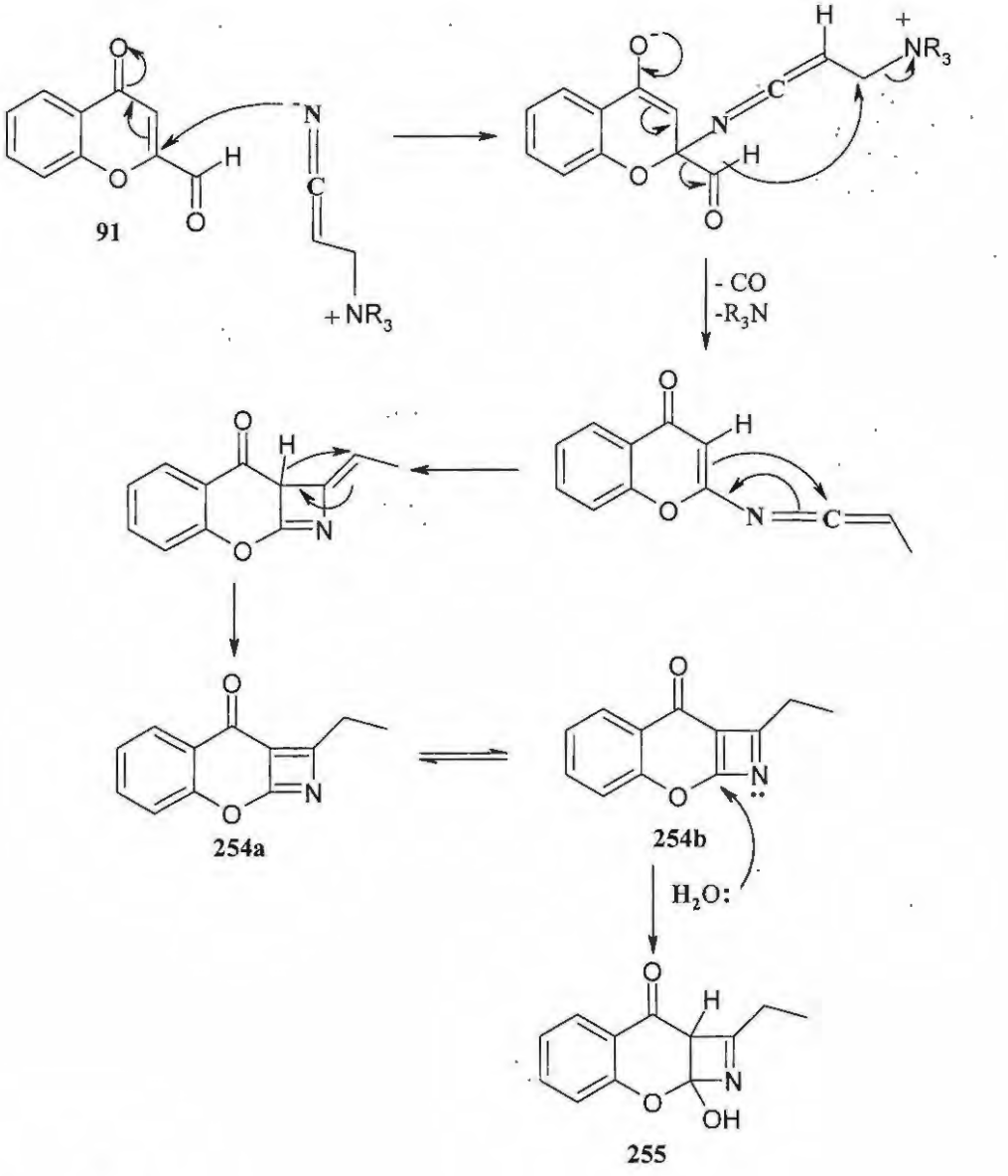

Scheme 59

Table 10. Isolated yields (%) of compounds **255-257** using different solvents.

R	Compound	$CHCl_3$	CH_2Cl_2
H	**255**	47	22
Br	**256**	40	15
MeO	**257**	55	25

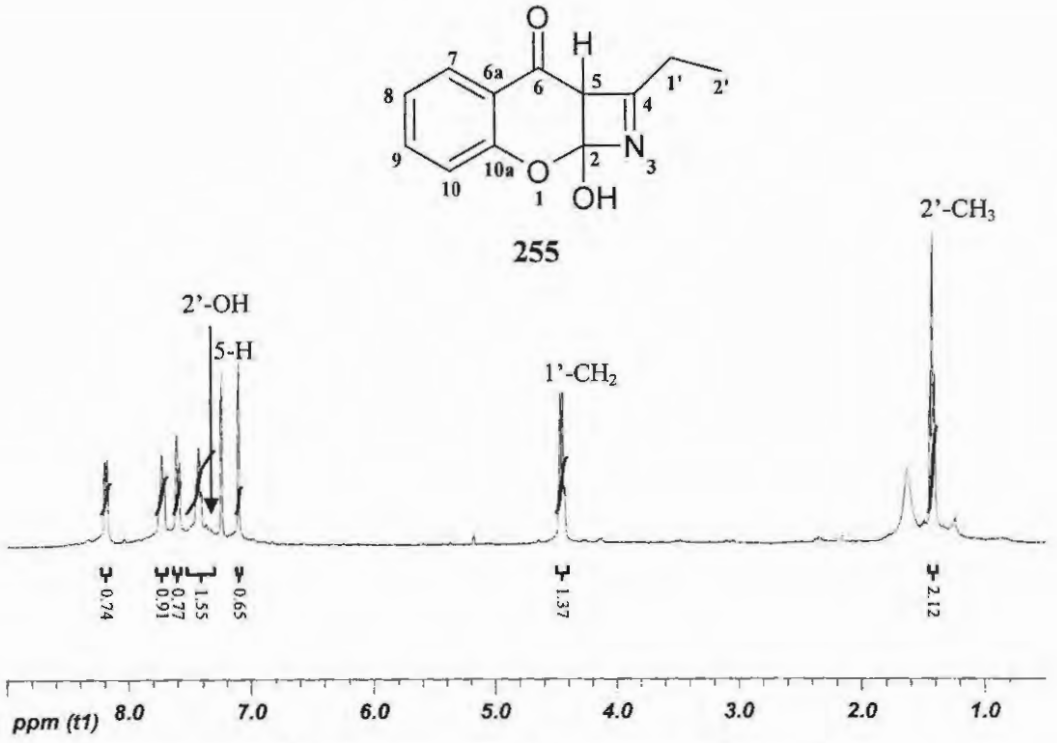

Figure 41. 400 MHz ^{1}H NMR spectrum of compound **255** in $CDCl_3$.

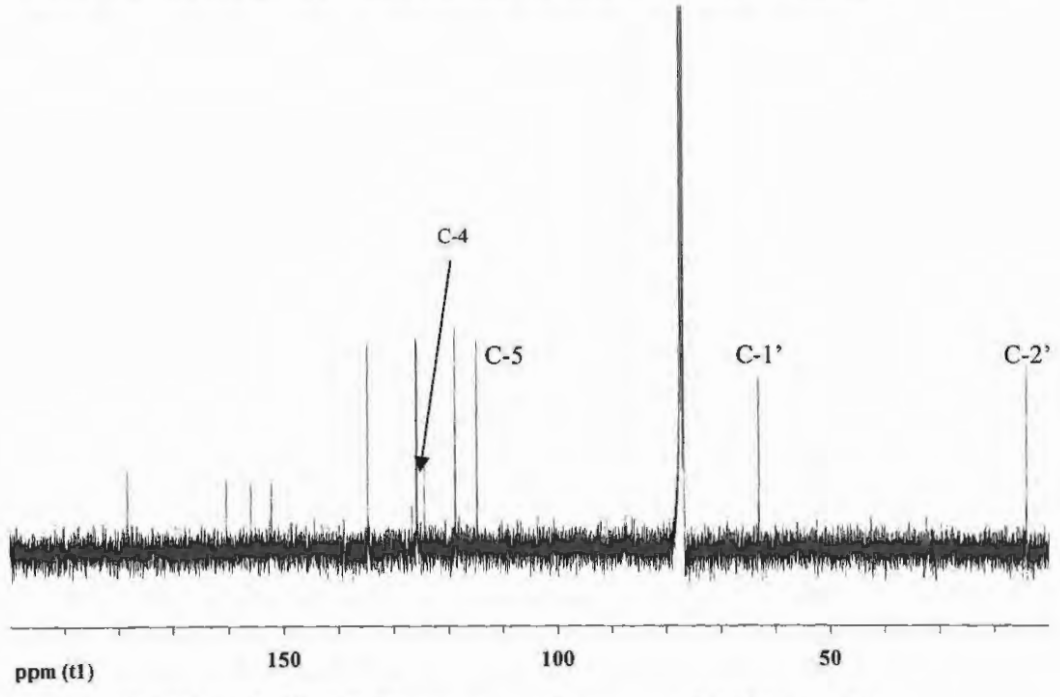

Figure 42. 100 MHz ^{13}C NMR spectrum of compound **255** in $CDCl_3$.

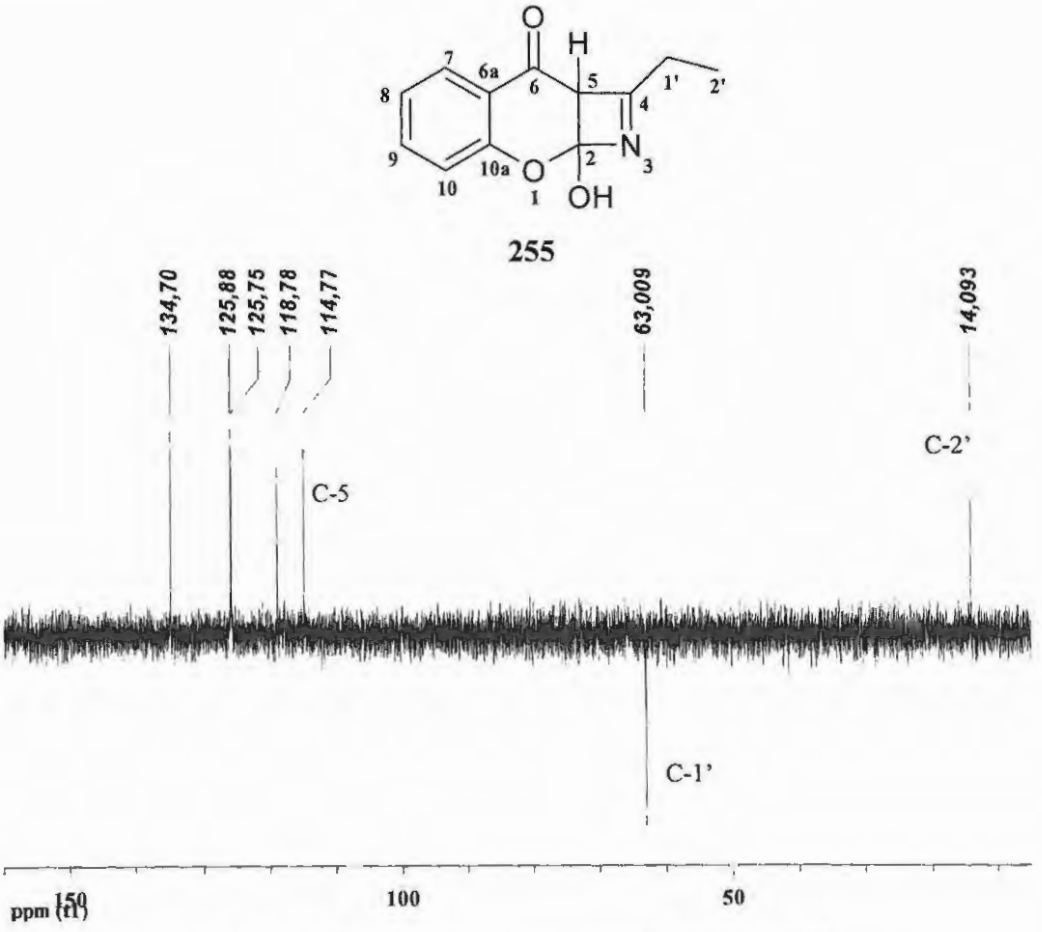

Figure 43. DEPT 135 NMR spectrum of compound **255** in $CDCl_3$.

For example, the ^1H NMR spectrum (Figure 41) of compound **255** reveals a triplet at 1.43 ppm which corresponds to the 2'-methyl protons, a quartet at 4.46 ppm which corresponds to the 1'-methylene protons, a singlet at 7.11 ppm which corresponds to the 5-methine proton and a broad signal at 7.36 ppm corresponding to the hydroxyl proton. The ^{13}C NMR spectrum (Figure 42) reveals 12 carbon signals as expected. The methyl carbon C-2' resonates at 14.1 ppm, the methylene carbon C-1' at 63.0 ppm, the methine carbon C-5 at 114.8 ppm, the imine carbon C-4 at 124.4 ppm and the carbonyl carbon at 178.4 ppm. The DEPT 135 spectrum (Figure 43) confirms the presence of the methyl carbon C-2', the methylene carbon C-1' and the presence of four five methine carbons

with C-5 resonates at 114.8 ppm. The COSY spectrum (Figure 44) reveals the vicinal coupling (at the cross peak **A**) between the 2' methyl and the 1'-methylene protons. The HMQC spectrum (Figure 45) reveals that in cross peak **A** that the 2'-methyl protons are bonded to the carbon that resonates at 14.1 ppm, cross peak **B** reveals that the 1'-methylene protons are bonded to the carbon that resonates at 63.0 ppm, and cross peak **C** reveals that the 5-methine proton is bonded to the carbon that resonates at 114 ppm. The HMBC spectrum (Figure 46) was also used to support the structural assignment with 1'-methylene protons connects to C-4 and 5-methine proton connects to C-4, C-2 and carbonyl carbon.

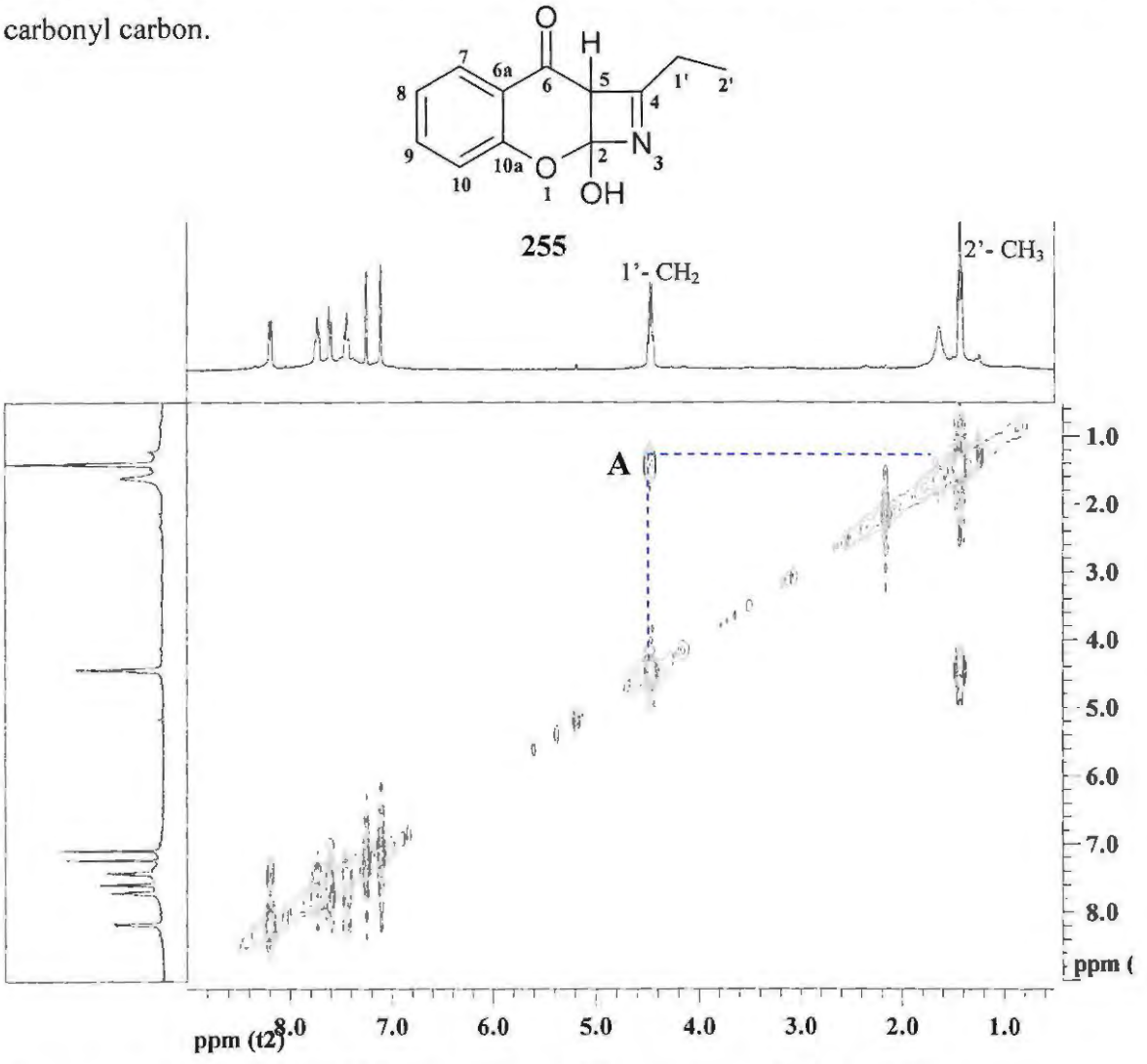

Figure 44. 400 MHz COSY NMR spectrum of the compound **255** in $CDCl_3$.

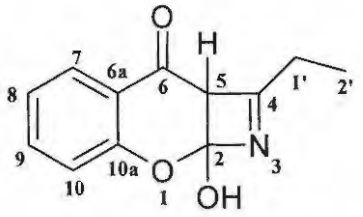

255

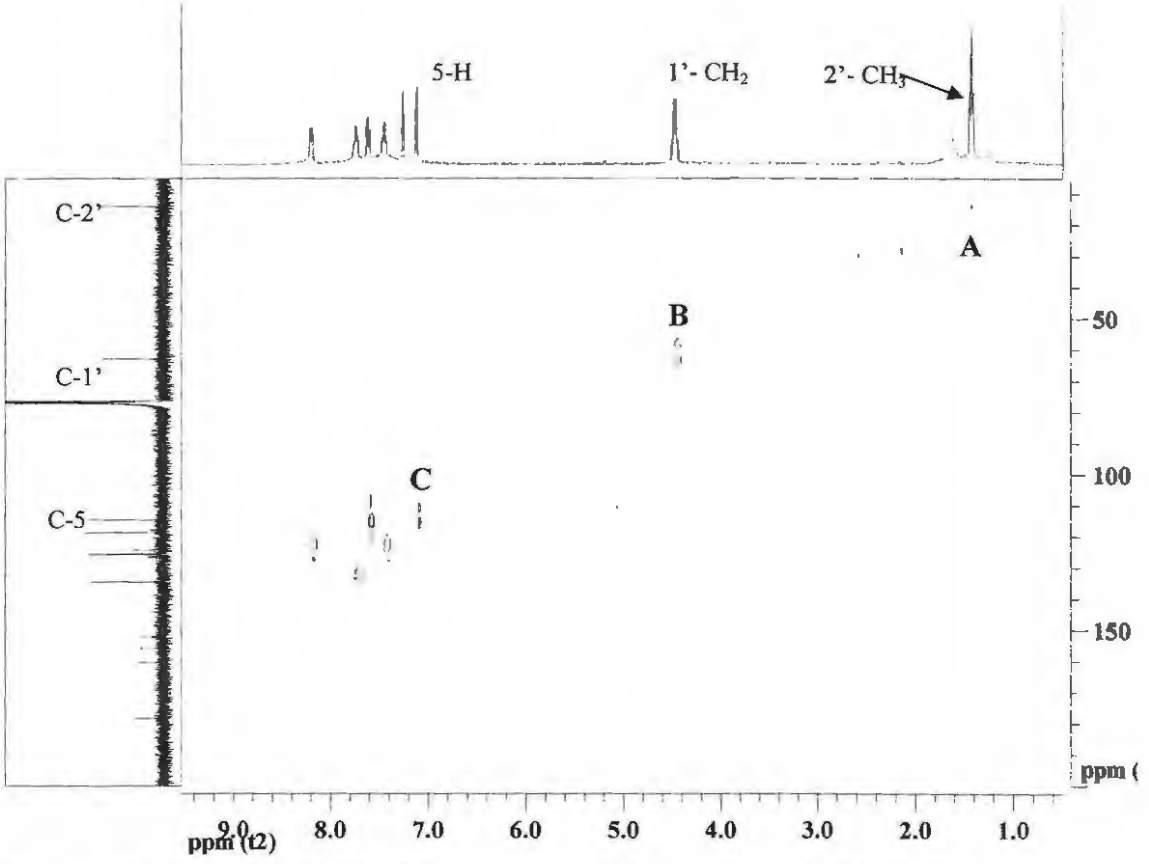

Figure 45. 400 MHz HMQC NMR spectrum of the compound **255** in $CDCl_3$.

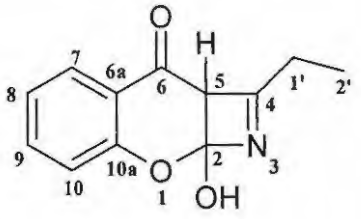

255

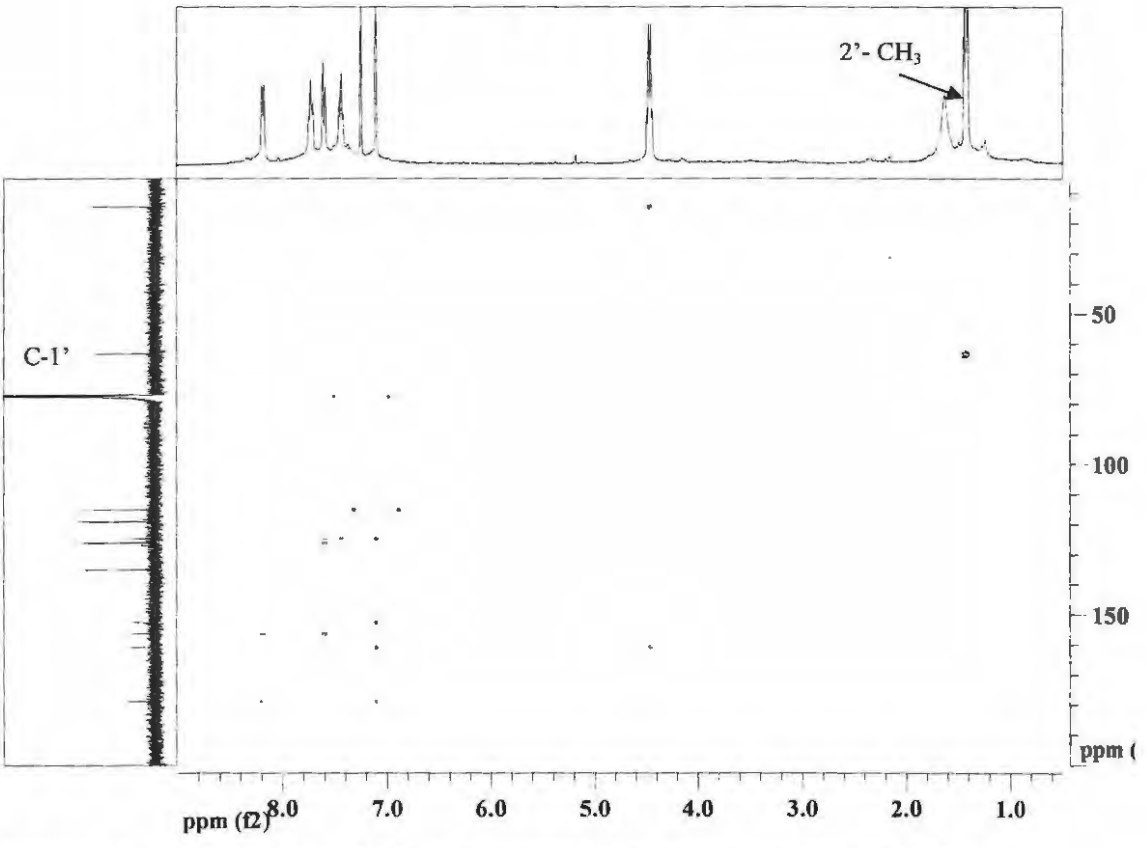

Figure 46. 400 MHz HMBC NMR spectrum of the compound **255** in $CDCl_3$.

2.3 Aza-Michael reactions of Baylis-Hillman products with amine derivatives

These reactions involve the intermolecular addition of nitrogen-centered nucleophiles to a suitably activated alkenes, under strongly basic conditions either in the presence or absence of a catalyst.[189] They provide a convenient method for the formation of β-amino carbonyl compounds and for generating carbon-nitrogen bonds.[190-194] In the present study, the approach has been applied to Baylis-Hillman derived α, β-unsaturated carbonyl compounds or nitriles.

2.3.1 Reactions of Baylis-Hillman products with (S)-benzylcysteamine hydrochloride

The series of Baylis-Hillman products **212-216** were treated with (*S*)-benzylcysteamine hydrochloride and sodium acetate in EtOH at 25°C for 6 weeks (**Scheme 60**). Purification of the crude products using flash chromatography afforded the corresponding aza-Michael products **258-262** in yields ranging from 35 to 51% (Table 11). It was observed that (*S*)-benzylcysteamine hydrochloride was insoluble in most organic solvent and it was decided to explore use of the amine. This was first achieved by treating the hydrochloride salt with aqueous sodium hydroxide and extracting the free amine into diethyl ether. Evaporation of organic solvent afforded the free amine, (*S*)-benzylcysteamine, as an oil, some of which crystallized to give white needles. The reactions (**Scheme 60**) were repeated under similar conditions but employing the free amine, (*S*)-benzylcysteamine. The same products **258-262** were obtained but, surprisingly, the yields were lower, ranging from 15 to 45%. It was then decided to neutralize the (*S*)-benzylcysteamine hydrochloride *in situ*. Thus, the Baylis-Hillman products **212-216** were treated with (*S*)-benzylcysteamine hydrochloride and sodium acetate (NaOAc) in the presence of tetrabutylammonium bromide, (TBAB), as catalyst, in EtOH at 25°C. It was found that the reaction time could be effectively reduced to 5 days, but still afford the chromatographed aza-Michael products **258-262** in yields

ranging from 40 to 60% (Table 11). When the ionic liquid, 3-butyl-1-methylimidazoleboranetetrafluoride ($BmimBF_4$) was employed as catalyst in the presence of water, the reaction did not take place since the substrates **212-216** were insoluble in water. When the reactions were attempted in organic solvents such as chloroform, dichloromethane, THF, methanol and DMF, the substrates **212-216** were recovered unchanged due, it seems, to the fact that $BmimBF_4$ failed to dissolve. However, when the EtOH was used as the solvent, even though the 3-butyl-1-methylimidazolium tetrafluoroborate ($BmimBF_4$) appeared to be immiscible, the reaction took place and yielded products in purified yields ranging from 50 to 68% (Table 11). From the results summarized in Table 11 that the highest yields were obtained using $BmimBF_4$ in EtOH. The novel aza-Michael products **258-262** were fully characterized by spectroscopic (IR, 1- and 2-dimensional NMR) and elemental (HREIMS) analysis. The nitrile function in these compounds is, of course, capable of elaboration to, for example, amine or carboxylic acid groups. Such functional groups could hydrogen-bond with amino acid residues in the HIV-1 protease binding site. It should also be noted that a number of nitrile-containing compounds have been shown to exhibit useful pharmacological properties.

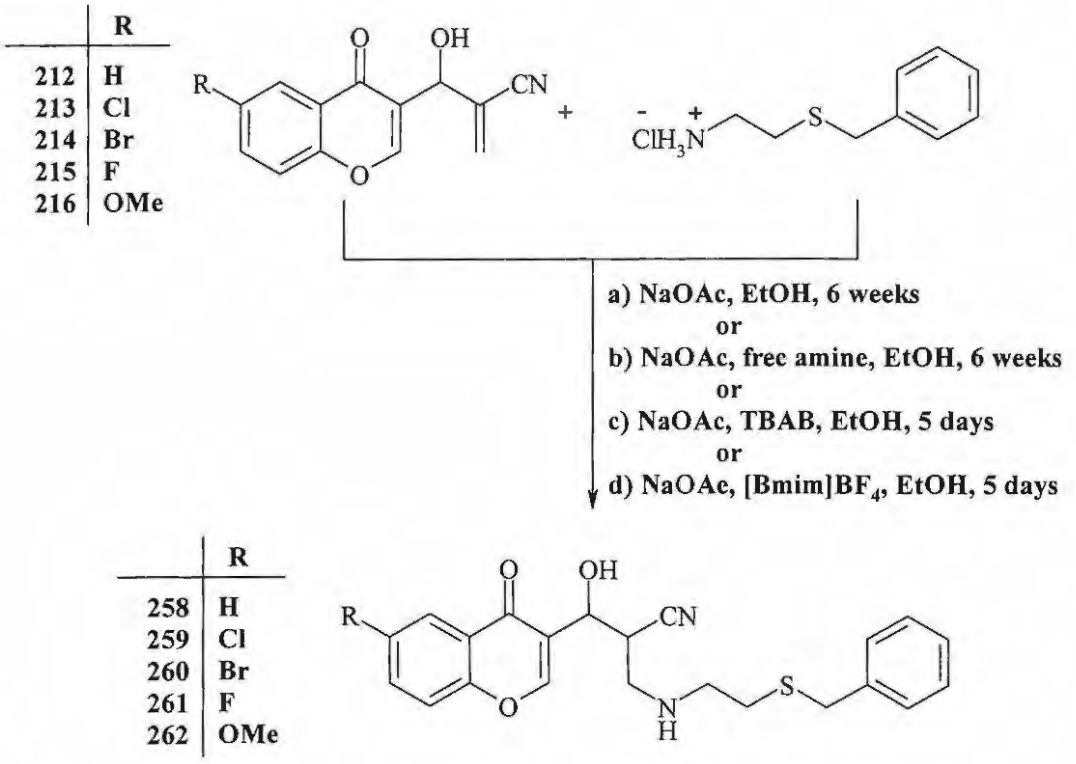

Scheme 60

Table 11. Isolated yields (%) of the aza-Michael adducts **258-262** obtained under various conditions.

R	Compound	A (6 weeks)	B (6 weeks)	C (5 days)	D (5 days)
H	**258**	51	45	51	68
Cl	**259**	46	40	48	64
Br	**260**	42	33	43	56
F	**261**	35	15	40	50
MeO	**262**	47	27	60	66

A = using the using hydrochloride amine salt; **B** = using the free amine;
C= using TBAB; **D**= using [bmim]BF_4

The ^{1}H NMR spectrum (Figure 47) of the aza-Michael product **258** reveals a triplet at 2.64 ppm which corresponds to the diastereotopic 6'–methylene protons, a multiplet at 3.15 ppm which corresponds to the 2'-methine proton, a multiplet at 3.21 ppm which

corresponds to the diastereotopic 5'–methylene protons, a doublet of doublets at 3.24 ppm corresponding to one hydrogen of the diastereotopic 4'–methylene group, a broad peak at 3.53 ppm which corresponds to the 4'-amine proton, a doublet of doublets at 3.57 ppm corresponding to another hydrogen of the 3'-methylene diastereotopic protons, a broad singlet at 3.73 ppm which corresponds to the diastereotopic 8'-methylene protons and a doublet at 4.98 ppm which corresponds to the 1'-methine proton. The series of signals in the region 7.21-7.27 ppm correspond to the aromatic protons and a broad signal at 10.93 ppm corresponds to the 1'hydroxyl proton. The ^{13}C NMR spectrums reveals 22 carbon signals as expected, and are assigned as indicated in (Figure 48).

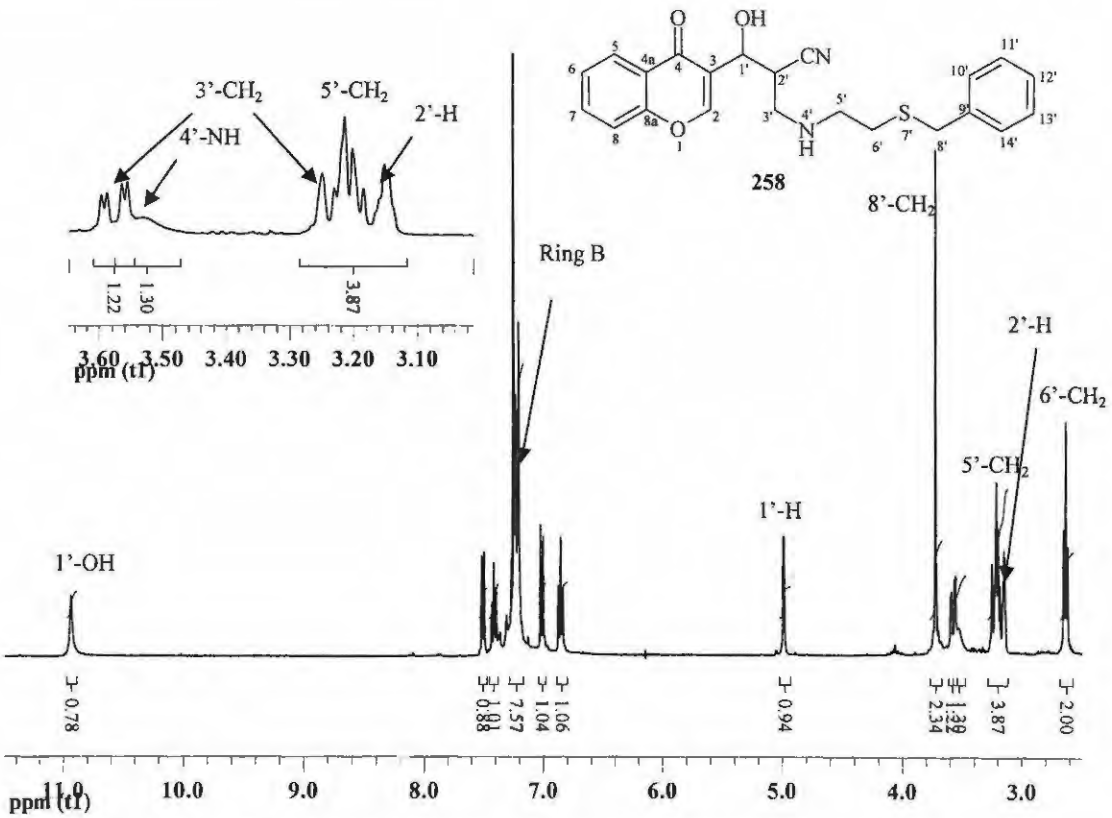

Figure 46. 400MHz ^1H NMR spectrum of the aza-Michael product **258** in $CDCl_3$.

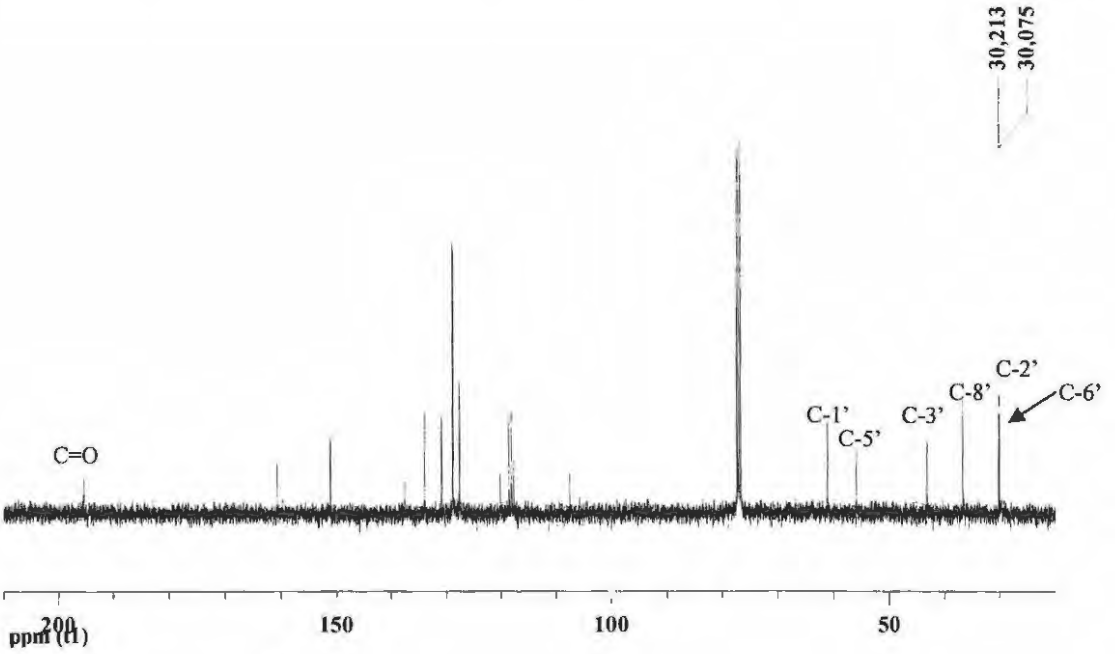

Figure 47. 100MHz ^{13}C NMR spectrum of the aza-Michael product **258** in $CDCl_3$.

The DEPT 135 spectrum (Figure 48) confirms the presence of four methylene carbons, C-6', C-8', C-3' and C-5' which resonate at 30.1, 30.2, 43.2 and 55.9 ppm, respectively. In the HMQC spectrum (Figure 49) the cross peak **A** reveals that the 2'-methine proton is bonded to the carbon at 30.2 ppm, while cross peak **B** reveals that the diastereotopic 3'-methylene protons are bonded to the carbon that resonates at 43.2 ppm, cross peak **C** reveals that the 1'-methine proton is bonded to the carbon resonating at 61.1 ppm. In the HMBC spectrum (Figure 50), the cross peak **A** reveals that the diastereotopic 2'-methine proton is coupling with 3'-methylene carbon through a two-bond connectivity ($^2J_{C,H}$), while the cross peak **B** reveals that the diastereotopic 3'-methylene protons are coupling with the 1'-methine carbon through three-bond connectivity ($^3J_{C,H}$).

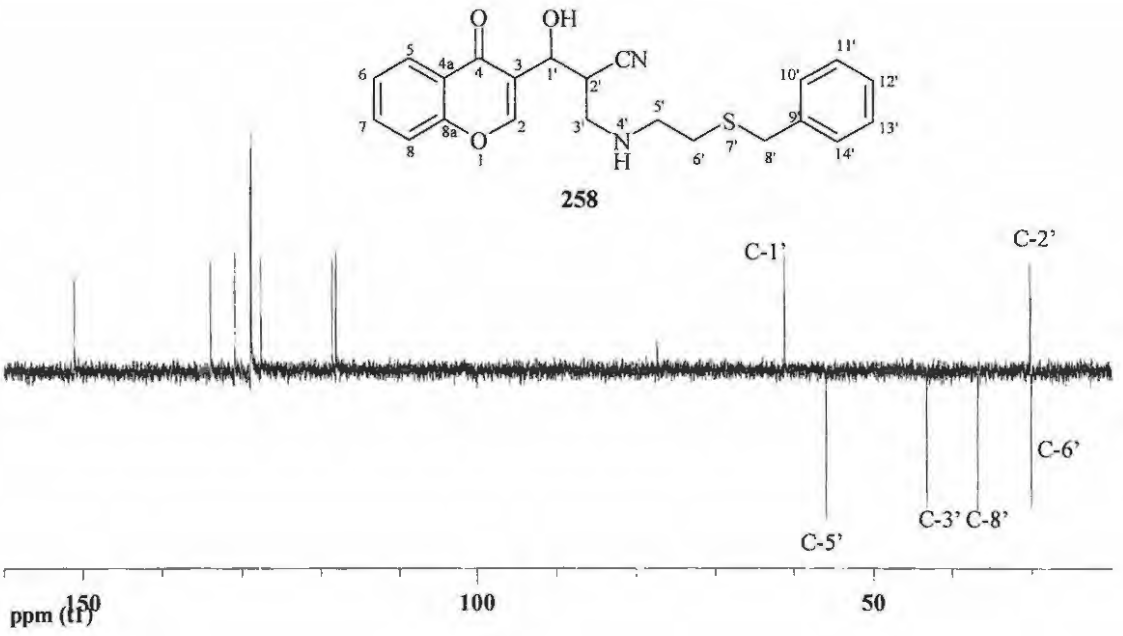

Figure 48. DEPT 135 NMR spectrum of the aza-Michael product **258** in $CDCl_3$.

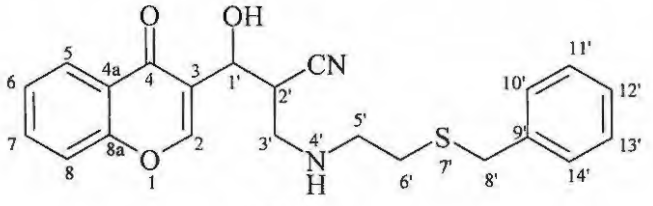

258

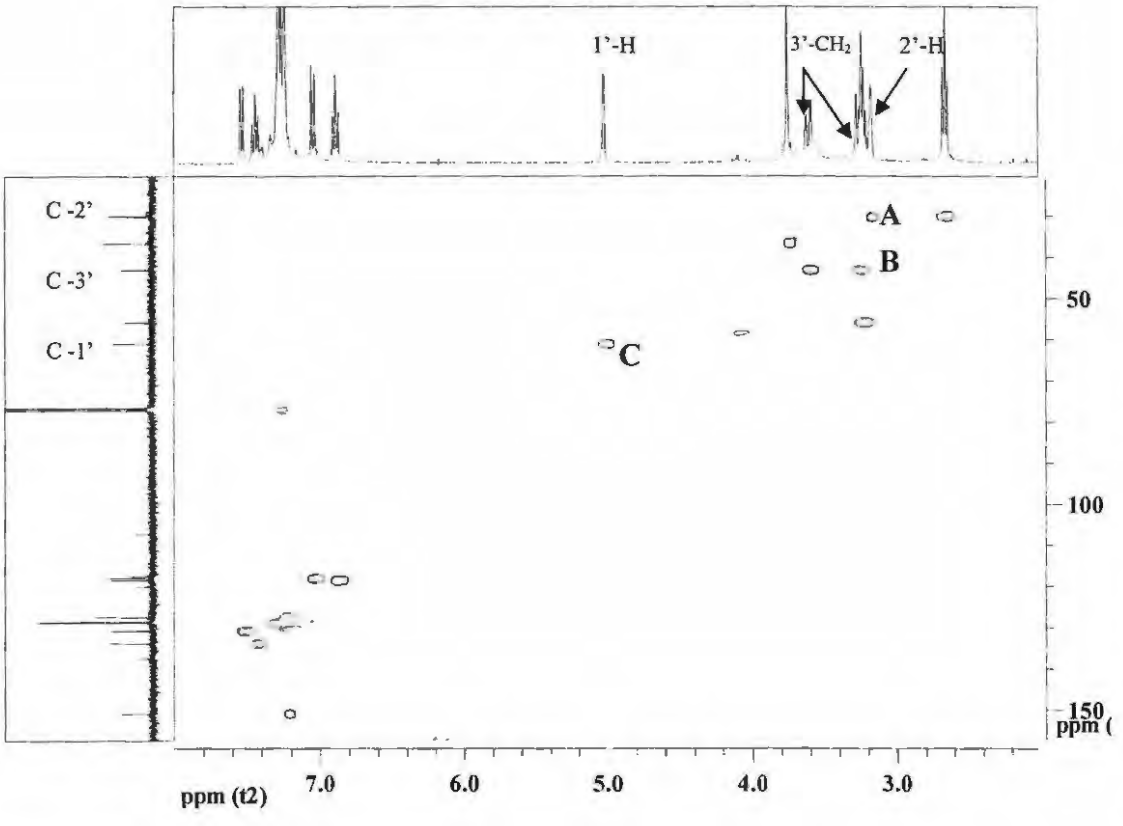

Figure 49. HMQC NMR spectrum of the aza-Michael product **258** in $CDCl_3$.

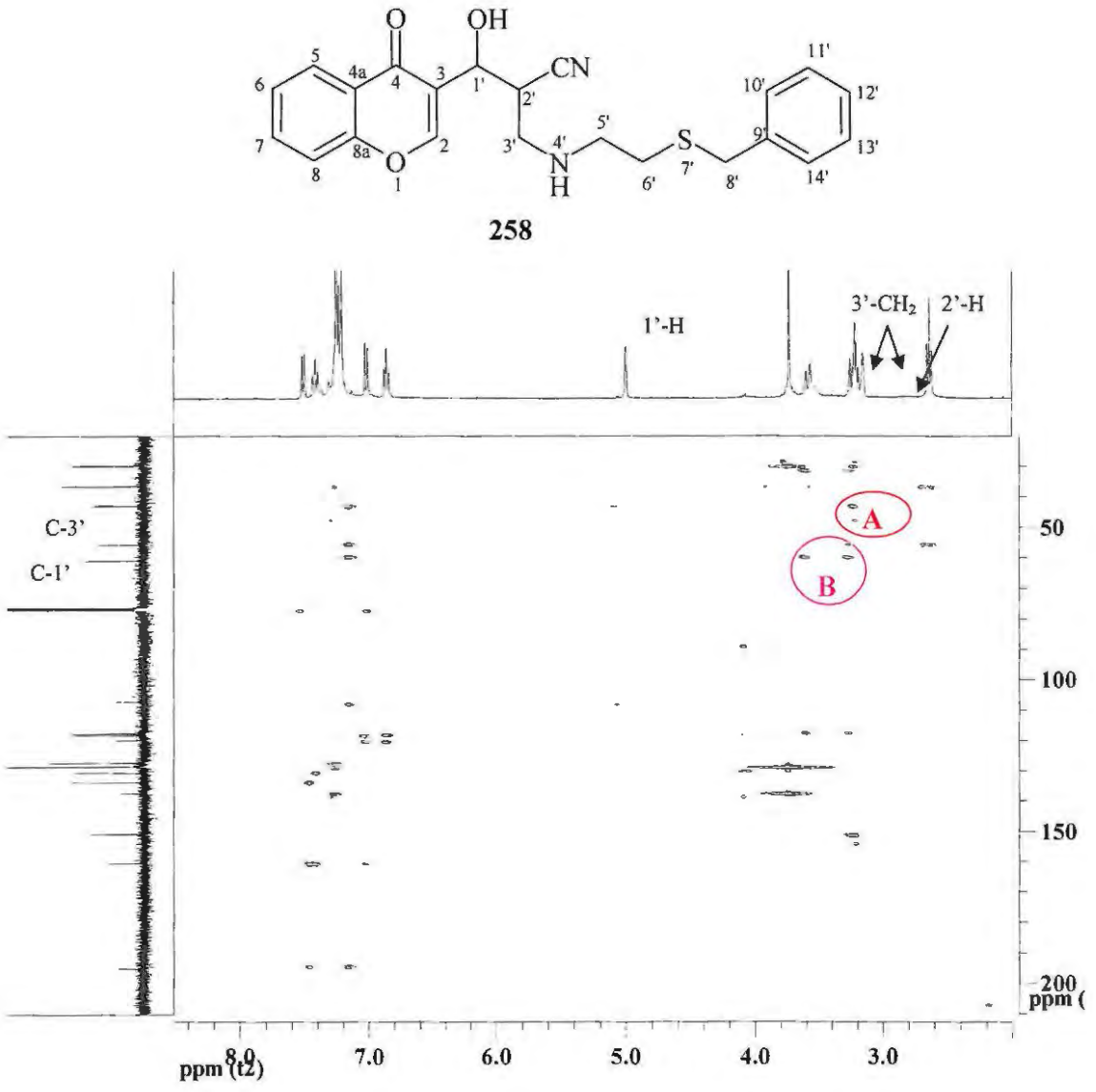

Figure 50. HMBC NMR spectrum of the aza-Michael product **258** in $CDCl_3$.

2.3.2 Reactions of Baylis-Hillman products with ethyl glycinate hydrochloride

The Baylis-Hillman products **212**, **213** and **215** were reacted with ethyl glycinate hydrochloride and sodium acetate in EtOH at 25°C for 6 weeks (**Scheme 61**). Purification of the crude products using flash chromatography afforded the aza-Michael products **263-265** in yields ranging from 15 to 45% (Table 12). The hydrochloride salt was again insoluble in most organic solvents and, as with the reaction with (*S*)-benzylcysteamine hydrochloride, alternative approaches were explored. When reactions (**Scheme 61**) were repeated under similar conditions using free amine, ethyl glycinate (produced by neutralizing ethyl glycinate hydrochloride salt), the same products **263-265** were obtained in yields ranging from 41 to 54%. It was also decided to neutralize the (*S*)-benzylcysteamine *in situ*. Thus, the Baylis-Hillman products **212**, **213** and **215** were treated with ethyl glycinate hydrochloride and sodium acetate in the presence of tetrabutylammonium bromide (TBAB) as catalyst, in EtOH at 25°C for 5 days. Purification using the flash chromatography afforded the aza-Michael products **263-265** in yields ranging from 50 to 60% (Table 12). When an ionic liquid, 3-butyl-1-methylimidazolium tetrafluoroborate (BmimBF$_4$), was employed as catalyst in the presence of sodium acetate in EtOH, the yields ranged from 56 to 68% (Table 12). When MeOH or THF were used as the solvent in the presence of BmimBF$_4$ the reaction did not take place. These novel aza-Michael products **263-265** were fully characterized by spectroscopic (IR, 1- and 2-dimensional NMR) and elemental (HREIMS) analysis.

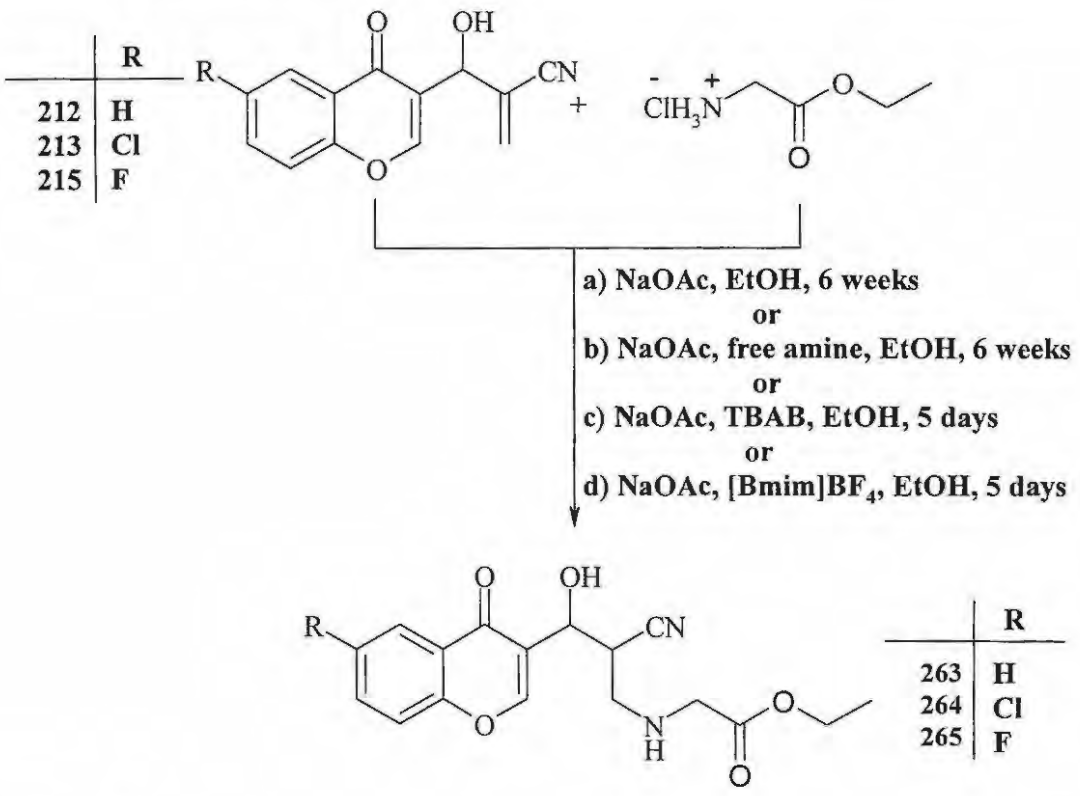

Scheme 61

Table 12. Isolated yields (%) of the aza-Michael products **263-265** under various conditions.

R	Compound	A after 6 weeks	B after 6 weeks	C after 5 days	D after 5 days
H	**263**	45	48	58	68
Cl	**264**	37	54	65	64
F	**265**	15	41	50	56

A = using the using hydrochloride amine salt; **B** = using the free amine;
C= using TBAB; **D**= using [bmim]BF_4

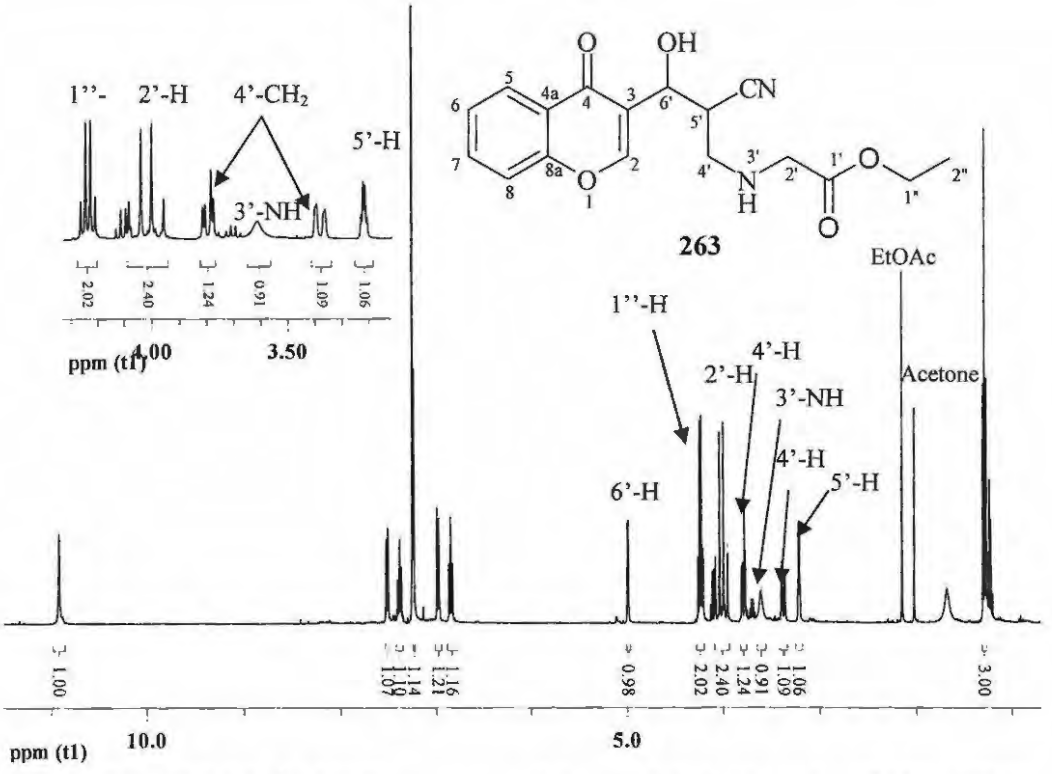

Figure 51. 400 MHz ^{1}H NMR spectrum of the aza-Michael product **263** in $CDCl_3$.

The ^{1}H NMR spectrum (Figure 51) of the aza-Michael **263** reveals a triplet at 1.29 ppm which corresponds to the 2''–methyl protons, a multiplet at 3.21 ppm corresponding to the 5'-methine proton, a doublet of doublets at 3.38 ppm corresponding to one of the 4'-methylene protons, a broad singlet at 3.61 ppm which corresponds to NH, another doublet of doublets at 3.79 corresponding to the second 4'-methylene proton, a doublet at 4.99 ppm corresponding to the 6'-methine proton and a broad signal at 10.9 ppm which corresponds to the 6'-hydroxyl proton. The ^{13}C NMR spectrum (Figure 52) reveals 17 carbon signals as expected. The 5'-methine carbon resonates at 30.3 ppm, the 4'-methylene carbon at 44.2 ppm, the 6'-methine carbon at 61.0 ppm and the 1'- and 4-carbonyl carbons at 167.9 and 195.9 ppm, respectively. The DEPT 135 spectrum (Figure 53) confirms the presence of three methylene carbons, C-2', C-4' and C-1'', which resonate at 57.1, 44.2 and 62.2 ppm, respectively, and the two 5'- and 6'-methine carbons at 30.3 and 61.0 ppm.

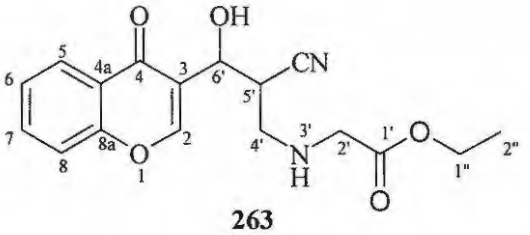

263

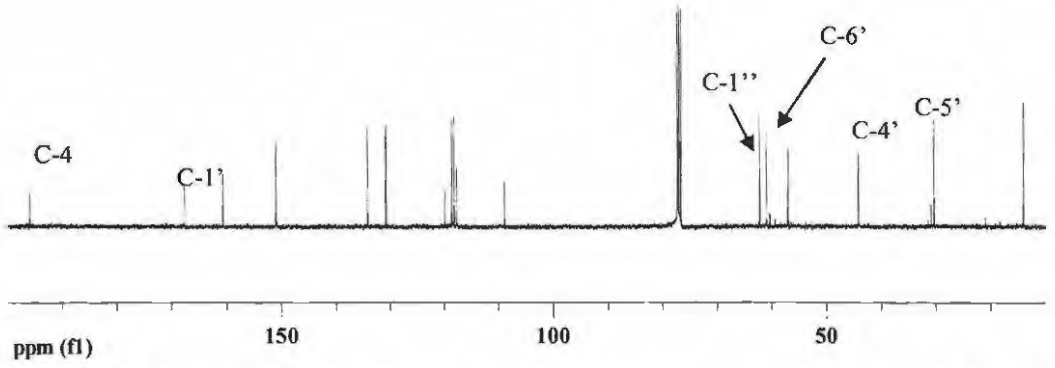

Figure 52. 100 MHz ^{13}C NMR spectrum of the new aza-Michael product **263** in $CDCl_3$.

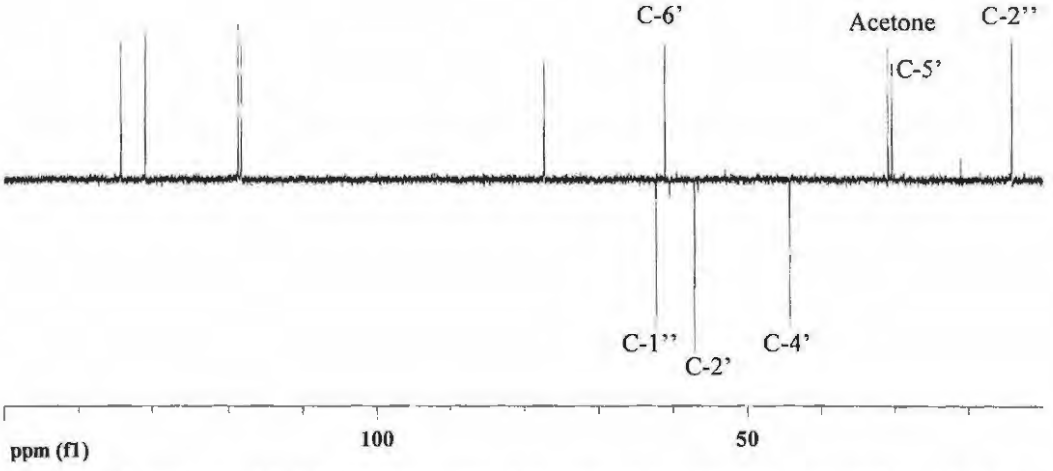

Figure 53. DEPT 135 NMR spectrum of the aza-Michael product **263** in $CDCl_3$.

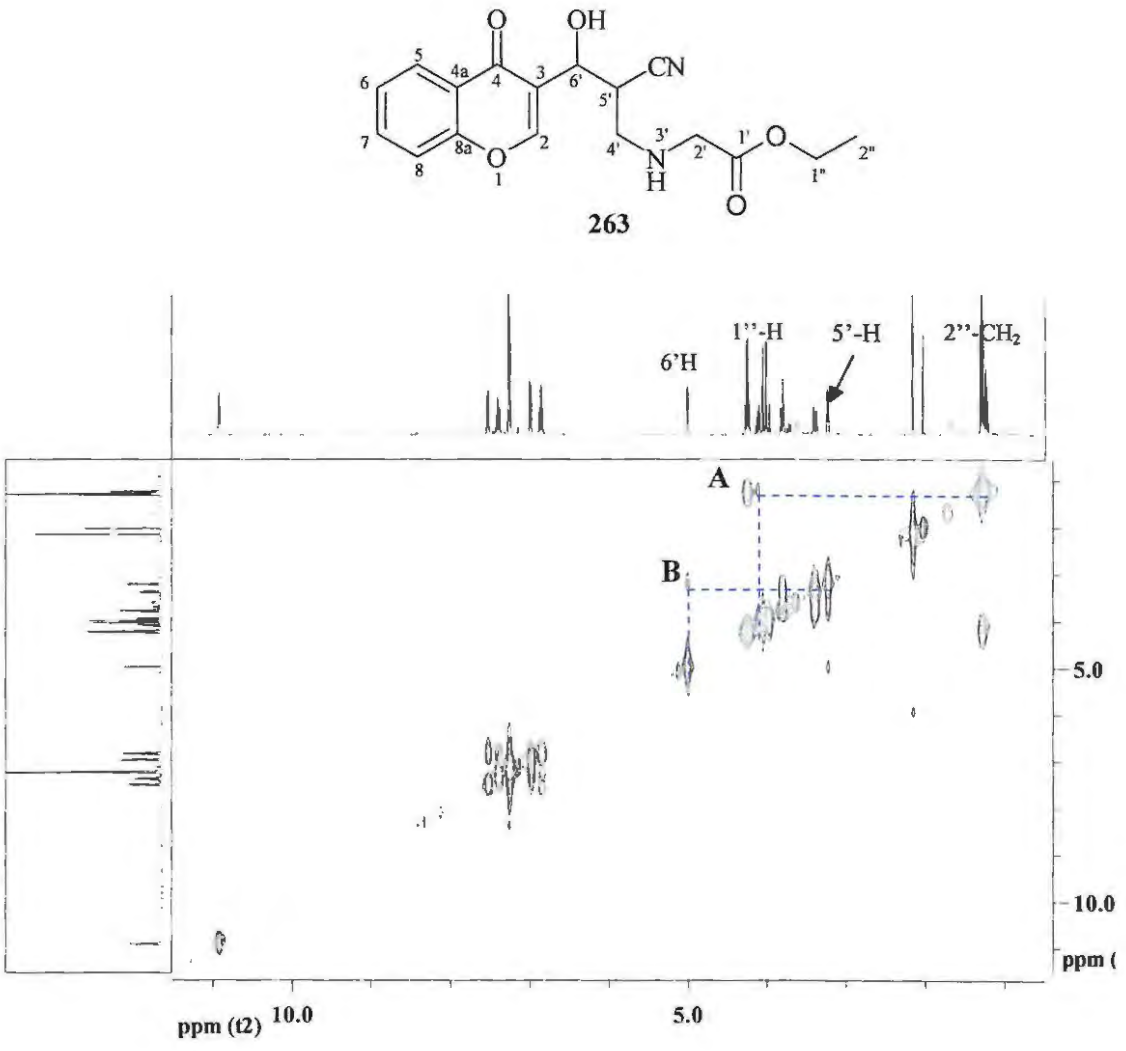

Figure 54. COSY NMR spectrum of the aza-Michael product **263** in $CDCl_3$.

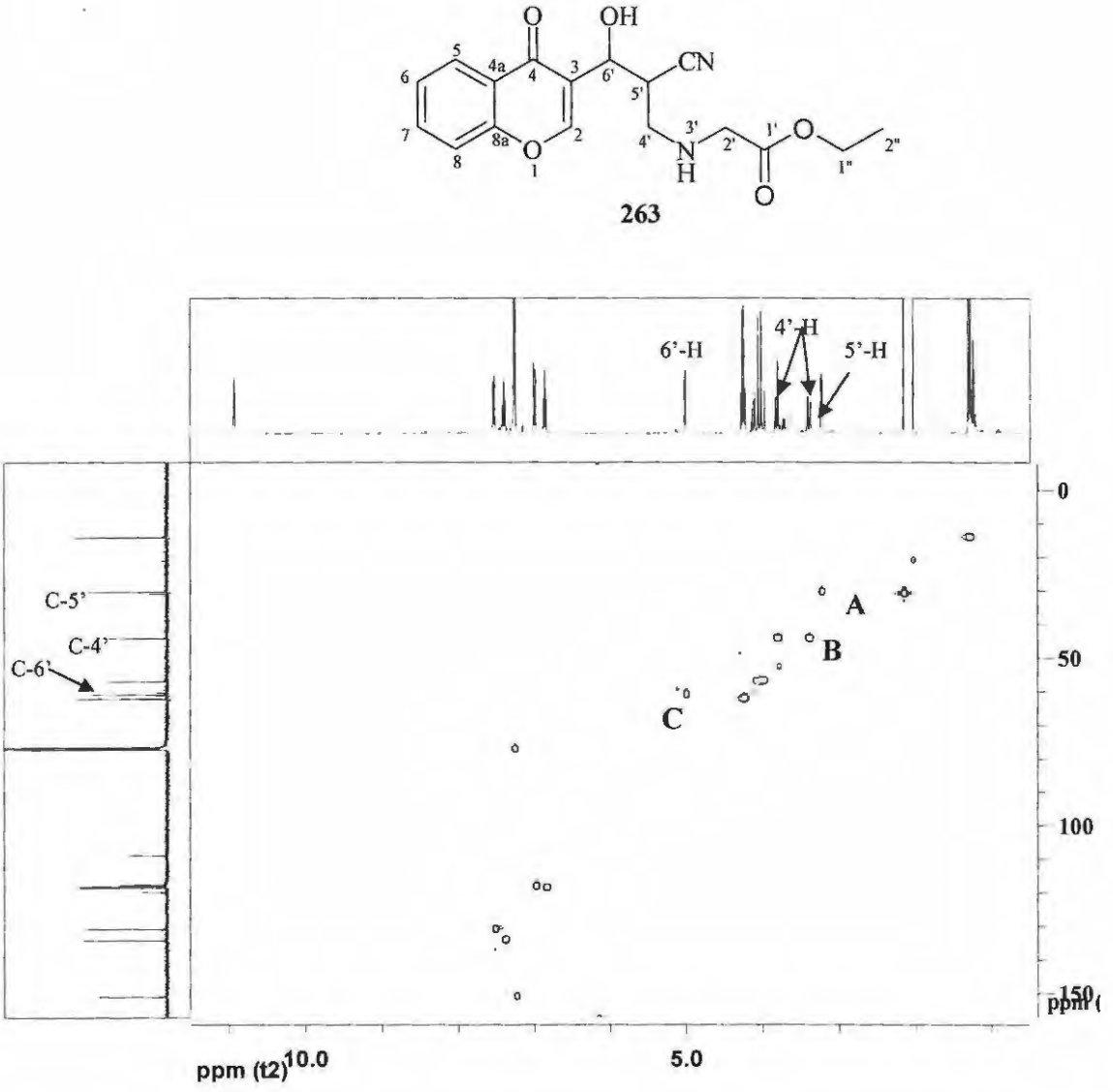

Figure 55. HMQC NMR spectrum of the aza-Michael product **263** in $CDCl_3$.

The COSY spectrum (Figure 54) reveals vicinal coupling (**A**) between the 2''-methyl protons and the diastereotopic 1''-methylene protons, and also another vicinal coupling (**B**) between the 5'-methine proton and the 6'-methine proton.. In the HMQC spectrum (Figure 55) the cross peak **A** reveals that the 5'-methine proton is bonded to the carbon that resonates at 62.2 ppm, cross peaks **B** reveal that 4'-methylene diastereotopic protons are bonded to carbon that resonates at 44.2 ppm, and the cross peak **C** reveals that the 6'-methine proton is bonded to carbon that resonates at 61.0 ppm.

2.3.3 Reaction of Baylis-Hillman products with D-serine methyl ester hydrochloride

The Baylis-Hillman products **212**, **213** and **216** were reacted with D-serine methyl ester hydrochloride and sodium acetate in EtOH at 25°C for 6 weeks (**Scheme 62**). Purification of the crude products using flash chromatography afforded the aza-Michael products **266-268** in yields ranging from 15 to 31% (Table 13). However, when these reactions were run for 5 days using similar conditions and TBAB as catalyst the aza-Michael products **266-268** were obtained in yields ranging from 20 to 40% (Table 13). The aza-Michael products **266-268** were fully characterized by spectroscopic (IR, 1- and 2-dimensional NMR) and elemental (HREIMS) analysis.

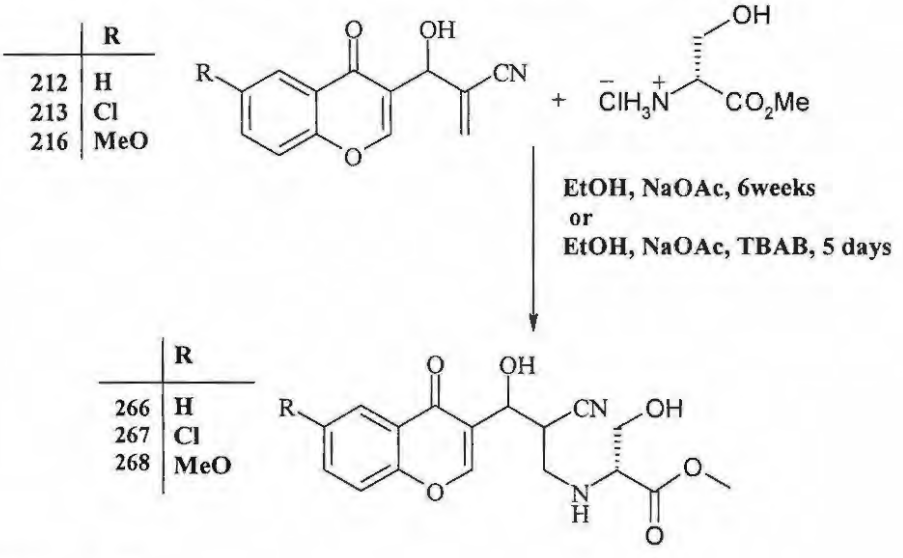

Scheme 62

Table 13. Isolated yields (%) of the aza-Michael compounds **266-268** obtained under various conditions.

R	Compound	After 6 weeks using NaOAc	After 5 days using TBAB
H	**266**	31	40
Cl	**267**	15	20
MeO	**268**	27	33

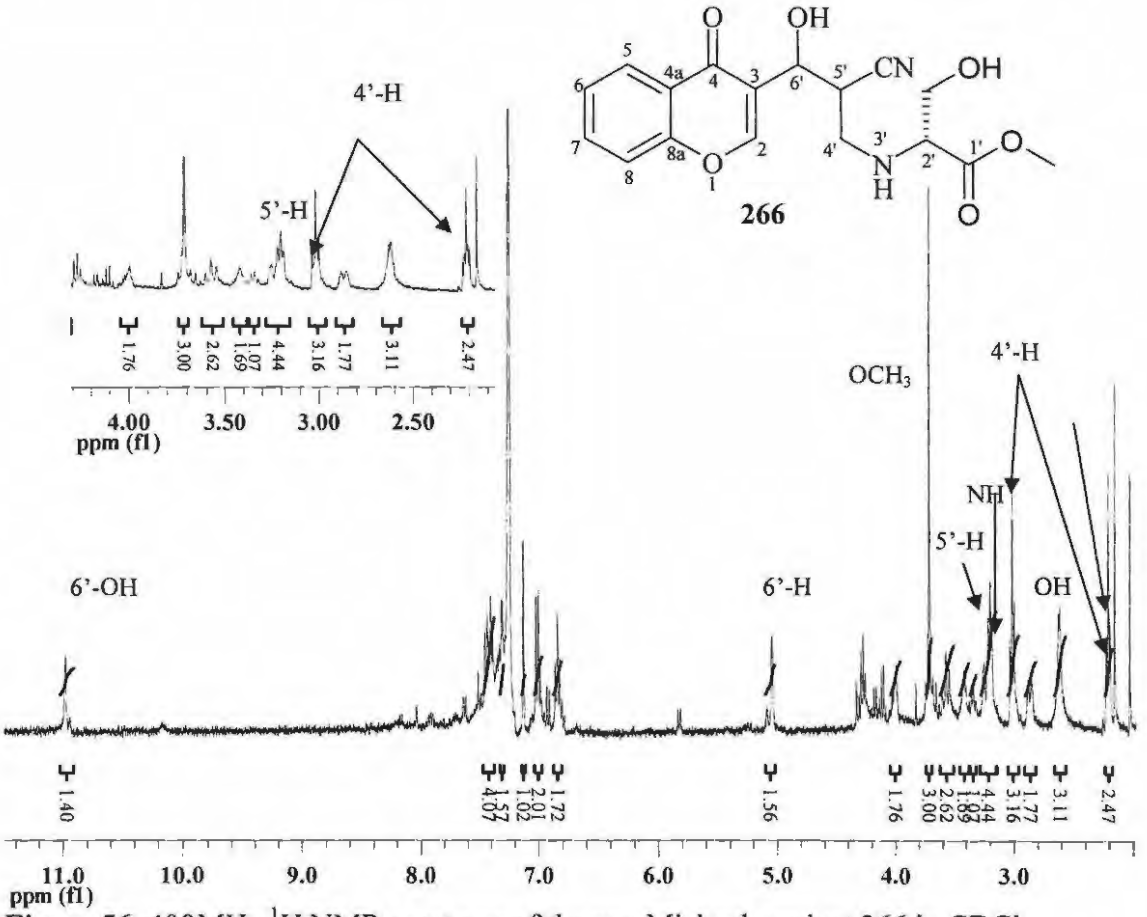

Figure 56. 400MHz ^{1}H NMR spectrum of the aza-Michael product **266** in $CDCl_3$.

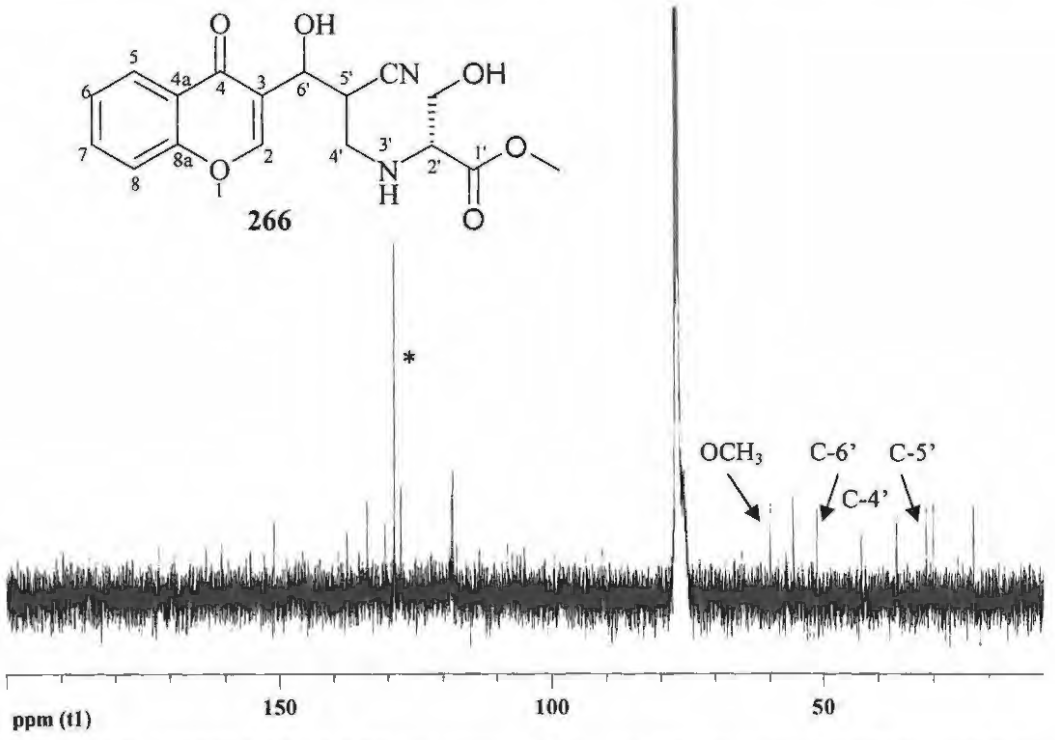

Figure 57. 100MHz ^{13}C NMR spectrum of the aza-Michael product **266** in $CDCl_3$.

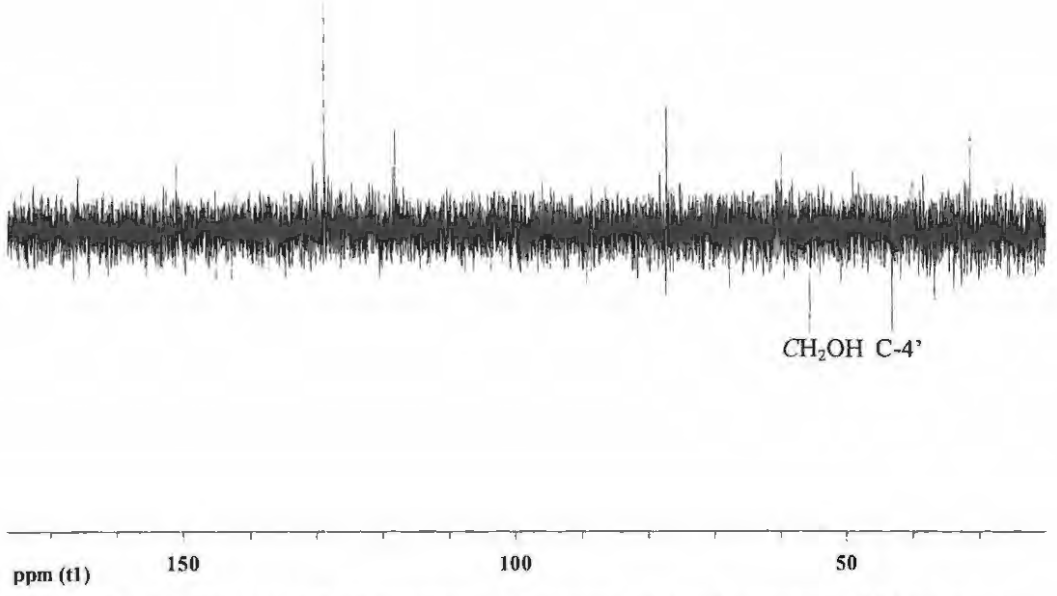

Figure 58. DEPT 135 NMR spectrum of the aza-Michael product **266** in $CDCl_3$.

The ^{1}H NMR spectrum (Figure 56) of the aza-Michael product **266** reveals a broad signal at 2.21 ppm corresponding to the 2'-methylene hydroxyl proton, two triplets at 2.21 and 3.02 ppm corresponding to the diastereotopic 4'-methylene protons, a broad singlet at 3.16 ppm which corresponds to NH, a multiplet at 3.21 ppm which corresponds to the 5'–methine proton, a broad singlet at 4.98 ppm corresponding to the 6'–methine proton, and a broad singlet at 10.98 ppm which corresponds to the 6'-hydroxyl proton. The ^{13}C NMR spectrum (Figure 57) reveals 17 carbon signals as expected with the extra signals due to the diastereomers. The 5'-methine carbon resonates at 31.3 ppm, a 4'-methylene carbon resonates at 43.1 ppm, a 6'-methine carbon resonates at 55.5 ppm, a methoxy carbon resonates at 59.8 ppm, the signal marked with an asterisk, which resonates at 128.8 ppm, indicates that there are four methine carbons which are overlapping which implies the presence of four isomers. The DEPT 135 spectrum (Figure 58) confirms the presence of two diastereotopic 4'- and 8'-methylene carbons which resonate at 43.1 and 55.5 ppm respectively.

2.3.4 Reaction of Baylis-Hillman products with L-serine ethyl ester

The Baylis-Hillman products **212**, **213** and **216** were reacted with L-serine ethyl ester hydrochloride and sodium acetate NaOAc in EtOH at 25°C for 6 weeks (**Scheme 63**). Purification of the crude products using flash chromatography afforded the aza-Michael products **269-271** in yields ranging from 26 to 45% (Table 14). However, when these reactions were reacted using L-serine ethyl ester hydrochloride, sodium acetate (NaOAc) and tetrabutylammonium bromide (TBAB), as catalyst, in EtOH at 25°C for 5 days they gave yields ranging from 28 to 40%. The products **269-271** were fully characterized by spectroscopic (IR, 1- and 2-dimensional NMR) and elemental (HREIMS) analysis. The ^{1}H NMR spectrum (Figure 59) of the aza-Michael product **269** reveals a triplet at 1.33 ppm corresponding to the 8'-methyl protons, a broad singlet at 3.19 ppm which corresponds to the 3'-amine proton, a multiplet at 3.57 and 3.79 ppm corresponding to the diastereotopic 4'-methylene protons, a multiplet at 3.80 ppm corresponding to the

5'–methine proton, a singlet at 5.02 ppm corresponding to the 6'–methine proton, and a broad singlet at 11.4 ppm which corresponds to 6'-hydroxyl proton. The ^{13}C NMR spectrum (Figure 60) reveals 17 carbon signals as expected. The 5'-methine carbon resonates at 47.4 ppm, the 4'-methylene carbon at 53.4 ppm, and the 6'-methine carbon at 68.4 ppm. The DEPT 135, COSY, HSQC and HMBC and elemental (HREIMS) analysis data were all used to facilitate the assignment of signals in of these compounds.

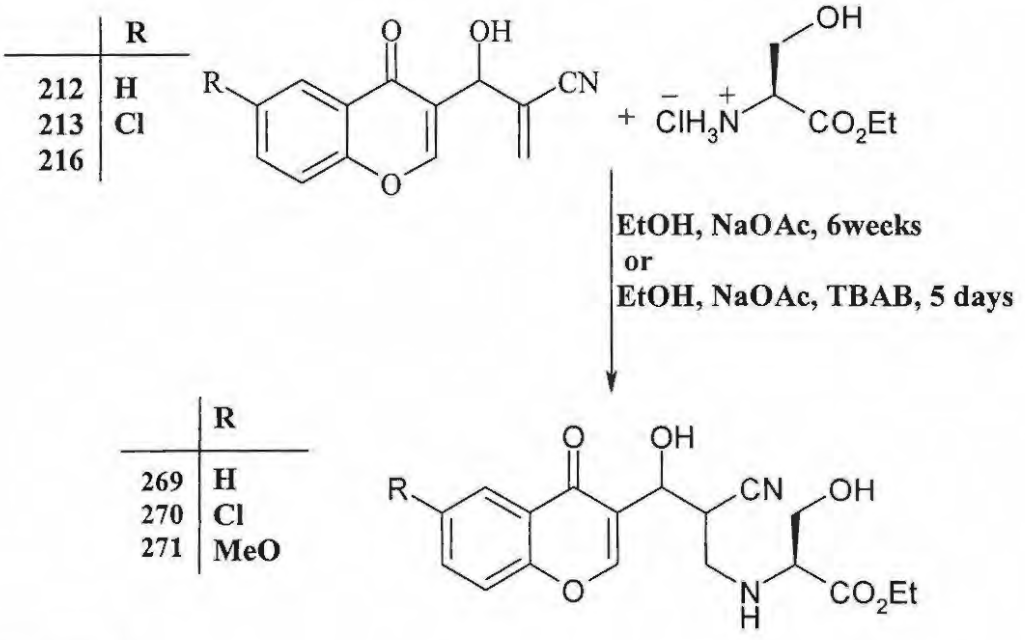

Scheme 63

Table 14. Isolated yields (%) of the aza-Michael compounds **269-271** obtained under various conditions.

R	Compound	After 6 weeks using NaOAc	After 5 days using TBAB
H	**269**	26	30
Cl	**270**	29	45
MeO	**271**	27	33

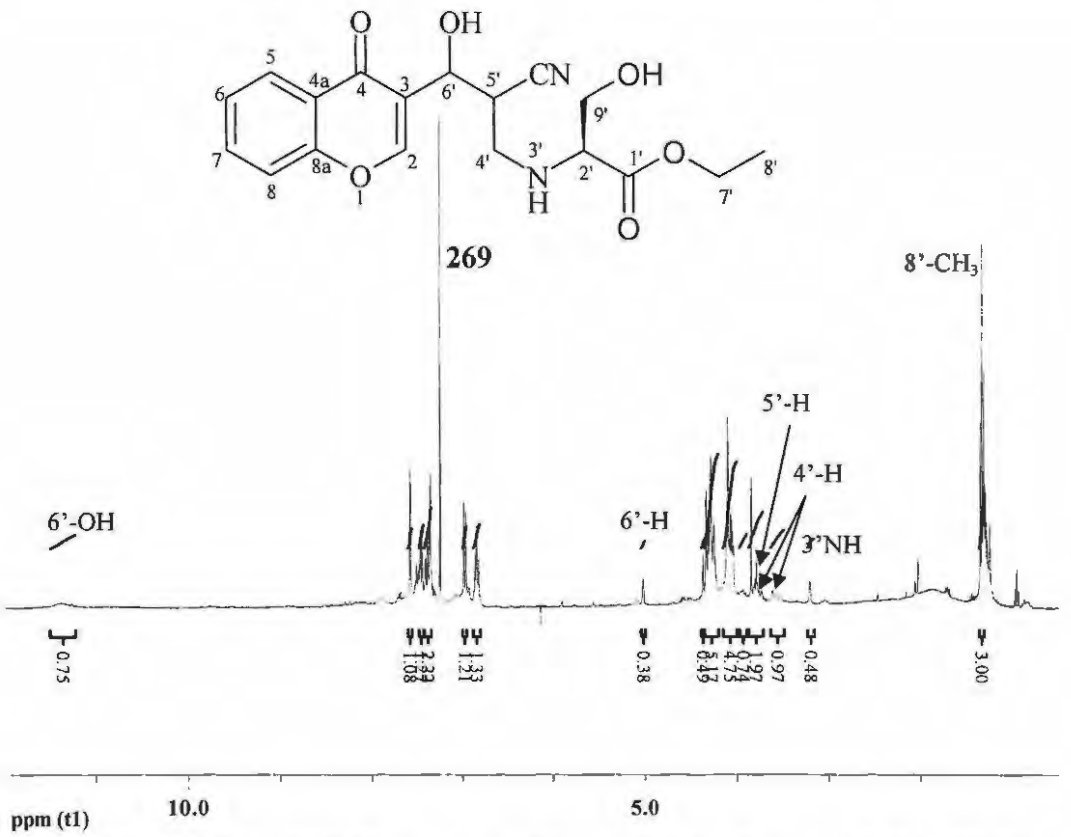

Figure 59. 400MHz ^{1}H NMR spectrum of the aza-Michael product **269** in $CDCl_3$.

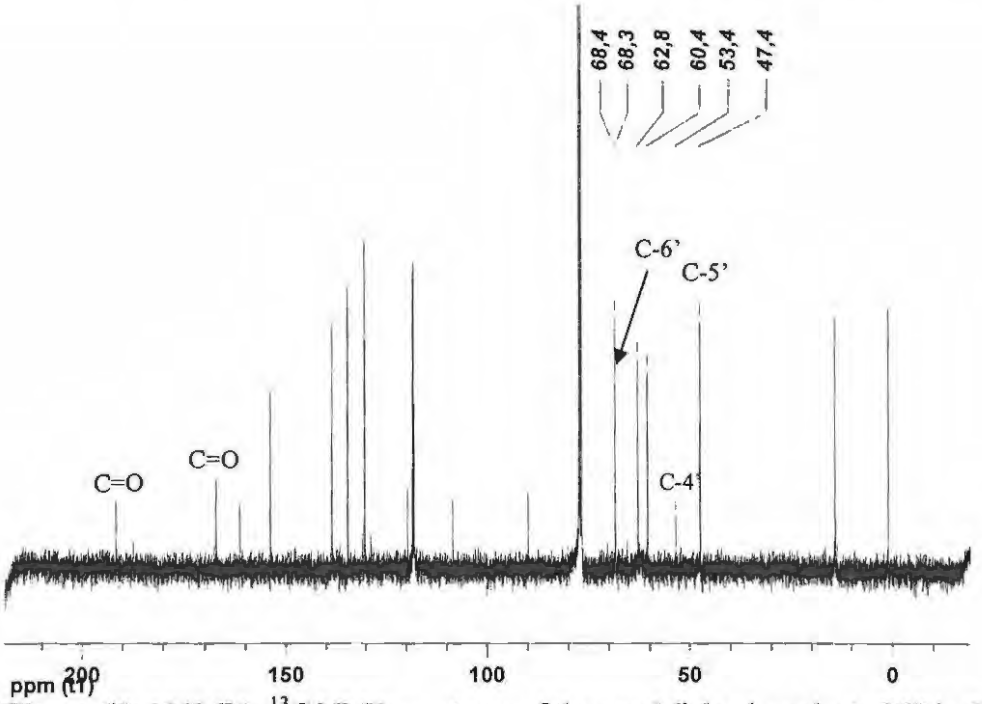

Figure 60. 100MHz ^{13}C NMR spectrum of the aza-Michael products **269** in $CDCl_3$.

2.3.5 Reaction of Baylis-Hillman products with L-threonine methyl ester hydrochloride

The Baylis-Hillman products **212** and **213** were reacted with L-threonine methyl ester hydrochloride and sodium acetate in EtOH at 25°C for 6 weeks (**Scheme 64**). Purification of the crude products using flash chromatography afforded the aza-Michael products **272** and **273** in relatively low yield (25-31%; Table 15). However, repetition of these reactions using L-threonine methyl ester hydrochloride and sodium acetate (NaOAc) and tetrabutylammonium bromide, as catalyst, in EtOH at 25°C for 5 days gave improved yields (37-45%).

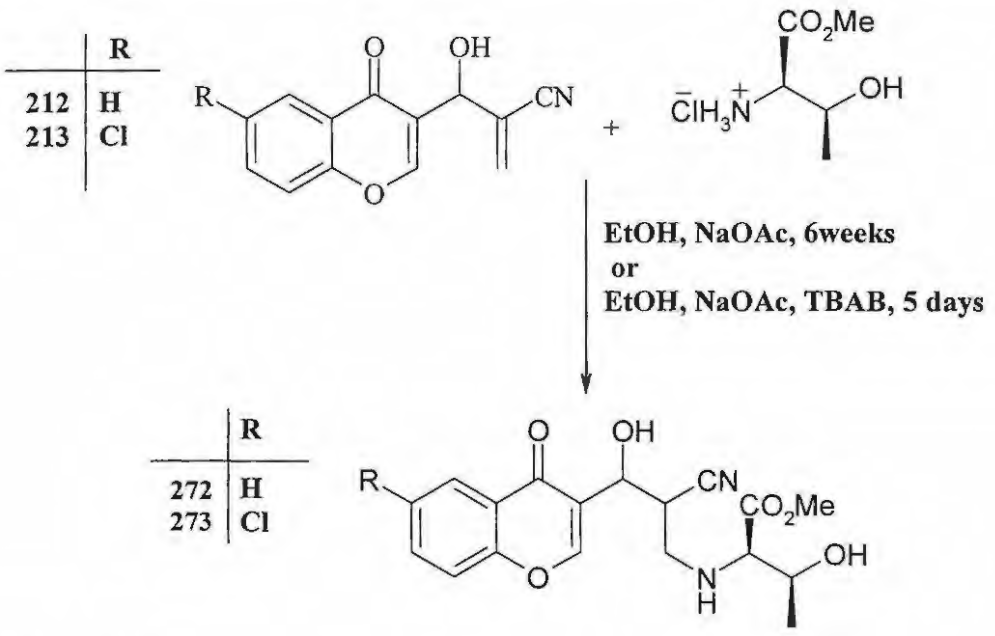

Scheme 64

Table 15. Isolated yields of aza-Michael compounds **272** and **273** obtained at various reaction times.

R	Compound	After 6 weeks using NaOAc	After 5 days using TBAB
H	**272**	25	37
Cl	**273**	31	45

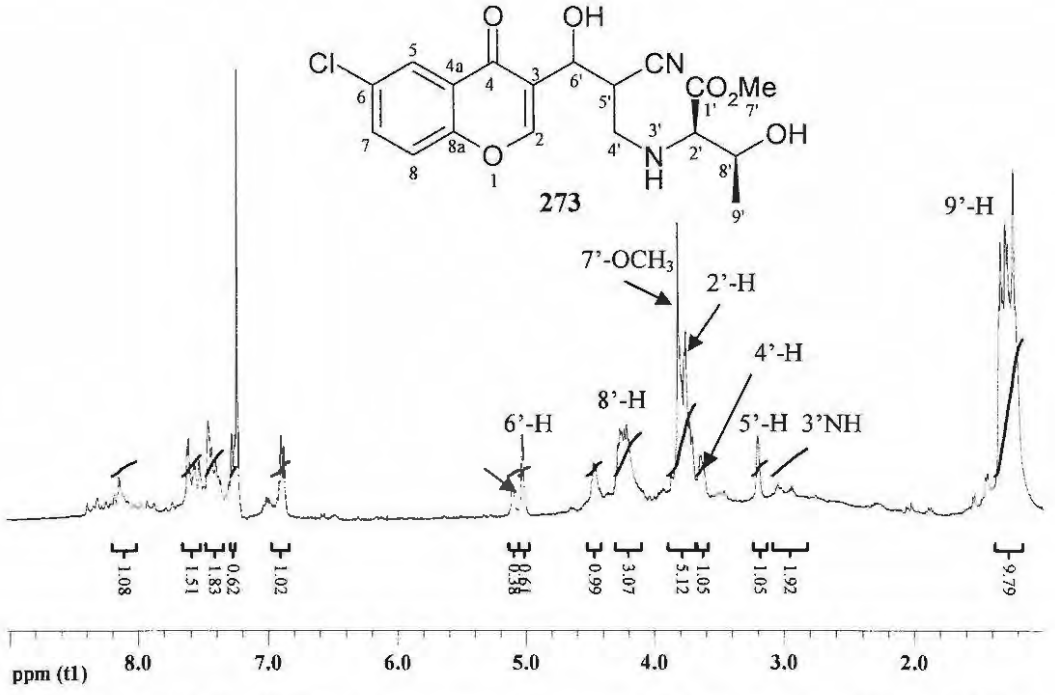

Figure 61. 400MHz ^{1}H NMR spectrum of the aza-Michael product **273** in $CDCl_3$.

While the ^{1}H NMR spectra of the corresponding benzyl cysteamine, glycine and serine derivatives exhibit relatively sharp signals, the ^{1}H NMR spectrum (Figure 61) of the aza-Michael product **273** is characterized by poorly resolved signals attributed to the presence, in this case, of diastereomeric products. The ^{13}C NMR spectrum (Figure 62) reveals more than 18 carbon signals, which was expected, which confirms the presence of diastereomeric products. The DEPT 135, COSY, HMBC (Figures 62-64) and elemental (HREIMS) analysis data were used to facilitate the assignment of signals in these compounds.

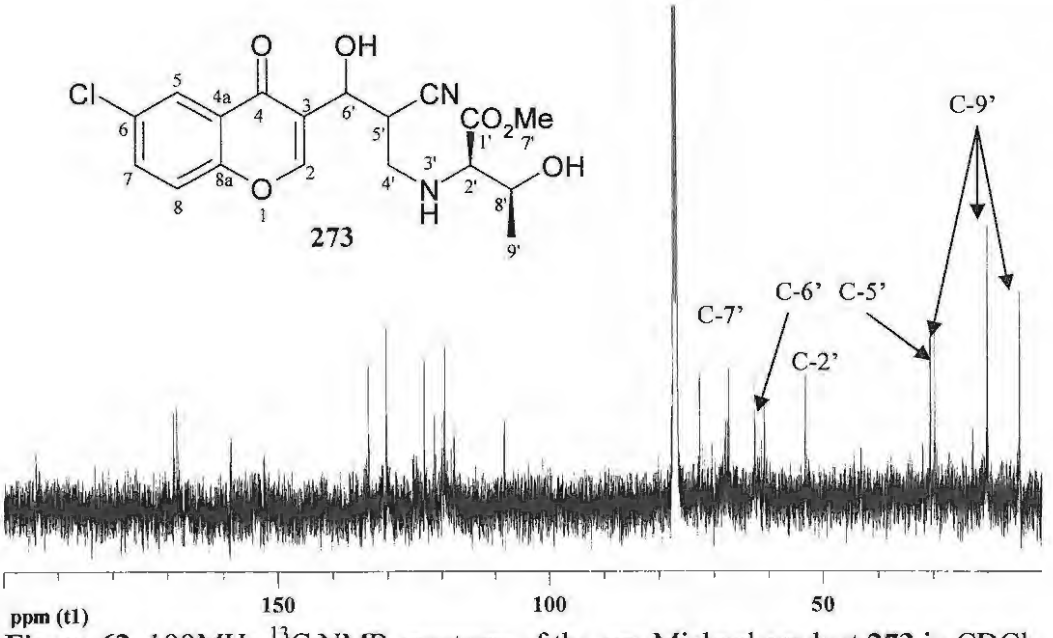

Figure 62. 100MHz ^{13}C NMR spectrum of the aza-Michael product **273** in $CDCl_3$.

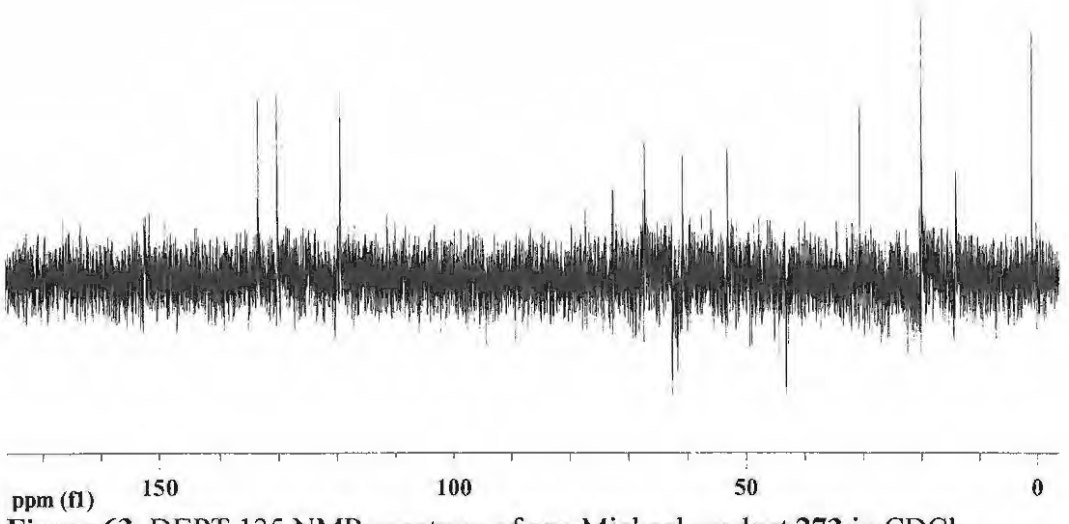

Figure 63. DEPT 135 NMR spectrum of aza-Michael product **273** in $CDCl_3$.

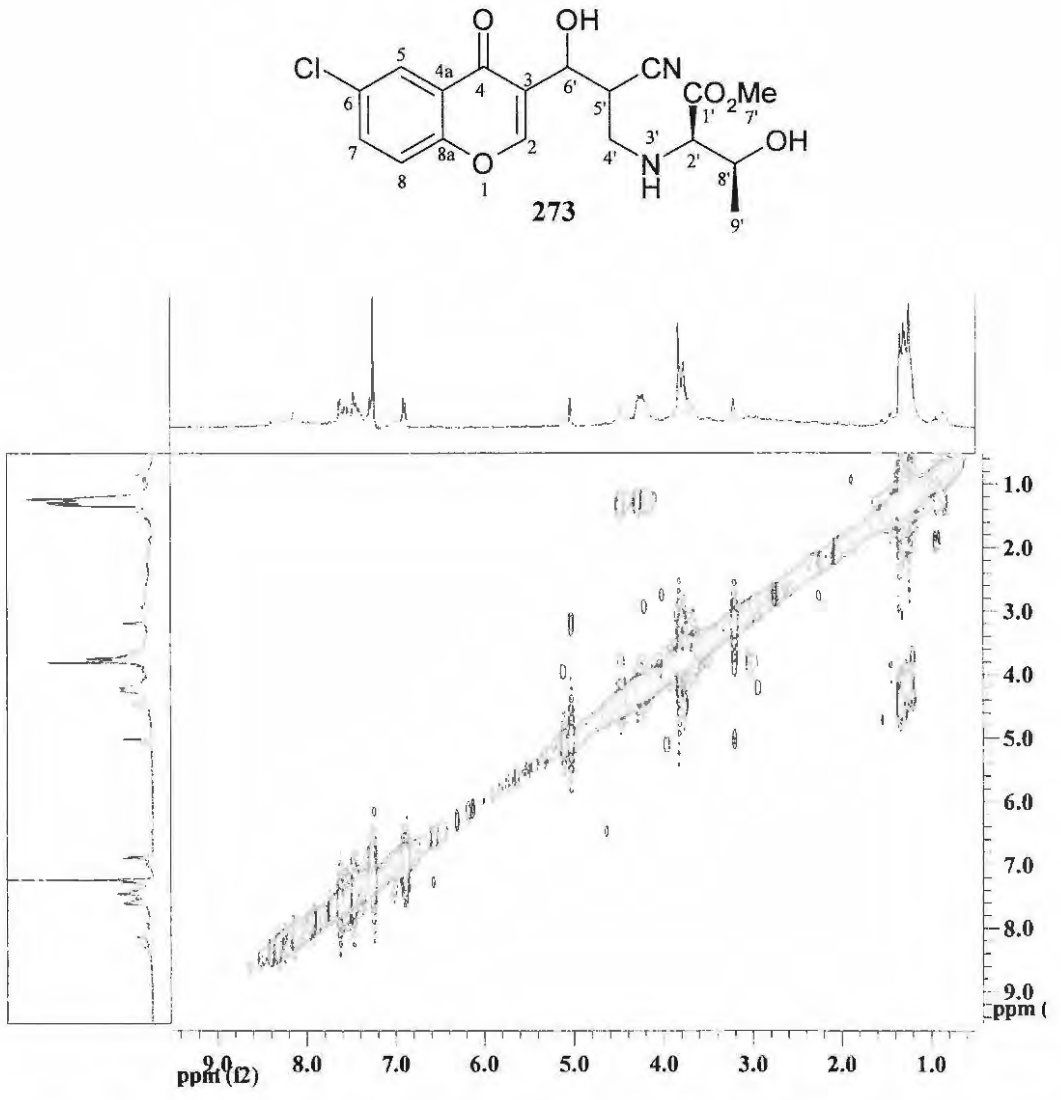

Figure 64. 400 MHz COSY NMR spectrum of aza-Michael product **273** in $CDCl_3$.

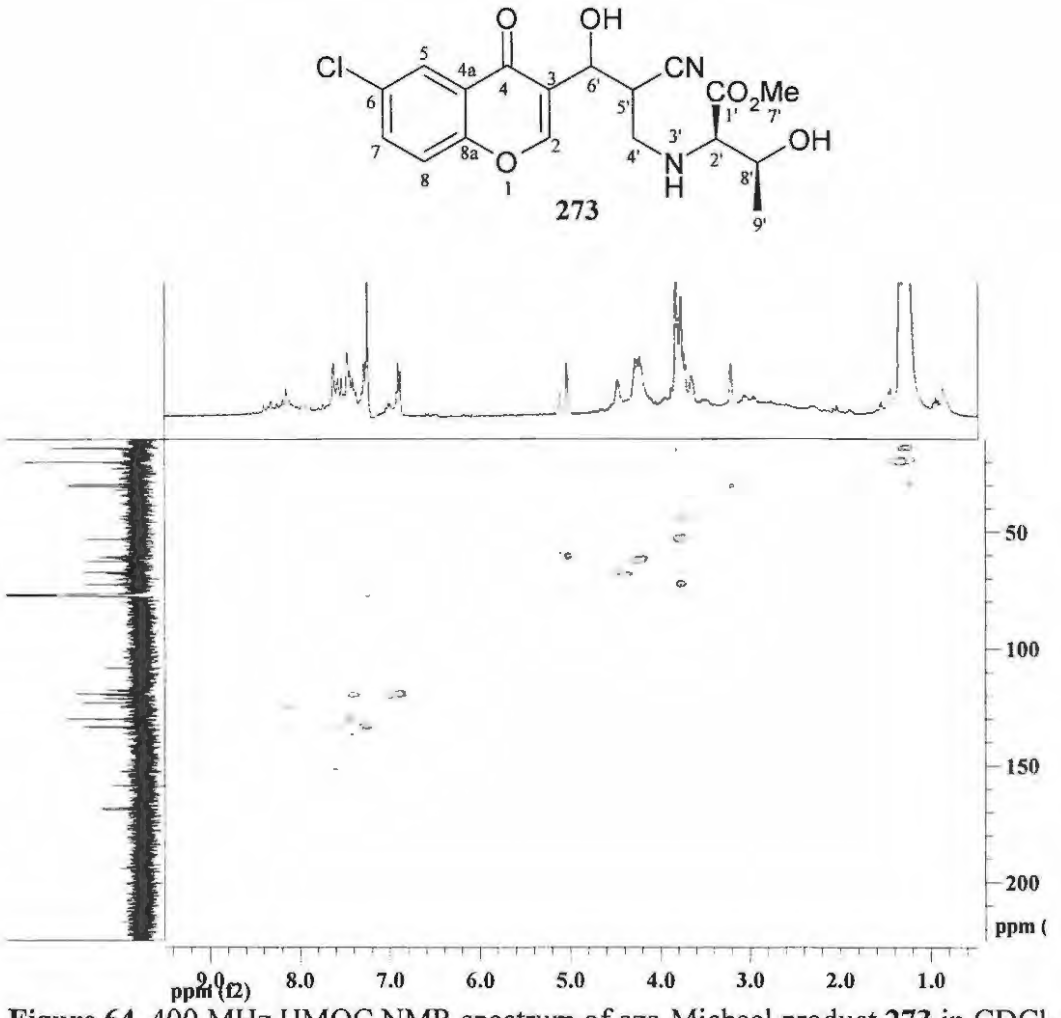

Figure 64. 400 MHz HMQC NMR spectrum of aza-Michael product **273** in $CDCl_3$.

2.4 HIV-1 Protease Kinetics

Enzyme kinetics studies were undertaken in order to explore the catalytic activity of HIV-1 protease in the presence of the commercially available "HIV substrate III" and the representative chromone derivatives **258**, **263** and **266**, our inhibitors (Figure 65). The chromone derivatives **258**, **263** and **266** were selected for examination as potential inhibitors as they possess some features in common with ritonavir, a clinically approved HIV-1 protease inhibitor. K_m, V_{max} and K_i are the parameters typically used to measure changes in catalytic activity. The Michaelis constant, K_m, reflects the binding affinity between the HIV substrate III and HIV-1 protease, while V_{max}, the maximum velocity, corresponds to the maximum catalytic activity. These parameters provide measures of the catalytic activity of the enzyme, in the presence of substrate, informing the intermediate HIV-1 protease-HIV substrate III complex. It is assumed that the interaction between the enzyme and substrate in this case is reversible (Equation 5), but that the decomposition of the HIV-1 protease-HIV substrate III complex to form product and free enzyme is sufficiently slow to be considered negligible.

[HIV-1 protease] + [HIV substrate III] $\underset{k_{-1}}{\overset{k_1}{\rightleftharpoons}}$ **[HIV-1 protease—HIV substrate III].....(5)**

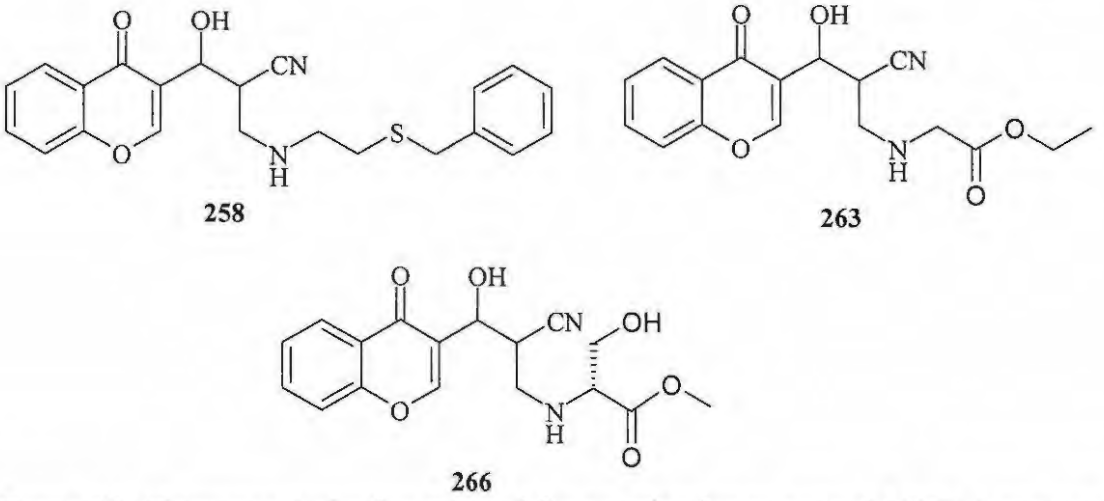

Figure 65. Chromone derivative selected for examination as potential HIV-1 protease inhibitors

The rate of the enzyme-catalysed reaction is therefore directly proportional to the concentration of the enzyme and this linearity is important for accurate measurement of the enzyme activity.[79] This requires that the enzyme concentrations used during the assay should lie within the linear region and that the pH and temperature be kept constant. K_m, the substrate concentration at which the HIV-1 protease receptor sites are half filled ($1/V_{max}$), and V_{max}, the rate at which the HIV-1 protease activity is saturated, can be determined using Michaelis-Menten, Lineweaver-Burk, and Hanes and Wool plots, as described in the Introduction.

Normally, the units of initial velocity, v_0, are expressed as μmoles of substrate cleaved per minute.[77] But in this section, the units used to express v_0 are defined as the amount of enzyme that will cause a change in absorbance at 300nm of 0.00001 per minute, under the assay conditions described.

2.4.1 HIV-1 Protease Linearity

The linear range of the HIV-1 protease was determined from assays in which the enzyme concentrations were varied while keeping the HIV substrate concentration constant at 18.5 μM (Figure 66).

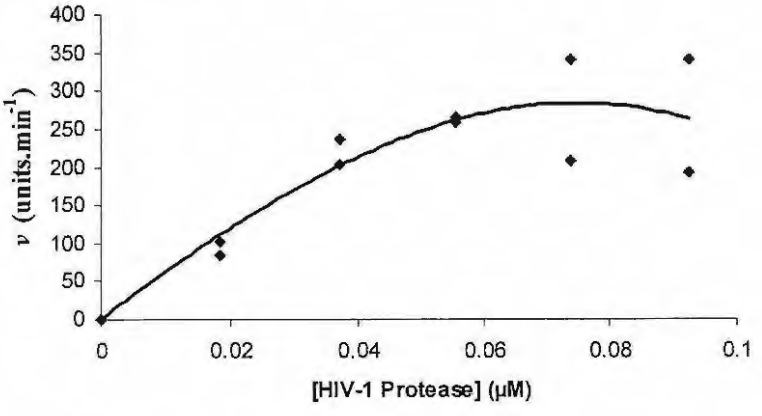

Figure 66. Plot of v_0 **versus** HIV-1 protease concentration for determining the linearity dependence of HIV-1 PR. This assay was generated from duplicate assays in which [HIV-1 protease] was varied from 0 to 0.093 μM using a constant HIV protease substrate III concentration of 18.5 μM, at 25°C and pH 4.9.

A plot of the resulting data (Figure 66) reveals reasonable linearity up to *ca.* 0.05 μM in the concentration of HIV-1 protease. An HIV-1 protease concentration of 0.039 μM was therefore selected for all subsequent assays, while the pH and temperature were kept constant at 4.5 and 25 °C, respectively.

2.4.2 HIV-1 Protease Substrate Dependence

The substrate dependence assays involved collecting kinetic data for a series of substrate concentrations ranging from 0 – 73.96 μM while keeping the HIV-1 protease concentration constant at 0.037 μM. Figure 67 illustrates the graphical determination of K_m and V_{max} using (a) a Michaelis-Menten plot, (b) a Lineweaver-Burk plot, and (c) a Hanes and Woolf plot. These assays were run in triplicate at constant temperature 25 °C and a pH of 4.5. Comparison of the K_m and V_{max} values obtained with those reported in literature.

The Michaelis-Menten plot, Figure 67a, was constructed using the following equation:

$$v = \frac{\text{Vmax x [HIV PR substrate III]}}{K_m + \text{[HIV PR substrate III]}} \qquad \text{.....(6)}$$

This plot clearly shows that at low substrate concentrations the rate of reaction, v_0, increases more or less linearly with the substrate concentration while, at higher substrate concentrations the rate becomes constant. The Michaelis constant, K_m, can be obtained by interpolation since it is the substrate concentration at which the reaction rate is half of its maximum value ($V_{max}/2$), which is the reason why K_m is also called the half-saturation value.[80] However, it is difficult to specify the exact substrate concentration corresponding to K_m from this hyperbolic plot. Consequently, the linear Lineweaver-Burk and Hanes-Woolf plots were constructed (Figures 67b and c), thus permitting accurate measurements of the values of both K_m and V_{max} even at higher substrate concentrations.[78] The Lineweaver-Burk plot (Figure 67b) was constructed using equation 7, [75, 80] while the Hanes-Woolf plot was constructed using equation 8.

$$\frac{1}{v} = \frac{K_m}{V_{max} * [\text{HIV protease substrate III}]} + \frac{1}{V_{max}} \quad \text{.....(7)}$$

$$\frac{[\text{HIV protease substrate III}]}{v} = \frac{1}{V_{max}} * [\text{HIV protease substrate III}] + \frac{K_m}{V_{max}} \quad \text{.....(8)}$$

From these plots, K_m and V_{max} were found to be 27.97 μM and 322.58 units.min^{-1}, respectively. The K_m obtained for HIV PR substrate III lies in the same range as the Km value found in literature, *viz.* 28.00 μM.[84] The catalytic efficiency of HIV-1 protease was found to be 311.7 min^{-1}, and was obtained by dividing V_{max} by the K_m value.

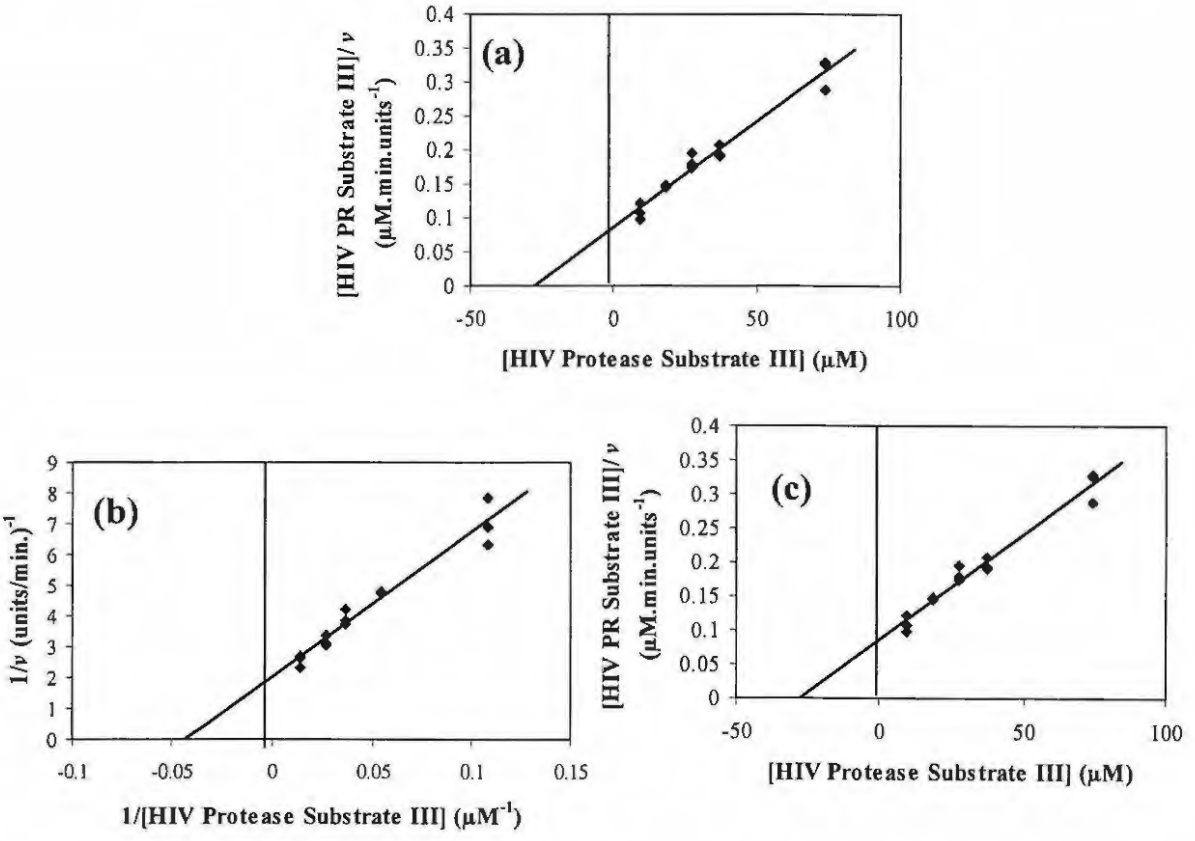

Figure 67. Kinetic analysis of HIV Protease substrate dependence: (a) Michaelis-Menten plot; (b) Lineweaver-Burk plot ($r^2 = 0.954$); (c) Hanes-Woolf plot ($r^2 = 0.969$).

2.4.3 HIV-1 Protease Inhibition Studies

2.4.3.1 Effect of Inhibitors

The chromone derivatives **258**, **260** and **266** were then examined in a series of HIV-1 protease inhibition assays. In triplicate runs exploring the effect of varying the concentration of the potential inhibitors on the activity of HIV-1 protease at pH 4.5 and 25°C, it became apparent that compounds **258** and **266** exhibit some inhibitory effect (see Figure 68). In the case of chromone derivative **260,** however, no inhibition was observed even at a concentration as high as 44.23 μM.

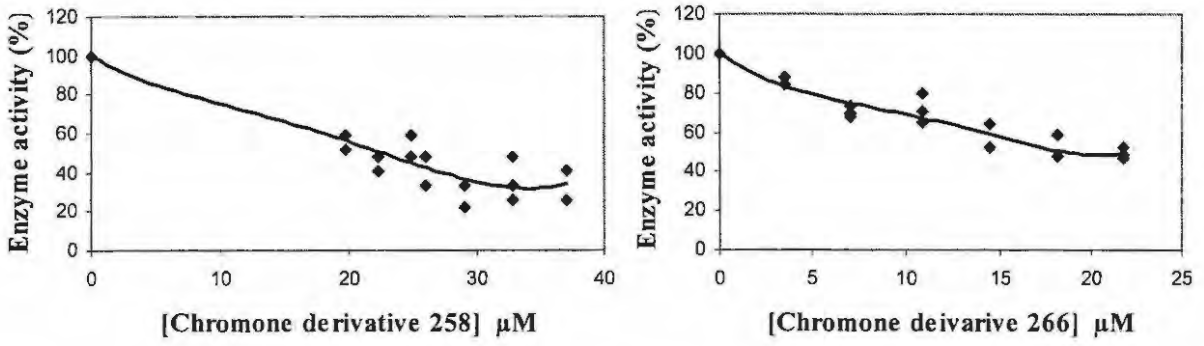

Figure 68. (a) Effect of chromone derivative **258** and (b) chromone derivative **266** on HIV-1 protease activity. The assays were run in triplicate at pH 4.5 and 25°C.

The observed decrease in enzymatic activity implies interaction between the HIV-1 protease enzyme and these inhibitors.[78] In the case of chromone derivative **258** (Figure 68a), the remaining enzyme activity was *ca.* 52% at 20 μM decreasing to *ca.* 33% at 25 μM and then remaining constant *ca.* 26 % at 32.7 μM. However, in the case of chromone derivative **266** (Figure 68b) the residual enzyme activity was *ca.* 52% at 14.5 μM and decreased to *ca.* 48% at 21.7 μM. The fact that neither of these inhibitors resulted in zero residual enzyme activity implies that they don't fill the entire receptor cavity of the HIV-1 protease enzyme. In order to establish the type of inhibition involved, Lineweaver-

Burk and Dixon plots were constructed using concentrations of the inhibitors that gave up to *ca.* 50% residual enzyme activity.

2.4.3.2 Determination of the K_m, V_{max} and K_i values

Inhibition assays for the chromone derivative **258** were performed using inhibitor concentrations of 0 to 22μM, while concentrations ranging from 0 to 21.75μM were used for the chromone derivative **266**. The K_m and V_{max} values were obtained from Lineweaver-Burk plots, while the K_i values were obtained from Dixon plots. The corresponding plots for the chromone derivatives **258** and **266** are illustrated in Figures 69 and 70, respectively.

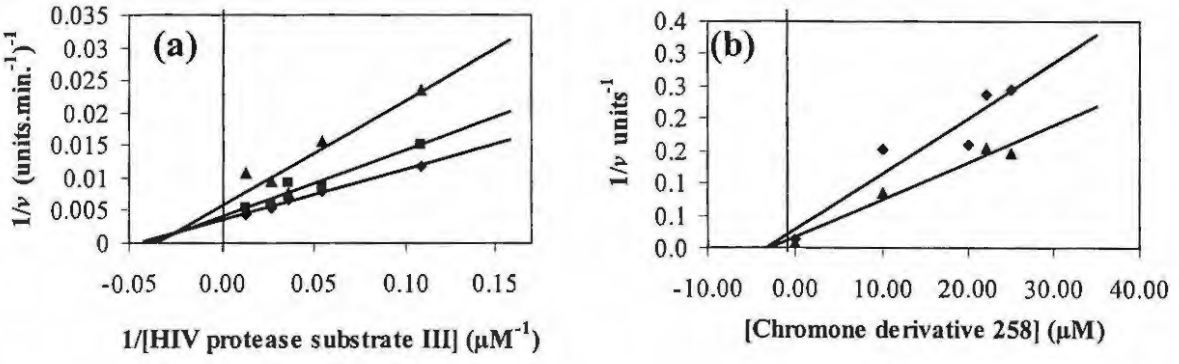

Figure 69. (a) Lineweaver-Burk plots for the inhibition of HIV-1 protease by chromone derivative **258** using the concentrations of 0μM (r^2 = 0.989), ♦, 10μM (r^2 = 0.935), ■, and 22μM (r^2 = 0.847), ▲, in the presence of HIV protease substrate III. (b) Dixon plots for the effect of chromone derivative **258** on HIV-1 protease activity when the HIV protease substrate III concentration was 9.25 μM (r^2 = 0.896), ♦, and 18.25μM (r^2 = 0.960), ▲.

Figure 69 reveals the chromone derivative **258** to be a non-competitive inhibitor. The Lineweaver-Burk plot, Fig. 69a, indicates that different concentrations [0.00μM (standard), 10μM and 22μM] give straight lines with K_m values of 23.02, 25.04 and 28.07 μM, respectively. The K_m values in the presence of the inhibitor are higher than

the K_m value in its absence (23.02 μM), meaning that the chromone derivative **258** does, in fact, interfere with the catalytic activity of HIV-1 protease. Furthermore, use of the different concentrations (0.00 μM, 25.04 μM and 28.07 μM) afforded V_{max} values of 294.12, 250.0 and 175.4 units.min.$^{-1}$, respectively. The progressive decrease in V_{max} on increasing the concentration are features which describe non-competitive inhibition.[80] The Dixon plot (Figure 69b) confirms that the chromone derivative **258** is a non-competitive inhibitor; the straight lines intersect at abscissa indicating an inhibition constant (K_i) of *ca.* 3.2 μM (0.0032nM). However, with a K_i value of 0.015nM, [91] ritonavir has higher binding affinity for HIV-1 protease than chromone derivative **258**. The results indicate that the chromone derivative **258** interferes with both the binding of the HIV protease substrate III and HIV-1 protease catalytic activity. This may be attributed to the chromone derivative **258** binding either to the free enzyme or to the protease-HIV protease substrate III (ES) complex (Equation 3, p. 13).

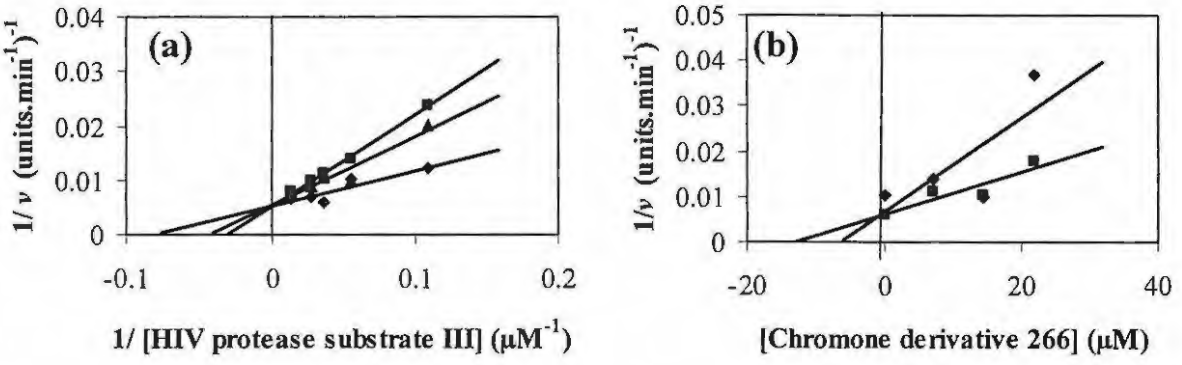

Figure 70. (a) Lineweaver-Burk plots for the inhibition of HIV-1 protease by chromone derivative **266** with concentrations of 0μM (r^2 = 0.820), ♦, 7.03 μM (r^2 = 0.997), ■, and 14.5μM (r^2 = 0.9197), ▲, in the presence of HIV protease substrate III. (b) Dixon plot for the effect of chromone derivative **266** in HIV-1 protease activity when the HIV protease substrate III concentration was 18.25 μM(r^2 = 0.896) ♦, and 27.73μM(r^2 = 0.960) ▲.

Figure 70 shows the chromone derivative **266** is a competitive inhibitor as defined in Equation 2 (p. 13). The Lineweaver-Burk plot (Fig. 70a) reveals that the assay data for

different concentrations (0.00 , 7.03 and 14.5 μM) afford the straight lines, (with the K_m values of 12.45, 32.50 and 23.44 μM, respectively) which intersect at the same 1/ V_{max} value of about 188.7 units.min.$^{-1}$ (Figure 70b). It is also evident that the K_m values (32.5 and 23.44 μM) in the presence of this chromone derivative **266** are much higher than the K_m value (12.45 μM) in its absence. This implies that the chromone derivative **266** has a higher binding affinity than the HIV protease substrate III and thus competes with the protease substrate for binding to HIV-1 protease enzyme. The Dixon plot (Figure 70b) confirms that the chromone derivative **266** is a competitive inhibitor since plots of the different concentrations (0.00 , 7.03 and 14.5 μM) of compound **266** at constant substrate concentrations (18.5 and 27.73 μM) gave K_i values of 6.4 μM (0.0064 nM) and 13.3 μM (0.00133 nM), respectively. However, these values are lower than for the ritonavir K_i value of 0.015 nM,[91] which means that the binding affinity of chromone derivative **266** for HIV-1 protease is lower than for the ritonavir. The various kinetic parameters determined in the enzyme kinetic studies are summarized in Table 16.

Table 16. Kinetic parameters obtained during the kinetic studies.

[Chromone derivative **258**] (μM)	K_m (μM)	V_{max} (units.min^{-1})	K_i (nM)
0 10 22	23.01 25.04 28.07	294.12 250.0 175.4	0.015
[Chromone derivative **266**] (μM)			
0.00 7.03 14.5	12.45 32.50 23.44	188.7	0.0064

2.5 Computer Modelling Studies of Chromone Derivatives as Potential HIV-1 Protease Inhibitors

Computer modelling has become a crucial drug-designing technique.[13] Such studies typically involve modelling of the putative inhibitor and exploring its docking into a known enzyme receptor cavity, permitting elucidation of the interactions involved in the enzyme receptor-inhibitor complex.[57] The structure of the receptor cavity of the HIV-1 protease enzyme has been well established by X-ray crystallography and the structure reported by Kempf *et al.*[195] was used in our investigation. The structure of this homodimeric enzyme is illustrated in Figure 71 with the orange ribbon denoting monomer A and the blue ribbon denoting the monomer B.[195]

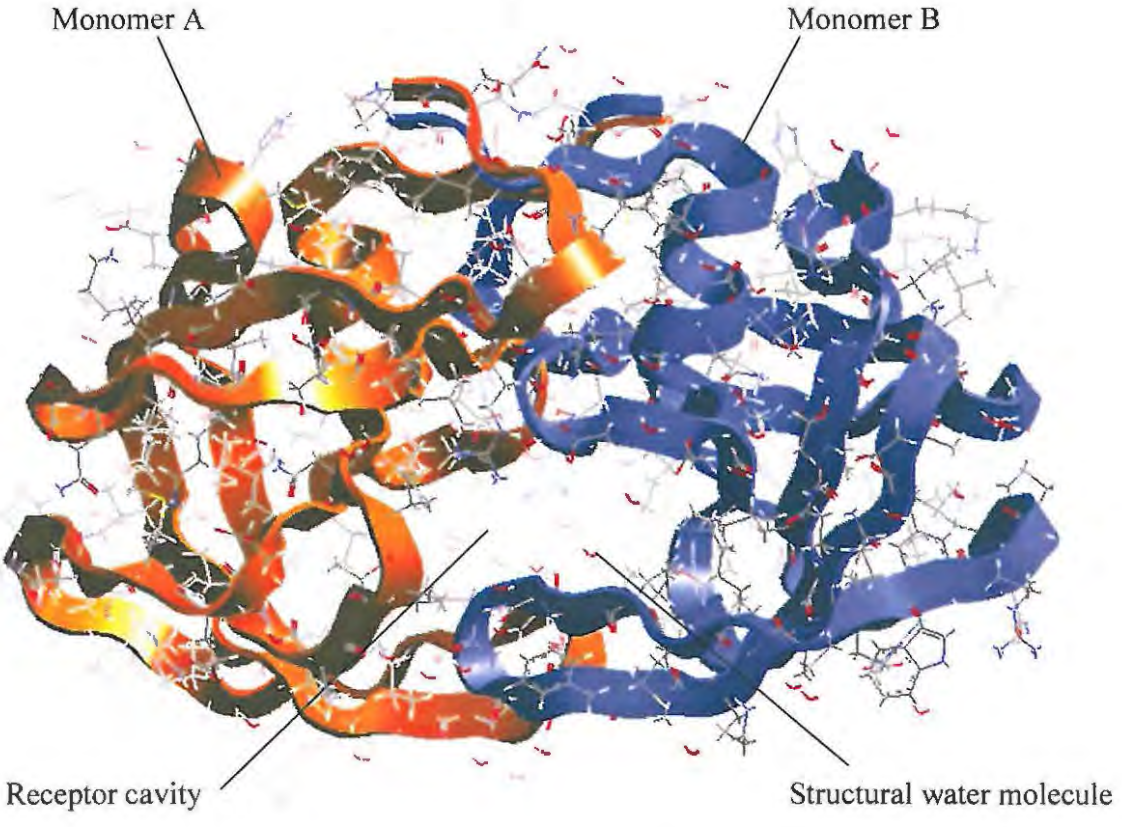

Figure 71. X-ray crystal structure of HIV-1 protease.[195]

The chromone-containing derivatives **222, 241, 258, 260, 266, 269, 272,** and **274** developed as truncated ritonavir analogues and the dimers **222** and **241** were selected as representative structures of several series of compounds prepared in this study, and were docked into this HIV-1 protease receptor cavity, using the ACCELRYS Cerius^2 module, LigandFit. Conformational space was explored for each structure using molecular dynamics and the ten highest and ten lowest energy conformations in the resulting trajectory were subjected to energy minimization. The common minimum energy structure was then presumed to correspond to the global minimum. The resulting structures, illustrated in Figures 72-73, represent the global minimum in each case. The intention was to:- i) compare the minimum energy conformations of ritonavir **2** and each of the chromone derivatives **222, 241, 258, 260, 266, 269, 272,** and **274**; ii) explore the docking of ritonavir **2** and the chromone derivatives into the enzyme receptor cavity; and iii) compare the favoured *binding* conformation of each of the compounds with their respective minimum energy conformations.

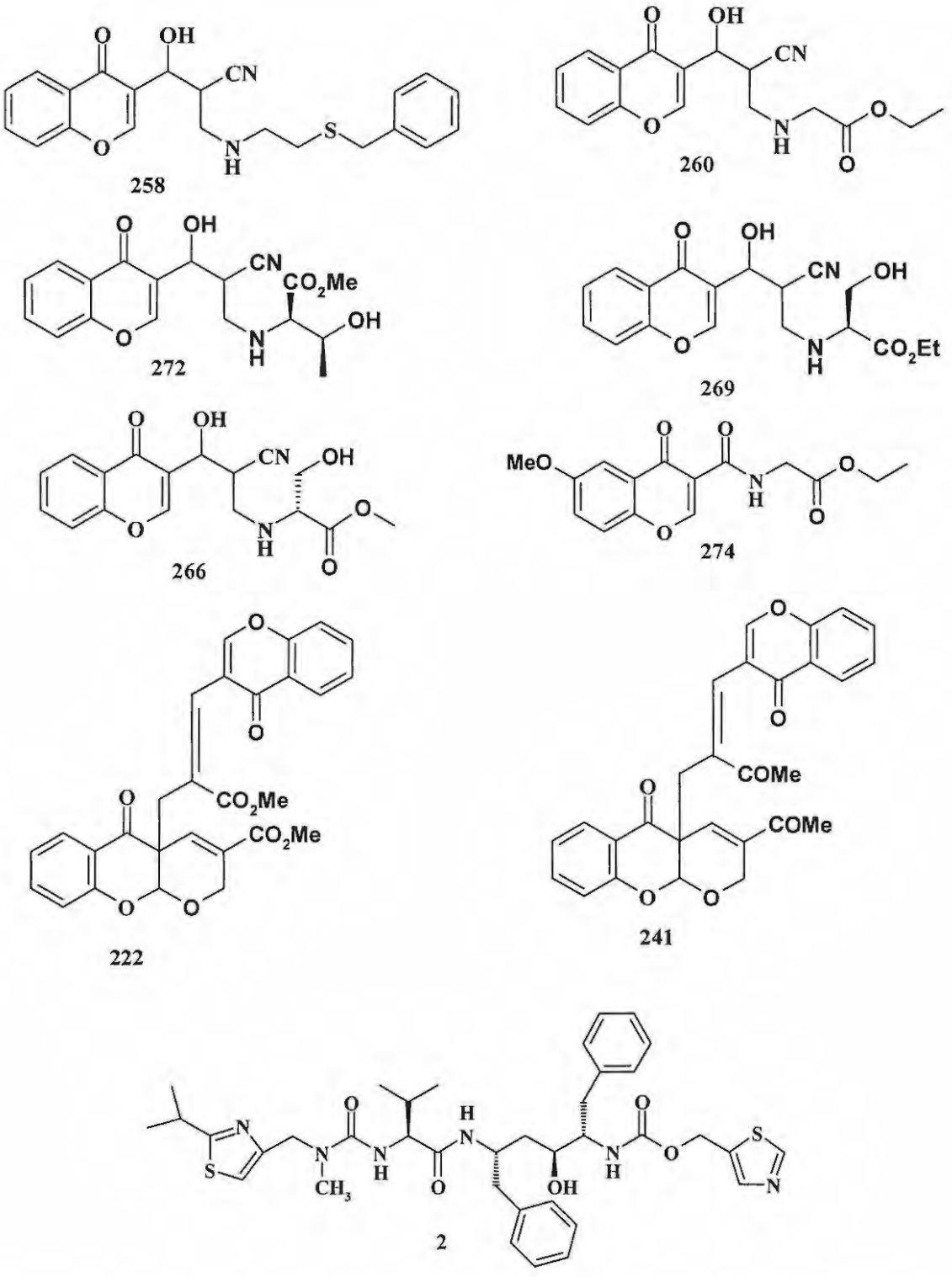

Figure 72. Structures of compounds **2**, **222**, **241**, **258**, **260**, **266**, **269**, **272** and **274**.

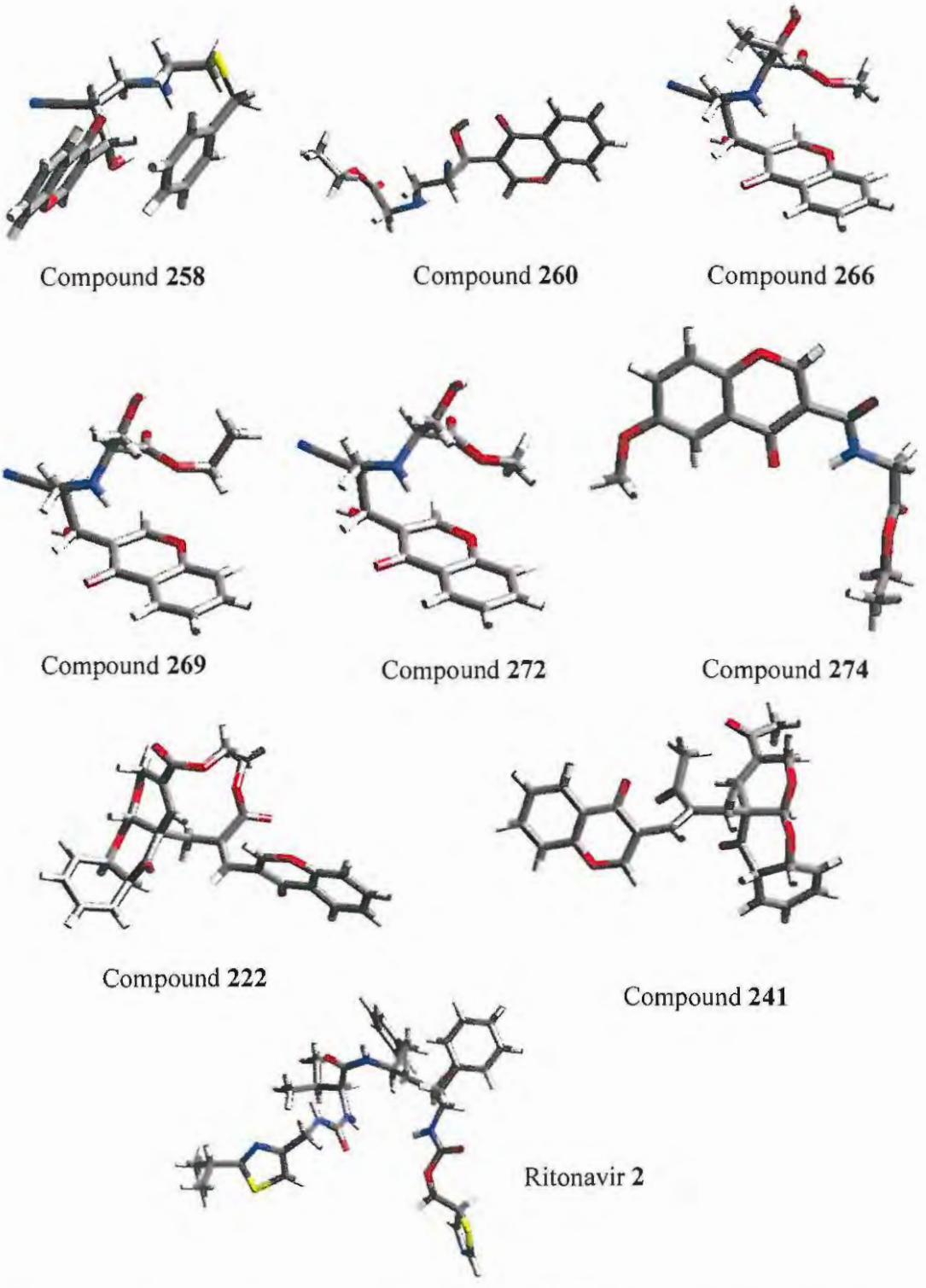

Figure 73. Energy-minimized conformers of the truncated, chromone-containing compounds **222**, **241**, **258**, **260**, **266**, **269**, **272** and **274** and ritonavir **2**.

The Cerius^2 SITE SEARCH module was used to define the binding site of HIV-1 protease (Figure 74). The inhibitor is expected to be able to interact with the receptor provided it is situated within the vicinity of the site and, ideally, fills the entire region. Overlaying the energy-minimized structure of ritonavir **2** on this binding site reveals that this clinically useful inhibitor does not, in fact, encompass the entire space of the site nor is it completely accommodated within it (Figure 75). However, when overlaying both ritonavir **2** and lopinavir **5**, a mixture of which comprises the combination drug, kaletra,[72] it is apparent that more space in the binding site is occupied (Figure 76). This illustrates a possible advantage of using HIV protease inhibitors as combination drugs. Alignment of the chromone-derivatives **222**, **241**, **258**, **260**, **266**, **269**, **272** and **274** also revealed, not unexpectedly, that these compounds are not long enough to occupy the entire binding site (Figure 77). What is critical, of course, is the nature and strength of the interactions between the ligand and the receptor, and their effect on the relative receptor binding and plasma solvation energies.

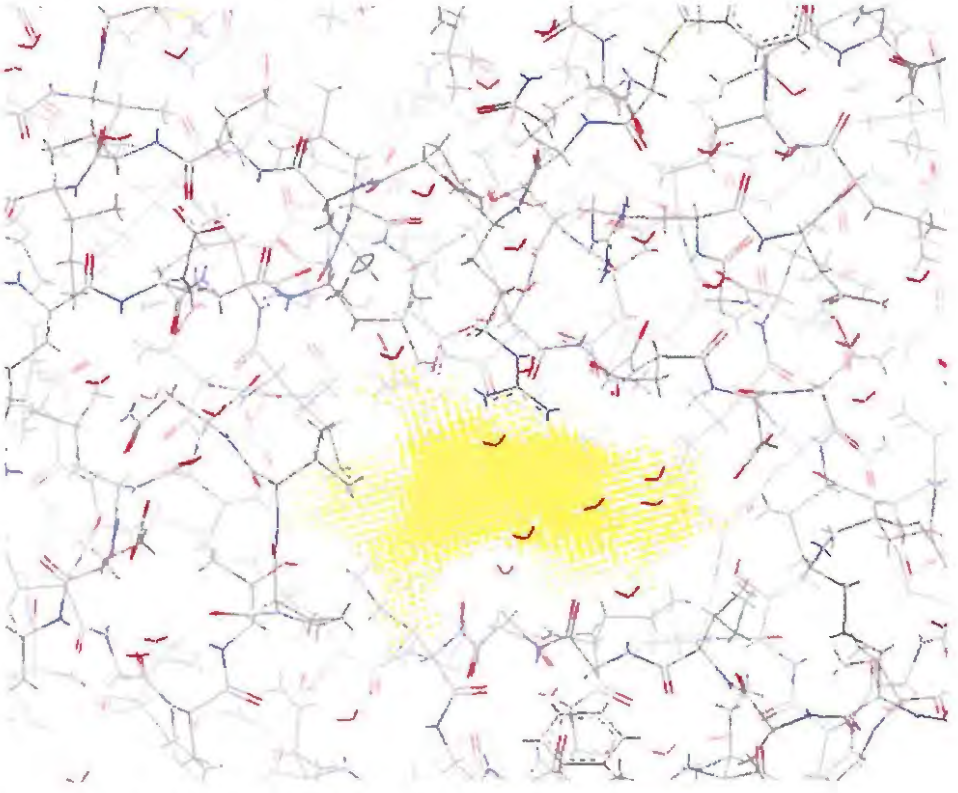

Figure 74. Binding site of the HIV-1 protease receptor cavity.

It should be noted, however that Figures 75-77 illustrate *in vacuo* rather than binding conformations of the compounds examined. The binding conformations were explored using a docking routine (see below).

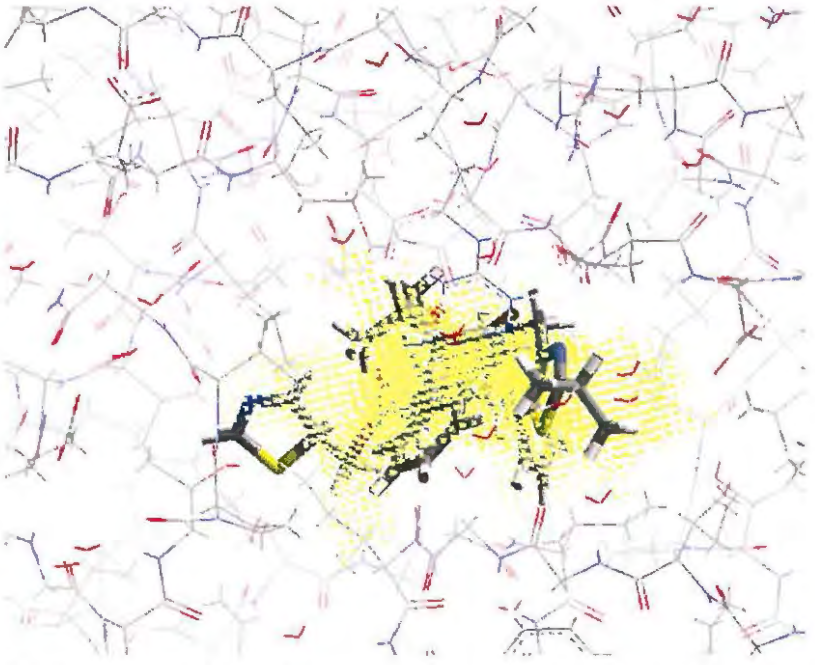

Figure 75. Energy-minimized *in vacuo* structure of ritanovir **2** in the binding site of HIV-1 protease.

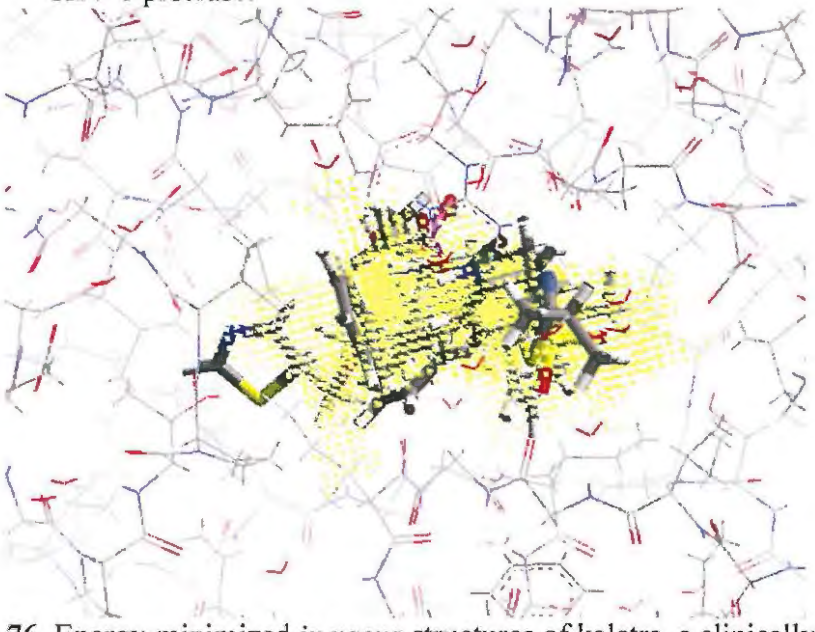

Figure 76. Energy-minimized *in vacuo* structures of kaletra, a clinically approved combination of ritanovir **2** and liponavir **5** in the binding site of HIV-1 protease.

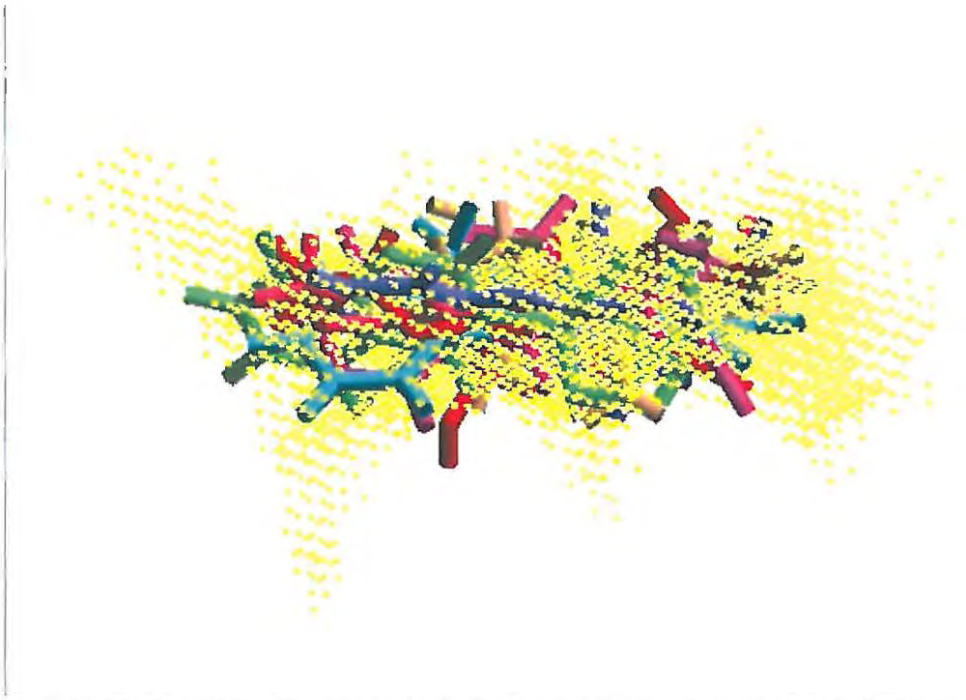

Figure 77. Overlay of energy-minimized *in vacuo* structures of the chromone-containing analogues **222**, **241**, **258**, **260**, **266**, **269**, **272** and **274**.

Since the chromone containing-analogues **222**, **241**, **258**, **260**, **266**, **269**, **272** and **274** were expected to exhibit some structural similarity with ritonavir **2**, their *in silico* alignment with ritonavir **2** was examined. This involved matching, where possible, corresponding groups, such as the characteristic 3-hydroxyl group in compounds **222**, **241**, **258**, **260**, **266**, **269**, **272** and **274**, the amide group in compound **274** as well as the aromatic groups.

There are numerous reports on X-ray crystal structures of complexes of linear inhibitors with the HIV-1 protease dimer.[47,195-196] Two important common features have been observed in the binding of peptidomimetic inhibitors and these are illustrated for the model isostere in Figure 78.[16,73,196] The first feature involves linkage of the inhibitor to the flexible glycine-rich "flaps" through hydrogen-bonding with a structural water molecule. This water molecule interacts with the amide hydrogens of the isoleucine residues, Ile 50A-NH and Ile 50B-NH and carbonyl oxygens of the inhibitor molecule. The second feature is the hydrogen-bonding between the inhibitor hydroxyl group and

the catalytic aspartic acid residues Asp 25A-COOH and Asp 25B-COO$^-$, situated in the S_1 and $S_{1'}$ binding pockets of the enzyme. The bond marked with an asterisk (*) in Figure 78 corresponds to the cleavage site in an enzyme substrate. The inhibitor residues P_1, P_2, P_3 *etc.* bind to the S_1, S_2, S_3 *etc.* pockets of the HIV-1 protease enzyme situated in monomer A (Figure 79), while the $P_{1'}$, $P_{2'}$, $P_{3'}$ residues bind to the $S_{1'}$, $S_{2'}$, $S_{3'}$ enzyme binding pockets situated in monomer B. Table 1 summarizes the amino acid residues which form the specific enzyme binding pockets.

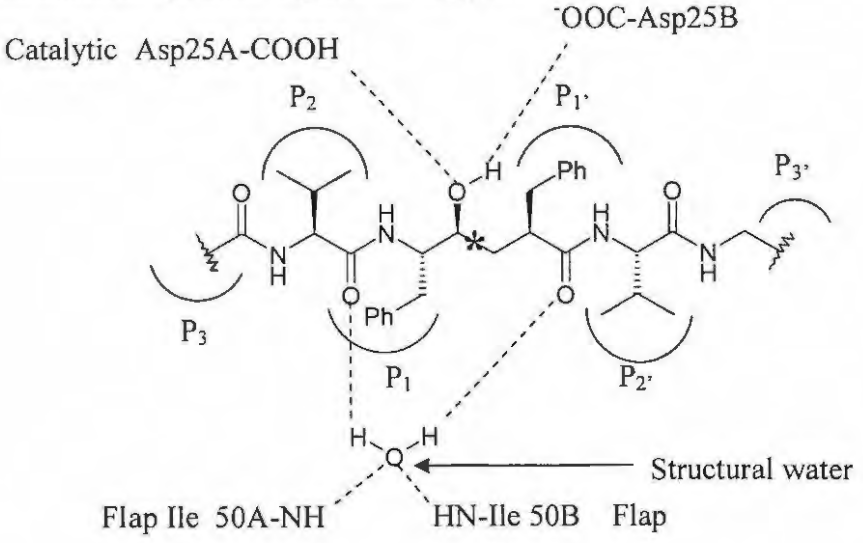

Figure 78. Schematic representation of the hydrogen-bonding interactions observed when typical peptidomimetic inhibitors, such as ritonavir, bind to the HIV-1 protease active site.[16, 204]

Table 1. Amino acid sequences forming the HIV-1 Protease subsites.[41]

Subsite	HIV-1 PR
S_4	$Asp^{30'}$ $Ile^{50'}$ $Ile^{54'}$
S_3	Arg^{8} $Asp^{29'}$ Leu^{23} Val^{82} $Arg^{87'}$
S_2	Ala^{28} Val^{82} $Phe^{53'}$ $Ile^{54'}$ $Leu^{76'}$ $Thr^{80'}$ $Ile^{84'}$
S_1	Leu^{23} Asp^{25}* Phe^{53} Pro^{81} Val^{82} Ile^{84}
$S_{1'}$	$Leu^{23'}$ $Asp^{25'}$* $Phe^{53'}$ $Ile^{84'}$
$S_{2'}$	Ala^{28} Asp^{30} Val^{32} Phe^{53} Ile^{54} Leu^{76} Ile^{84}
$S_{3'}$	Arg^{8} Asp^{29} Ile^{50} $Pro^{81'}$ Arg^{87}

Primes (') distinguish the residues from the two subunits in the dimer of HIV-1PR.
* Catalytic Asp residue.

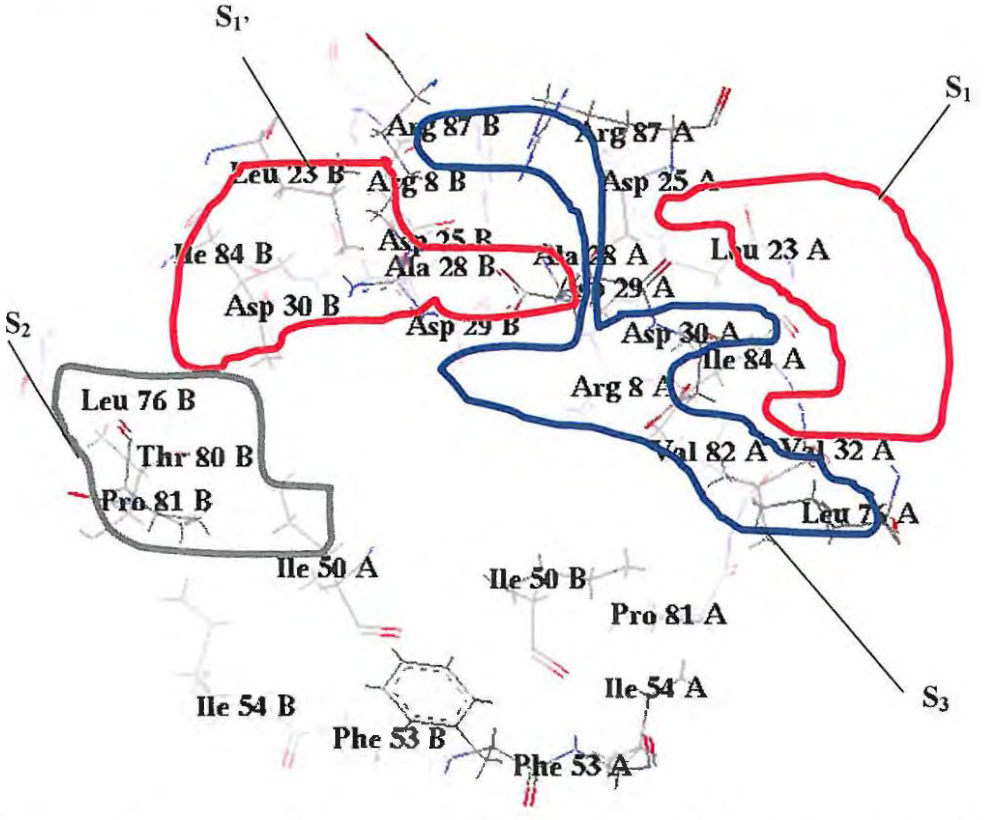

Figure 79. X-ray crystal structure of HIV-1 protease with the amino acid residues that form the enzyme binding pockets in both monomers A and B.[41, 195]

The interaction between compounds **222**, **241**, **258**, **260**, **266**, **269**, **272** and **274** and the HIV-1 protease receptor cavity was explored using the Cerius^2 docking module, "LigandFit". In this approach, the docking of various conformations of the ligand into the receptor site is examined while the enzyme remains rigid. Initially, the active binding site of the HIV-1 protease (Figure 71) was exposed by removing the ligand occupying the receptor cavity in the enzyme-ligand complex in the structure reported by Kempf *et al.*[203] Figure 80 shows the complex of the HIV-1 protease enzyme with ritonavir **2**, covered by a Connoly surface, and it is evident that this inhibitor occupies a significant volume of the receptor cavity.[197] The van der Waals energy of interaction between ritonavir and the receptor cavity was found to be 903.5 kcal mol^{-1}. The van der Waals binding energy reflects the stability provided by hydrophobic interactions between the enzyme and the inhibitor. The ligand scoring option was used to select the conformation with the best binding based on both hydrogen-bonding and van der Waals interactions. Twenty conformers were so scored in each case with conformer 1 having the best interaction since it exhibits the highest binding energy of the set. This ranking is supported by the hydrogen-bonding distances, which are shorter and, hence, stronger in conformer 1 than in conformer 20. Figure 81 illustrates the interactions observed between conformer 1 of the docked ritonavir **2** molecule and the HIV-1 protease receptor cavity-interactions which include some of the common features characteristic of peptidomimetic inhibitors.[198]

Figure 80. Structure of ritonavir **2** docked into the HIV-1 protease receptor cavity.

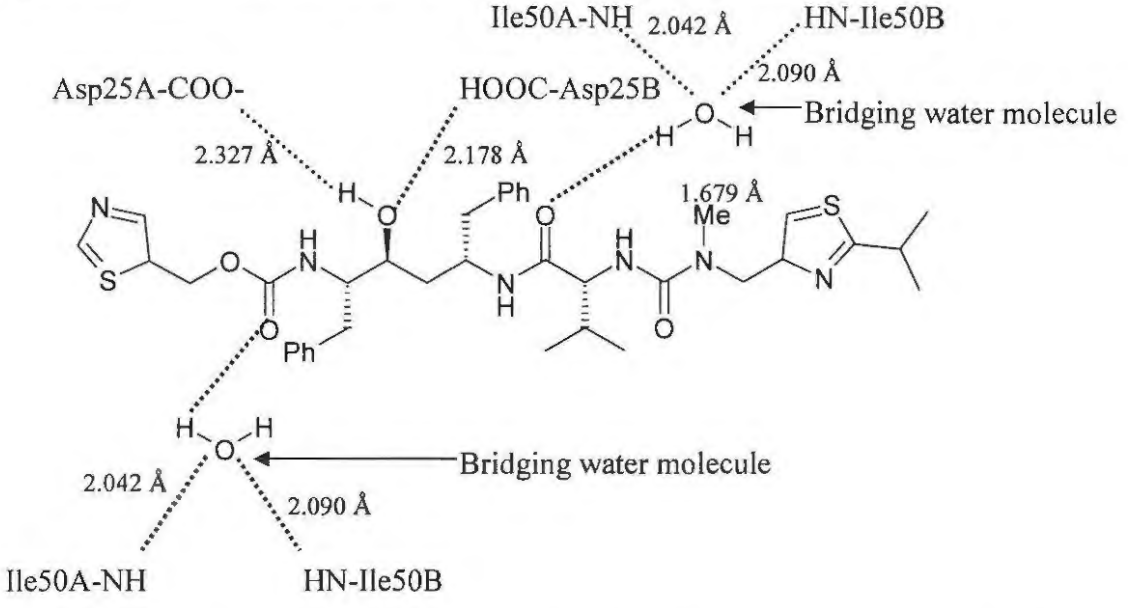

Figure 81. Schematic representation of hydrogen-bonding interactions between ritonavir **2** and the HIV-1 protease receptor cavity in the presence of bridging, structural water molecules.

The docking of compound **258** revealed water-mediated interactions with the HIV-1 protease receptor cavity (Figures 82 to 85). Hydrogen-bonding interactions (≤ 2.1 Å) were predicted between the isoleucine residues, Ile 50A-NH and Ile 50B-NH, a bridging water molecule, and both the amino nitrogen and hydrogen atoms in compound **258**. Hydrogen bonding interaction was also apparent between the same bridging water molecule and the nitrile nitrogen (C≡N), and between the hydroxyl hydrogen and the catalytic aspartic acid residue (Asp 25A-COO^-). Compound **258** appears to interact with the S_1, S_3, and S_4 enzyme-binding pockets with a van der Waals binding energy of -45.29 kcal mol^{-1}, which is far lower than for ritonavir **2** (903.5 kcal mol^{-1}). Clearly, compound **258** seems to exhibit fewer hydrogen-bonding interactions inside the receptor cavity and a much lower overall receptor binding energy (164.2 kcal mol^{-1}) than ritonavir **2**. Compound **258** also occupies 0.336 $Å^3$ of the receptor cavity whereas ritonavir **2** occupies 0.612 $Å^3$. Comparison of the interactions for conformer 1 with the highest binding energy (Figures 82 and 83) and conformer 20 with the lowest binding energy (Figures 84 and 85), reveals that the latter exhibits weaker binding interactions. Attempts to dock compound **258** into the enzyme receptor cavity in the absence of a water molecule failed to show any hydrogen-bond interactions with the amino acid residues forming the enzyme binding pockets, indicating the absence of direct interaction between the ligand and the amino acids residues situated in the enzyme binding pocket. Table 17 details the overall binding energies for the twenty conformers scored for compound **258**.

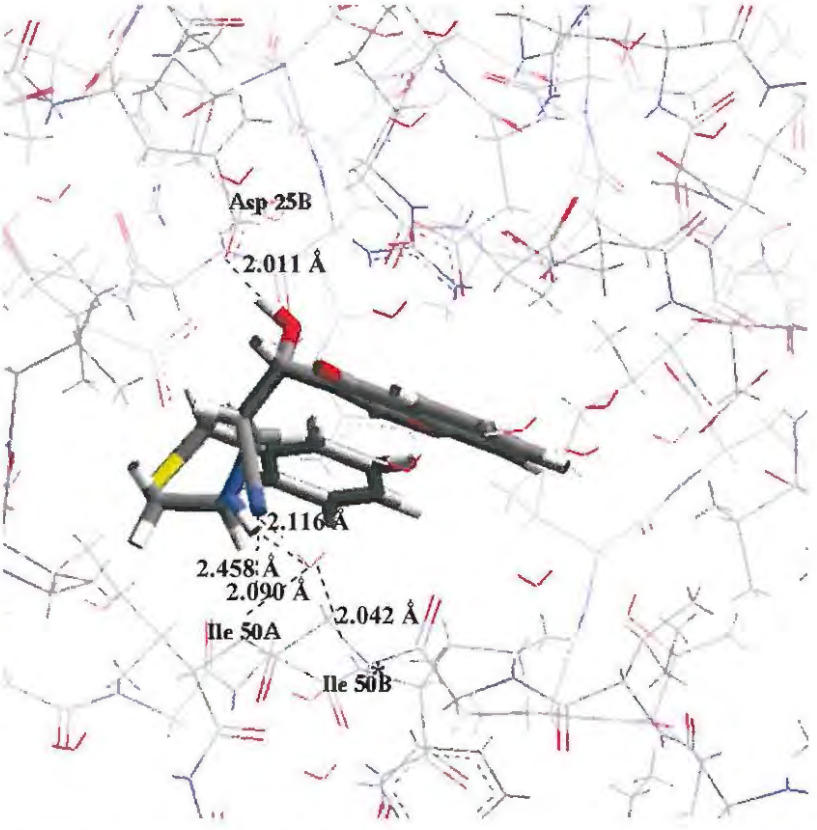

Figure 82. Complex of compound **258** (conformer 1) with the HIV-1 protease receptor cavity showing interactions with a structural water molecule. (Asterisk indicates structural water molecule.)

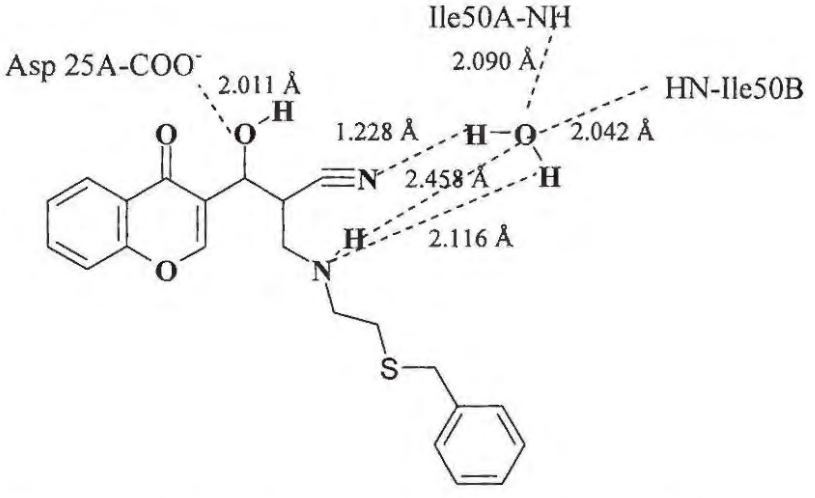

Figure 83 Schematic representation of hydrogen-bonding interactions between compound **258** (conformer 1) and the HIV-1 protease receptor cavity in the presence of a structural water molecule.

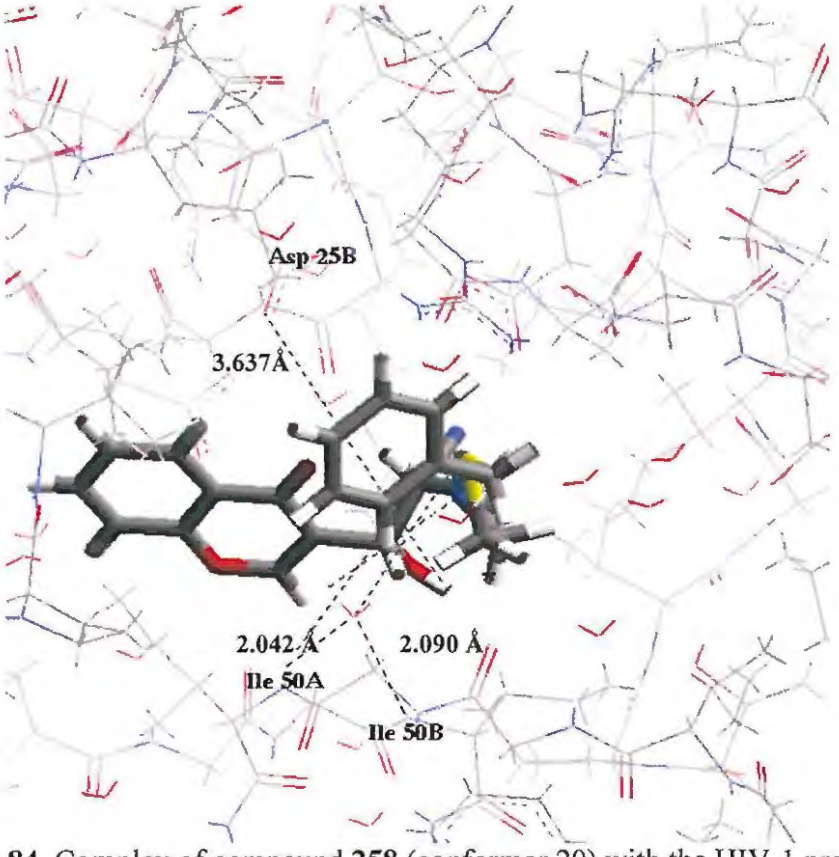

Figure 84. Complex of compound **258** (conformer 20) with the HIV-1 protease receptor cavity showing interactions with a structural water molecules. (Asterisk indicates structural water molecule.)

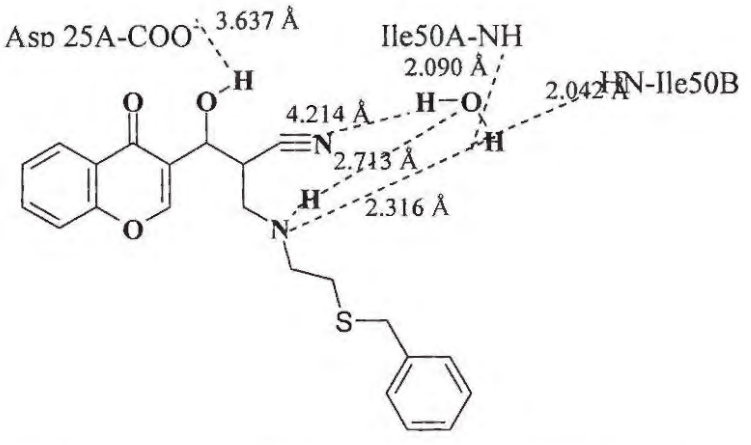

Figure 85. Schematic representation of hydrogen-bonding interactions between compound **258** (conformer 20) and the HIV-1 protease receptor cavity in the presence of a structural water molecule.

Table 17. The binding energies for the twenty scored conformers of compound **258**.

Conformer no.	Binding energy for compound **258** (kcal.mol^{-1})
1	164.2
2	133.1
3	104.3
4	97.3
5	73.1
6	60.5
7	53.7
8	53.3
9	52.8
10	50.3
11	45.8
12	40.0
13	30.6
14	22.1
15	22.0
16	21.9
17	21.8
18	18.5
19	17.3
20	17.1

The docking of compound **263** (conformer 1) revealed water-mediated interactions with the HIV-1 protease receptor cavity (Figures 86 to 88). Hydrogen-bonding interaction was observed between a bridging water molecule and the amino hydrogen (NH) in compound **263**. Comparison of conformer 1, with lowest energy (Figures 86 and 87) and conformer 20 (Figure 88), with highest energy, shows that the latter exhibits longer NH-H_2O separation meaning a weaker interaction. Compound **263** appears to interact with the S_4-S_3'enzyme binding pockets with a van der Waals energy of -16.73 kcalmol^{-1} and overall binding energy of 156.4 kcalmol^{-1} again far lower than for ritonavir **2** and also appears to occupy 0.320 Å^3 of the receptor cavity. Attempts to dock this compound in a receptor cavity in the absence of structural water revealed no hydrogen-bonding interaction.

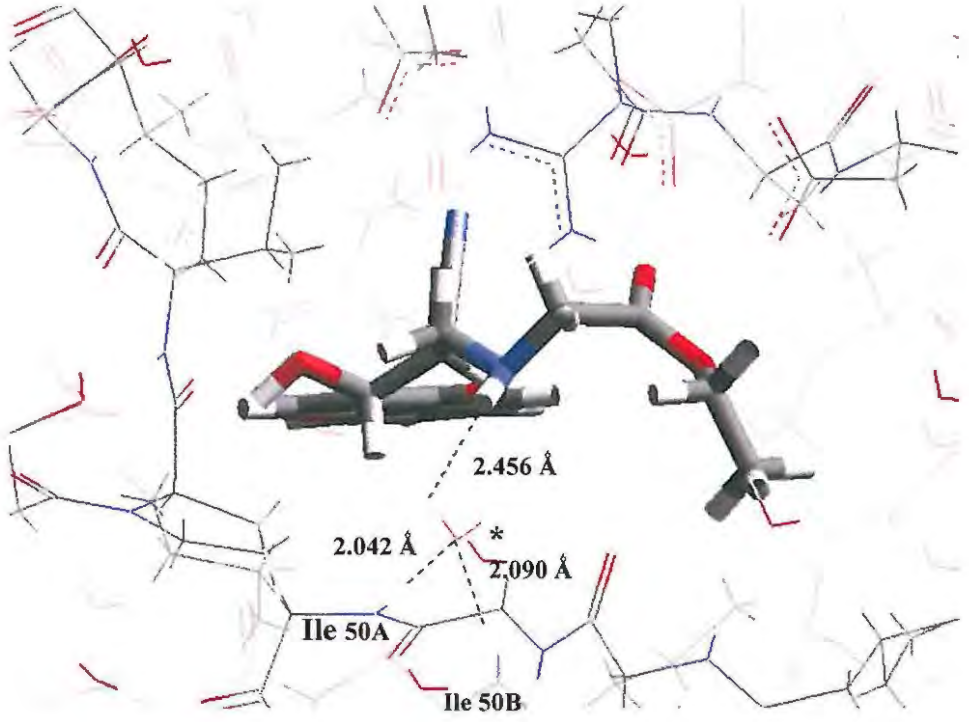

Figure 86. Complex of compound **263** (conformer 1) with the HIV-1 protease receptor cavity showing interactions with a structural water molecule. (Asterisk indicates structural water molecule.)

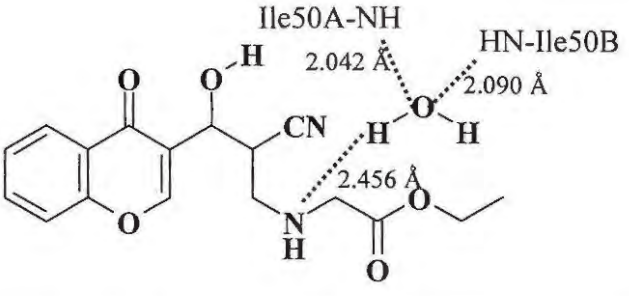

Figure 87. Schematic representation of hydrogen-bonding interactions between compound **263** (conformer 1) and the HIV-1 protease receptor cavity in the presence of a structural water molecule.

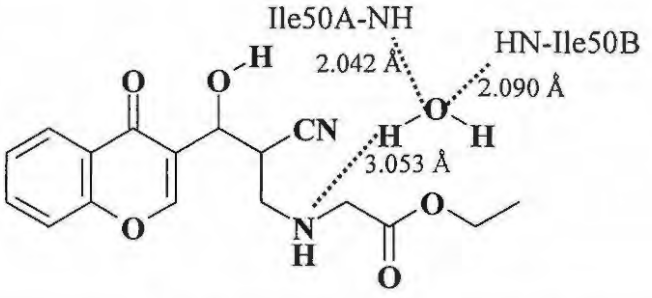

Figure 88. Schematic representation of hydrogen-bonding interactions between compound **263** (conformer 20) and the HIV-1 protease receptor cavity in the presence of a structural water molecule.

The hydrogen-bonding interactions observed on docking compound **272** into the HIV-1 protease receptor cavity are illustrated in Figures 89-92. This compound **272** appears to interact with the S_1, S_4 and S_3'enzyme binding pockets with van der Waals energy of -27.5 kcal mol^{-1} and an overall binding energy of 139.9 kcal mol^{-1} and was found to occupy *ca.* 0.331 $Å^3$ of the receptor cavity. In this case, the substrate hydrogen bonds directly to Asp 25ACO_2^- *via* the threonine hydroxyl hydrogen and *via* a structural water molecule as illustrated in Figures 89,90. In the case of conformer 20, however, the separations are all so large (*ca.* 8-10 Å) as to preclude hydrogen-bonding interactions (Figures 91, 92). Attempts to dock compound **272** into the receptor cavity in the absence of a structural water molecule again revealed no interactions with the amino acid residues in the enzyme binding pockets.

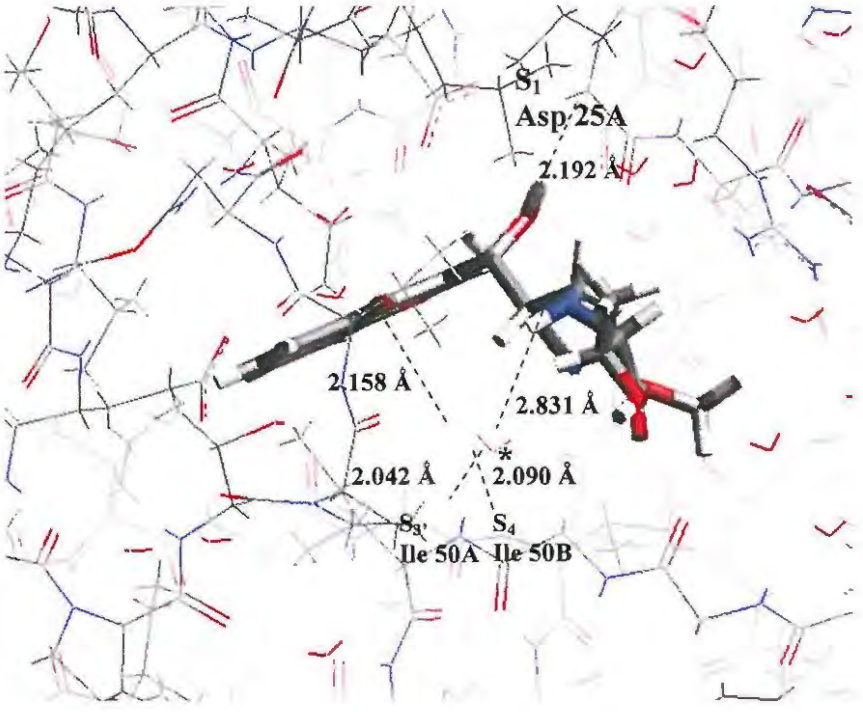

Figure 89. Complex of compound **272** (conformer 1) with the HIV-1 protease receptor cavity showing interactions with a structural water molecule. (Asterisk indicates structural water molecule.)

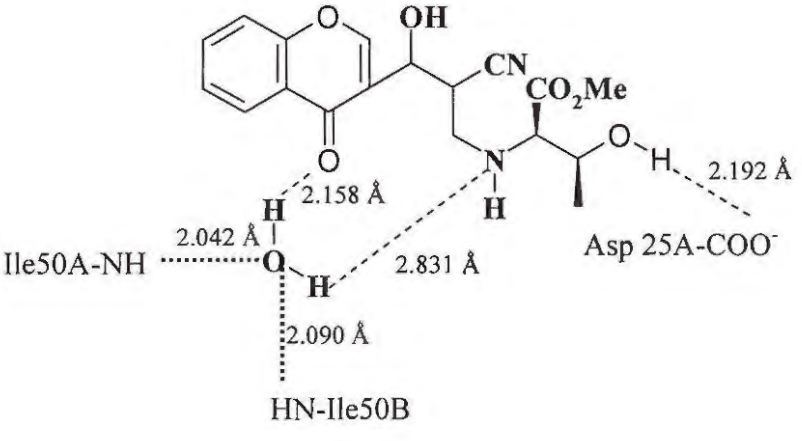

Figure 90. Schematic representation of hydrogen-bonding interactions between compound **272** (conformer 1) and the HIV-1 protease receptor cavity in the presence of a structural water molecule.

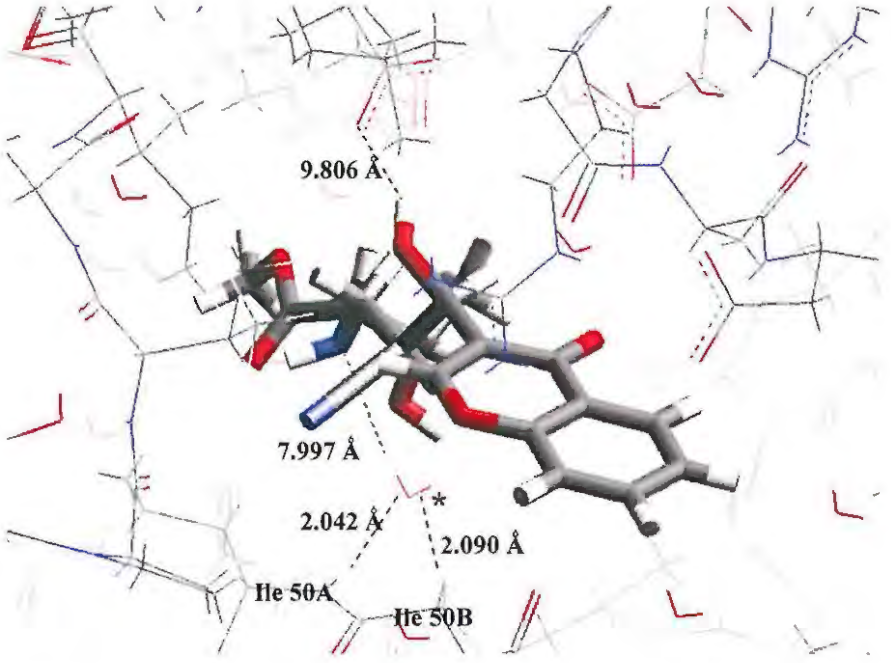

Figure 91. Complex of compound **272** (conformer 20) with the HIV-1 protease receptor cavity showing distances between the substrate and potential hydrogen-bonding moieties. (Asterisk indicates structural water molecule.)

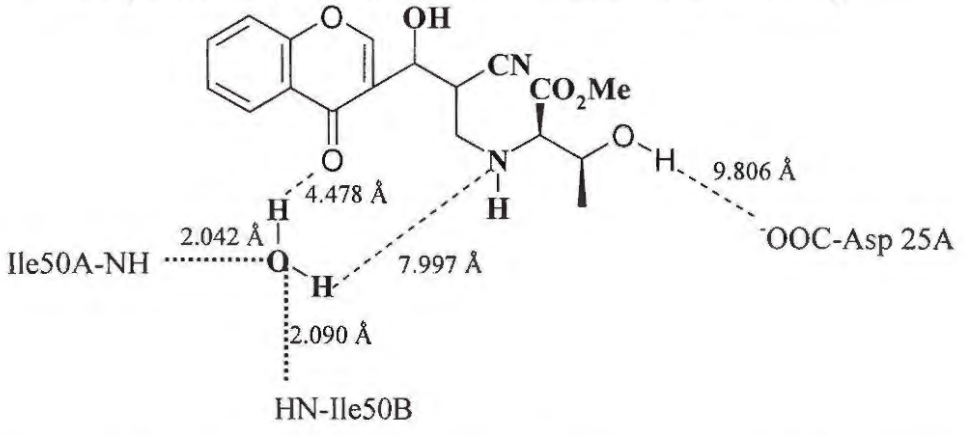

Figure 92. Schematic representation of distances between compound **272** (conformer 20) and potential hydrogen-bonding moieties in the HIV-1 protease receptor cavity.

Docking of the compounds **222, 241, 266, 269** and **274** into the HIV-1 protease receptor cavity, has revealed some hydrogen-bonding interactions which are illustrated schematically in Figure 93. In each case, conformer 1 shows appropriate atomic separations consistent with effective hydrogen-bonding interaction, whereas conformer

20 exhibits separations so large as to preclude hydrogen-bonding interaction. Table 18 details the enzyme binding pockets which interact with these compounds; their van der Waal energies and overall binding energies and also the space they appear to occupy in the receptor cavity. Attempts to dock these compounds into the receptor cavity in the absence of structural water molecule, reveals that none of them were sufficiently close to the amino acid residues in the enzyme binding pockets to experience receptor-substrate hydrogen bonding.

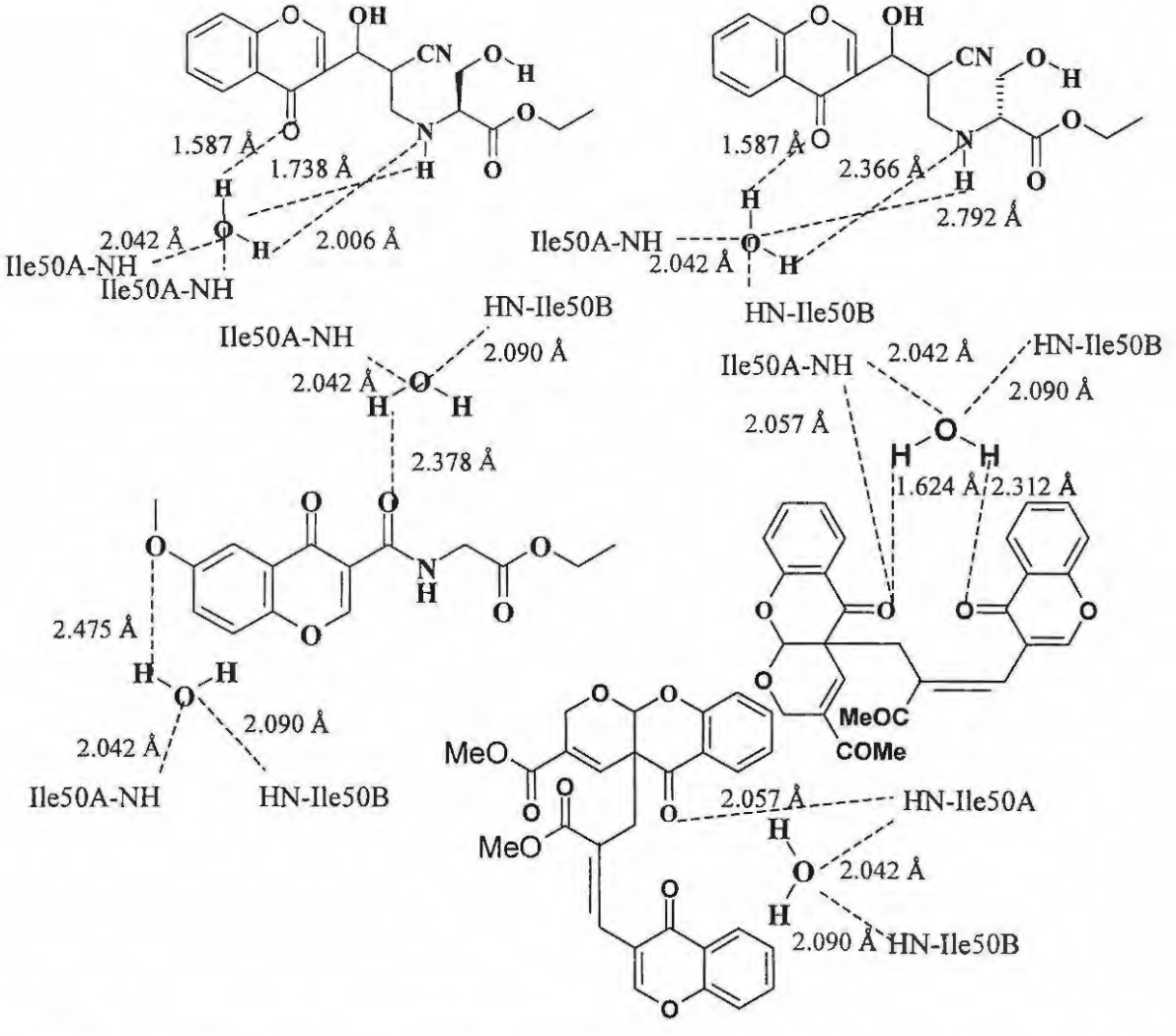

Figure 93. Schematic representation of hydrogen-bonding interactions between "conformer 1" of compounds **222, 241, 266, 269** and **274** and the HIV-1 protease receptor cavity in the presence of structural water molecules.

Table 18. Results obtained when compounds **2**, **222**, **222**, **241**, **258**, **260**, **266**, **269**, **272** and **274** were docked in the HIV-1 Protease receptor cavity.

Compound	Binding Energy / kcal.mol^{-1}		Space occupied Å^3	Enzyme binding pockets nteracting
	Van der Waals	Overall		
Ritanovir	903.5	15171.7	0.612	$S_{3'}$,$S_{2'}$, $S_{1'}$, S_1, S_2,
222	241.8	252.2	0.408	S_4
241	65.46	204.7	0.394	$S_{3'}$ and S_4
258	-45.29	164.2	0.336	$S_{1'}$, $S_{3'}$ and S_4
263	-16.73	156.4	0.321	$S_{3'}$ and S_4
266	-27.50	155.2	0.319	$S_{3'}$ and S_4
269	-24.04	160.3	0.308	$S_{3'}$ and S_4
272	-17.19	139.9	0.331	$S_{1'}$, $S_{3'}$ and S_4
274	-38.26	156.1	0.287	$S_{3'}$ and S_4

These *in silico* studies certainly indicate the capacity of the chromone containing-analogues **2, 222, 222, 241, 258, 260, 266, 269, 272** and **274** to interact with the receptor cavity, but further modification of these compounds may well be necessary to increase the number of efficient hydrogen-bonding interactions with critical enzyme binding pockets. Careful consideration of their potential for binding *via* hydrophobic interactions will also be critical. The observation that there were, in general, no hydrogen-bonding interactions in the absence of structural water molecules in the receptor cavity, suggest the possibility of introducing a group on the inhibitor which will replace the need for structural water. It is perhaps significant that compound **263**, which showed no activity at all in the enzyme inhibition studies (Section 2.4.3), exhibits a much higher *in silico* van der Waals binding energy (-16.73 kcal.mol^{-1}) than the competitive inhibition **266** (-27.50 kcal.mol^{-1}) and the non-competitive inhibition **258** (-45.29 kcal.mol^{-1}). In all cases, the favoured bound conformation was found to have a similar conformation to that of the 'isolated' global minimum conformation.

2.6 KINETIC MECHANISTIC STUDY of the BAYLIS-HILLMAN REACTION OF 2-NITROBENZALDEHYDES

Shi *et al*, [199-201] have recently reported the formation of the bis-MVK Baylis-Hillman adducts **278a-d** and **279a-d**, together with the normal Baylis-Hillman products **277a-d**, when certain arylaldehydes **275a-d** are reacted with the Michael acceptor MVK **276**, **(Scheme 65)**. They observed that an excess of MVK **276** was found to promote formation of the bis-MVK products and the MVK dimer **246**.[199, 202-203]

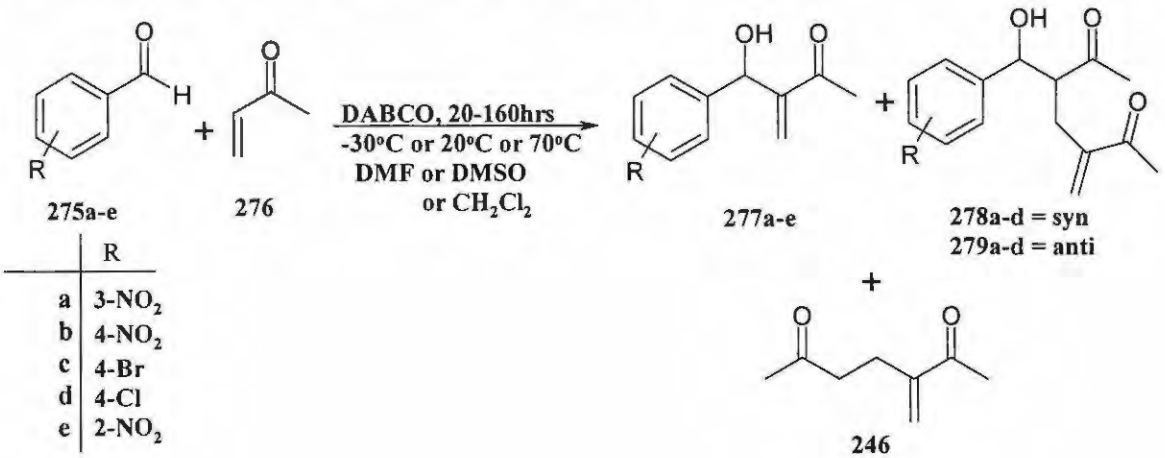

	R
a	3-NO_2
b	4-NO_2
c	4-Br
d	4-Cl
e	2-NO_2

Scheme 65

When 2-nitrobenzaldeyde **275e** was reacted with MVK **276**, Shi *et al*[199] did not obtain the diastereomeric adducts **278e** and **279e** but only the normal Baylis-Hillman product **277e**. However, Pakade working on a project in our group on the application of Baylis-Hillman methodology in the construction quinoline derivatives,[193,194] was able to isolate both the normal Baylis-Hillman product **277f** and the corresponding diastereomeric adducts **278f** and **279f** from the reaction of 3-methoxy-2-nitrobenzaldehyde **275f** with MVK **276** (**Scheme 66**). This observation has prompted us to explore the mechanism of these Baylis-Hillman reactions, focusing, initially, on the reaction of 3-methoxy-2-nitrobenzaldehyde **275f** with MVK **276** in the presence of diazabicyclo[5.5.5.]octane (DABCO) in $CHCl_3$ or $CDCl_3$.

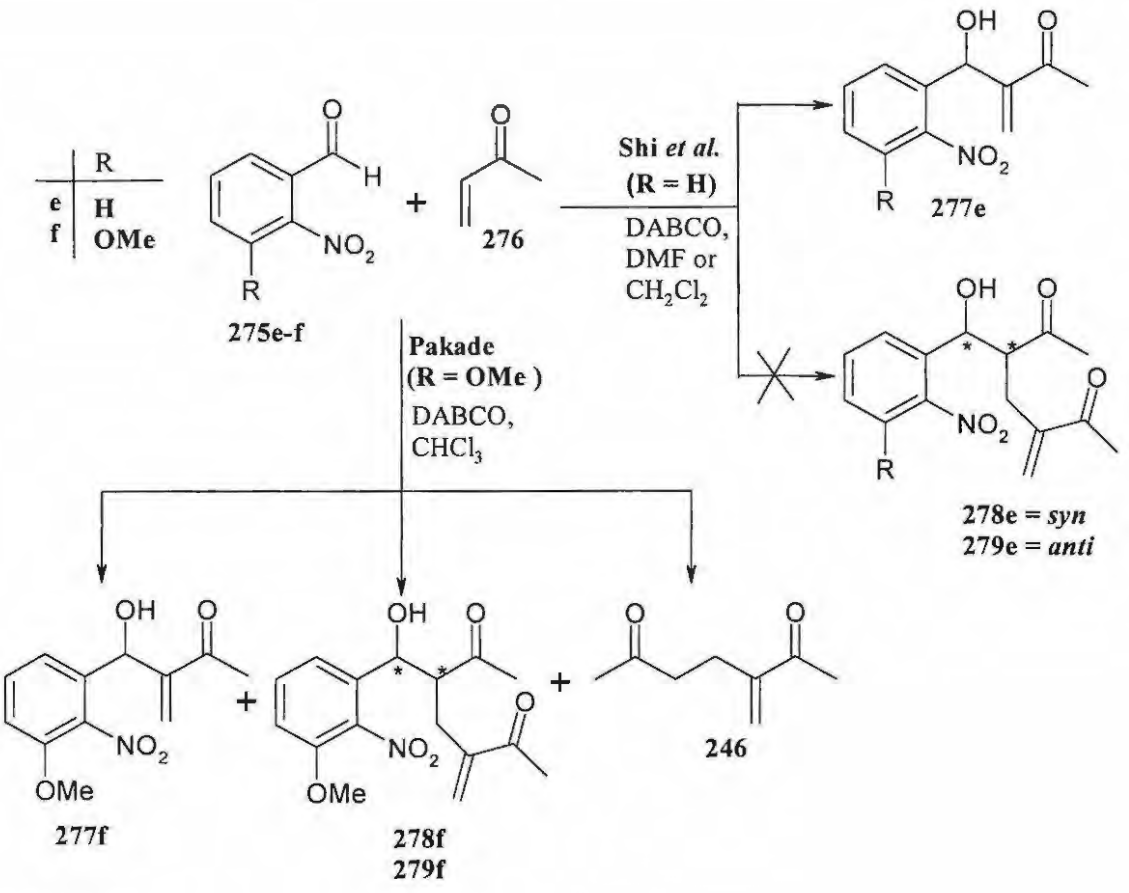

Scheme 66

The formation of adducts of type **278** and **279** from 3-methoxy-2-nitrobenzaldehyde **275f** but not 2-nitrobenzaldehyde **275e** raises interesting mechanistic questions. While Shi *et al.*[200] had proposed the possibility of two possible mechanistic pathways, which are outlined for the reaction of 3-nitrobenzaldehyde **275a** in **Scheme 67**, they favoured the **Path I** since there was no reaction when **Path II** was explored by treating 3-nitrobenzaldehyde **275a** with MVK dimer **246** in the presence of DABCO. Shi *et al.*[200] indicated that **Paths I** and **II** would be expected to involve the steps detailed in **Scheme 67**, which has also provided the framework for a parallel theoretical study in our group. **Path I** involves the nucleophilic addition of DABCO (**C**) to the activated alkene, MVK **276**, to form a zwitterionic enolate (**D**), followed by addition of this intermediate **D** to the aldehyde **275a**; proton transfer and release of the catalyst, DABCO (**C**), then affords the normal Baylis-Hillman product **277a.** This product (**277a**) then reacts with a second

zwitterionic enolate species (**D**) to yield the *syn*- and *anti*-adducts **278a** and **279a**. **Path II**, on the other hand, involves the reaction of MVK **276** with DABCO (**C**) to form the zwitterionic enolate (**D**), which then attacks another MVK molecule **276**, to form the bis-MVK zwitterionic enolate (**G**). Instead of releasing DABCO to afford the MVK dimer **246** the enolate **G** can now attack the aldehyde **275a** resulting in the formation of the *syn* and *anti* adducts **278a** and **279a** after release of DABCO (**C**). It should be noted that in **Path I**, the diastereomers **278a** and **279a** are produced *via* the formation of the normal Baylis-Hillman product **277a**, whereas in **Path II**, they are produced directly from the reaction of 3-nitrobenzaldehyde **275a**.

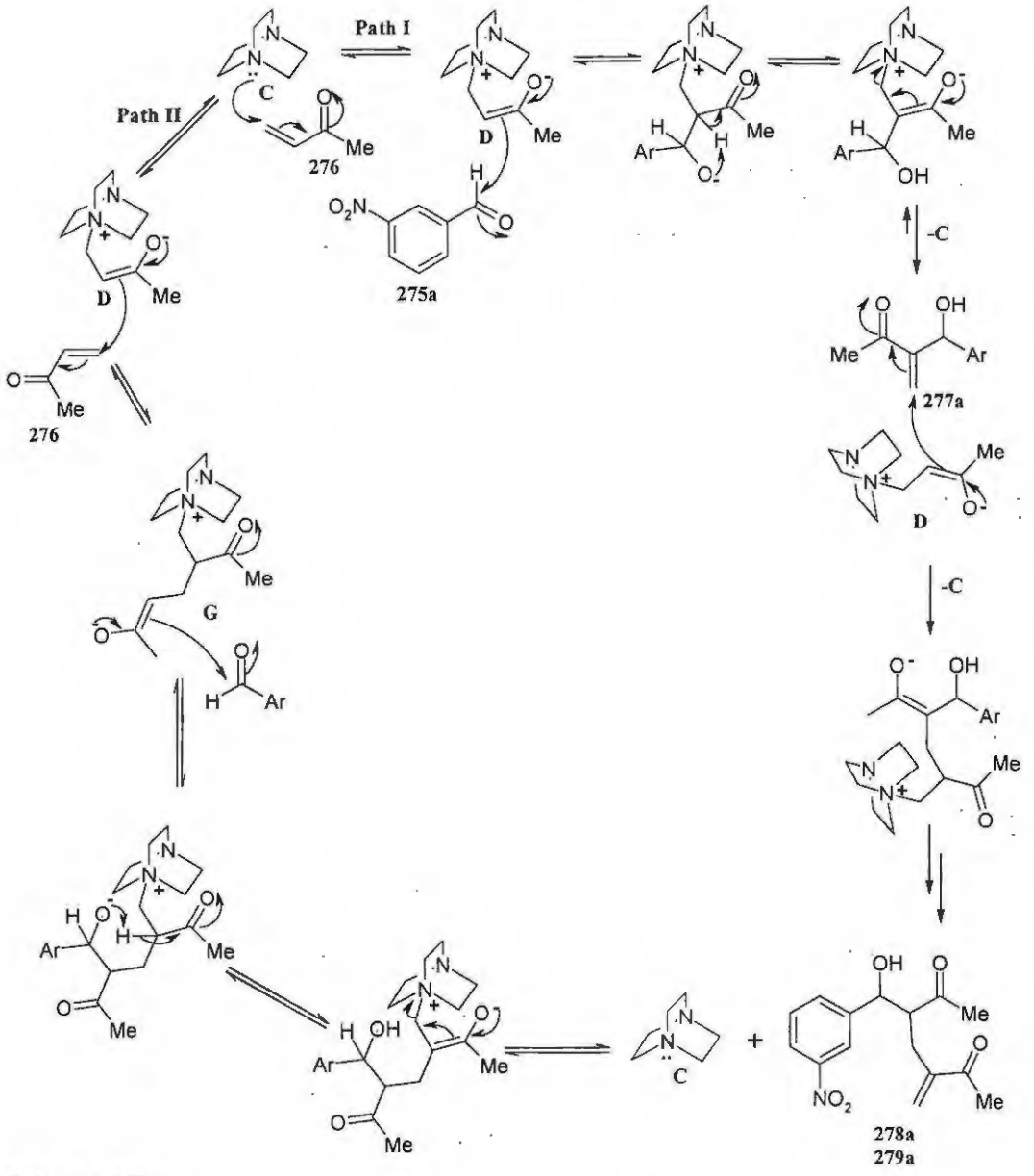

Scheme 67

It was decided to investigate the use of NMR methods to monitor the progress of the reaction. This required:- i) separation and characterization of each of the components in the reaction mixture; and ii) sufficient resolution of significant signals in the spectrum of the mixture to permit identification and integration of structure-specific signals.

2.6.1 Isolation of the reaction products

The reaction between 3-methoxy-2-nitrobenzaldehyde **275f** and MVK **276** (**Scheme 66**) was repeated. Flash chromatography of the crude product formed after 24h yielded the pure MVK dimer **246** and a mixture of the *syn*-and *anti*-diastereomers **278f** and **279f**, respectively. Since flash and radial chromatography failed to separate the diastereomeric adducts **278f** and **279f**, HPLC was used to obtain the pure diastereomers. The normal Baylis-Hillman product **277f** could not be observed when the reaction was stopped after 24 hours and, consequently, was isolated by stopping the reaction after 2 hours. The ^{1}H NMR spectra of the Baylis-Hillman product **277f**, the *syn*-and *anti*-diastereomers, **278f** and **279f**, respectively, and the MVK dimer **246** are illustrated in Figures 94-97. The ^{1}H NMR spectrum (Figure 94) for the Baylis-Hillman product **271f** reveals:- singlets at 2.33 and 3.88 ppm which correspond to the 5'-acetyl and 3-methoxy protons, respectively; a broad signal at 3.45 ppm corresponding to the hydroxyl proton; a singlet at 5.67 ppm corresponding to the 3'-methine proton; two singlets at 5.95 and 6.22 ppm corresponding to the diastereotopic 1'-methylene protons; and the three aromatic signals further downfield. The ^{1}H NMR spectrum (Figure 95) of the *syn*-diastereomer **278f** reveals an additional singlet at 2.35 ppm, which corresponds to the 9'-methyl protons, multiplets at 2.35 and 2.61 ppm, which correspond to the diastereotopic 3'-methylene protons, and a multiplet at 3.21 ppm corresponding to the 4'-methine proton. The ^{1}H NMR spectrum (Figure 96) of the *anti*-diastereomer **279f**, exhibits the same spectroscopic pattern as the *syn*-diastereomer but with obvious differences in the chemical shift values. For comparative purposes, the ^{1}H NMR spectrum of the MVK dimer **246** is illustrated in Figure 97. Examination of the spectra of the reactants and all three products permitted identification of the signals to be used as NMR probes in the kinetic studies.

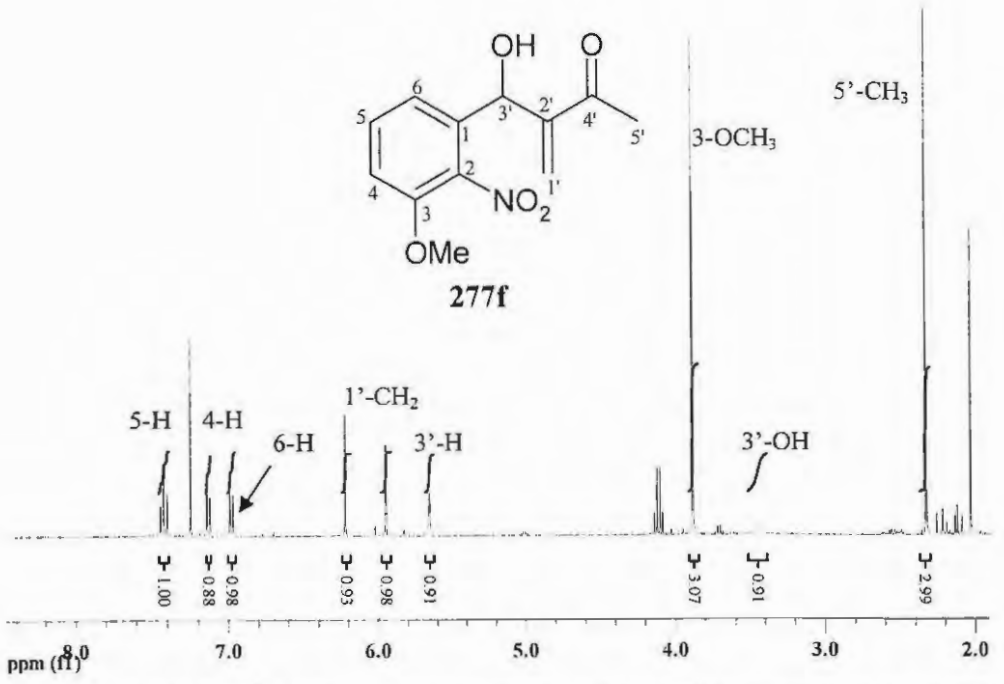

Figure 94. 400 MHz ^{1}H NMR spectrum of the Baylis-Hillman product **277f** in $CDCl_3$.

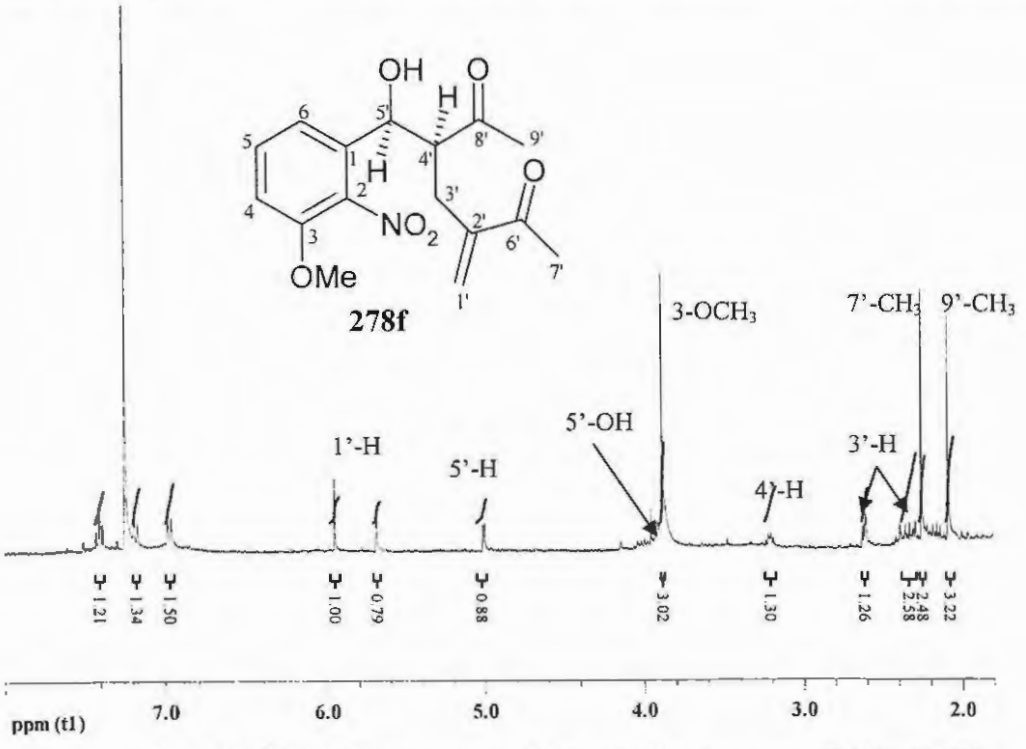

Figure 95. 400 MHz ^{1}H NMR spectrum of the *syn*-diastereomer **278f** in $CDCl_3$.

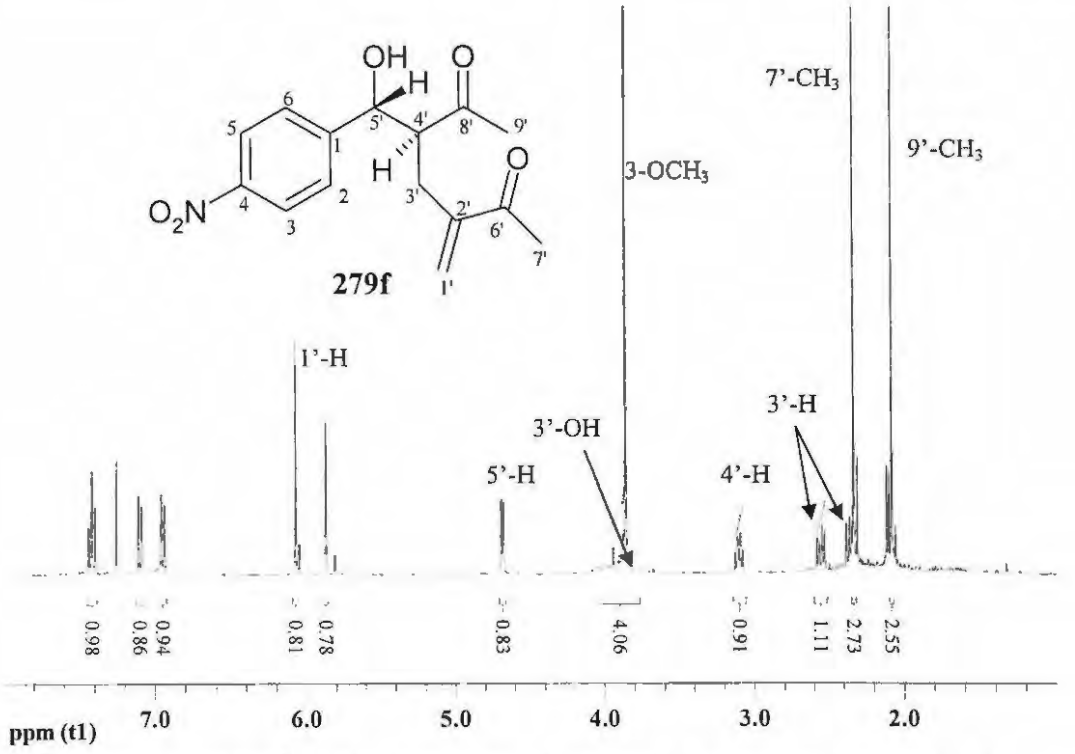

Figure 96. 400 MHz ^{1}H NMR spectrum of the *anti*-diastereomer **279f** in $CDCl_3$.

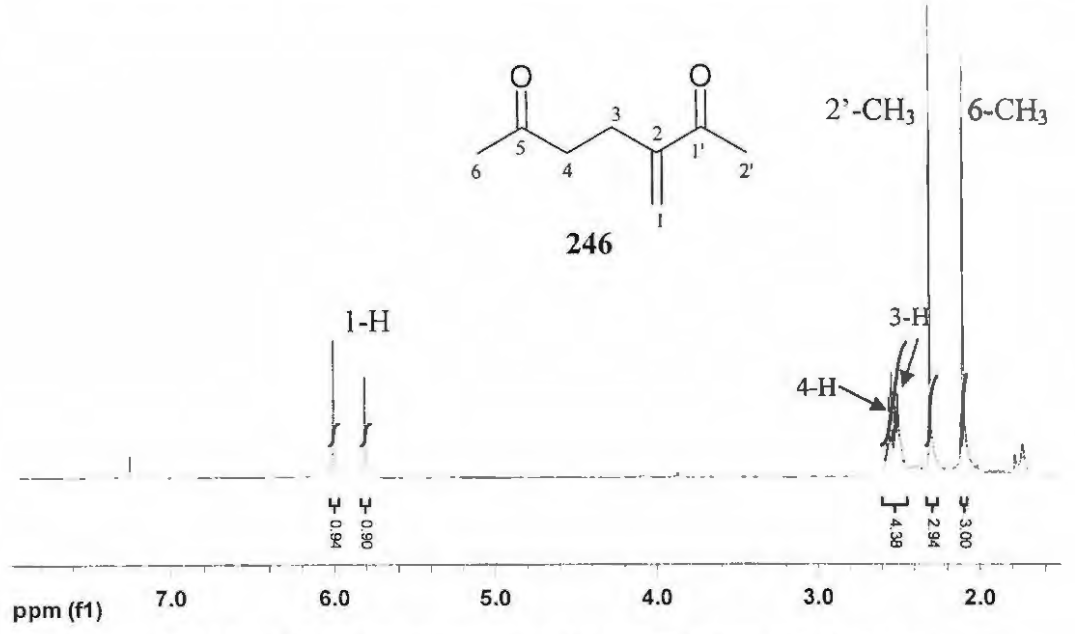

Figure 97. 400 MHz ^{1}H NMR spectrum of the MVK dimer **246** in $CDCl_3$.

2.6.2 Optimization of the spectroscopic analysis methodology

Figure 98 illustrates the ^{1}H NMR spectrum for the reaction after 1minute, with the arrow indicating the region where the vinylic protons normally resonate. Initially, it was hoped that the vinylic methylene proton signals for each species (between 5.6 and 6.9 ppm) could be used to monitor the progress of the reaction. However, signal overlap made it difficult to integrate the signals for the individual products (Figure 99). An attempt was made to address this problem by employing a deconvolution method.[205] This method permits multipoint baseline correction and curve fitting (Figure 100), which enhances peak resolution and peak visibility (Figure 101). Unfortunately, this method could not be used since careful analysis of the results revealed some obvious errors, and attention was turned to the use of ^{13}C NMR spectroscopy. However, since different carbon nuclei typically exhibit different relaxation times, signal integration cannot normally be used for quantitative purposes.

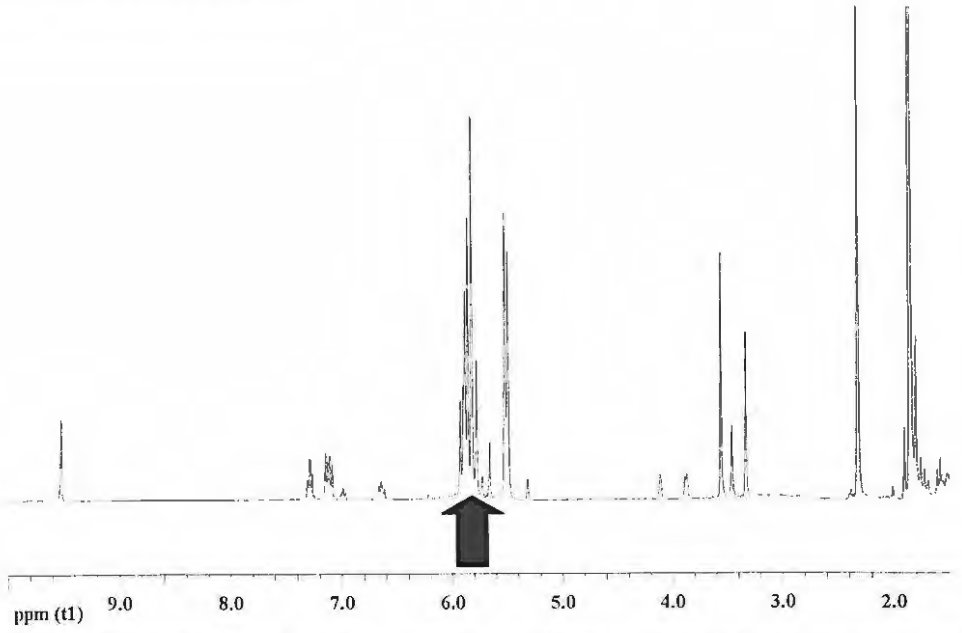

Figure 98. 400 MHz ^{1}H NMR spectrum reflecting the DABCO-catalysed reaction of 3-methoxy-2-nitrobenzaldehyde **275f** with MVK **276** in $CDCl_3$ after 1min.

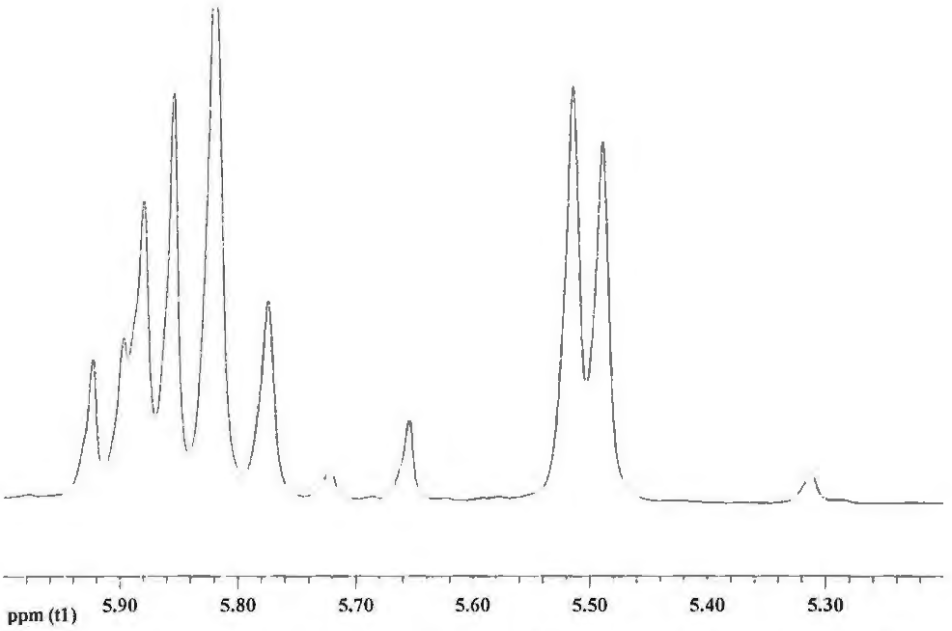

Figure 99. Expansion of a region of the 400MHz ^{1}H NMR spectrum (Fig. 98) reflecting the DABCO-catalysed reaction of 3-methoxy-2-nitrobenzaldehyde **275f** with MVK **276** in $CDCl_3$ after 1min, *before* multipoint baseline correction.

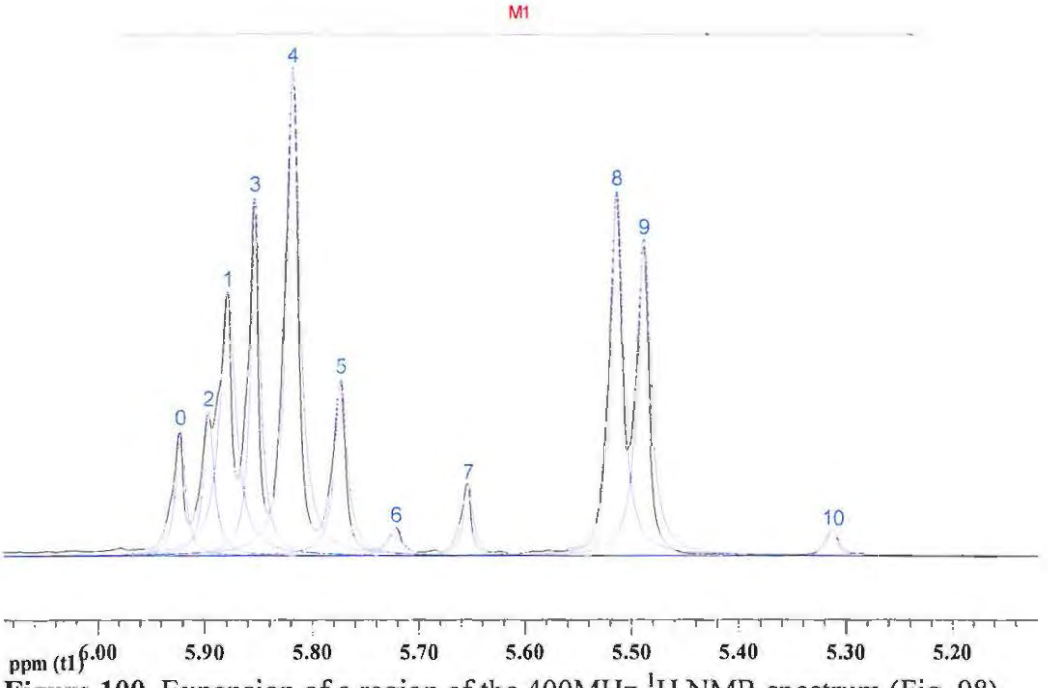

Figure 100. Expansion of a region of the 400MHz ^{1}H NMR spectrum (Fig. 98) reflecting the DABCO-catalysed reaction of 3-methoxy-2-nitrobenzaldehyde **275f** with MVK **276** in $CDCl_3$ after 1min, with the curve fitted spectrum, after multipoint baseline correction, in blue.

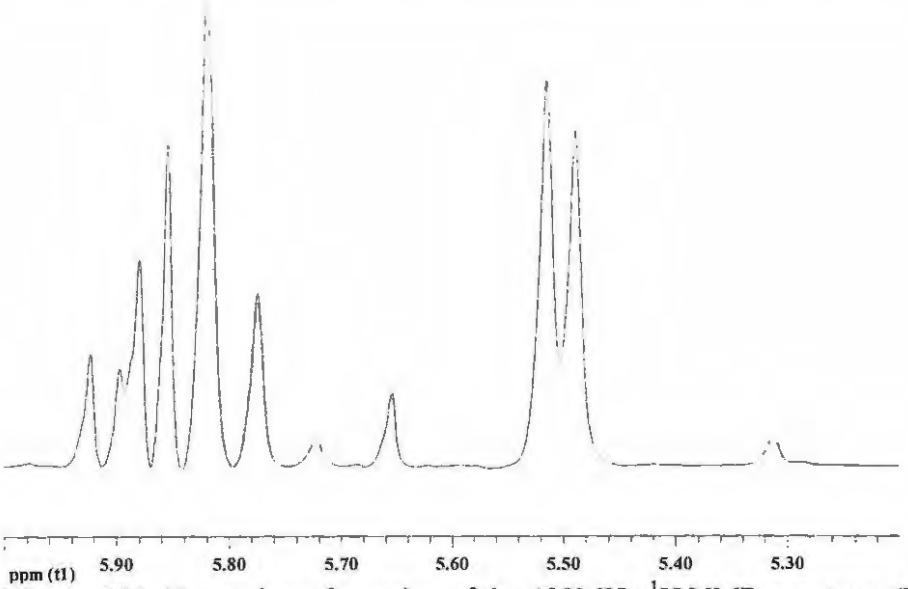

Figure 101. Expansion of a region of the 400MHz ^{1}H NMR spectrum (Fig. 98) reflecting the DABCO-catalysed reaction of 3-methoxy-2-nitrobenzaldeyde **275f** with MVK **276** in $CDCl_3$ after 1min, following multipoint baseline correction and curve fitting.

This problem can be obviated by introducing a pulse delay long enough to ensure complete relaxation of the nuclei of interest. In order to establish the relevant spin-lattice relaxation times (T_1), an inversion recovery sequence was employed (Figure 102). Since the vinylic methylene carbon signals for the reactants and products were expected to be used to monitor the reaction, particular attention was given to the spectral region between 126 and 129 ppm. In this approach, the magnetization of the carbon nuclei is inverted towards the –z axis with a π pulse, the nuclei are allowed to relax back towards the +z axis and then subjected to a $\pi/2$ pulse before the signal intensity is measured. It can be observed (Figure 102) that all the signals are negative up to 10s. As the pulse delay is increased some of the signals remain negative while others become positive. The relaxation time for a given nucleus can be determined using the following equation:[206]

$$T_1 = \tau_{null} / \ln 2 = 1.443 \times \tau_{null}$$

Unfortunately, even after 50s (T_1 = 72.2s) the vinylic methylene carbon signals (marked by the bracket) are still negative. Given the need for multiple acquisitions and the observed rate of the reaction, it was evident that it would be impractical to use ^{13}C NMR spectroscopy to monitor the reaction since it would take too long.

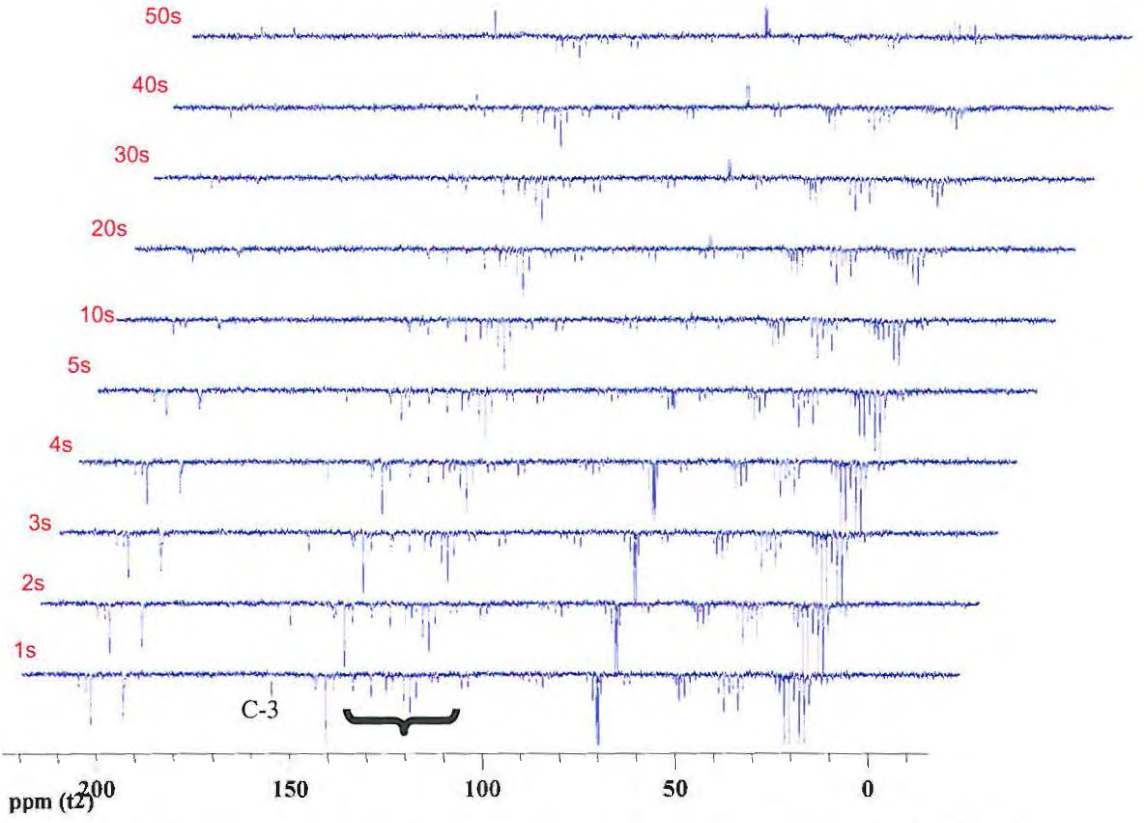

Figure 102. Stack-plot of inversion recovery spectra of the mixture obtained in the DABCO-catalysed reaction of 3-methoxy-2-nitrobenzaldehyde **275f** with MVK **276** in $CDCl_3$, recorded after specified pulse delays.

An alternative approach, which was finally used and which worked effectively, was to select other signals in the ^1H NMR spectra which correspond uniquely to the reactants **275f** and **276** and the products **277f, 278f** and **279f,** and **246**. Thus, formation of the MVK dimer **246** was monitored using the multiplet at 2.15 ppm (corresponding to the 3- and 4-methylene protons), the diastereomers **278f** and **279f**, using the singlets at 5.34

using the singlet at 5.74 ppm (corresponding to one of the 1'-methylene protons). For monitoring consumption of starting materials, use was made of the doublet at 5.54 ppm (due to the vinylic protons in MVK **276**) and the singlet at 9.51 ppm (due to the aldehydic proton in the substrate **275f**).

2.6.3. Analysis of the kinetic data

The kinetic studies were conducted on an NMR-tube scale, as described in the experimental section. 1,3,5-Trimethoxybenzene (TMB) was used as an internal standard and Figure 103 illustrates the ^{1}H NMR spectra recorded : a) after 1 minute and b) after 14 hours, as well as the signals used to monitor each species. In the spectrum recorded after 1 minute (Fig. 103a), the substrate **275f** aldehyde signal is evident at 9.50 ppm, but is clearly absent in the spectrum recorded after 14 h (Fig. 103b), indicating that after 14 h all of the aldehyde starting material had been consumed. The integrals were corrected using TMB – an internal standard which gives rise to a singlet at 3.30 ppm, corresponding to three methoxy groups. The changes in the spectra with time are clearly illustrated in the stack-plot reproduced in Figure 104. Although spectra were run at 10 minute intervals, the stack-plot reflects the change at 1 hourly intervals.

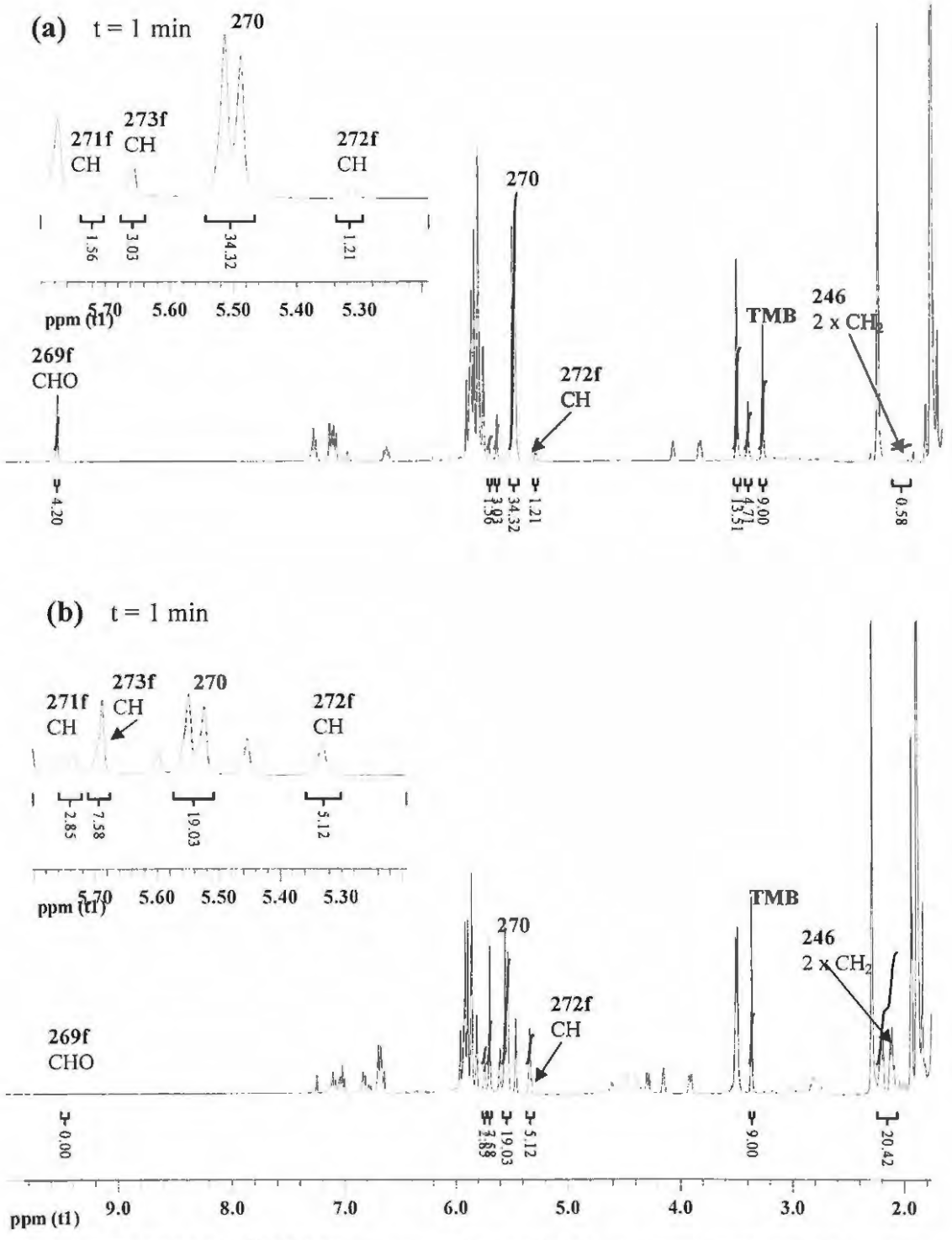

Figure 103. 400 MHz ^{1}H NMR spectra of the DABCO-catalysed reaction of 3-methoxy-2-nitrobenzaldehyde **275f** with MVK **276** in $CDCl_3$: (a) at the beginning of the reaction and (b) when the reaction was stopped after 14 h.

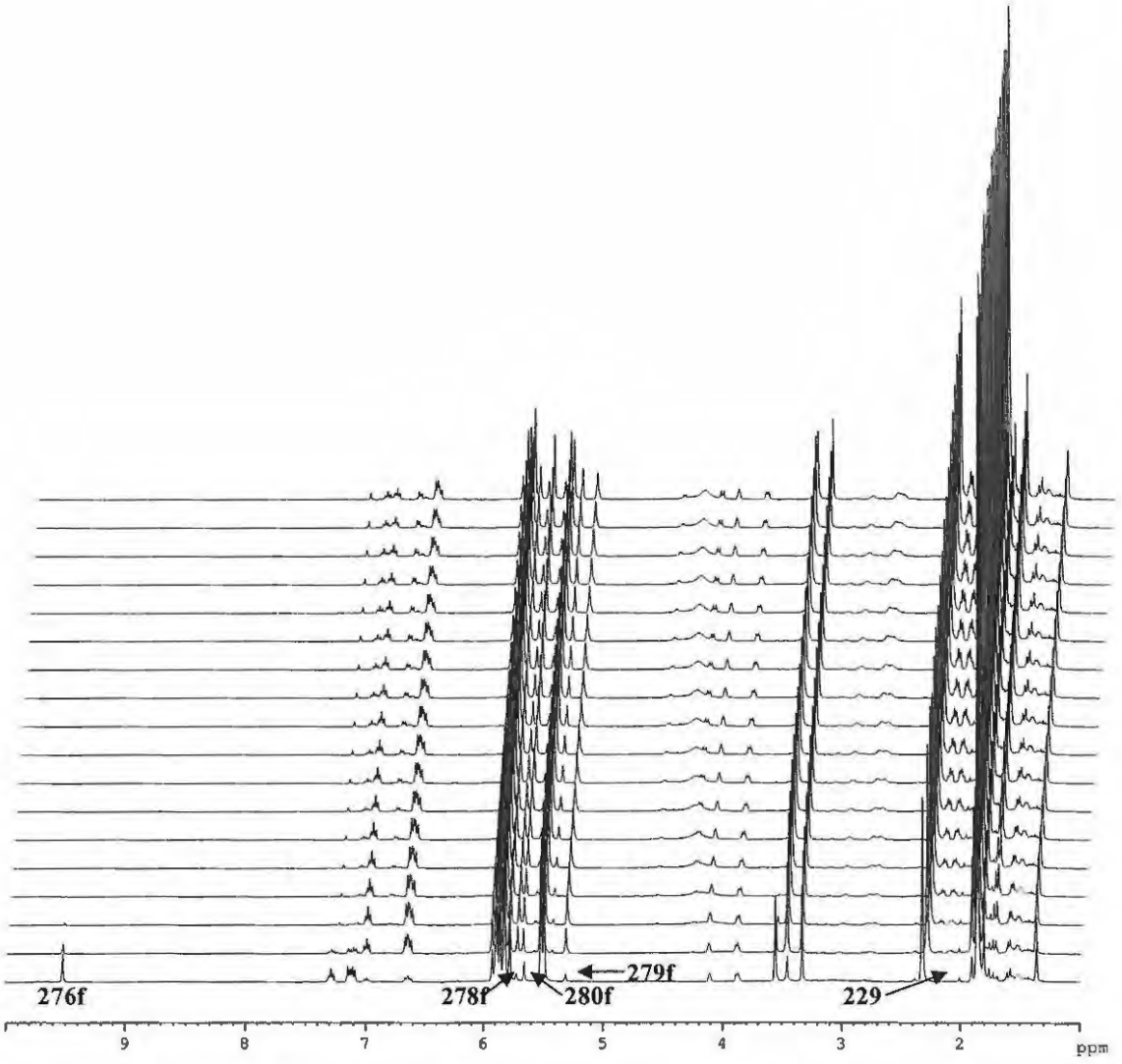

Figure 104. Stack-plot of 400 MHz ^{1}H-NMR spectra for the DABCO-catalysed reaction of 3-methoxy-2-nitrobenzaldehyde **275f** with MVK **276** in $CDCl_3$, recorded at 1 hour intervals.

In order to simplify analysis of the kinetic data, the structures detailed in **Scheme 67** are represented in **Scheme 68** by the letters A-H where A ≡ **269f**; B ≡ **270**; C ≡ **DABCO**; D ≡ zwitterionic intermediate; E ≡ **271f**; F_{syn} ≡ **272f**; F_{anti} ≡ **273f**; G ≡ MVK dimer enolate; and H ≡ **246**. The simplified sequence is illustrated in Figure 105.

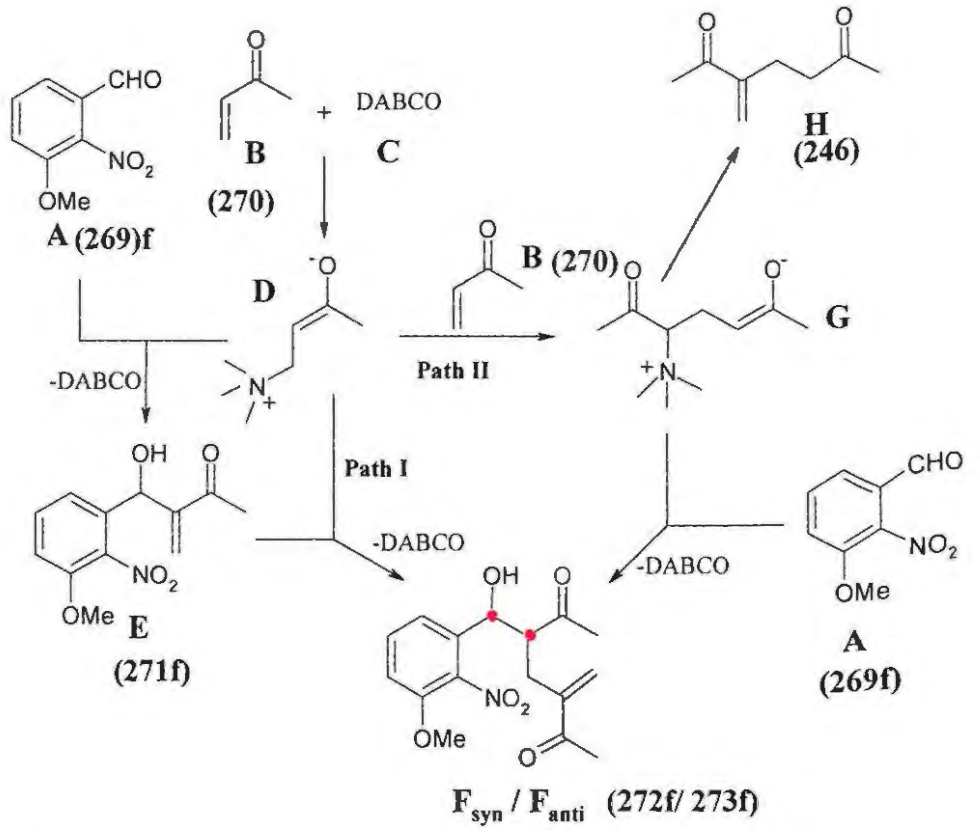

Scheme 68

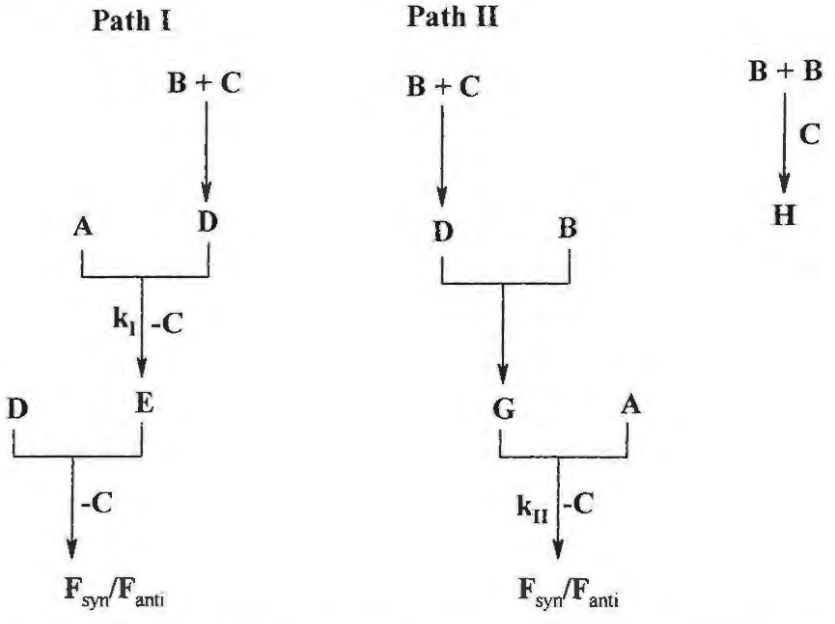

Figure 105. Simplified schematic diagram illustrating possible reaction pathways (*cf.* Schemes 67 and 68).

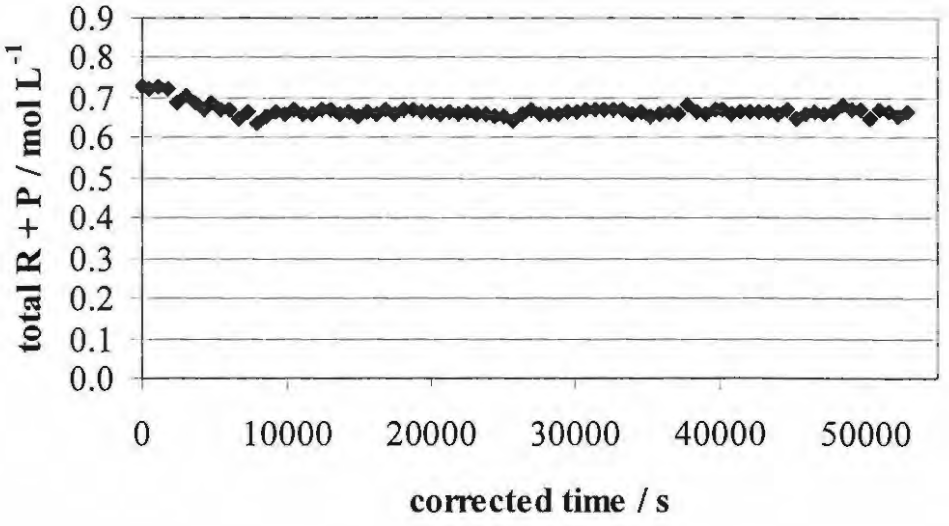

Figure 111. Time-corrected plot of the sum of the concentrations of the aldehyde **275f** [**A**] and the substrate-derived products **277f** [**E**], **278f** [$\mathbf{F}_{syn}$] and **279f** [$\mathbf{F}_{anti}$] with time.

$\mathbf{F}_{anti}$ and $\mathbf{F}_{syn}$ are presumed to be formed initially *via* two routes, *viz.*, **Path I**, in which 3-methoxy-2-nitrobenzaldehyde **275f** (**A**) is converted to the diastereomeric adducts **278f** ($\mathbf{F}_{syn}$) and **279f** ($\mathbf{F}_{anti}$) *via* the formation of the normal Baylis-Hillman product **277f** (**E**) and path II, in which the diastereomeric adducts **278f** ($\mathbf{F}_{syn}$) and **279f** ($\mathbf{F}_{anti}$) are formed without the intermediate **277f** (**E**) (refer to **Scheme 68** and Figure 105). After 9910 s, (Figure 112).

$$[\mathbf{A}] \approx 0 \text{ mol.L}^{-1}$$

$$[\mathbf{E}] \approx 0.24 \text{ mol.L}^{-1}$$

$$[\mathbf{F}_{anti}] \approx 0.16 \text{ mol.L}^{-1}$$

$$[\mathbf{F}_{syn}] \approx 0.26 \text{ mol.L}^{-1}$$

Since $[\mathbf{E}] + [\mathbf{F}_{anti}] + [\mathbf{F}_{syn}] = 0.66 \text{ mol.L}^{-1} \approx [\mathbf{A}]_o$

then, at any time t,

$[\mathbf{F}]_{final} - [\mathbf{E}]$ is the amount of $\mathbf{F}_{total}$ = ($\mathbf{F}_{anti}$ and $\mathbf{F}_{syn}$) formed *via* path II.

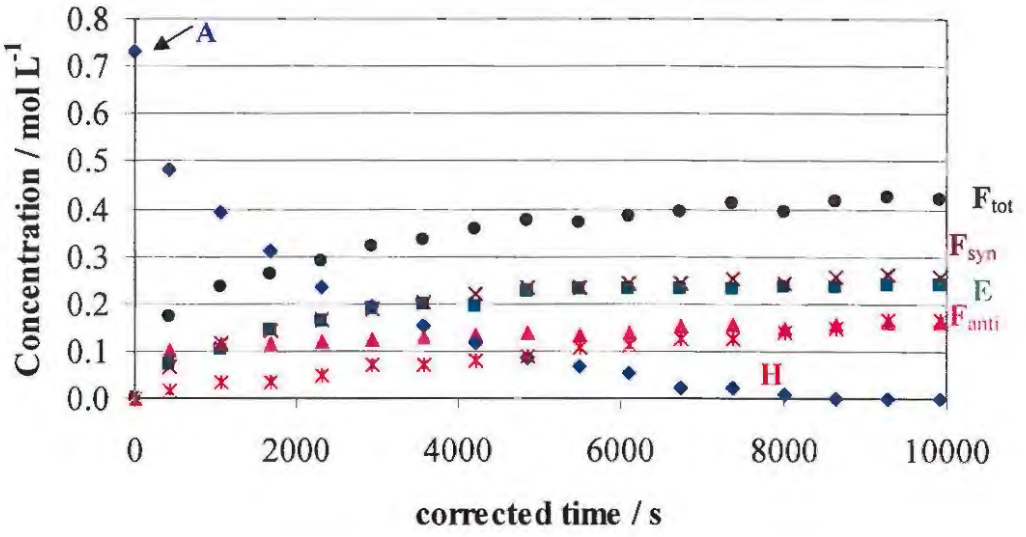

Figure 112. Time-corrected plots of the changes in concentrations of 3-methoxy-2-nitrobenzaldehyde **275f** (**A**), the Baylis-Hillman product **277f** (**E**), the Baylis-Hillman diadducts **278f** ($\mathbf{F}_{syn}$) and **279f** ($\mathbf{F}_{anti}$), the MVK dimer **246** (**H**) and [$\mathbf{F}_{total}$] with time, during the initial stage of the reaction.

Initially, $\mathbf{F}_{syn}$ is formed more rapidly than $\mathbf{F}_{anti}$ but, after reaching a maximum concentration of about 0.26 mol L^{-1} at about 10 000 s, $\mathbf{F}_{syn}$ begins to decrease linearly (Figure 113). On the other hand, [$\mathbf{F}_{anti}$] increases almost linearly after rapidly reaching about 0.16 mol L^{-1}. [$\mathbf{F}_{syn}$] and [**E**] reach a maximum at about the same time that the aldehyde [**A**] has been consumed (Figure 113). Clearly, once [**A**] has reached zero, the formation of [$\mathbf{F}_{anti}$] and [$\mathbf{F}_{syn}$] *via* path II will cease. After about 10 000 s [$\mathbf{F}_{tot}$] increases approximately linearly and after 50 000 s approaches the value of $[\mathbf{A}]_o$.

Thus, after about 10 000 s, $[\mathbf{F}_{tot}] = k_F t + [\mathbf{F}_{tot}]_{10000}$

Where $k_F = 2.79 \times 10^{-6}$ mol L^{-1} s^{-1} and $[\mathbf{F}_{tot}]_o = 0.405$ mol L^{-1}

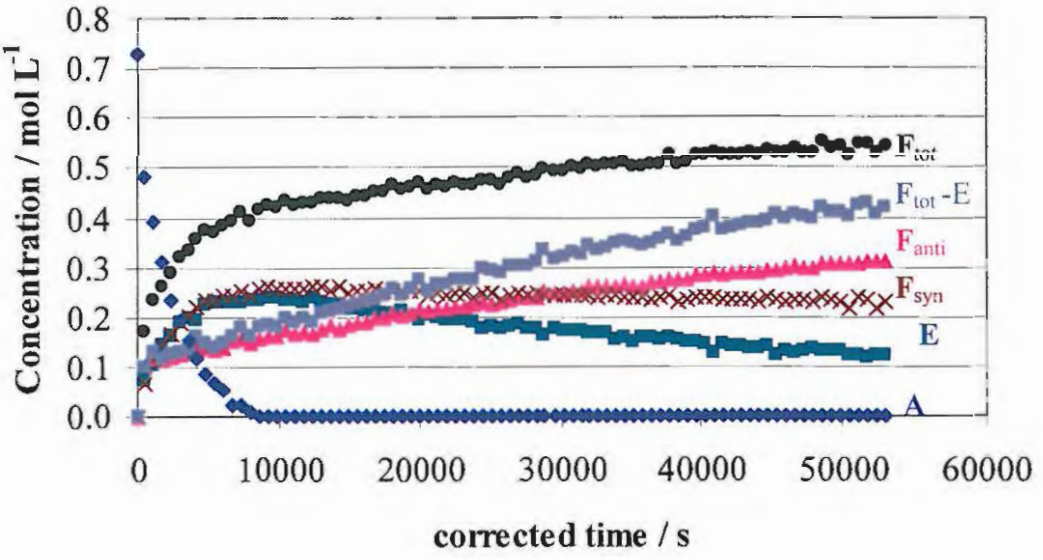

Figure 113. Plots of the changes in [F_{tot}], [F_{anti}] and [F_{syn}], [**E**] and [F_{tot}]–[**E**] against corrected time.

The plots in the approximately linear region (Figure 113) afford slopes and intercepts and, hence, rate constants for the formation of F_{anti} and the consumption of F_{syn} and E and their concentrations at t = 10 000 s (Table 17).

Table 17. Kinetic data for the approximately linear region after *ca.* 10 000s in (Figure 105).

Component	Rate constant / mol L^{-1} s^{-1}	Concentration at t =10 000 s / mol L^{-1}
F_{tot} – E (path I)	5.52×10^{-6}	0.147
F_{tot}	2.79×10^{-6}	0.405
F_{anti}	3.45×10^{-6}	0.105
F_{syn}	-2.07×10^{-6}	0.042
E	-2.66×10^{-6}	0.256

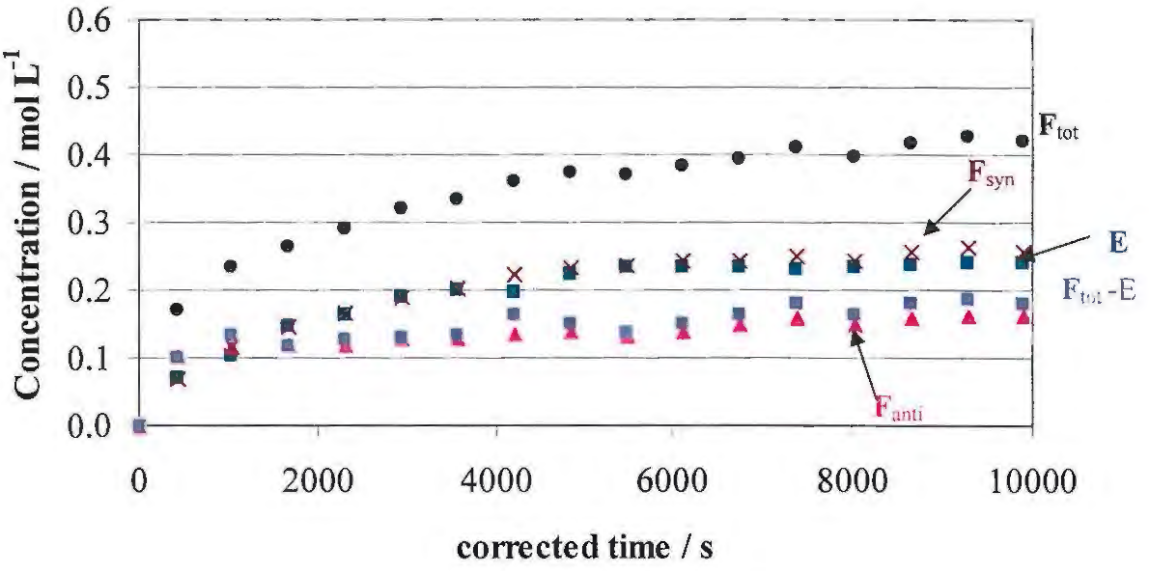

Figure 114. Time-corrected plots of change in [$\mathbf{F}_{tot}$], [$\mathbf{F}_{anti}$] and [$\mathbf{F}_{syn}$], [**E**] and [$\mathbf{F}_{tot}$]–[**E**] against time for the initial stage of the reaction.

In the initial stage of the reaction the product distribution is essentially kinetically controlled and [$\mathbf{F}_{syn}$] > [**E**] > [$\mathbf{F}_{anti}$] (Figure 114). After 10 000 s, however, the substrate concentration [**A**] = 0 and the formation of $\mathbf{F}_{syn}$ and/or $\mathbf{F}_{anti}$ is assumed to proceed *via* **Path I** alone and require the equilibration:

$$\mathbf{F}_{syn} \rightleftharpoons \mathbf{E} \rightleftharpoons \mathbf{F}_{anti}$$

The final product distribution is thus thermodynamically controlled, with $\mathbf{F}_{anti}$ being the most stable product, produced by concomitant consumption of both the normal Baylis-Hillman product **E** and the diadduct $\mathbf{F}_{syn}$. From the product distribution after about 50 000 s, it is apparent that the equilibrium constant at 298 K is approaching a value of 1.3), (*i.e.* K = 0.31/0.24 = 1.3).

The reaction using the aldehyde **275f (A)** was repeated at various temperatures (295-315 K) with the intention of accessing activation energy data. However, no consistent trends were observed. This is, perhaps, not surprising given the complexity of the transformation and the reversibility of the various steps.

The formation of the MVK dimer **246** (**H**) should be third-order, *i.e.* Rate = k $[\mathbf{B}]^2[\mathbf{D}]$ but, since the catalyst concentration [**D**] is constant, it may be expected to be pseudo second-order, as reflected in the linear second-order plot (after about 10 000 s) shown in Figure 115, the slope affording a pseudo-second-order rate constant of 3.97×10^{-6} mol L^{-1} s^{-1} with $r^2 = 0.975$.

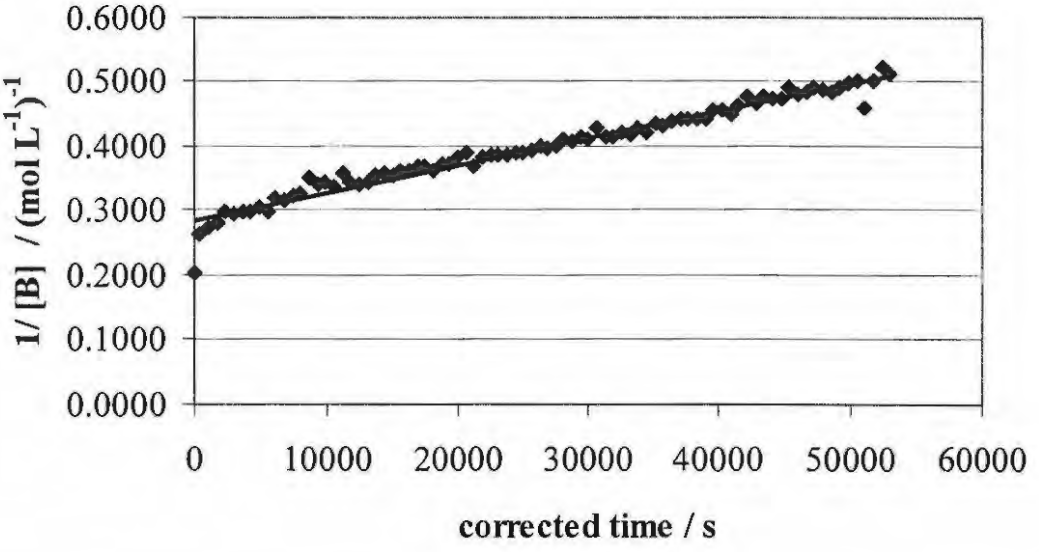

Figure 115. Pseudo-second-order plot reflecting the formation of the MVK dimer (**H**) from MVK (**B**) with respect to MVK [**B**] ($r^2 = 0.975$).

Kinetic studies were also undertaken using MVK **276** and the arylaldehydes **275a, 280** and **281** with the aim of exploring the effect of different substituents on reactivity. These compounds all follow the same trend as 3-methoxy-2-nitrobenzaldehyde **275f** affording the corresponding Baylis-Hillman products and *syn*-and *anti*-diadducts. Table 18 summarizes the rate constants for the disappearance of the substrates **275f, 275a, 280** and **281** and of MVK **276** in each case.

Table 18. Comparison of the rate constants (k_a) for the consumption of the aldehyde substrates during Baylis-Hillman reactions.

Entry	Benzaldehyde substituents	Compound	k_a / (s^{-1})
1	3-MeO, 2-NO_2	**275f**	4.74×10^{-4}
2	4-NO_2	**275a**	4.02×10^{-4}
3	5-Cl, 6-NO_2	**280**	3.78×10^{-4}
4	2-Cl, 6-NO_2	**281**	3.85×10^{-5}

It seems that 3-methoxy-2-nitrobenzaldehyde **275f** (entry 1) is the most reactive of the set of four benzaldehyde derivatives examined. The 4-nitro- and 5-chloro-6-nitrobenzaldehydes exhibit similar rates of consumption (entries 2 and 3), but the 2-chloro-6-nitro analogue **281** reacts an order of magnitude more slowly (entry 4). The pair of substituents *ortho* to the aldehyde group in compound **281** may force the aldehyde moiety to adopt an arrangement perpendicular to the aromatic ring and thus sterically inhibiting attack by nucleophilic species.

These kinetic studies have revealed that both mechanistic pathways (**Scheme 67**) operate during the formation of the *syn*-and *anti*-diadducts **272f** ($\mathbf{F}_{syn}$) and **273f** ($\mathbf{F}_{anti}$), and that product selectivity is kinetically controlled in the early stage of the reaction, but that the final product distribution is thermodynamically controlled. The rejection, by Shi *et al.*[200] of Path II, was based on the fact that treatment of 3-methoxy-2-nitrobenzaldehyde **269a** with the MVK dimer **246** in the presence of DABCO failed to afford the bis-MVK adducts **278a** and **279a**. However, Path II requires the zwitterionic enolate **G** (**Scheme 67**) whereas, once formed, the MVK dimer **246** may be expected to form the isomeric intermediate **I** (**Scheme 69**) not **G**.

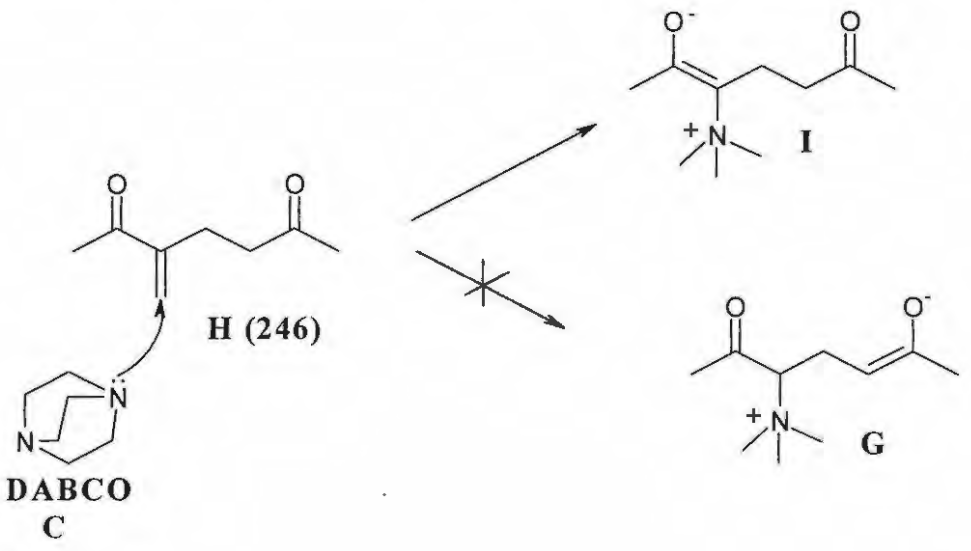

Scheme 69

2.7 CONCLUSION

Many chromone derivatives are known to exhibit pharmacological activity,[88,89] and in this study, chromone derivatives have been explored as scaffolds for the construction of HIV-1 protease inhibitors. Chromone-3-carbaldehydes have been successfully synthesized using Vilsmeier-Haack methodology in yields ranging from 43 to 85%, while chromone-2-carbaldehydes have been obtained *via* the Kostanecki–Robinson reactions in yields ranging from 46 to 65%. The chromone-2-carbaldehyde yields were increased from 50 to 70% when the reaction time was extended from 12 hours to 20 hours; use of 1-chloronaphthalene or dioxane instead of xylene as solvent was also investigated but the results confirmed that xylene was the best solvent for these reactions.

Application of the Baylis-Hillman reaction to the chromone-3-carbaldehydes and chromone-2-carbaldehydes has been studied using three different catalysts, *viz.*, 1,4-diazabicyclo[2.2.2]octane (DABCO), 1,8-diazabicyclo[5.4.0]-undec-7-ene (DBU) and 3-hydroxyquinuclidine (3HQ), and three different activated alkenes, *viz.*, acrylonitrile, methyl acrylate and methyl vinyl ketone. These reactions generally afforded both normal Baylis-Hillman and dimeric Baylis-Hillman products in high yields when chromone-3-carbaldehydes were used as substrates. Both the yields and the reaction rates were increased when DABCO was employed in the presence of the ionic liquid, 1-methyl-2-pyrrolidine (1-NMP).[167] However, only dimeric products were isolated when this reaction was performed at 0°C in the presence of organic solvents. DBU was found to be a more efficient catalyst than 3HQ since it afforded the Baylis-Hillman products in good yields over shorter reaction periods. Interestingly, when the chromone-3-carbaldehydes were reacted with methyl vinyl ketone, dimeric Baylis-Hillman products were obtained together with novel tricyclic adducts, but none of normal Baylis-Hillman products were isolated. The tricyclic adducts appear to be formed *via* an unprecedented transformation

involving attack of the zwitterionic enolate at C(2) of the chromone-3-carbaldehyde which then undergoes proton transfer and, finally, elimination of the catalyst.

When chromone-2-carbaldehydes were used as substrates in the presence of methyl vinyl ketone, the MVK dimer together with *syn*- and *anti*-diastereomeric adducts were obtained. Furthermore, unprecedented reactions were also observed when these substrates were reacted with methyl acrylate and acrylonitrile, as activated alkenes, which afforded interesting novel products in low yields. These reactions indicate that the electrophilicity of C(2) renders it more susceptible to nucleophilic attack than carbonyl carbon of the aldehyde group. This is illustrated by the attack of the zwitterionic enolate at C(2) followed by displacement of the 2-aldehyde group. When DBU was used as the catalyst in the presence of MVK, neither chromone-2-carbaldehydes nor chromone-3-carbaldehydes appeared to react, confirming that DBU is not a good catalyst for reactions with MVK.[186]

Reactions between the normal Baylis-Hillman adducts derived from the chromone-3-carbaldehydes and acrylonitrile, on one hand, and various amino derivatives, on the other, afforded aza-Michael products. Tetrabutylammonium bromide (TBAB) and the ionic liquid, 3-butyl-1-methylimidazoleboranetetrafluoride ($BmimBF_4$), were used as catalysts and the products were typically obtained in yields of 20–68%. These aza-Michael products (or compounds derived therefrom) had been targeted as truncated ritonavir analogues for investigation as potential HIV-1 protease inhibitors, designed to partially resemble the clinically useful hydroxyethylene dipeptide drug. This design strategy involved elongation of the Baylis-Hillman products with amino derivatives to form aza-Michael products containing a hetero-aromatic system at one end attached to a chain containing hydroxyl and other functional groups capable of hydrogen-bonding interactions with the protease receptor. In the absence of catalyst, the aza-Michael products were obtained after 6 weeks, whereas in the presence of catalyst, they were obtained in 5 days! Although use of $BmimBF_4$ resulted in products in higher yields, this

catalyst was not miscible with all the organic solvents examined. Consequently, TBAB, which proved to dissolve more readily, was used in all reactions.

Analysis of the HIV-1 protease enzyme-inhibition activity of selected aza-Michael products revealed that one compound exhibited non-competitive inhibition [with an inhibition constant (K_i) of *ca.* 0.0032 nM], while another exhibited competitive inhibition (with a K_i value of *ca.* 0.0064 nM). However, one of the three compounds examined did not show any activity.

Computer modelling studies were conducted on a range of the synthesized chromone-containing derivatives using the Cerius2 LigandFit module. These *in silico* studies clearly indicated the capacity of the chromones-containing analogues to interact with the receptor cavity through hydrogen-bonding interactions. However, these interactions did not involve all of the significant binding pockets in the receptor and, moreover, depended on the presence of a structural water molecule in the receptor cavity. In all cases, the favoured bound conformation was found to have a similar conformation to that of the 'isolated' global minimum.

Finally, attention was given to the mechanism of the Baylis-Hillman reaction of selected 2-nitrobenzaldehydes with MVK in the presence of DABCO – a reaction which affords the normal Baylis-Hillman product, the MVK dimer as well as *syn*- and *anti*-bis-MVK Baylis-Hillman adducts. Kinetic studies were perfomed using NMR spectroscopy and confirmed the simultaneous operation of two mechanistic pathways during the formation of the *syn*- and *anti*-diadducts during the early stage of the reaction. These diadducts were successfully separated using HPLC. The *anti*-diadduct was found to be the more stable and, hence, thermodynamically favored product. The *syn*-diadduct, on the other hand, is kinetically favoured (being formed during the initial stage of the reaction) and is converted to the *anti*-diadduct at a later stage. The kinetic study afforded rate constants for the formation of the various products as well as the consumption of the reactants, and provided useful insights into the complex mechanism.

Future research in this area is expected to involve the following.

(i) Confirmation of the structures of the products of unexpected reactions using single crystal X-ray analysis.

(ii) Elaboration of the aza-Michael products to increase the number of efficient hydrogen-bonding interactions with critical enzyme binding pockets and to replace the need for structural water.

(iii) Hydrolysis of nitriles obtained in the aza-Michael reaction to affords amides and acids as potential HIV-1 protease inhibitors.

(iv) Application of the aza-Michael reaction to Baylis-Hillman products derived from α,β-unsaturated carbonyl compounds.

(v) Modification of the Baylis-Hillman dimers by incorporating functional groups which will enhance hydrogen-bonding interaction with critical enzyme binding pockets and also replace the need for structural water.

3. EXPERIMENTAL

3.1 General Directions

^{1}H and ^{13}C-NMR spectra were recorded on a Bruker Avance 400MHz spectrometer at 303K, and were calibrated using the solvent signals; coupling constants are given in Hertz (Hz). Melting points were determined using a Kofler hot-stage apparatus, and are uncorrected. IR spectra were recorded on a Perkin Elmer Spectrum 2000 FT-IR spectrometer. Low-resolution mass spectra were obtained on a Finnegan–Mat GCQ mass spectrometer, and high-resolution mass spectra were recorded on a VG70-SEQ double-focusing magnetic sector instrument (University of the Witwatersrand Mass Spectrometry Unit) and on a Micromass 70-70E spectrometer (Universiteit vir Hoër Christelike Onderwys in Potchefstroom Mass Spectrometry Unit).

Flash chromatography was carried out using Merck silica gel 60 [230 – 400 mesh (particle size 0.040 – 0.063mm)] and preparative layer chromatography was conducted using silica gel 60 PF_{254}. Chromatotron plates were prepared using silica gel 60 PF_{254} containing $CaSO_4$. Thin layer chromatography (TLC) was carried out on pre-coated Merck silica gel F_{254} plates, visualization being achieved by inspection under UV light (254nm) or following exposure to iodine.

Solvents were dried using the procedures prescribed by Perrin and Armarego.[49] *N,N*-Dimethylformamide (DMF) was pre-dried and distilled from 3Å molecular sieves under reduced pressure. Ethanol and methanol were dried by reaction with Mg turnings and iodine and then distilled from the resulting magnesium alkoxide under nitrogen. THF and diethyl ether were pre-dried over CaH_2 and then distilled from Na wire in the presence of benzophenone under nitrogen.

3.2 Preparation of chromone derivatives

3.2.1 Synthesis of chromone-3-carbaldehydes

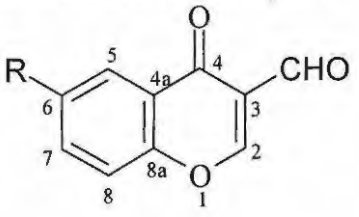

Chromone-3-carbaldehyde **83** [127]

$POCl_3$ (9.4 mL, 0.10mol) was added dropwise, during a period of 0.5h., to a stirred solution of *o*-hydroxyacetophenone **84** (3.0 mL, 25 mmol) in dry DMF (25 mL) under N_2, while maintaining the temperature at –23°C using a liquid N_2-carbon tetrachloride bath. The resulting mixture was stirred overnight at room temperature and then poured into ice-water (50 mL). The resulting precipitate was filtered off, and washed successively with water and EtOH. Recrystallisation from acetone afforded chromone-3-carbaldehyde **83** as a colourless crystalline solid (3.09g, 71%), m.p. 153-154°C (lit., [127] 152- 153°C); ν_{max} (KBr)/cm^{-1} 1649 and 1690 (2x C=O); δ_H (400 MHz; $CDCl_3$) 7.49 (1H, t, *J*=7.1 Hz, 6-H), 7.53 (1H, d, *J*= 8.8 Hz, 8-H), 7.74 (1H, t, *J*= 7.8 Hz, 7-H), 8.23 (1H, d, *J*= 8.0 Hz, 5-H), 8.54 (1H, s, 2-H) and 10.38 (1H, s, CHO); δ_C (100MHz; $CDCl_3$) 118.6 (C-8), 120.4 (C-3), 125.3 (C-4a), 126.2 (C-5), 126.6 (C-6), 134.8 (C-7), 156.2 (C-8a), 160.6 (C-2), 176.0 (C=O) and 188.6 (CHO); *m/z* 174 (M^+, 6%) and 146 (100).

6-Chlorochromone-3-carbaldehyde **184**[127]

The experimental procedure employed for the synthesis of chromone-3-carbaldehyde **83** was followed, using $POCl_3$ (18.7 mL, 200 mmol), 5-chloro-2-hydroxyacetophenone **180** (8.53 g, 50.0 mmol) and dry DMF (50 mL). Work-up afforded 6-chlorochromone-3-carbaldehydes **184** as a yellow crystalline solid (8.45 g, 81%), m.p. 165-167 °C (lit.,[207] 166-168°C); ν_{max} (KBr)/cm^{-1} 1655 and 1695 (2x C=O); δ_H (400 MHz; $CDCl_3$) 7.49 (1H,

d, *J*=8.9 Hz, 8-H), 7.68 (1H, dd, *J*=2.6 and 8.9 Hz, 7-H), 8.25 (1H, d, *J*=2.5 Hz, 5-H), 8.52 (1H, s, 2-H) and 10.36 (1H, s, CHO); δ_C (100MHz; $CDCl_3$) 120.3 (C-8), 125.6 (C-5), 126.3 (C-4a), 132.8 (C-6 and C-3), 135.0 (C-7), 154.5 (C-8a), 160.6 (C-2), 174.8 (C=O) and 188.1 (CHO); *m/z* 208 ($\mathbf{M}^+$, 4%) and 180 (100).

6-Bromochromone-3-carbaldehyde **185** [127]

The experimental procedure employed for the synthesis of chromone-3-carbaldehyde **83** was followed, using $POCl_3$ (8.4 mL, 90 mmol), 5-bromo-2-hydroxyacetophenone **181** (5.0 g, 23 mmol) and DMF (25 mL). Work-up afforded 6-bromochromone-3-carbaldehyde **185** as a yellow crystalline solid (4.92 g, 85%), m.p. 187-189 °C (lit., [127] 186-188°C); ν_{max} (KBr)/cm^{-1} 1655 and 1699 (2x C=O); δ_H (400 MHz; $CDCl_3$) 7.42 (1H, d, *J*=8.9 Hz, 8-H), 7.83 (1H, dd, *J*=8.9 and 2.3 Hz, 7-H), 8.41 (1H, d, *J*=2.4 Hz, 5-H), 8.53 (1H, s, 2-H) and 10.35 (1H, s, CHO); δ_C (100MHz; $CDCl_3$) 120.3 (C-3), 120.4 (C-6), 120.5 (C-8), 126.6 (C-4a), 128.8 (C-5), 137.8 (C-7), 155.0 (C-8a), 160.6 (C-2), 174.7 (C=O) and 188.1 (CHO); $C_{10}H_5O_3Br$, *m/z* 252 ($\mathbf{M}^+$, 4%) and 226 (100).

6-Fluorochromone-3-carbaldehyde **186** [127]

The experimental procedure employed for the synthesis of chromone-3-carbaldehyde **83** was followed, using $POCl_3$ (4.2 mL, 45 mmol), 5-fluoro-2-hydroxyacetophenone **182** (2.5 g, 16 mmol) and dry DMF (13 mL). Work-up afforded 6-fluorochromone-3-carbaldehyde **186** as a yellow crystalline solid (2.5 g, 83%), m.p. 157-159 °C (lit., [198] 158°C); ν_{max} (KBr)/cm^{-1} 1657 and 1701(2x C=O); δ_H (400 MHz; $CDCl_3$) 7.46 (1H, m, 8-H), 7.55 (1H, dd, *J*= 4.1 and 9.1 Hz, 7-H), 7.93 (1H, d, *J*= 3.0 and 7.9 Hz, 5-H), 8.53 (1H, s, 2-H) and 10.34 (1H, s, CHO); δ_C (100MHz; $CDCl_3$) 111.2 (J_{CF}=24.0 Hz, C-5), 119.7 (C-4a), 120.8 (J_{CF}= 8.1 Hz, C-8), 123.0 (J_{CF}= 25 Hz, C-7), 126.8 (C-3 and C-6), 152.4 (C-8a), 160.6 (C-2), 175.2 (C=O) and 188.2 (CHO); *m/z* 192 ($\mathbf{M}^+$, 4%) and 164 (100).

6-Methoxychromone-3-carbaldehyde **187** [127]

The experimental procedure employed for the synthesis of chromone-3-carbaldehyde **83** was followed, using $POCl_3$ (13.5 mL, 144 mmol), 2-hydroxy-6-methoxyacetophenone **183** (6.0 g, 36 mmol) and dry DMF (25 mL). Work-up afforded 6-methoxychromone-3-carbaldehyde **187** as a yellow crystalline solid (4.3 g, 59%), m.p. 164-165 °C (lit.,[127] 164-166°C); ν_{max} (KBr)/cm^{-1} 1657 and 1701 (2x C=O); δ_H (400 MHz; $CDCl_3$) 3.92 (3H, s, OCH_3), 7.31 (1H, dd, *J*=9.2 and 3.1 Hz, 7-H), 7.46 (1H, d, *J*=9.1 Hz, 8-H), 7.64 (1H, d, *J*=3.1 Hz, 5-H), 8.51 (1H, s, 2-H) and 10.39 (1H, s, CHO); δ_C (100MHz; $CDCl_3$) 56.1 (OCH_3), 105.5 (C-5), 119.6 (C-3), 120.0 (C-8), 124.4 (C-7), 126.1 (C-4a), 151.0 (C-6), 158.0 (C-8a), 160.2 (C-2), 175.9 (C=O) and 188.7 (CHO); m/z 204 ($\mathbf{M}^+$, 1%) and 176 (100).

3.2.2 *Synthesis of chromone-2-carbaldehydes*

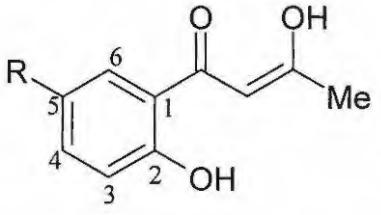

1-(2-Hydroxyphenyl)-1,3-butanedione **192**[86, 208]

A solution of *o*-hydroxyacetophenone **84** (10 mL, 83 mmol) in dry EtOAc (35 mL, 0.36 mol) was added dropwise to a stirred suspension of NaOEt [generated *in situ* by adding Na metal lumps (8.0 g, 0.35 mol) to dry EtOH (40 mL)]. The resulting yellow mixture was boiled gently under reflux for *ca* 8h, until a thick yellow slurry was formed. After cooling, the mixture was poured into Et_2O (200 mL) and allowed to stand for 1h. The resulting precipitate was filtered off, washed with Et_2O and dissolved in ice-cold water (100 mL). The resulting solution was acidified with acetic acid and the resulting precipitate was filtered off and recrystallized from petroleum ether (b.p. 60-80°C) to afford 1-(2-hydroxyphenyl)-1,3-butanedione **192** as a yellow solid (8.2g, 57%), which was used immediately without further purifications.

1-(5-Chloro-2-hydroxyphenyl)-1,3-butanedione **193**[86, 208]

The experimental procedure employed in the synthesis of 1-(2-hydroxyphenyl)-1,3-butanedione **192** was followed, using 5-chloro-2-hydroxyacetophenone **188** (3.0 g, 18 mmol), dry EtOAc (7.0 mL, 70 mmol) and NaOEt [generated *in situ* by adding Na metal (1.6 g, 70 mmol) to dry EtOH (9.0 mL)]. Work-up afforded 1-(5-chloro-2-hydroxychlorophenyl)-1,3-butanedione **182** as yellow solid (2.8g, 74%), which was used immediately without further purification.

1-(5-Bromo-2-hydroxy-phenyl)-1,3-butanedione **194**[86, 208]

The experimental procedure employed in the synthesis of 1-(2-hydroxyphenyl)-1,3-butanedione **192** was followed, using 5-bromo-2-hydroxyacetopheone **189** (10.0 g, 47 mmol), dry EtOAc (18.2 mL, 186 mmol) and NaOEt [generated *in situ* by adding Na metal (4.28 g, 186 mmol) to dry EtOH (45 mL)]. Work-up afforded 1-(5-bromo-2-hydroxy-phenyl)-1,3-butanedione **194** as yellow solid (4.7g, 39%), which was used immediately without further purification.

1-(5-Fluoro-2-hydroxyphenyl)-1,3-butanedione **195**[86, 208]

The experimental procedure employed in the synthesis of 1-(2-hydroxyphenyl)-1,3-butanedione **192** was followed, using 5-fluoro-2-hydroxyacetopheone **190** (3.0 g, 19.4 mmol), dry EtOAc (7.6 mL, 78 mmol) and NaOEt [generated *in situ* by adding Na metal (1.79 g, 78 mmol) to dry EtOH (29 mL)]. Work-up afforded 1-(5-fluoro-2-hydroxyphenyl]-1,3-butanedione **195** as yellow solid (1.6 g, 47%), which was used immediately without further purification.

1-(2-Hydroxy-5-methoxyphenyl)-1,3-butanedione **185**[86, 208]

The experimental procedure employed in the synthesis of 1-(2-hydroxyphenyl)-1,3-butanedione **192** was followed, using 2-hydroxy-5-methoxyacetopheone **191** (10 g, 60 mmol), dry EtOAc (26 mL, 0.3 mol) and NaOEt [generated *in situ* by adding Na metal (5.80 g, 252 mmol) to dry EtOH (29 mL)]. Work-up afforded 1-(2-hydroxy-5-

methoxyphenyl)-1,3-butanedione **196** as yellow solid (7.1 g, 73%), which was used immediately without further purification.

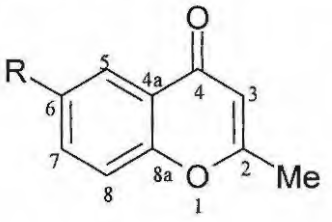

2-Methylchromone **90**[86, 208]

A stirred solution of 1-(2-hydroxyphenyl)-1,3-butanedione **192** (2.0 g, 11 mmol), glacial acetic acid (10 mL) and H_2SO_4 (98%, 0.4 mL) was boiled gently under reflux for 4h. The resulting, hot, brick-red solution was poured into ice-cold water (50 mL) and basified with 10% aq. $NaHCO_3$. The resulting precipitate was filtered, washed with ice-cold water, and recrystallized from hexane to afford 2-methylchromone **90** as a yellow solid (1.2 g, 68%), m.p. 68-70°C (lit[209] 69-70°C), ν_{max} (KBr)/cm^{-1}, 1654 (C=O); δ_H (400 MHz; $CDCl_3$) 2.36 (3H, s, CH_3), 6.15 (1H, s, 3-H), 7.38 (1H, m, 8-H), 7.62 (1H, m, 7-H), and 8.16 (1H, dd, *J*=8.0 and 1.6 Hz, 5-H); δ_c(100 MHz; $CDCl_3$) 20.5 (CH_3), 110.5 (C-3), 117.7 (C-8), 123.5 (C-4a), 124.9 (C-6), 125.6 (C-5), 133.4 (C-7), 156.5 (C-8a), 166.2 (C-2) and 178.2 (C=O); *m/z* 160 ($\mathbf{M}^+$, 100%).

6-Chloro-2-methylchromone **197**

The experimental procedure employed in the synthesis of 2-methylchromone **90** was followed, using 1-(5-chloro-2-hydroxyphenyl)-1,3-butanedione **193** (2.0 g, 9.4 mmol), glacial acetic acid (11 mL) and H_2SO_4 (98%, 0.4 mL). Work-up afforded 6-chloro-2-methylchromone **197** as a yellow solid (1.6 g, 86%). m.p. 112-114°C; ν_{max} (KBr)/cm^{-1}, 1674 (C=O), (Found: $\mathbf{M}^+$194.0139. Calc. for $C_{10}H_7ClO_2$, *M*: 194.9904); δ_H (400 MHz; $CDCl_3$) 2.38 (3H, s, CH_3), 6.16 (1H, s, 3-H), 7.36 (1H, d, *J*=8.9 Hz, 8-H), 7.57 (1H, dd, *J*=8.9 and 2.6 Hz, 7-H), and 8.12 (1H, d, *J*=2.6 Hz, 5-H); δ_c (100 MHz; $CDCl_3$) 20.9 (CH_3), 110.5 (C-3), 119.5 (C-5), 124.5 (C-7), 125.1 (C-6), 130.9 (C-8), 133.6 (C-4a), 154.8 (C-8a), 166.5 (C-2) and 177.0 (C=O); *m/z* 194($\mathbf{M}^+$, 100%).

6-Bromo-2-methylchromone **198**[86, 208]

The experimental procedure employed in the synthesis of 2-methylchromone **90** was followed, using 1-(5-bromo-2-hydroxyphenyl)-1,3-butanedione **194** (3.0 g, 12 mmol), glacial acetic acid (13 mL) and H_2SO_4 (98%, 0.4 mL). Work-up afforded 6-bromo-2-methylchromone **198** as a yellow solid (1.9 g, 69%). m.p.118-120°C; ν_{max} (KBr)/cm-^{1}, 1676 (C=O), (Found: $\mathbf{M}^+$ 239.9607. Calc. for $C_{10}H_7BrO_2$, *M*: 239.8622); δ_H (400 MHz; $CDCl_3$) 2.38 (3H,s, CH_3), 6.17 (1H, s, 3-H), 7.31 (1H, d, *J*= 8.9 Hz, 8-H), 7.71 (1H, dd, *J*=8.9 and 2.5 Hz, 7-H), and 8.30 (1H, d, *J*=2.5 Hz, 5-H); δ_c (100 MHz; $CDCl_3$) 20.6 (CH_3), 110.6 (C-3), 118.3 (C-5), 119.8 (C-7), 124.9 (C-6), 128.3 (C-8), 136.4 (C-4a), 155.2 (C-8a), 166.5 (C-2) and 176.8 (C=O); *m/z* 239 ($\mathbf{M}^+$, 100%).

6-Fluoro-2-methylchromone **199**[86, 208]

The experimental procedure employed in the synthesis of 2-methylchromone **90** was followed, using 1-(5-fluoro-2-hydroxyphenyl)-1,3-butanedione **195** (0.5 g, 2.6 mmol), glacial acetic acid (6.0 mL) and H_2SO_4 (98%, 0.4 mL). Work-up afforded 6-fluoro-2-methylchromone **199** as a yellow solid (0.4 g, 88 %), m.p. 102-103°C (lit[210] 101-102°C), ν_{max} (KBr)/cm-, 1685 (C=O); δ_H (400 MHz; $CDCl_3$) 2.37 (3H,s, CH_3), 6.14 (1H, s, 3-H), 7.35-7.42 (2H, m, 7-H and 8-H), 7.78 (1H, dd, *J*=8.4 and 3.3Hz, 5-H); δ_c (100 MHz; $CDCl_3$) 20.5 (CH_3), 109.9 (C-3), 110.6 (C-5), 119.8 (C-7), 119.9 (C-6), 121.4 (C-8), 121.6 (C-4a), 160.6 (C-8a), 166.4 (C-2) and 177.3 (C=O); *m/z* 178 ($\mathbf{M}^+$, 100%).

6-Methoxy-2-methylchromone **200**[86, 208]

The experimental procedure employed in the synthesis of 2-methylchromone **90** was followed, using 1-[2-hydroxy-5-methoxyphenyl]-1,3-butanedione **196** (4.0 g, 20 mmol), glacial acetic acid (21.5 mL) and H_2SO_4 (98%, 0.9 mL). Work-up afforded 6-methoxy-2-methylchromone **200** as a yellow solid (2.64 g, 69%). m.p. 107-108°C (lit[211] 107-108°C), ν_{max} (KBr)/cm-, 1675 (C=O); δ_H (400 MHz; $CDCl_3$) 2.35 (3H, s, CH_3), 3.86 (3H, s, OCH_3), 6.14 (1H, s, 3-H), 7.20 (2H, m, 6-H and 8-H), 7.72 (1H, d, *J*= 9.1 Hz, 7-H) and 7.53 (1H, d, *J*=3.0 Hz, 5-H); δ_c (100MHz; $CDCl_3$) 20.5 (CH_3), 55.9 (OCH_3), 104.9

(C-5), 109.8 (C-3), 119.1 (C-7), 123.4 (C-8), 124.1 (C-4a), 151.3 (C-6), 156.8 (C-8a), 165.9 (C-2), and 178.0 (C=O); *m/z* 190 (M^+, 100%).

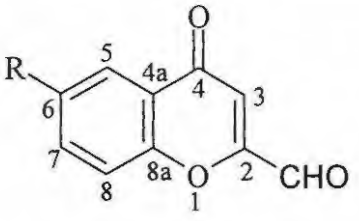

Chromone-2-carbaldeyde **91**[130-131]

A stirred mixture of 2-methylchromone **90** (2.0 g, 11 mmol), SeO_2 (6.1 g, 31 mmol) and xylene (50 mL) was boiled under reflux at for 12 h. The resulting mixture was filtered while hot to remove the black selenium, and the filtrate concentrated *in vacuo*. Flash chromatography of the residue on silica (elution with $CHCl_3$) afforded chromone-2-carbaldeyde **91** as a brown solid (1.2 g, 65%). Repeating this reaction for 20 h afforded chromone-2-carbaldeyde **91** as a brown solid (1.3 g, 70%), m.p. 161-162°C (lit[58]160-163°C), ν_{max} (KBr)/cm^{-1}, 1664 and 1700 (2xC=O); δ_H (400 MHz; $CDCl_3$) 6.18 (1H, s, 3-H), 7.38 (1H, m, 6-H), 7.62 (1H, m, 8-H), 7.77 (1H, m, 7-H), 8.20 (1H, m, 5-H) and 9.79 (1H, s, CHO); δ_c(100 MHz; $CDCl_3$) 117.0 (C-3), 118.8 (C-8), 124.9 (C-4a), 125.9 (C-6), 126.2 (C-5), 135.2 (C-7), 155.6 (C-8a), 156.0 (C-2), 178.3 (C=O) and 185.5 (CHO); *m/z* 174 (M^+, 100%).

6-Chlorochromone-2-carbaldeyde **201**

The experimental procedure employed in the synthesis of chromone-2-carbaldeyde **91** was followed, using 6-chloro-2-methylchromone **197** (2.00 g, 10.3 mmol), SeO_2 (5.70 g, 51.4 mmol) and xylene (25 mL). Work-up afforded 6-chlorochromone-2-carbaldehyde **201** as a yellow solid (g, 46%). m.p. 162-164°C, ν_{max} (KBr)/cm^{-1}, 1674 and 1717 (2xC=O), (Found: M^+:207.9911. Calc. for $C_{10}H_5ClO_3$, *M*: 208.9353); δ_H (400 MHz; $CDCl_3$) 6.90 (1H, s, 3-H), 7.57 (1H, d, *J*=9.0 Hz, 8-H), 7.71 (1H, dd, *J*=9.0 and 2.6 Hz, 7-H), 8.17 (1H, d, *J*=2.6 Hz, 5-H) and 9.79 (1H, s, CHO); δ_c (100 MHz; $CDCl_3$) 116.6

(C-3), 120.5 (C-5), 125.3 (C-7), 125.7 (C-6), 132.3 (C-8), 135.4 (C-4a), 153.9 (C-8a), 156.0 (C-2), 177.1 (C=O) and 185.0 (CHO); *m/z* 208 ($\mathbf{M}^+$, 100%).

6-Bromochromone-2-carbaldeyde **202**

The experimental procedure employed in the synthesis of chromone-2-carbaldeyde **91** was followed, using 6-bromo-2-methylchromone **198** (2.0 g, 8.4 mmol), SeO_2 (4.6 g, 42 mmol) and xylene (30 mL). Work-up afforded 6-bromochromone-2-carbaldehyde **202** as a yellow solid (1.0 g, 47%). m.p.170-172°C, ν_{max} (KBr)/cm^{-1}, 1675 and 1717 (2xC=O); (Found: $\mathbf{M}^+$: 254.9506. Calc. for $C_{10}H_5BrO_3$, *M*: 254.8571); δ_H (400 MHz; $CDCl_3$) 6.91 (1H, s, 3-H), 7.50 (1H, d, *J*=8.9 Hz, 8-H), 7.84 (1H, dd, *J*=8.9 and 2.5 Hz, 7-H), 8.31 (1H, d, *J*=2.4 Hz, 5-H) and 9.78 (1H, s, CHO); δ_c (100 MHz; $CDCl_3$) 116.8 (C-3), 119.8 (C-5), 120.7 (C-7), 126.0 (C-6), 128.6 (C-8), 138.2 (C-4a), 154.4 (C-8a), 156.0(C-2), 176.9 (C=O) and 185.0 (CHO); *m/z* 254($\mathbf{M}^+$, 100%).

6-Fluorochromone-2-carbaldeyde **203**[212]

The experimental procedure employed in the synthesis of chromone-2-carbaldeyde **91** was followed, using 6-fluoro-2-methylchromone **199** (2.0 g, 11 mmol), SeO_2 (6.2 g, 56 mmol) and xylene (30 mL). Work-up afforded 6-fluorochromone-2-carbaldehyde **203** as a yellow solid (1.1 g, 52%). m.p. 155-157 °C (lit[212] 156-158°C), ν_{max} (KBr)/cm^{-1}, 1675 and 1719 (2xC=O); δ_H (400 MHz; $CDCl_3$) 6.89 (1H, s, 3-H), 7.49 (1H, m, 7-H), 7.63 (1H, m, 8-H), 7.84 (1H, m, 5-H) and 9.79 (1H, s, CHO); δ_c (100MHz; $CDCl_3$) 110.8 (C-3), 111 (C-5), 115.7 (C-7), 121.0 (C-6), 121.1 (C-8), 123.6 (C-4a), 156.1 (C-8a), 160.8 (C-2), 177.5 (C=O) and 185.1 (CHO); *m/z* 192 ($\mathbf{M}^+$, 100%).

6-Methoxychromone-2-carbaldeyde **204**[212]

The experimental procedure employed in the synthesis of chromone-2-carbaldeyde **91** was followed, using 6-methoxy-2-methylchromone **200** (2.0 g, 11 mmol), SeO_2 (5.8 g, 53 mmol) and xylene (30 mL). Work-up afforded 6-methoxychromone-2-carbaldehyde **204** as a yellow solid (1.37 g, 64%), m.p.174-176 °C (lit[212] 174-176 °C), ν_{max} (KBr)/cm^{-1},

1678 and 1719 (2xC=O); δ_H (400 MHz; $CDCl_3$) 3.91 (3H, s, OCH_3), 6.88 (1H, s, 3-H), 7.34 (1H, m, 8-H), 7.53-7.56 (2H, m, 5-H and 7-H) and 9.80 (1H, s, CHO); δ_c (100 MHz; $CDCl_3$) 56.0 (OCH_3), 104.9 (C-5), 115.8 (C-3), 120.2 (C-7), 124.5 (C-8), 125.7 (C-4a), 152.0 (C-6), 156.0 (C-8a), 157.8 (C-2), 178.1 (C=O) and 185.5 (CHO); *m/z* 204 ($\mathbf{M}^+$, 100%)

3.3 Baylis-Hillman reactions of chromone-3-carbaldehydes

3.3.1 Reactions of chromone-3-carbaldehydes with acrylonitrile

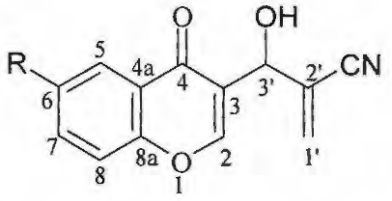

3-(2-cyano-3-hydroxypropen-3-yl)-4H-1-benzopyran-4-one **212**

Acrylonitrile (0.56mL, 8.6 mmol) was added to a stirred solution of chromone-3-carbaldehyde **83** (1.0g, 5.8 mmol) and 3-hydroxyquinuclidine (3.7 g, 29 mmol) in $CHCl_3$ (7.0 mL). The resulting mixture was stirred vigorously at room temperature for 25h. Evaporation of solvent *in vacuo* gave a brown oily residue which was purified by flash chromatography [on silica; elution with hexane-EtOAc (2:3)] to afford 3-(2-cyano3-hydroxypropen-3-yl)-4*H*-1-benzopyran-4-one **212** as a yellow crystalline solid (0.24 g, 98%). m.p. 68-70 °C, (lit.,[212] 68-70°C), (Found $\mathbf{M}^+$: 227.0570. Calc. for $C_{13}H_9NO_3$, *M*: 227.0582), ν_{max} (KBr)/cm^{-1} 3430 (br, OH), 2225 (CN) and 1630 (C=O); δ_H (400 MHz; $CDCl_3$) 4.22 (1H, br s, 3'-OH), 5.29 (1H, s, 3'-H), 6.13 and 6.32 (2H, 2xs, 1'-CH_2), 7.44 (1H, t, *J*=7.6 Hz, 6-H), 7.50 (1H, d, *J*= 8.5 Hz, 8-H), 7.72 (1H, t, *J*= 7.8 Hz, 7-H), 8.05 (1H, s, 2-H) and 8.18 (1H, d, *J*= 8.0 Hz, 5-H); δ_C (100MHz; $CDCl_3$) 69.3 (C-3'), 116.7 and 124.3 (C-2' and CN), 118.3 (C-8), 121,3 (C-3), 123,8 (C-4a), 125.5 (C-5), 125.6 (C-6), 131.0 (C-1'), 134.4 (C-7), 153.8 (C-2), 156.4 (C-8a) and 177.6 (C=O); *m/z* 227 ($\mathbf{M}^+$, 46%) and 210 (100).

Note:

i) This reaction was repeated using DBU (2.2 mL, 15 mmol) as catalyst for 6 and 24 hours. The reaction was then quenched, in each case, by diluting with diethyl ether (20 mL), and the resulting mixture was washed with aq. HCl (2-M, 20 mL) and then withwater (20 mL) and dried over $NaSO_4$. Evaporation of the solvent *in vacuo* gave a brown oily residue which was purified by flash chromatography [on silica; elution with hexane-EtOAc (2:3)] to afford 3-(2-cyano-3-hydroxypropen-3-yl)-4*H*-1-benzopyran-4-one **212 as** a yellow crystalline solid (0.15 g, 60%) and (0.20 g, 80%), respectively.

ii) The reaction was repeated for 24 hours using DABCO (0.27g, 2.4 mmol) as catalyst and an ionic liquid, 1-methyl-2-pyrollidine (1-NMP), (4 mL) as solvent. The reaction was quenched by dilution with water (15 mL) followed by extraction with EtOAc (3 x 10 mL). Evaporation of the organic solvent *in vacuo* gave a brown oily residue which was purified by flash chromatography [on silica; elution with hexane-EtOAc (1:2)] to afford 3-(2-cyano-3-hydroxypropen-3-yl)-4*H*-1-benzopyran-4-one **212** as a yellow crystalline solid (0.15 g, 60%).

*6-Chloro-3-(2-cyano-3-hydroxypropen-3-yl)-4*H*-1-benzopyran-4-one* **213**

The experimental procedure employed for the synthesis of 3-(2-cyano-3-hydroxypropen-3-yl)-4*H*-1-benzopyran-4-one **212** was followed, using 6-chlorochromone-3-carbaldehyde **184** (0.50 g, 2.4 mmol), acrylonitrile (0.24 mL, 3.6 mmol), 3-hydroxyquinuclidine (1.53 g, 12.0 mmol) and $CHCl_3$ (7.0mL). Work-up afforded 6-chloro-3-(2-cyano-3-hydroxypropen-3-yl)-4*H*-1-benzopyran-4-one **213** as a yellow crystalline solid (0.42g, 66%), m.p. 132-133°C (lit.,[212] 131-133°C); (Found $\mathbf{M}^+$: 261.0196. Calc. for $C_{13}H_8O_3N^{35}Cl$, *M*: 261.0193); ν_{max} (KBr)/cm^{-1} 3440 (br, OH), 2300 (CN) and 1653 (C=O); δ_H (400 MHz; $CDCl_3$) 4.04 (1H, br s, 3'-OH), 5.34 (1H, s, 3'-H), 6.12 and 6.30 (2H, 2xs, 1'-CH_2), 7.45 (1H, dd, *J*=8.9 and 2.1 Hz, 7-H), 7.64 (1H, d, *J*=8.9 Hz, 8-H), 8.08 (1H, s, 2-H) and 8.12 (1H, d, *J*= 2.1 Hz, 5-H); δ_C (100 MHz; $CDCl_3$) 69.5 (C-3'), 104.3 (C-5), 116.8 (C-3), 119.8 (C-8), 120.2 (C-4a), 124.2 and

124.3 (C-2' and CN), 124.7 (C-7), 131.0 (C-1'), 151.2 (C-8a), 153.4 (C-2), 157.4 (C-6) and 177.6 (C=O); *m/z* 261 ($\mathbf{M}^+$, 52%) and 209 (100).

Note:

i) When DBU (0.91g, 6.2 mmol) was used as catalyst, work-up after 6 hours and 24 hours afforded 6-chloro-3-(2-cyano-3-hydroxypropen-3-yl)-4*H*-1-benzopyran-4-one **213** as a yellow crystalline solid (0.36 g, 56%) and (0.45 g, 71%), respectively.

ii) When DABCO (0.14 g, 1.2 mmol) and 1-NMP (2 mL) were used as catalyst and solvent, respectively, work-up afforded 6-chloro-3-(2-cyano-3-hydroxypropen-3-yl)-4*H*-1-benzopyran-4-one **213** as a yellow crystalline solid (0.32g, 50%).

*6-Bromo-3-(2-cyano-3-hydroxypropen-3-yl)-4*H*-1-benzopyran-4-one* **214**

The experimental procedure employed for the synthesis of 3-(2-cyano3-hydroxypropen-3-yl)-4*H*-1-benzopyran-4-one **212** was followed, using 6-bromochromone-3-carbaldehyde **185** (1.00 g, 3.95 mmol), acrylonitrile (0.39 mL, 5.9 mmol), 3-hydroxyquinuclidine (2.5 g, 20 mmol) and $CHCl_3$ (7.0 mL). Work-up afforded 6-bromo-3-(2-cyano-3-hydroxypropen-3-yl)-4*H*-1-benzopyran-4-one **214** as an orange-yellow crystalline solid (0.88 g, 73%), m.p.124-125 °C (lit.[52], 122-125°C); (Found $\mathbf{M}^+$: 304.9724. Calc. for $C_{13}H_8O_3N^{79}Br$, *M*: 304.9688), ν_{max} (KBr)/cm^{-1} 3420 (br, OH), 2225 (CN) and 1648 (C=O); δ_H (400 MHz; $CDCl_3$) 4.18 (1H, br s, 3'-OH), 5.33 (1H, s, 3'-H), 6.12 and 6.31 (2H, 2xs, 1'-CH_2), 7.40 (1H, d, *J*=8.9 Hz, 8-H), 7.79 (1H, dd, *J*= 8.9 and 2.40 Hz, 7-H), 8.09 (1H, s, 2-H) and 8.28 (1H, d, *J*= 2.4 Hz, 5-H); δ_C (100MHz; $CDCl_3$) 69.0 (C-3'), 116.5 (CN), 119.3 (C-6), 120.3 (C-8), 121.6 (C-2'), 123.9 (C-3), 124.9 (C-4a), 128.2 (C-5), 131.5 (C-1'), 137.5 (C-7), 154.0 (C-2), 155.1 (C-8a) and 176.1 (C=O); *m/z* 305 ($\mathbf{M}^+$, 44%) and 253 (100).

Note:

i) When DBU (2.2 g, 15 mmol) was used as catalyst, work-up after 6 hours and 24 hours afforded 6-bromo-3-(2-cyano-3-hydroxypropen-3-yl)-4*H*-1-benzopyran-4-one **214** as a yellow crystalline solid (0.63 g, 52%) and (0.78 g, 63%), respectively.

ii) When DABCO (0.14 g, 1.2 mmol) and 1-NMP (2 mL) were used as catalyst and solvent, respectively, work-up afforded 6-bromo-3-(2-cyano-3-hydroxypropen-3-yl)-4*H*-1-benzopyran-4-one **214** as a yellow crystalline solid (0.60 g, 50%).

6-Fluoro-3-(2-cyano-3-hydroxy propen-3-yl)-4H-1-benzopyran-4-one **215**

The experimental procedure employed for the synthesis of 3-(2-cyano-3-hydroxy propen-3-yl)-4*H*-1-benzopyran-4-one **212** was followed, using 6-fluorochromone-3-carbaldehyde **186** (0.50 g, 2.6 mmol), acrylonitrile (0.26 mL, 3.9 mmol), 3-hydroxyquinuclidine (1.6 g, 13 mmol) and $CHCl_3$ (7.0 mL). Work-up afforded 6-fluoro-3-(2-cyano-3-hydroxy propen-3-yl)-4*H*-1-benzopyran-4-one **215** as a yellow crystalline solid (0.38 g, 60%), m.p. 59-60 °C (lit.,[212] 58-60°C), (Found: $\mathbf{M}^+$, 245.0490, $C_{13}H_8O_3NF$ requires *M*, 245.0488), ν_{max} (KBr)/cm^{-1} 3200 (br, OH), 2235 (CN) and 1640 (C=O); δ_H (400 MHz; $CDCl_3$) 4.08 (1H, br s, 3'-OH), 5.31 (1H, s, 3'-H), 6.15 and 6.33 (2H, 2xs, 1'-CH_2), 7.45 (1H, m, 7-H), 7.53 (1H, m, 8-H), 7.81 (1H, dd, *J*=8.1 and 3.1 Hz, 5-H) and 8.08 (1H, s, 2-H); δ_C (100MHz; $CDCl_3$) 69.1 (C-3'), 110.3 (J_{CF} = 23 Hz, C-5), 116.6 and 124.0 (C-2' or CN), 120.5 (J_{CF} = 8.1 Hz, C-8), 120.7 (C-3), 122.9 (J_{CF} = 25 Hz, C-7), 124.9 (J_{CF} = 7.6 Hz, C-4a), 131.4 (C-1'), 152.5 (C-8a), 154.0 (C-2), 160.0 (C-6) and 176.5 (C=O); *m/z* 245 ($\mathbf{M}^+$, 57%) and 193 (100).

Note:

i) When DBU (1.0 g, 6.7 mmol) was used as catalyst, work-up after 6 hours and 24 hours afforded 6-fluoro-3-(2-cyano-3-hydroxy propen-3-yl)-4*H*-1-benzopyran-4-one **215** as a yellow crystalline solid (0.32 g, 50%) and (0.38 g, 60%), respectively.

ii) When DABCO (0.14 g, 1.2 mmol) and 1-NMP (2mL) were used as catalyst and solvent, respectively, work-up afforded 6-fluoro-3-(2-cyano-3-hydroxy propen-3-yl)-4*H*-1-benzopyran-4-one **215** as a yellow crystalline solid (0.31 g, 48%).

*3-(2-cyano-3-hydroxypropen-3-yl)-6-methoxy-4*H*-1-benzopyran-4-one* **216**

The experimental procedure employed for the synthesis of 3-(2-cyano-3-hydroxy propen-3-yl)-4H-1-benzopyran-4-one **212** was followed, using 6-methoxychromone-3-carbaldehyde **187** (1.0 g, 4.9 mmol), acrylonitrile (0.48 mL, 7.3 mmol), 3-hydroxyquinuclidine (3.1 g, 25 mmol) and $CHCl_3$ (10 mL). Work-up afforded 3-(2-cyano-3-hydroxypropen-3-yl)-6-methoxy-4*H*-1-benzopyran-4-one **216** as a yellow crystalline solid (0.89 g, 71%), m.p. 114-115 °C (lit., [212] 114-117°C), (Found: $\mathbf{M}^+$: 257.0686. Calc. for $C_{14}H_{11}O_4N$, *M*: 257.0688), ν_{max} (KBr)/cm^{-1} 3400 (br, OH), 2225 (CN) and 1650 (C=O); δ_H (400 MHz; $CDCl_3$) 3.89 (3H, s, OCH_3), 4.41 (1H, br s, 3'-OH), 5.28 (1H, s, 3'-H), 6.14 and 6.34 (2H, 2xs, 1'-CH_2), 7.32 (1H, dd, *J*=9.2 and 3.1 Hz, 7-H), 7.45 (1H, d, *J*= 9.2 Hz, 8-H), 7.52 (1H, d, *J*= 3.1 Hz, 5-H) and 8.08 (1H, s, 2-H); δ_C (100 MHz; $CDCl_3$) 55.9 (OCH_3), 69.1 (C-3'), 104.4 (C-5), 116.8 and 124.2 (C-2' or CN), 119.8 (C-8), 120.3 (C-3), 124.3 (C-7), 124.8 (C-4a), 131.0 (C-1'), 151.3 (C-8a), 154.0 (C-2), 160.0 (C-6) and 176.5 (C=O); *m/z* 257 ($\mathbf{M}^+$, 46%) and 205 (100).

Note:

i) When DBU (1.85 g, 12.6 mmol) was used as catalyst, work-up after 6 hours and 24 hours the work-up afforded 3-(2-cyano-3-hydroxypropen-3-yl)-6-methoxy-4*H*-1-benzopyran-4-one **216** as a yellow crystalline solid (0.69 g, 55%) and (0.97 g, 77%), respectively.

ii) When DABCO (0.14 g, 1.2 mmol) and 1-NMP (2mL) were used as catalyst and solvent, respectively, the work-up afforded 3-(2-cyano-3-hydroxypropen-3-yl)-6-methoxy-4*H*-1-benzopyran-4-one **216** as a yellow crystalline solid (0.56 g, 45%).

3.3.2 Reactions of chromone-3-carbaldehydes with methyl acrylate

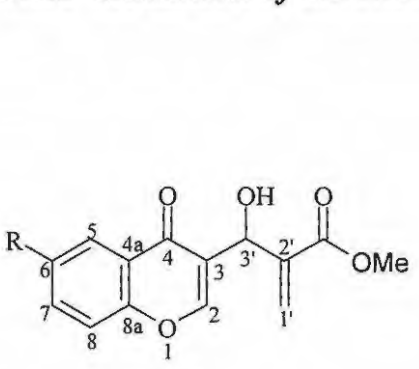

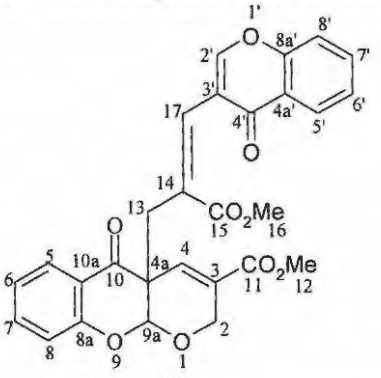

*3-[3-Hydroxy-2-(methoxycarbonyl)-1-propen-3-yl]-4*H*-1-benzopyran-4-one **217** and the corresponding dimer **222***

Methyl acrylate (0.56mL, 8.6 mmol) was added to a stirred solution of chromone-3-carbaldehyde **83** (1.0 g, 5.8 mmol) and 3-hydroxyquinuclidine (3.7 g, 29 mmol) in $CHCl_3$ (7.0 mL). The resulting mixture was stirred vigorously at room temperature for 24h. Evaporation of the solvent *in vacuo* gave a brown oily residue, which was purified by flash chromatography [on silica; elution with hexane-EtOAc (1:2)] afforded two fractions.

i) 3-[3-Hydroxy-2-(methoxycarbonyl)-1-propen-3-yl]-4*H*-1-benzopyran-4-one **217** as a yellow solid (1.21 g, 80%), m.p. 109-110 °C (lit.,[212] 109-112 °C); (Found $\mathbf{M}^+$: 260.0690. Calc. for $C_{14}H_{12}O_5$, *M*: 260.0685); ν_{max} (KBr)/cm^{-1}3423 (br, OH), 1723 and 1655 (2 x C=O); δ_H (400 MHz; $CDCl_3$) 3.74 (3H, s, OCH_3), 4.57 (1H, br s, 3'-OH), 5.59 (1H, s, 3'-H), 6.14 and 6.43 (2H, 2xs, 1'-CH_2), 7.41 (1H, m, 6-H), 7.45 (1H, d, *J*=8.0 Hz, 8-H), 7.68 (1H, m, 7-H), 8.02 (1H, s, 2-H) and 8.18 (1H, dd, *J*=8.0 and 1.4 Hz, 5-H); δ_C (100 MHz; $CDCl_3$) 52.0 (OCH_3), 67.6 (C-3'), 118.3 (C-8), 123.0 (C-3), 124.0 (C-4a), 125.4 (C-6), 125.6 (C-5), 126.8 (C-1'), 134.0 (C-7), 139.5 (C-2'), 154.3 (C-2), 156.3 (C-8a), 166.5 (CO.O) and 177.9 (C=O); *m/z* 260 ($\mathbf{M}^+$, 7%) and 200 (100)

ii) The chromone dimer **222** as a pale yellow solid (0.73 g, 25%), m.p. 193-195 °C (lit.,[52] 193-194°C), (Found: $\mathbf{M}^+$, 502.1250. Calc. for $C_{28}H_{22}O_9$, *M*: 502.1257); ν_{max} (KBr)/cm^{-1} 1712, 1707, 1653 and 1631 (4 x C=O); δ_H (400 MHz; $CDCl_3$) 3.12 and 3.37 (2H, 2x d, *J*=14.7 Hz, 13-CH_2), 3.61 and 3.65 (6H, 2xs, 12-and 16-CH_3), 4.50 (2H, dd, *J*=17 and 1.6 Hz, 2-CH_2), 5.05 (1H, s, 9a-H), 6.90 (1H, t, *J*=7.8 Hz, 6-H), 6.97 (1H, d, *J*=8.4 Hz, 5-H), 7.30 (1H, s, 4-H), 7.35 (1H, t, *J*=8.4 Hz, 7-H) 7.40 (2H, m, 7'-H and 8'-H), 7.50 (1H, s, 17-H), 7.69 (1H, t, *J*=7.2 Hz, 6'-H), 7.72 (1H, dd, *J*=7.9 and 1.5 Hz, 8-H), 7.90 (1H, s, 2'-H) and 8.16 (1H, d, *J*=7.2 Hz, 5'-H); δ_C (100MHz; $CDCl_3$) 28.4 (C-13), 50.3 (C-4a), 51.8 (C-12), 52.1 (C-16), 65.8 (C-2), 99.9 (C-9a), 117.7 (C-8), 117.9 (C-8'), 119.9 (C-10a), 120.5 (C-4a'), 122.7 (C-6), 123.9 (C-3'), 125.5 (C-6'), 126.2 (C-5), 127.7 (C-5'), 129.1 (C-3), 130.8 (C-14), 133.1 (C-17), 133.8 (C-4), 136.0 (C-7), 136.1 (C-7'), 154.9 (C-2'), 157.1 (C-8a), 155.8 (C-8a'), 163.8 (C-11), 167.3 (C-15), 174.9 (C-4') and 191.4 (C-10); *m/z* 502 ($\mathbf{M}^+$, 24%) and 243 (100)

Note:

i) The reaction was repeated using DBU (2.19 mL, 15 mmol) as catalyst. After 24 hours, the reaction was quenched by diluting with diethyl ether (20 mL). The resulting solution was washed with aq. HCl (2-M, 20 mL), followed by water (20 mL) and then dried over $NaSO_4$. Evaporation of the solvent *in vacuo* gave a brown oily residue which was purified by flash chromatography [on silica; elution with hexane-EtOAc (2:3)] to afford 3-[3-hydroxy-2-(methoxycarbonyl)-1-propen-3-yl]-4*H*-1-benzopyran-4-one **217** as a yellow solid (0.98 g, 65%).

ii) The reaction was repeated using DABCO (0.27 g, 2.4 mmol) as catalyst and -NMP (4 mL) as solvent. After 24h, the reaction was quenched by dilution with water (15 mL) and the resulting mixture was extracted with EtOAc (3 x 10 mL). Evaporation of the organic solvent *in vacuo* gave a brown oily residue, which was purified by flash chromatography [on silica gel and elution with hexane-EtOAc (1:2)] to afford 3-[3-

hydroxy-2-(methoxycarbonyl)-1-propen-3-yl]-4*H*-1-benzopyran-4-one **217** as a yellow crystalline solid (0.75 g, 50%).

*6-Chloro-3-[3-hydroxy-2-(methoxycarbonyl)-1-propen-3-yl]-4*H*-1-benzopyran-4-one* **218** *and the corresponding dimer* **223**

The experimental procedure employed for the synthesis of 3-[3-hydroxy-2-(methoxycarbonyl)-1-propen-3-yl]-4*H*-1-benzopyran-4-one **217** and the corresponding dimer **222** was followed, using 6-chlorochromone-3-carbaldehyde **184** (1.0 g, 4.8 mmol), methyl acrylate (0.48 mL, 7.2 mmol), 3-hydroxyquinuclidine (3.1 g, 24 mmol) and $CHCl_3$ (7.0 mL). Work-up and flash chromatography afforded two fractions.

i) 6-Chloro-3-[3-hydroxy-2-(methoxycarbonyl)-1-propen-3-yl]-4*H*-1-benzopyran-4-one **218** as yellow solid (0.96 g, 68%), m.p. 108-110 °C (lit.,[212] 108-110°C), (Found $\mathbf{MH}^+$: 295.0373. Calc. for $C_{14}H_{11}{}^{35}ClO_5$, *M+1*: 295.0373), ν_{max} (KBr)/cm^{-1} 3423 (br, OH), 1718 and 1650 (2 x C=O); δ_H (400 MHz; $CDCl_3$) 2.90 (1H, br s, 3'-OH), 3.74 (3H, s, OCH_3), 5.60 (1H, s, 3'-H), 6.14 and 6.44 (2H, 2xs, 1'-CH_2), 7.42 (1H, d, *J*=8.9 Hz, 8-H), 7.61 (1H, dd, *J*=8.9 and 2.5 Hz, 7-H), 8.04 (1H, s, 2-H) and 8.13 (1H, d, *J*=2.5 Hz, 5-H); δ_C (100MHz; $CDCl_3$) 52.0 (OCH_3), 67.4 (C-3'), 120.0 (C-8), 123.2 (C-3), 124.8 (C-6), 125.1 (C-4a), 125.6 (C-5), 127.0 (C-1'), 131.4 (C-5), 134.2 (C-7), 154.5 (C-2), 154.6 (C-8a), 166.5 (CO.O) and 176.6 (C=O); *m/z* 294 ($\mathbf{M}^+$, 33%) and 234 (100).

ii) The chromone dimer **223** as yellow solid (0.60 g, 22%), m.p. 210-212 °C (lit.,[52] 210-213°C), (Found $\mathbf{M}^+$: 572.0636. Calc. for $C_{28}H_{20}O_9{}^{35}Cl_2$, *M*: 572.0641), ν_{max} (KBr)/cm^{-1}, 1715, 1710, 1650 and 1646 (4 x C=O); δ_H (400 MHz; $CDCl_3$) 3.10 and 3.35 (2H, 2xd, *J*=14.7 Hz, 13- CH_2), 3.67 and 3.69 (6H, 2xs, 12 and 16-OCH_3), 4.52 (2H, dd, *J*=17 and 2.0 Hz, 2-CH_2), 5.04 (1H, s, 9a-H), 6.93 (1H, d, *J*=8.9 Hz, 8-H), 7.27 (1H, m, 4-H), 7.29 (1H, m, 7-H) 7.42 (1H, d, *J*=9 Hz, 8'-H), 7.48 (1H, s, 17-H), 7.61 (1H, m, 7'-H), 7.65 (1H, d, *J*=2.4 Hz, 5-H), 8.00 (1H, s, 2'-H) and 8.10 (1H, d, *J*=2.5 Hz, 5'-H); δ_C (100MHz; $CDCl_3$) 28.4 (C-13), 50.3 (C-4a), 51.9 (C-12), 52.3 (C-16), 66.0 (C-2), 100.0 (C-9a), 119.5 (C-8), 119.8 (C-8'), 120.5 (C-4a), 120.8 (C-3'), 125.5 (C-5'), 127.0 (C-5),

128.5 (C-10a), 129.4 (C-3), 131.2 (C-14), 131.7 (C-6'), 132.3 (C-17), 134.4 (C-7'), 135.4 (C-7), 136.0 (C-4), 154.0 (C-8a), 155.1 (C-2'), 155.5 (C-8a'), 163.8 (C-6), 167.8 (C-11), 173.6 (C-15), 175.7 (C-4') and 190.3 (C-10); *m/z* 571 ($\mathbf{M}^+$, 38%) and 277 (100)

Note:

i) When DBU (1.8 g, 12 mmol) was used as the catalyst, work-up after 24 hours afforded 6-chloro-3-[3-hydroxy-2-(methoxycarbonyl)-1-propen-3-yl]-4*H*-1-benzopyran-4-one **218** as a yellow crystalline solid (0.89 g, 63%).

ii) When DABCO (1.1 g, 9.6 mmol) was used as catalyst and 1-NMP (5 mL) as solvent, work-up after 24 hours afforded 6-chloro-3-[3-hydroxy-2-(methoxycarbonyl)-1-propen-3-yl]-4*H*-1-benzopyran-4-one **218** as a yellow crystalline solid (0.66 g, 47%).

*6-Bromo-3-[3-hydroxy-2-(methoxycarbonyl)-1-propen-3-yl]-4*H*-1-benzopyran-4-one* **219** *and the corresponding dimer* **224**

The experimental procedure employed for the synthesis of 3-[3-hydroxy-2-(methoxycarbonyl)-1-propen-3-yl]-4*H*-1-benzopyran-4-one **217** and the corresponding dimer **222** was followed, using 6-bromochromone-3-carbaldehyde **185** (1.1 g, 4.4 mmol), methyl acrylate (0.44 mL, 6.6 mmol), 3-hydroxyquinuclidine (2.8 g, 22 mmol) and $CHCl_3$ (7.0 mL). Work-up and flash chromatography afforded two fractions.

i) 6-Bromo-3-[3-hydroxy-2-(methoxycarbonyl)-1-propen-3-yl]-4*H*-1-benzopyran-4-one **219** as a yellow solid (1.1 g, 70%), m.p. 114-116 °C (lit., [212] 114-116°C), (Found $\mathbf{M}^+$: 337.9790. Calc. for $C_{14}H_{11}{}^{79}BrO_5$, *M*: 337.9789), ν_{max} (KBr)/cm^{-1} 3440 (br, OH), 1716 and 1642 (2 x C=O); δ_H (400 MHz; $CDCl_3$) 3.75 (3H, s, OCH_3), 4.38 (1H, d, *J*=8.0 Hz, 3'-OH), 5.59 (1H, d, *J*=8.0 Hz, 3'-H), 6.11 and 6.42 (2H, 2 x s, 1'- CH_2), 7.37 (1H, d, *J*=8.9 Hz, 8-H), 7.75 (1H, dd, *J*= 9.0 and 2.5 Hz, 7-H), 8.02 (1H, s, 2-H) and 8.28 (1H, d, *J*=2.5 Hz, 5-H); δ_C (100 MHz; $CDCl_3$) 52.0 (OCH_3), 67.5 (C-3'), 118.8 (C-8), 120.2 (C-6), 123.3 (C-3), 125.2 (C-4a), 125.6 (C-5), 127.0 (C-1'), 128.3 (C-5), 137.0 (C-7),

154.5 (C-2), 155.0 (C-8a), 166.5 (CO.O) and 176.5 (C=O); *m/z* 338 ($\mathbf{M}^+$, 17%) and 280 (100).

ii) The corresponding dimer **224** (0.52 g, 18%), m.p. 223-225 °C (lit., [52] 223-225 °C), (Found $\mathbf{M}^+$: 657.9471. Calc. for $C_{28}H_{20}{}^{79}Br_2O_5$, *M*: 657.9474), ν_{max} (KBr)/cm^{-1}1715, 1705, 1650 and 1646 (4 x C=O); δ_H (400 MHz; $CDCl_3$) 3.11 and 3.33 (2H, 2x d, *J*=14.7 Hz, 13-CH_2), 3.65 and 3.69 (3H, 2xs, 12 and 16-OCH_3), 4.51 (2H, dd, *J*=17.0 and 2.0 Hz, 2-CH_2), 5.02 (1H, s, 9a-H), 6.88 (1H, d, *J*=8.8 Hz, 8-H), 7.27 (1H, m, 4-H), 7.35 (1H, d, *J*=8.9 Hz, 7'-H) 7.41 (1H, dd, *J*=9.0 and 2.5 Hz, 7-H), 7.48 (1H, s, 17-H), 7.78 (1H, dd, *J*=9.0 and 2.5 Hz, 8'-H), 7.81 (1H, d, *J*=2.5 Hz, 5-H), 7.88 (1H, s, 2'-H) and 8.26 (1H, d, *J*= 2.5 Hz, 5'-H); δ_C (100MHz; $CDCl_3$) 28.4 (C-13), 50.3 (C-4a), 52.0 (C-12), 52.3 (C-16), 66.0 (C-2), 100.0 (C-9a), 115.7 (C-8), 119.2 (C-4a'), 119.8 (C-8'), 120.1 (C-10a), 120.6 (C-6), 121.3 (C-6'), 125.0 (C-3'), 128.8 (C-5'), 129.3 (C-3), 130.1 (C-5), 131.2 (C-14), 132.8 (C-17), 135.4 (C-7'), 137.0 (C-7), 138.8 (C-4), 154.4 (C-2'), 155.0 (C-8a'), 156.0 (C-8a), 163.8 (C-11), 167.1 (C-15), 173.5 (C-4') and 190.2 (C-10); *m/z* 658 ($\mathbf{M}^+$, 10%) and 323 (100).

Note:

i) When DBU (1.8 g, 12 mmol) was used as catalyst, work-up after 24 hours afforded 6-bromo-3-[3-hydroxy-2-(methoxycarbonyl)-1-propen-3-yl]-4*H*-1-benzopyran-4-one **219** as a yellow solid (0.86 g, 57%).

ii) When DABCO (0.99 g, 8.8 mmol) was used as the catalyst and 1-NMP (5 mL) as solvent, work-up after 24 hours afforded 6-bromo-3-[3-hydroxy-2-(methoxycarbonyl)-1-propen-3-yl]-4*H*-1-benzopyran-4-one **219** as a yellow solid (0.57 g, 38%).

*6-Fluoro-3-[3-hydroxy-2-(methoxycarbonyl)-1-propen-3-yl]-4*H*-1-benzopyran-4-one* **220** *and the corresponding dimer* **225**

The experimental procedure employed for the synthesis of 3-[3-hydroxy-2-(methoxycarbonyl)-1-propen-3-yl]-4*H*-1-benzopyran-4-one **217** and the corresponding dimer **222** was followed, using 6-fluorochromone-3-carbaldehyde **186** (0.50 g, 2.6 mmol), methyl acrylate (0.20 mL, 3.9 mmol), 3-hydroxyquinuclidine (1.7 g, 13 mmol) and $CHCl_3$ (7.0 mL). Work-up and flash chromatography afforded two fractions.

i) 6-Fluoro-3-[3-hydroxy-2-(methoxycarbonyl)-1-propen-3-yl]-4*H*-1-benzopyran-4-one **220** as a yellow solid (0.46 g, 63%), m.p. 139-141 °C (lit.,[212] 140-142 °C), (Found $\mathbf{M}^+$: 278.0596. Calc. for $C_{14}H_{11}FO_5$, *M*: 278.0591); ν_{max} (KBr)/cm^{-1} 3423 (br, OH), 1716 and 1640 (2 x C=O); δ_H (400 MHz; $CDCl_3$) 3.75 (3H, s, OCH_3), 4.43 (1H, d, *J*=7.8 Hz, 3'-OH), 5.60 (1H, d, *J*=7.8 Hz, 3'-H), 6.12 and 6.46 (2H, 2xs, 1'- CH_2), 7.40 (1H, m, 7-H), 7.48 (1H, dd, *J*=9.1 and 4.2 Hz, 8-H), 7.81 (1H, dd, *J*=8.3 and 3.0 Hz, 5-H) and 8.05 (1H, s, 2-H); δ_C (100 MHz; $CDCl_3$) 52.0 (OCH_3), 67.6 (C-3'), 110.5 (C-5), 120.4 (C-8), 122.3 (C-7), 122.5 (C-3), 125.8 (C-4a), 126.9 (C-1'), 139.2 (C-2'), 152.5 (C-8a), 154.6 (C-2), 159.6 (C-6), 166.5 (CO.O) and 177.1 (C=O); *m/z* 278 ($\mathbf{M}^+$, 34%) and 193 (100).

ii) The chromone dimer **225** as yellow solid (70 mg, 5%), m.p. 198-200 °C (lit.,[212] 198-200°C), (Found: $\mathbf{M}^+$: 538.1074. Calc. for $C_{28}H_{20}F_2O_5$, *M*: 538.1075), ν_{max} (KBr)/cm^{-1} 1727, 1713, 1650 and 1648 (4 x C=O); δ_H (400 MHz; $CDCl_3$) 3.10 and 3.35 (2H, 2xd, *J*=14.7 Hz, 13- CH_2), 3.64 and 3.70 (3H, 2xs,12 and 16-OCH_3), 4.51 (2H, dd, *J*=17.0 and 2.0 Hz, 2-CH_2), 5.01 (1H, s, 9a-H), 6.97 (1H, dd, *J*=9.0 and 4.0 Hz, 5-H), 7.05 (1H, m, 7-H), 7.24 (1H, s, 4-H), 7.33 (1H, dd, *J*=8.3 and 2.8 Hz, 8-H), 7.38-7.48 (2H, m, 5'-H and 7'-H), 7.50 (1H, s, 17-H), 7.78 (1H, dd, *J*=8.3 and 2.8 Hz, 8'-H) and 7.90 (1H, s, 2'-H); δ_C (100 MHz; $CDCl_3$) 28.4 (C-13), 50.2 (C-4a), 51.9 (C-12), 52.2 (C-16), 65.9 (C-2), 100.1 (C-9a), 111.0 (C-8'), 112.7 (C-8), 119.5 (C-5), 119.8 (C-3'), 120.2 (C-5'), 120.6 (C-10a), 122.3 (C-7'), 123.6 (C-7), 124.9 (C-4a'), 129.4 (C-3), 131.1 (C-14), 132.8 (C-17), 135.4 (C-4), 151.9 (C-8a'), 153.3 and 157.8 (C-8a and C-6'), 155.1 (C-2'),

159.7 (C-6), 163.8 (C-11), 167.1 (C-15), 174.0 (C-14') and 190.6 (C-10); *m/z* 538 ($\mathbf{M}^+$, 21%) and 261 (100).

Note:
i) When DBU (0.99 g, 6.7 mmol) was used as the catalyst, work-up after 24 hours afforded 6-fluoro-3-[3-hydroxy-2-(methoxycarbonyl)-1-propen-3-yl]-4*H*-1-benzopyran-4-one **220** as a yellow solid (0.37 g, 50%).

ii) When DABCO (0.585 g, 5.20 mmol) was used as the catalyst and 1-NMP (5 mL) as solvent, work-up after 24 hours afforded 6-fluoro-3-[3-hydroxy-2-(methoxycarbonyl)-1-propen-3-yl]-4*H*-1-benzopyran-4-one **220** as a yellow solid (2.2 mg, 30%).

*3-[3-Hydroxy-2-(methoxycarbonyl)-1-propen-3-y]-6-methoxy-4*H*-1-benzopyran-4-one* **221** *and the corresponding dimer* **226**

The experimental procedure employed for the synthesis of 3-[3-hydroxy-2-(methoxycarbonyl)-1-propen-3-yl]-4*H*-1-benzopyran-4-one **217** and the corresponding dimer **222** was followed, using 6-methoxychromone-3-carbaldehyde **187** (1.0 g, 4.9 mmol), methyl acrylate (0.49 mL, 7.3mmol), 3-hydroxyquinuclidine (3.1 g, 25 mmol) and $CHCl_3$ (7.0 mL).Work-up and flash chromatography afforded two fractions.

i) 3-[3-Hydroxy-2-(methoxycarbonyl)propen-3-y]-6-methoxy-4*H*-1-benzopyran-4-one **221** as yellow oil (1.1 g, 75%), (Found $\mathbf{M}^+$: 290.0780. Calc for $C_{15}H_{14}O_6$, *M*: 290.0790); ν_{max} (KBr)/cm^{-1} 3426 (br, OH), 1723 and 1643 (2 x C=O); δ_H (400 MHz; $CDCl_3$) 3.70 (3H, s, CO.*OCH*$_3$), 3.81 (3H, s, 6-OCH_3), 4.68 (1H, d, *J*=4.5 Hz, 3'-OH), 5.60 (1H, d, *J*=2.5 Hz, 3'-H), 6.10 and 6.39 (2H, 2 x s, 1'-H), 7.18 (1H, dd, *J*=9.1 and 3.0 Hz, 7-H), 7.30 (1H, d, *J*= 9.0 Hz, 8-H), 7.44 (1H, d, *J*= 3.0 Hz, 5-H) and 7.98 (1H, s, 2-H); δ_C (100MHz; $CDCl_3$) 51.7 ($CO.OCH_3$), 55.6 (6-OCH_3), 67.1 (C-3'), 104.3 (C-5), 119.4 (C-8), 122.2 (C-3), 123.9 (C-7), 124.3 (C-4a), 126.3 (C-1'), 139.7 (C-2'), 150.9 (C-8a),

154.0 (C-2), 156.8 (C-6), 166.3 (CO.O) and 177.4 (C=O); m/z 290 ($\mathbf{M}^+$, 26%) and 151(100).

ii) The corresponding dimer **226** (0.41 g, 15%) as a yellow viscous oil, (Found: $\mathbf{M}^+$, 562.1467. Calc. for $C_{30}H_{26}O_{11}$, *M*: 562.1475), ν_{max} (KBr)/cm^{-1}, and 1722, 1715, 1650 and 1646 (4 x C=O); δ_H (400 MHz; $CDCl_3$) 3.10 and 3.35 (2H, 2xd, *J*=14.7 Hz, 13-CH_2), 3.60 (3H, s, 12-H), 3.70 (3H, s, 6-OCH_3), 3.78 (3H, s, 16-H), 3.89 (3H, s, 6'-OCH_3), 4.39-4.53 (2H, dd, *J*=17 and 2.0 Hz, 2-CH_2), 5.45 (1H, s, 9a-H), 6.70 (1H, s, 4-H), 6.73 (1H, d, *J*=9.0 Hz, 9-H), 7.00 (1H, m, 7-H), 7.10 (1H, d, *J*=3.0 Hz, 5-H), 7.26 (1H, dd, *J*=9.0 and 3.0 Hz, 7'-H), 7.38 (1H, d, *J*=9.1 Hz, 8'-H), 7.50 (1H, d, *J*=3.2 Hz, 5'-H), 7.55 (1H, s, 17-H) and 7.91 (1H, s, 2'-H); δ_C (100MHz; $CDCl_3$) 31.2 (C-13), 51.0 (C-4a), 51.7 (C-12), 52.2 (C-16), 55.7 (6-OCH_3), 55.9 (6'-OCH_3), 62.9 (C-2), 99.2 (C-9a), 105.3 (C-5'), 107.6 (C-5), 119.0 (C-10a), 119.2 (C-8), 119.4 (C-8'), 119.6 (C-3'), 123.9 (C-7'), 124.5 (C-4a'), 125.6 (C-7), 129.9 (C-3), 130.6 (C-14), 133.3 (C-17), 135.0 (C-4), 150.7 (C-8a'), 151.8 (C-8a), 154.3 (C-2'), 154.7 (C-6), 157.1 (C-6'), 163.9 (C-11), 167.8 (C-15), 175.1 (C-4') and 192.4 (C-10); *m/z* 562 ($\mathbf{M}^+$, 37%) and 289 (100).

Note:

i) When DBU (1.9 g, 13 mmol) was used as the catalyst, work-up after 24 hours afforded 3-[3-hydroxy-2-(methoxycarbonyl)-1-propen-3-y]-6-methoxy-4*H*-1-benzopyran-4-one **221** as a yellow solid (0.86 g, 61%).

ii) When DABCO (1.10 g, 9.78 mmol) was used as the catalyst and 1-NMP (5 mL) as the solvent, work-up after 24hours afforded 3-[3-hydroxy-2-(methoxycarbonyl)-1-propen-3-y]-6-methoxy-4*H*-1-benzopyran-4-one **221** as a yellow solid (0.62 g, 44%).

3.3.3 Reactions of chromone-3-carbaldehydes with methyl vinyl ketone

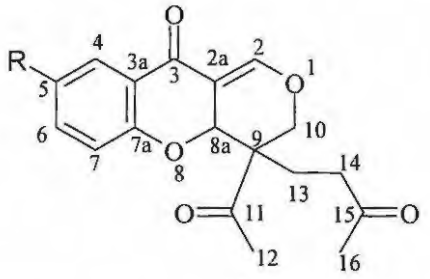

i

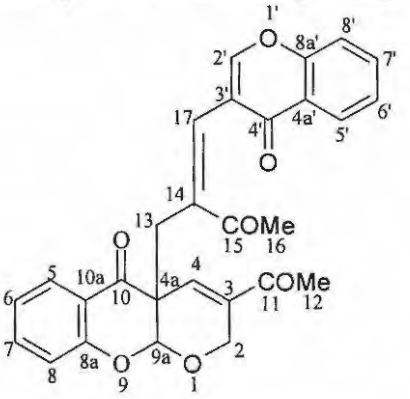

ii

*9-[11-acetyl-(15-oxo-butyl)-10-dihydro-3*H*-pyrano(9,2a)]chromen-3-one* **231** *and the corresponding dimer* **241**

Methyl vinyl ketone (0.56mL, 8.6 mmol) was added to a stirred solution of chromone-3-carbaldehyde **83** (1.0 g, 5.8 mmol) and 3-hydroxyquinuclidine (3.7 g, 29 mmol) in $CHCl_3$ (7.0 mL). The resulting mixture was stirred vigorously at room temperature for 24h. Evaporation of solvent *in vacuo* gave a brown oily residue which was purified by flash chromatography [on silica; elution with hexane-EtOAc (1:2)] afforded two fractions.

i) *9-[11-Acetyl-(15-oxo-butyl)-10-dihydro-3*H*-pyrano(9,2a)]chromen-3-one* **231** as a brown viscous oil (1.3 g, 69%), (Found $\mathbf{M}^+$: 314.1131. Calc. for $C_{18}H_{18}O_5$, *M*: 314.1154) ν_{max} (KBr)/cm^{-1}1700, 1665 and 1650 (3 x C=O); δ_H (400 MHz; $CDCl_3$) 1.98 and 2.25 (2H, 2 x m, CH_2CH_2CO), 2.07 (3H, s, $CH_2CH_2COCH_3$), 2.39 (3H, s, $COCH_3$), 2.40 and 2.60 (2H, 2xm, CH_2CH_2CO), 4.59 (1H, dd, *J*= 17.2 and 1.9 Hz, 10-H_a), 4.79 (1H, dd, *J*= 17.2 and 1.5 Hz, 10-H_b), 5.13 (1H, s, 8a-H), 7.13 (2H, m, 5-H and 7-H), 7.30 (1H, br s, 2-H), 7.57 (1H, t, *J*=6.9 Hz, 6-H) and 7.90 (1H, d, *J*=6.5 Hz, 4-H); δ_C (100 MHz; $CDCl_3$) 24.8 (CH_2CH_2CO), 25.5 ($CH_2CH_2COCH_3$), 30.0 ($COCH_3$), 37.8 (CH_2CH_2CO), 49.1 (C-9), 65.9 (C-10), 99.9 (C-8a), 118.2 (C-7), 119.5 (C-2a), 123.0 (C-4), 127.9 (C-5), 135.4 (C-6), 136.8 (C-2), 138.3 (C-3a), 157.6 (C-7a), 192.6 (3-C=O), 196.6 (15-C=O) and 206.7 (11-C=O); *m/z* 314 ($\mathbf{M}^+$, 2%) and 193 (100).

ii) The chromone dimer **241** as a yellow solid (0.96 g, 35%), m.p. 193-195 °C (lit., [213] 193-194°C), (Found $\mathbf{M}^+$: 470.1364. Calc. for $C_{28}H_{22}O_7$, *M*: 470.1366); ν_{max} (KBr)/cm^{-1}, 1698, 1669, 1642 and 1606 (4 x C=O); δ_H (400 MHz; $CDCl_3$) 2.29 and 2.42 (6H, 2xs, 12- and 16-CH_3), 3.23 (2H, 2x d, *J*=14.7 Hz, 13-CH_2), 4.52 (2H, dd, *J*=17 and 1.7 and Hz, 2-CH_2), 5.00 (1H, s, 9a-H), 6.83-6.90 (2H, m, 6- and 5-H), 7.17 (1H, s, 4-H), 7.27 (1H, m, 8-H), 7.40-7.47 (3H, m, 17-H, 7'-H and 8'-H), 7.69-7.75 (2H, m, 6'- and 7-H), 7.90 (1H, s, 2'-H), and 8.13 (2H, dd, *J*=8.0 and 1.3 Hz, 5'-H); δ_C (100 MHz; $CDCl_3$) 25.3 (C-12), 25.8 (C-16), 30.9 (C-13), 50.1 (C-4a), 65.9 (C-2), 99.9 (C-9a), 117.5 (C-5), 118.1 (C-7'), 120.0 (C-10a), 120.3 (C-4a'), 122.9 (C-6), 123.5 (C-8a'), 125.8 (C-8'), 126.1 (C-5'), 128.0 (C-7), 133.6 (C-17), 134.2 (C-6'), 136.1 (C-8), 136.6 (C-3), 136.7 (C-4), 139.1 (C-14), 154.1 (C-2'), 155.9 (C-3'), 157.0 (C-8a), 175.6 (C-4'), 191.5 (C-10), 196.9 (C-11) and 199.0 (C-15); *m/z* 470 ($\mathbf{M}^+$, 24%) and 185 (100).

Note:

i) When DABCO (0.38 g, 2.9mmol) was used as catalyst and 1-NMP (3mL) as solvent, work-up afforded 9-[11-acetyl-(15-oxo-butyl)-10-dihydro-3H-pyrano (9,2a)]chromen-3-one **231** as a light brown viscous oil (0.82 g, 45%).

*9-[11-Acetyl-(15-oxo-butyl)-10-dihydro-3*H*-pyrano(9,2a)]-5-chloro-chromen-3-one* **232** *and the corresponding dimer* **242**

The experimental procedure employed for the synthesis of 9-[11-Acetyl-(15-oxo-butyl)-10-dihydro-3H-pyrano(9,2a)]chromen-3-one **231** and the chromone dimer **241** was followed, using 6-chlorochromone-3-carbaldehyde **184** (1.0 g, 4.8 mmol), methyl vinyl ketone (0.48 mL, 7.2 mmol), 3-hydroxyquinuclidine (3.1 g, 24 mmol) and $CHCl_3$ (7.0 mL). Work-up and flash chromatography afforded two fractions.

i) *9-[11acetyl-(15-oxo-butyl)-10-dihydro-3*H*-pyrano(9.2a)]-5-chloro-chromen-3-one* **232** as a reddish oil (1.3 g, 80%), (Found $\mathbf{MH}^+$: 349.0843. Calc. for $C_{18}H_{17}{}^{35}ClO_5$, *M*: 349.0848); ν_{max} (KBr)/cm^{-1} 1717, 1699 and 1674 (3 x C=O); δ_H (400 MHz; $CDCl_3$) 2.13

(3H, s, $CH_2CH_2COCH_3$), 2.15-2.25 (2H, 2 x m, CH_2CH_2CO), 2.31 (3H, s, $COCH_3$), 2.46-2.59 (2H, 2xm, CH_2CH_2CO), 4.48 (1H, dd, *J*=17.1 and 2.0 Hz, 10-H_a), 4.63 (1H, dd, *J*=17.0 and 1.5 Hz, 10-H_b), 5.40 (1H, s, 8a-H), 6.65 (1H, br s, 2-H), 6.69 (1H, d, *J*=8.8 Hz, 7-H), 7.48 (1H, dd, *J*=8.8 and 2.7 Hz, 6-H) and 7.80 (1H, d, *J*=2.7 Hz, 4-H); δ_C (100MHz; $CDCl_3$) 25.2 ($CH_2CH_2COCH_3$), 27.6 ($CH_2CH_2COCH_3$), 30.0 ($COCH_3$), 37.6 ($CH_2CH_2COCH_3$), 48.8 (C-9), 62.7 (C-10), 99.6 (C-8a), 118.8 (C-2a), 120.0 (C-7), 126.6 (C-4), 135.4 (C-6), 136.9 (C-2), 139.4 (C-3a), 143.5 (C-5), 155.9 (C-7a), 192.0 (3-C=O), 196.4 (15-C=O) and 205.3 (11-C=O); *m/z* 349 (**MH^+**, 9%) and 154 (100).

ii) The *chromone dimer* **242** as a yellow solid (0.80 g, 33%), m.p. 112-114°C, (Found **M^+**:538.0587. Calc. for $C_{28}H_{21}ClO_7$, *M*: 538.0586); ν_{max} (KBr)/cm^{-1}, 1653,1678, 1684 and 1701 (4 x C=O); δ_H (400 MHz; $CDCl_3$) 2.31 and 2.44 (6H, 2xs, 12-and 16-CH_3), 3.00 (2H, 2xd, *J*=14.7 Hz, 13-CH_2), 5.16 (2H, dd, *J*=17 and 1.7 and Hz, 2-CH_2), 5.39 (1H, s, 9a-H), 6.93 (1H, s, 4-H), 7.12 (1H, d, *J*=8.9 Hz, 8-H), 7.30 (1H, s, 17-H), 7.44 (1H, d, *J*=8.9 Hz, 8'-H), 7.45 (1H, d, *J*=8.9 and 2.0 Hz, 7'-H), 7.76 (1H, dd, *J*=8.0 and 2.0 Hz, 7-H), 8.08 (1H, d, *J*=2.0 Hz, 5-H), 8.66 (1H, s, 2'-H), and 8.18 (1H, d, *J*=1.3 Hz, 5'-H); δ_C (100 MHz; $CDCl_3$) 25.4 (C-12), 25.9 (C-16), 31.2 (C-13), 50.5 (C-4a), 66.1(C-2), 100.2 (C-9a), 116.6 (C-5), 118.0 (C-7'), 121.6 (C-10a), 122.2 (C-4a'), 124.4 (C-5'), 128.4 (C-8'), 128.5 (C-7), 133.6 (C-17), 134.0 (C-6), 136.6 (C-3), 136.7 (C-8), 139.3 (C-14), 141.4 (C-6'), 143.7 (C-4), 148.6 (C-8a'), 154.2 (C-2'), 156.2 (C-3'), 158.5 (C-8a), 174.8 (C-4'), 190.8 (C-10), 196.9 (C-11) and 199.0 (C-15); *m/z* (**M^+**, %) and (100).

Note:

i) When DABCO (0.31 g, 2.4 mmol) was used as the catalyst and 1-NMP (3 mL) as solvent, work-up afforded *9-[11-acetyl-(15-oxo-butyl)-10-dihydro-3H-pyrano(9,2a)]-5-chloro-chromen-3-one* **232** as a light brown viscous oil (0.67 g, 40%).

*9-[11-acetyl-(15-oxo-butyl)-10-dihydro-3*H*-pyrano(9,2a)]-5-bromo-chromen-3-one* **233** *and the corresponding dimer* **243**

The experimental procedure employed for the synthesis of 9-[11-acetyl-(15-oxo-butyl)-10-dihydro-3H-pyrano(9,2a)]chromen-3-one **231** and the corresponding dimer **241** was followed, using 6-bromochromone-3-carbaldehyde **177** (1.0 g, 4.0 mmol), methyl vinyl ketone (0.48 mL, 5.93 mmol), 3-hydroxyquinuclidine (2.51 g, 19.8 mmol) and $CHCl_3$ (7.0 mL). Work-up and flash chromatography afforded two fractions.

i) *9-[11acetyl-(15-oxo-butyl)-10-dihydro-3*H*-pyrano(9.2a)]-5-bromo-chromen-3-one* **233** as a reddish oil (0.98 g, 63%), (Found: $\mathbf{M}^+$, 392.9466. Calc. for $C_{18}H_{17}BrO_5$, *M*: 391.9446), ν_{max} (KBr)/cm^{-1}, 1600, 1674 and 1716 (3 x C=O); δ_H (400 MHz; $CDCl_3$) 1.94-2.24 (2H, 2xm, CH_2CH_2CO), 2.08 (3H, s, $CH_2CH_2COCH_3$), 2.26-2.58 (2H, m, CH_2CH_2CO), 2.39 (3H, s, $COCH_3$), 4.58 (1H, dd, *J*=17.2 and 1.7 Hz, 10-H_a), 4.79 (1H, dd, *J*=17.2 and 1.5 Hz, 10-H_b), 5.11 (1H, s, 8a-H), 6.73 (1H, m, 2-H), 7.02 (1H, d, *J*=8.81 Hz, 7-H), 7.64 (1H, dd, *J*=8.8 and 2.5 Hz, 6-H) and 7.99 (1H, d, *J*=2.4 Hz, 4-H); δ_C (100 MHz; $CDCl_3$) 24.7 (C-13), 25.5 (C-16), 30.0 (C-12), 37.6 (C-14), 49.0 (C-9), 65.9 (C-10), 100.0 (C-8a), 118.1 (C-2a), 120.2 (C-7), 130.3 (C-4), 134.8 (C-6), 139.4 (C-2), 138.4 (C-3a), 143.5 (C-5), 156.5 (C-7a), 191.4 (3-C=O), 196.4 (15-C=O) and 206.5 (11-C=O); *m/z* 392 ($\mathbf{M}^+$, 2%) and 194 (100).

ii) The *chromone dimer* **243** as a yellow solid oil (0.62 g, 28%), (Found $\mathbf{M}^+$:625.9579 Calc. for $C_{28}H_{21}BrO_7$, *M*: 625.9576); ν_{max} (KBr)/cm^{-1}, 1600, 1670, 1675 and 1710 (4 x C=O); δ_H (400 MHz; $CDCl_3$) 2.31 and 2.44 (6H, 2 x s, 12-and 16-CH_3), 3.50 (2H, 2xd, *J*=14.7 Hz, 13-CH_2), 5.17 (2H, dd, *J*=17 and 1.7 and Hz, 2-CH_2), 5.81 (1H, s, 9a-H), 7.16 (1H, s, 4-H), 7.28 (1H, s, 17-H), 7.38 (1H, d, *J*=8.9 Hz, 8'-H), 7.61 (1H, d, *J*=8.9 Hz, 8-H), 7.62 (1H, d, *J*=8.9 and 2.0 Hz, 7'-H), 7.79 (1H, s, 2'-H), 8.00 (1H, dd, *J*=8.0 and 2.0 Hz, 7-H), 8.35 (1H, d, *J*=2.0 Hz, 5-H), and 8.32 (1H, d, *J*=1.3 Hz, 5'-H); δ_C (100 MHz; $CDCl_3$) 25.5 (C-12), 26.1 (C-16), 31.6 (C-13), 50.8 (C-4a), 66.8 (C-2), 100.4 (C-9a), 118.8 (C-10a), 119.3 (C-4a'), 120.3 (C-5), 121.3 (C-7'), 123.2 (C-6), 128.9 (C-5'),

130.1 (C-8'), 131.1 (C-7), 133.7 (C-17), 133.8 (C-6'), 136.7 (C-3), 138.5 (C-8), 139.2 (C-14), 143.7 (C-4), 149.2 (C-8a'), 154.6 (C-2'), 156.2 (C-3'), 157.9 (C-8a), 174.6 (C-4'), 190.6 (C-10), 196.6 (C-11) and 197.8 (C-15); m/z 626 ($\mathbf{M}^+$, 16%) and 136 (100).

Note:

i) When DABCO (0.26 g, 2.0 mmol) was used as the catalyst and 1-NMP (3 mL) as solvent, work-up afforded *9-[11-acetyl-(15-oxo-butyl)-10-dihydro-3*H*-pyrano(9,2a)]-5-bromo-chromen-3-one* **233** as a light brown viscous oil (0.51 g, 33%).

9-[11-acetyl-(15-oxo-butyl)-10-dihydro-3H-pyrano(9,2a)]-5-fluoro-chromen-3-one **234** *and the corresponding dimer* **244**

The experimental procedure employed for the synthesis of 9-[11-Acetyl-(15-oxo-butyl)-10-dihydro-3H-pyrano(9,2a)]chromen-3-one **231** and the corresponding dimer **241** was followed, using 6-fluorochromone-3-carbaldehyde **178** (1.0 g, 4.0 mmol), methyl vinyl ketone (0.48 mL, 5.9 mmol), 3-hydroxyquinuclidine (2.5 g, 20 mmol) and $CHCl_3$ (7.0 mL). Work-up and flash chromatography afforded two fractions.

i) *9-[11acetyl-(15-oxo-butyl)-10-dihydro-3H-pyrano(9.2a)]-5-fluoro-chromen-3-one* **234** as a light brown oil (0.79 g, 60%), (Found: $\mathbf{M}+H^+$, 332.1051. Calc. for $C_{18}H_{17}FO_5$, *M*:332.1060), ν_{max} (KBr)/cm^{-1}, 1674, 1687 and 1699 (3 x C=O); δ_H (400 MHz; $CDCl_3$) 1.97-2.23 (2H, 2xm, C*H*$_2$CH$_2$CO), 2.08 (3H, s, CH$_2$CH$_2$COC*H*$_3$), 2.35-2.45 (2H, 2xm, CH$_2$C*H*$_2$CO), 2.39 (3H, s, COC*H*$_3$), 4.57 (1H, dd, *J*= 17.2 and 1.9 Hz, 10-H$_a$), 4.79 (1H, dd, *J*=17.2 and 1.7 Hz, 10-H$_b$), 5.11 (1H, s, 8a-H), 7.12 (1H, dd, *J*=9.1 and 4.2 Hz, 7-H), 7.27 (1H, br s, 2-H), 7.30 (1H, m, 6-H) and 7.54 (1H, dd, *J*=8.0 and 3.1 Hz, 4-H); δ_C (100MHz; $CDCl_3$) 24.7 (*C*H$_2$CH$_2$CO), 25.5 (CH$_2$CH$_2$CO*C*H$_3$), 30.0 (CO*C*H$_3$), 37.6 (CH$_2$*C*H$_2$CO), 49.0 (C-9), 65.9 (C-10), 100.1 (C-8a), 113.0 (J_{CF}=24.0 Hz, C-7), 119.93 (J_{CF}=7.6 Hz, C-4), 124.4 (J_{CF}=24.6 Hz, C-6), 126.2 (C-2a), 134.9 (C-2), 138.4 (C-3a), 147.7 (C-5), 153.8 (C-7a), 191.9 (3-C=O), 196.5 (15-C=O) and 206.5 (11-C=O); *m/z* 392 ($\mathbf{M}^+$, 2%) and 154 (100).

ii) The *chromone dimer* **243** as a yellow solid oil (0.45 g, 23%), (Found $\mathbf{M}^+$: 507.1251. Calc. for $C_{28}H_{21}FO_7$, *M*: 507.1255); ν_{max} (KBr)/cm^{-1}, 1674, 1683, 1699 and 1717 (4 x C=O); δ_H (400 MHz; $CDCl_3$) 2.32 and 2.45 (6H, 2 x s, 12-and 16-CH_3), 3.52 (2H, 2xd, *J*=14.7 Hz, 13-CH_2), 5.18 (2H, dd, *J*=17 and 1.7 and Hz, 2-CH_2), 5.85 (1H, s, 9a-H), 7.17 (1H, s, 4-H), 7.26 (1H, d, *J*=8.9 and 2.0 Hz, 7'-H), 7.30 (1H, s, 17-H), 7.48 (1H, d, *J*=8.9 Hz, 8'-H), 7.72 (1H, d, *J*=8.9 Hz, 8-H), 7.64 (1H, dd, *J*=8.0 and 2.0 Hz, 7-H), 7.93 (1H, s, 2'-H), 7.94 (1H, d, *J*=2.0 Hz, 5-H), and 7.96 (1H, d, *J*=1.3 Hz, 5'-H); δ_C (100 MHz; $CDCl_3$) 25.6 (C-12), 25.9 (C-16), 31.6 (C-13), 52.5 (C-4a), 66.9 (C-2), 100.3 (C-9a), 119.6 (C-5), 119.9 (C-5'), 120.3 (C-7'), 121.0 (C-4a'), 121.9 (C-10a), 129.2 (C-8'), 130.5 (C-7), 133.8 (C-17), 136.7 (C-3), 138.4 (C-8), 139.1 (C-14), 143.7 (C-4), 144.7 (C-8a'), 154.6 (C-2'), 156.6 (C-3'), 157.2 (C-8a), 163.5 (C-6), 164.3 (C-6'), and 174.7, 190.5, 196.6, 197.8 (4 x C=O); *m/z* 507 ($\mathbf{M}^+$, 30%) and (100).

Note:

i) When DABCO (0.26 g, 2.0mmol) was used as catalyst and 1-NMP (3mL) as solvent, work-up afforded *9-[11-acetyl-(15-oxo-butyl)-10-dihydro-3*H*-pyrano(9,2a)]-5-bromo-chromen-3-one* **234** as a light brown viscous oil (0.40 g, 30%).

9-[11-acetyl-(15-oxo-butyl)-10-dihydro-3H-pyrano(9,2a)]-5-methoxy-chromen-3-one **235** *and the corresponding dimer* **245**

The experimental procedure employed for the synthesis of 9-[11-Acetyl-(15-oxo-butyl)-10-dihydro-3H-pyrano(9,2a)]chromen-3-one **231** and the corresponding dimer **241** was followed, using 6-bromochromone-3-carbaldehyde **187** (1.0 g, 4.9 mmol), methyl vinyl ketone (0.60 mL, 7.4 mmol), 3-hydroxyquinuclidine (3.1 g, 25 mmol) and $CHCl_3$ (7.0 mL).Work-up and flash chromatography afforded.

i) *9-[11acetyl-(15-oxo-butyl)-10-dihydro-3H-pyrano(9.2a)]-5-methoxy-chromen-3-one* **235** as a reddish oil (1.23 g, 73%), (Found: $\mathbf{M}^+$, 344.1252. Calc. for $C_{19}H_{20}O_6$, *M*: 344.1259), ν_{max} (KBr)/cm^{-1}, 1652, 1665 and 1674 (3 x C=O); δ_H (400 MHz; $CDCl_3$)

2.09-2.23 (2H, 2xm, CH_2CH_2CO), 2.15 (3H, s, $CH_2CH_2COCH_3$), 2.39-2.51 (2H, 2xm, CH_2CH_2CO), 2.44 (3H, s, $COCH_3$), 3.91 (3H, s, 6-OCH_3), 4.55 (1H, dd, 10-H_a and H_b), 4.94 (1H, s, 8a-H), 6.69 (1H, br s, 2-H), 7.08 (1H, d, *J*=9.11 Hz, 7-H), 7.33 (1H, dd, *J*=2.32 and 9.11 Hz, 6-H) and 7.85 (1H, d, *J*=2.32 Hz, 4-H); δ_C (100MHz; $CDCl_3$) 24.7 (C-13), 25.5 (C-16), 30.0 (C-12), 37.6 (C-14), 50.1 (C-9), 55.9 (OCH_3), 65.9 (C-10), 99.8 (C-8a), 118.5 (C-2a), 119.4 (C-7), 124.1 (C-4), 133.9 (C-6), 137.3 (C-2), 139.0 (C-3a), 143.5 (C-5), 154.8 (C-7a), 191.4 (3-C=O), 197.1 (15-C=O) and 199.2 (11-C=O); *m/z* 344 ($\mathbf{M}^+$, 33%) and 193 (100).

ii) The *chromone dimer* **245** as a yellow solid oil (0.52 g, 20%), m.p. °C, (Found $\mathbf{M}^+$: 530.1578. Calc. for $C_{30}H_{26}O_9$, *M*:530.1576); ν_{max} (KBr)/cm^{-1}, 1653, 1674, 1677 and 1700 (4 x C=O); δ_H (400 MHz; $CDCl_3$) 2.28 and 2.33 (6H, 2x s, 12-and 16-CH_3), 3.14 (2H, 2xd, *J*=14.7 Hz, 13-CH_2), 3.68 and 3.80 (6H, 2xs, 6-and 6'-OCH_3), 5.09 (2H, dd, *J*=17 and 1.7 and Hz, 2-CH_2), 5.25 (1H, s, 9a-H), 6.95 (1H, s, 4-H), 6.98 (1H, d, *J*=8.9 Hz, 8-H), 7.27 (1H, s, 17-H), 7.44 (1H, d, *J*=8.9 and 2.0 Hz, 7'-H), 7.64 (1H, d, *J*=8.9 Hz, 8'-H), 7.73 (1H, dd, *J*=8.0 and 2.0 Hz, 7-H), and 8.16 (1H, d, *J*=1.3 Hz, 5'-H), 8.33 (1H, d, *J*=2.0 Hz, 5-H), and 8.70 (1H, s, 2'-H); δ_C (100 MHz; $CDCl_3$) 25.3 (C-12), 25.9 (C-16), 31.4 (C-13), 50.3 (C-4a), 55.7(6-O*C*H3), 55.8(6'-O*C*H3), 66.4(C-2), 100.5 (C-9a), 114.5 (C-5), 116.1 (C-7), 116.3 (C-7'), 120.7 (C-5'), 121.3 (C-4a'), 123.9 (C-10a), 128.7 (C-8'), 133.6 (C-17), 136.3 (C-8), 136.6 (C-3), 139.4 (C-14), 143.8 (C-4), 143.9 (C-8a'), 154.4 (C-2'), 158.5 (C-8a), 159.4 (C-6), 161.4 (C-6'), 156.2 (C-3'), and 174.9, 190.9, 196.8, 199.3 (C=O); m/z 530 ($\mathbf{M}^+$, 15%) and 43 (100).

Note:

i) When DABCO (0.32 g, 2.5 mmol) was used as the catalyst and 1-NMP (3 mL) as solvent, work-up afforded *9-[11-acetyl-(15-oxo-butyl)-10-dihydro-3*H*-pyrano(9,2a)]-5-methoxy-chromen-3-one* **235** as a light brown viscous oil (0.6 g, 37%).

3.4 Baylis-Hillman reactions of chromone-2-carbaldehydes

3.4.1 Reactions of chromone-2-carbaldehydes with methyl vinyl ketone

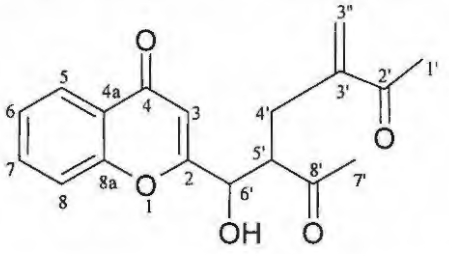

*5-Acetyl-6-(4*H*-1-benzopyran-4-on-2-yl)-6-hydroxy-3-(methylene)hexane-2-one* **247** and the MVK dimer **246**

Methyl vinyl ketone (0.36 mL, 4.3 mmol) was added to a stirred solution of chromone-2-carbaldehyde **91** (0.50 g, 2.9 mmol) and 3-hydroxyquinuclidine (1.8 g, 14 mmol) in $CHCl_3$ (7.0 mL). The resulting mixture was stirred vigorously at room temperature for 24h. Evaporation of solvent *in vacuo* gave a brown oily residue which was purified by flash chromatography [on silica; elution with hexane-EtOAc (1:2)] to afford MVK dimer **246** as yellow oil (0.24 g, 40%) and as brown oil *5-acetyl-6-(4*H*-1-benzopyran-4-on-2-yl)-6-hydroxy-3-(methylene)hexane-2-one* **247** in a mixture of the 2:3 *anti*-and *syn*-diastereomers as (0.63 g, 70%).

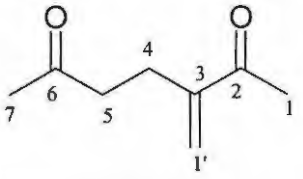

3-(Methylene)heptane-2,6-dione **246**

ν_{max}(KBr)/cm^{-1},1736 and 1694 (2 x C=O); δ_H (400 MHz; $CDCl_3$) 2.09 (3H, s, 7-CH_3), 2.30 (3H, s, 1-CH_3), 2.49 (2H, m, 4-H), 2.57 (2H, m, 5-H), 5.81 and 6.00 (2H, 2xs, 1'-CH_2); δ_C (100MHz; $CDCl_3$) 25.2 (C-4), 25.8 (C-7), 29.8 (C-1), 42.4 (C-5), 126.2 (C-1'), 147.6 (C-3), and 199.4 , 207.8 (2 x C=O).

*5-Acetyl-6-(4*H*-1-benzopyran-4-on-2-yl)-6-hydroxy-3-(methylene)hexane-2-one* (*syn*-**247a**):

(Calc. for $C_{18}H_{18}O_5$, *M*: 314.1154); ν_{max} (KBr)/cm^{-1}, (br, OH), and (3 x C=O); δ_H (400 MHz; $CDCl_3$) 2.18 (3H, s, 1-CH_3), 2.37 (3H, s, 5'-COC*H*$_3$), 2.46-2.60 (2H, m, 4'-H), 3.38 (1H, m, 5'-H), 3.37 (1H, br s, 6'-OH), 4.56 (1H, d, 6'-H), 5.79 and 5.99 (2H, 2xs, 3''-C*H*$_2$=C), 6.48 (1H, s, 3-H), 7.34-7.42 (2H, m, 6-H and 8-H), 7.64 (1H, t, *J*=7.8 Hz, 7-H) and 8.15 (1H, m, 5-H); δ_C (100MHz; $CDCl_3$) 25.6 (1'-COC*H*$_3$), 27.8 (C-4'), 30.1 (5'- COC*H*$_3$), 52.2 (C-5'), 69.3 (C-6'), 109.4 (C-3), 117.7 (C-8), 123.9(C-4a), 125.3 (C-5), 125.9 (C-6), 129.2 (C-3''), 133.8 (C-7), 144.8 (C-3'), 155.7 (C-2), 167.2(C-8a), 177.9, 199.5 and 211.4 (3xC=O); m/z 314 ($\mathbf{M}^+$, 25%) and 149(100).

*5-Acetyl-6-(4*H*-1-benzopyran-4-on-2-yl)-6-hydroxy-3-(methylene)hexane-2-one* (*anti*-**247b**):

ν_{max} (KBr)/cm^{-1}, (br, OH), and (3 x C=O); δ_H (400 MHz; $CDCl_3$) 2.08 (3H, s, 1'-COC*H*$_3$), 2.31 (3H, s, 5'-COC*H*$_3$), 2.61-2.78 (2H, m, 4'-H), 3.44 (1H, m, 5'-H), 4.05 (1H, br s, 6'-OH), 4.92 (1H, m, 6'-H), 5.82 and 6.14(1H, 2xs, 3''-H), 6.57 (1H, s, 3-H), 7.34-7.42 (2H, m, 6-H and 8-H), 7.64 (1H, t, *J*=7.8 Hz, 7-H) and 8.17 (1H, m, 5-H); δ_C (100 MHz; $CDCl_3$) 25.8 (1'-COC*H*$_3$), 30.3 (C-4'), 31.3 (5'-COC*H*$_3$), 52.3 (C-5'), 71.2(C-6'), 109.5 (C-3), 117.8 (C-8), 125.4(C-4a), 125.4 (C-5), 125.9 (C-6), 129.5 (C-3''), 133.9 (C-7), 145.1 (C-3'), 155.9 (C-2), 168.0 (C-8a), 180.0, 199.6 and 212.1 (3xC=O); *m/z* and (100).

Note:

i) When reaction was repeated using CH_2Cl_2 as solvent, workup afforded *5-acetyl-6-(4*H*-1-benzopyran-4-on-2-yl)-6-hydroxy-3-(methylene)hexane-2-one* **247** in a mixture of the 2:3 *syn*-and *anti*-diastereomers (0.56 g, 65%) and the MVK dimer **246** (0.21 g, 35%).

ii) When DABCO (1.6 g, 14 mmol) was used as the catalyst and $CHCl_3$ (7 mL) as the solvent, work-up afforded *5-acetyl-6-(4H-1-benzopyran-4-on-2-yl)-6-hydroxy-3-*

(methylene)hexane-2-one **247** in a mixture of the 2:3 syn and anti diastereomers as yellow thick oil (0.47 g, 55%) and the MVK dimer **246** (0.22 g, 37%).

iii) However, when DABCO (1.6 g, 14 mmol) was used as the catalyst and CH_2Cl_2 (7 mL) was used as solvent the work-up afforded *5-acetyl-6-(4*H*-1-benzopyran-4-on-2-yl)-6-hydroxy-3-(methylene)hexane-2-one* **247** as a mixture of the 2:3 *syn*-and *anti*-diastereomers (0.39 g, 45%) and the MVK dimer **246** (0.14 g, 23%).

*5-Acetyl-6-(6-bromo-4*H*-1-benzopyran-4-on-2-yl)-6-hydroxy-3-(methylene)hexane-2-one* **248** and the MVK dimer **246**

The experimental procedure employed for the synthesis of *5-acetyl-6-(4*H*-1-benzopyran-4-on-2-yl)-6-hydroxy-3-(methylene)hexane-2-one* **247** and the MVK dimer **246** was followed, using 6-bromochromone-2-carbaldehyde **202** (1.0 g, 4.0 mmol), methyl vinyl ketone (0.48 mL, 5.92 mmol), 3-hydroxyquinuclidine (2.5 g, 20 mmol) and $CHCl_3$ (7.0 mL).Work-up and flash chromatography afforded MVK dimer **246** as a pale yellow oil (0.31 g, 37%) and *5-acetyl-6-(6-bromo-4H-1-benzopyran-4-on-2-yl)-6-hydroxy-3-(methylene)hexane-2-one* **248** in a mixture of the 2 :3 *syn*-and *anti*-diastereomers as brown oil (0.98 g, 63%).

5-acetyl-6-(6-bromo-4H-1-benzopyran-4-on-2-yl)-6-hydroxy-3-(methylene)hexane-2-one (syn **248a**):

(Calc. for $C_{18}H_{17}BrO_5$ requires, *M*: 329.0259); ν_{max} (KBr)/cm^{-1}, (br, OH), and (3 x C=O); δ_H (400 MHz; $CDCl_3$) 2.27 (3H, s, 1'-COC*H*$_3$), 2.31 (3H, s, 9'-COC*H*$_3$), 2.53-2.77 (2H, m, 4'-H), 3.40 (1H, m, 5'-H), 3.89 (1H, br s, 6'-OH), 4.54 (1H, br d, *J*=3.6 Hz, 6'-H), 5.79 and 6.02 (2H, 2xs, 3''-C*H*$_2$=C), 6.50 (1H, s, 3-H), 7.29 (1H, d, *J*=7.5 Hz, 8-H), 7.73 (1H, dd, *J*=8.9 and 2.2 Hz, 7-H) and 8.29 (1H, d, *J*=2.48 Hz, 5-H); δ_C (100MHz; $CDCl_3$) 25.7 (1'-COCH$_3$), 27.9 (C-4'), 30.4 (5'-COCH$_3$), 52.0 (C-5'), 69.2 (C-6'), 109.4

(C-3), 119.6 (C-8), 128.6 (C-5), 129.4 (C-4a), 130.0 (C-3')141.7 (C-3''), 143.9 (C-7), 150.1 (C-6), 153.6 (C-8a), 155.7 (C-2), 169.5 ,179.8 and 194.0 (3xC=O);

5-acetyl-6-(6-bromo-4H-1-benzopyran-4-on-2-yl)-6-hydroxy-3-(methylene)hexane-2-one (anti **248b**):

ν_{max} (KBr)/cm^{-1}, (br, OH), and (3 x C=O); δ_H (400 MHz; $CDCl_3$) 2.05 (3H, s, 1'-COC*H*$_3$), 2.31 (3H, s, 9'-COC*H*$_3$), 2.53-2.77 (2H, m, 4'-H), 3.46 (1H, m, 5'-H), 4.15 (1H, br s, 6'-OH), 4.90 (1H, br d, *J*=2.51 Hz, 6'-H), 5.86 and 6.17 (2H, 2xs, 3''-C*H*$_2$=C), 6.59 (1H, s, 3-H), 7.31(1H, d, *J*=7.47 Hz, 8-H), 7.74 (1H, dd, *J*=2.20 and 8.94 Hz, 7-H) and 8.30 (1H, d, *J*=2.46 Hz, 5-H); δ_C (100MHz; $CDCl_3$) 25.8 (1'-COC*H*$_3$), 30.2 (C-4'), 31.3 (5'-COC*H*$_3$), 52.1 (C-5'), 71.0 (C-6'), 109.5 (C -3), 119.8 (C-8), 128.6 (C-5), 129.7 (C-4a), 130.8 (C-3'), 146.4 (C-7), 147.9 (C-3''), 150.1 (C-6), 153.7 (C-8a), 155.9 (C-2), 170.4, 179.8 and 203.1 (3xC=O);

Note:

i) This reaction was repeated using CH_2Cl_2 as solvent, work-up afforded *5-acetyl-6-(6-bromo-4H-1-benzopyran-4-on-2-yl)-6-hydroxy-3-(methylene)hexane-2-one* **248**, in a mixture of the 2:3 syn-and anti-diastereomers as a brown oil (0.78 g, 50%) and the MVK dimer **246** as (0.23 g, 28%).

ii) When DABCO (2.2 g, 20 mmol) was used as the catalyst and $CHCl_3$ (7 mL) as solvent, work-up afforded *5-acetyl-6-(6-bromo-4H-1-benzopyran-4-on-2-yl)-6-hydroxy-3-(methylene)hexane-2-one* **248**, in a mixture of the 2:3 syn and anti diastereomers as brown oil (0.73 g, 47%) and the MVK dimer **246** (0.16 g,19%).

iii) When DABCO (2.2 g, 20 mmol) was used as the catalyst and CH_2Cl_2 (7 mL) as solvent, work-up afforded *5-acetyl-6-(6-bromo-4H-1-benzopyran-4-on-2-yl)-6-hydroxy-*

3-(methylene)hexane-2-one **248**, in a mixture of the 2:3 syn and anti diastereomers as brown oil (0.55 g, 35%) and the MVK dimer **246** (0.14 g, 17%).

*5-Acetyl-6-(6-methoxy-4*H*-1-benzopyran-4-on-2-yl)-6-hydroxy-3-(methylene)hexane-2-one* **249** and the MVK dimer **246**

The experimental procedure employed for the synthesis of *5-acetyl-6-(4H-1-benzopyran-4-on-2-yl)-6-hydroxy-3-(methylene)hexane-2-one* **247** and the MVK dimer **246** was followed, using 6-methoxychromone-2-carbaldehyde **204** (1.0 g, 4.9 mmol), methyl vinyl ketone (0.60 mL, 7.35mmol), 3-hydroxyquinuclidine (3.1 g, 25 mmol) and $CHCl_3$ (7.0 mL). Work-up and flash chromatography afforded MVK dimer **246** as pale yellow oil (0.24 g, 23%) and the *5-acetyl-6-(6-methoxy-4*H*-1-benzopyran-4-on-2-yl)-6-hydroxy-3-(methylene)hexane-2-one* **249** in a mixture of the 2:3 *syn*-and *anti*-diastereomers as brown oil (0.92 g, 55%).

*5-Acetyl-6-(6-methoxy-4*H*-1-benzopyran-4-on-2-yl)-6-hydroxy-3-(methylene)hexane-2-one* (*syn* **249a**):

(Found: $\mathbf{M}^+$ 344.1247. Calc. for $C_{19}H_{20}O_6$, *M*: 344.1259); ν_{max} (KBr)/cm^{-1}, (br, OH), and (3 x C=O); δ_H (400 MHz; $CDCl_3$) 2.20 (3H, s, 1'-COC*H*$_3$), 2.31 (3H, s, 9'-COC*H*$_3$), 2.60-2.75 (2H, m, 4'-H), 3.46 (1H, m, 5'-H), 3.78 (3H, s, 6-OC*H*$_3$), 4.83 (1H, br s, 6'-OH), 4.94 (1H, br s, 6'-H), 5.76 and 6.04 (2H,2 x s, 3''-C*H*$_2$=C), 6.50 (1H, s, 3-H), 7.13 (2H, d, *J*= 8.9 Hz, 8-H), 7.32 (1H, dd, *J*=8.9 and 3.1 Hz, 7-H) and 7.54 (1H, d, *J*= 3.1 Hz, 5-H); δ_C (100MHz; $CDCl_3$) 25.3 (1'-COCH_3), 26.2 (C-4'), 28.0 (5'-COCH_3), 46.1 (C-5'), 62.2 (6-OCH_3), 69.2 (C-6'), 104.6 (C-3), 113.7 (C-8), 120.2 (C-5), 123.3 (C-4a), 124.8 (C-6), 129.7 (C-3'), 134.0 (C-3''), 147.7 (C-7), 149.7 (C-2), 152.0 (C-8a), 178.3, 180.8 and 193.3 (3xC=O); *m/z* 344 ($\mathbf{M}^+$, 25%) and 248 (100).

*5-Acetyl-6-(6-methoxy-4*H*-1-benzopyran-4-on-2-yl)-6-hydroxy-3-(methylene)hexane-2-one* (*anti* **249b**):

ν_{max} (KBr)/cm^{-1} (br, OH), and (3 x C=O); δ_H (400 MHz; $CDCl_3$) 2.02 (3H, s, 1'-COC*H*$_3$), 2.31 (3H, s, 9'-COC*H*$_3$), 2.53-2.77 (2H, s, 4'-H), 3.51 (1H, m, 5'-H), 3.89 (3H, s, 6-OC*H*$_3$), 4.90 (1H, br s, 6'-OH), 4.99 (1H, br s, 6'-H), 5.86 and 6.21 (2H, 2xs, 3'' C*H*$_2$=C), 6.59 (1H, s, 3-H), 7.13 (2H, d, *J*=8.9 Hz, 8-H), 7.32 (1H, dd, *J*=8.9 and 3.1 Hz, 7-H) and 7.54 (1H, d, *J*=3.1 Hz, 5-H); δ_C (100MHz; $CDCl_3$) 25.8 (1'-COCH$_3$), 29.9 (5'-COCH$_3$), 40.8 (C-4'), 56.0 (C-5'), 62.5 (6-OCH$_3$)71.0 (C-6'), 104.6 (C-3), 113.8 (C-8), 120.2 (C-5), 123.3 (C-4a), 125.0 (C-6), 129.7 (C-3'), 141.8 (C-3'), 147.7 (C-7), 150.8 (C-2), 157.50 (C-8a), 178.3, 181.8 and 201.0 (3xC=O);.

Note:

i) when this reaction was repeated using CH_2Cl_2 as solvent, workup afforded 5-acetyl-6-(4*H*-1-benzopyran-4-on-2-yl)-6-hydroxy-6-methoxy-3-(methylene)hexane-2-one **249**, in a mixture of the 2:3 *syn*-and *anti*-diastereomers as a brown oil (0.95 g, 57%) and the MVK dimer **246** as (0.29 g, 28%).

ii) When DABCO (2.8 g, 25 mmol) was used as the catalyst and $CHCl_3$ (7 mL) as the solvent, work-up afforded *5-acetyl-6-(6-methoxy-4*H*-1-benzopyran-4-on-2-yl)-6-hydroxy-3-(methylene)hexane-2-one* **249** in a mixture of the 2 :3 *syn*-and *anti*-diastereomers as brown oil (0.67 g, 40%) and MVK dimer **246** (0.16 g, 15%).

iii) When DABCO (2.8 g, 25 mmol) was used as the catalyst and CH_2Cl_2 (7 mL) as solvent, work-up afforded *5-acetyl-6-(6-methoxy-4*H*-1-benzopyran-4-on-2-yl)-6-hydroxy-3-(methylene)hexane-2-one* **249** (0.50 g, 30%) in a 2:3 mixture of *syn*-and *anti*-diastereomers as brown oil and the MVK dimer **246** (0.16 g, 15%).

3.4.2 Reactions of chromone-2-carbaldehydes with methyl acrylate

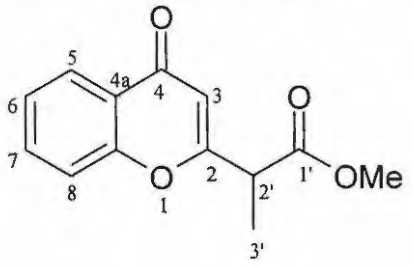

*Methyl-2-(6-methoxy-4*H*-1-benzopyran-4-one-2-yl)-2-methylpropanoate* **250**

Methyl acrylate (0.19 mL, 2.2 mmol) was added to a stirred solution of 6-methoxychromone-2-carbaldehyde **204** (0.3 g, 1.5 mmol), and 3-hydroxyquinuclidine (0.88 g, 7.3 mmol) in $CHCl_3$ (4.0 mL). The resulting mixture was stirred vigorously at room temperature for 24h. Evaporation of solvent *in vacuo* gave a brown oily residue which was purified by flash chromatography [on silica; elution with hexane-EtOAc (1:2)] to afford *Methyl-2-(6-methoxy-4*H*-1-benzopyran-4-one-2-yl)-2-methylpropanoate* **250** as white solid (0.17 g, 45 %). ν_{max} (KBr)/cm^{-1}, 1684 and 1653 (2 x C=O); δ_H (400 MHz; $CDCl_3$) 1.56 (3H, d, *J*=7.1 Hz, 3'-CH_3), 3.75 (3H, s, 6-OCH_3), 3.93 (3H, s, 1'-OCH_3), 4.31 (1H, q, *J*=7.1 Hz, 2'-H), 7.04 (1H, s, 3-H), 7.37 (1H, dd, *J*=9.2 and 3.1 Hz, 7-H), 7.47 (1H, d, *J*=9.2 Hz, 8-H) and 7.58 (1H, d, *J*=3.1 Hz, 5-H); δ_C (100MHz; $CDCl_3$) 12.6 (C-3'), 48.0 (C-2'), 56.0 (6-OCH_3), 64.0 (CO.OCH_3), 104.9 (C-3), 111.1 (C-8), 119.8 (C-5), 125.2 (C-4a), 125.4 (C-7), 150.1 (C-2), 155.6 (C-6), 157.8 (C-8a), 178.3 (4-C=O), 190.4 (1'-C=O), *m/z* 259 ($\mathbf{M}^+$,10 %) and 69 (100).

Note:

(i) When this reaction was repeated using CH_2Cl_2 as solvent, work-up afforded *methyl-2-(6-methoxy-4*H*-1-benzopyran-4-one-2-yl)-2-methylpropanoate* **250** as a brown oil (0.06 g, 12%).

3.4.3 Reactions of chromone-2-carbaldehydes with acrylonitrile

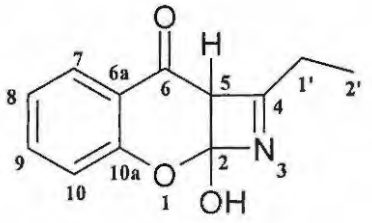

255

4-Ethyl-2-hydroxy-5,2-dihydro-4-oxa-3-aza-cyclobuta[b]naphthalene-6-one **255**

Acrylonitrile (0.37 mL, 4.3 mmol) was added to a stirred solution of chromone-2-carbaldehyde **91** (0.5 g, 2.9 mmol), and 3-hydroxyquinuclidine (1.7 g, 14 mmol) in $CHCl_3$ (7.0 mL). The resulting mixture was stirred vigorously at room temperature for 24h. Evaporation of solvent *in vacuo* gave a brown oily residue which was purified by flash chromatography [on silica; elution with hexane-EtOAc (1:2)] to afford *4-ethyl-2-hydroxy-5,2-dihydro-4-oxa-3-aza-cyclobuta[b]naphthalene-6-one* **255** as a white oil (0.38 g, 47 %). (Found: $\mathbf{M}^+$ 218.1632. Calc. for $C_{12}H_{11}O_2N$, *M*: 218.1630); ν_{max} (KBr)/cm^{-1}, 1465 (C=N); 1658 (C=O); 3397 (OH); δ_H (400 MHz; $CDCl_3$) 1.42 (3H, t, *J*=7.1 Hz, 2'-CH_3), 4.45 (2H, q, *J*= 7.1, 1'-H), 7.10 (1H, s, 5-H), 7.36 (1H, br peak, 2-OH), 7.43 (1H, t, *J*=7.5 Hz, 8-H), 7.60 (1H, d, *J*=8.6 Hz, 10-H), 7.73 (1H, t, *J*=6.7 Hz, 9-H), 8.80 (1H, d, *J*=7.9 Hz, 7-H); δ_C (100MHz; $CDCl_3$) 14.1 (C-2'), 63.0 (C-1'), 114.8 (C-5), 118.8 (C-10), 124.4 (C-6a), 125.7 (C-8), 125.9 (C-7), 134.7 (C-9), 152.2 (C-10a), 156.0 (C-2), 160.5 (C-4), 178.4 (C=O), *m/z* 218 ($\mathbf{M}^+$,42 %) and 89(100).

Note:

(i) When this reaction was repeated using CH_2Cl_2 (7 mL) as solvent, work-up afforded *4-ethyl-2-hydroxy-5,2-dihydro-4-oxa-3-aza-cyclobuta[b]naphthalene-6-one* **255** as white oil (0.18 g, 22 %).

8-Bromo-4-ethyl-2-hydroxy-5,2-dihydro-4-oxa-3-aza-cyclobuta[b]naphthalene-6-one **256**

The experimental procedure employed for the synthesis of *4-ethyl-2-hydroxy-5,2-dihydro-4-oxa-3-aza-cyclobuta[b]naphthalene-6-one* **255** was followed, using 6-bromochromone-2-carbaldehyde **202** (0.5 g, 1.98 mmol), acrylonitrile (0.25 mL, 2.97 mmol), 3-hydroxyquinuclidine (1.26 g, 9.90 mmol) and $CHCl_3$ (7.0 mL).Work-up and flash chromatography afforded *8-bromo-4-ethyl-2-hydroxy-5,2-hydro-4-oxa-3-aza-cyclobuta[b]naphthalene-6-one* **256** as brown oil (0.22 g, 40%). (Found: $\mathbf{M}^+ + H_2O$, 297.9679, $C_{12}H_{10}BrO_2N$ requires, *M*, 280.1173); ν_{max} (KBr)/cm^{-1}, 1558 (C=N); 1653 (C=O); 3430 (OH); δ_H (400 MHz; $CDCl_3$) 1.43 (3H, t, *J*=7.1 Hz, 2'-CH_3), 4.46 (2H, q, *J*=7.1, 1'-H), 7.11 (1H, s, 5-H), 7.49 (1H, br peak, 2-OH), 7.51 (1H, d, *J*=8.9 Hz, 10-H), 7.81 (1H, dd, *J*=8.9 and 2.5 Hz, 9-H), 8.32 (1H, d, *J*=2.4 Hz, 7-H); δ_C (100MHz; $CDCl_3$) 14.1 (C-2'), 63.2 (C-1'), 114.8 (C-5), 119.5 (C-6a), 120.7 (C-10), 128.4 (C-7), 129.4 (C-8), 137.7 (C-9), 152.4 (C-10a), 154.7 (C-2), 163.9 (C-4), 177.0 (C=O), *m/z* 29 ($\mathbf{M}^+$, 84%) and 298 (100).

Note:

(i) This reaction was repeated using CH_2Cl_2 (7.0 mL) as solvent and the workup afforded *8-bromo 4-ethyl-2-hydroxy-5,2-hydro-4-oxa-3-aza-cyclobuta[b]naphthalene-6-one* **256** as brown solid (0.08 g, 15%).

4-Ethyl-2-hydroxy-8-methoxy-5,2-dihydro-4-oxa-3-aza-cyclobuta[b]naphthalene-6-one **257**

The experimental procedure employed for the synthesis of *4-ethyl-2-hydroxy-5,2-dihydro-4-oxa-3-aza-cyclobuta[b]naphthalene-6-one* **255** was followed, using 6-methoxychromone-2-carbaldehyde **204** (0.5 g, 2.5 mmol), acrylonitrile (0.31 mL, 3.68mmol), 3-hydroxyquinuclidine (1.6 g, 12 mmol) and $CHCl_3$ (7.0 mL). Work-up and

flash chromatography afforded *4-ethyl-2-hydroxy-8-methoxy-5,2-dihydro-4-oxa-3-aza-cyclobuta[b]naphthalene-6-one* **257** as a brown oil (0.31 g, 55 %). (Calc. for $C_{13}H_{13}O_3N$, *M*: 231.2478); ν_{max} (KBr)/cm^{-1}, 1465 (C=N); 1653 (C=O); 3435 (OH); δ_H (400 MHz; $CDCl_3$) 1.42 (3H, t, *J*= 7.1 Hz, 2'-CH_3), 3.89 (3H, s, 8-OCH_3), 4.45 (2H, q, *J*=7.1, 1'-H), 7.09 (1H, s, 5-H), 7.27 (1H, d, *J*=3.2 Hz, 7-H), 7.32 (1H, dd, *J*=9.2 and 3.0 Hz, 9-H), 7.49 (1H, br peak, 2-OH), 8.02 (1H, d, *J*=8.02 Hz, 10-H); δ_C (100MHz; $CDCl_3$) 17.0 (C-2'), 56.0 (8-OCH_3), 64.4 (C-1'), 110.0 (C-5), 119.2 (C-6a), 120.7 (C-10) 128.9 (C-7), 130.5 (C-8), 132.4 (C-9), 158.6 (C-10a), 159.1 (C-2), 162.1 (C-4), 178.5 (C=O).

Note:

(i) When this reaction was repeated using CH_2Cl_2 (7.0 mL) as solvent and the workup afforded *4-ethyl-2hydroxy-8methoxy-5,2-dihydro-4-oxa-3-aza-cyclobita[b]naphthalene-6-one* **257** as brown oil (0.14 g, 25%).

3.5 aza-Michael reaction of Baylis-Hillman products with amine derivatives

3.5.1 Reactions of Baylis-Hillman products with S*-benzylcysteamine hydrochloride*

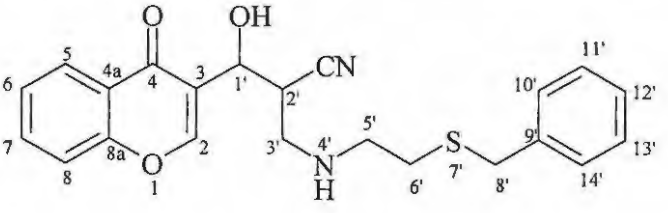

1-(4H-1-Benzopyran-4-on-3-yl)-2-cyano-8-phenyl-4-aza-7-thiaoctanol **258**

3-(2-cyano-3-hydroxy-1-propen-3-yl)-4*H*-1-benzopyran-4-one **212** (100 mg, 0.44 mmol) was added to a stirred solution of (*S*)-benzylcysteamine hydrochloride (179 mg, 0.88mmol) and sodium acetate (73 mg, 0.88 mmol) in EtOH (4 ml). The resulting mixture was stirred at room temperature for 6 weeks. Evaporation of the solvent *in*

vacuo gave a brown oily residue which was purified by flash chromatography [on silica; elution with hexane:EtOAc (3:2)] to afford *1-(4H-1-benzopyran-4-on-3-yl)-2-cyano-8-phenyl-4-aza-7-thiaoctanol* **258** as brown solid (89 mg, 51%), m.p. 90-92 °C, (Found: **MH**$^+$: 395.1425. Calc. for $C_{22}H_{22}O_3N_2S$ *M*: 394.1351); ν_{max} (KBr)/cm^{-1} 3300-3394 (OH and NH), 2360 (CN) and 1652 (C=O); δ_H (400 MHz; $CDCl_3$) 2.64 (2H, t, *J*=6.9 Hz, 6'-CH_2), 3.15 (1H, m, 2'-H), 3.21 (2H, m, 5'-CH_2), 3.24 (1H, dd, *J*=12.9 and 3.7 Hz, 3'-CH_2) 3.53 (1H, br s, NH), 3.57 (1H, dd, *J*=12.9 and 3.7 Hz, 3'-CH_2), 3.73 (2H, s, 8'-CH_2), 4.98 (1H, d, *J*=2.71 Hz, 1'-H), 6.86 (1H, t, *J*=7.53 Hz, 6-H), 7.01 (1H, d, *J*=8.29 Hz, 8-H), 7.19 (1H, s, 2-H), 7.21-7.27 (5H, m, Ar-H), 7.41 (1H, t, 7.8 Hz, 7-H), 7.50 (1H, d, *J*=7.8 Hz, 5-H), and 10.93 (1H, br s, OH); δ_C (100MHz; $CDCl_3$) 30.1 (C-6'), 30.2 (C-2'), 36.7 (C-8'), 43.2 (C-3'), 55.9 (C-5'), 61.1 (C-1'), 107.4 (CN), 117.6 (C-3), 120.1 (C-4a), 118.1 (C-8), 118.5 (C-6), 128.7 (C- 11' and C-13'), 128.8 (C-12'), 128.9 (C-10' and C-14'), 130.8 (C-5), 133.9 (C-7), 138.0 (C-9'), 151.1 (C-2), 160.6 (C-8a) and 195.3 (C=O) ; *m/z* 395 (**M**$^+$, 17%) and 154 (100%).

Note:

(i) When the reaction was run for 6 weeks using 3-(2-cyano-3-hydroxy-1-propen-3-yl)-4*H*-1-benzopyran-4-one **212** (100 mg, 0.44 mmol), (*S*)-benzylcysteamine (148 mg, 0.88 mmol) as free amine, and sodium acetate (73 mg, 0.88 mmol) in EtOH (4 ml), work-up and purification afforded *1-(4H-1-benzopyran-4-on-3-yl)-2-cyano-8-phenyl-4-aza-7-thiaoctanol* **258** as a brown solid (0.079 g, 45 %).

(ii) When the reaction was run for 6 weeks using 3-(2-cyano-3-hydroxy-1-propen-3-yl)-4*H*-1-benzopyran-4-one **201** (100 mg, 0.44 mmol), (*S*)-benzylcysteamine (179 mg, 0.88 mmol) as free amine, TBAB (284 mg, 0.88 mmol) as the catalyst and sodium acetate (73 mg, 0.88 mmol) in EtOH (4 ml), work-up and purification afforded *1-(4H-1-benzopyran-4-on-3-yl)-2-cyano-8-phenyl-4-aza-7-thiaoctanol* **258** as a brown solid (0.089 g, 51%).

(iii) When the reaction was run for 6 weeks using using 3-(2-cyano-3-hydroxy-1-propen-3-yl)-4*H*-1-benzopyran-4-one **212** (100 mg, 0.44 mmol), (*S*)-benzylcysteamine (179 mg, 0.88 mmol) as free amine, and $BmimBF_4$ (2.0 mL) as the catalyst in EtOH (4 ml), work-up and purification afforded *1-(4H-1-benzopyran-4-on-3-yl)-2-cyano-8-phenyl-4-aza-7-thiaoctanol* **258** as a brown solid (0.12 g, 68%).

*1-(6-chloro-4*H*-1-benzopyran-4-on-3-yl)-2-cyano-8-phenyl-4-aza-7-thiaoctanol* **259**

The experimental procedure employed for the synthesis of *1-(4H-1-benzopyran-4-on-3-yl)-2-cyano-8-phenyl-4-aza-7-thiaoctanol* **258** was followed, using 6-chloro-3-(2-cyano-3-hydroxy-1-propen-3-yl)-4*H*-1-benzopyran-4-one **213** (100 mg, 0.382 mmol), (*S*)-benzylcysteamine hydrochloride (128 mg, 0.76 mmol), and sodium acetate (63 mg, 0.76 mmol) in EtOH (4ml). The resulting mixture was stirred for 6 weeks and work-up afforded *1-(6-chloro-4*H*-1-benzopyran-4-on-3-yl)-2-cyano-8-phenyl-4-aza-7-thiaoctanol* **259** as yellow viscous oil (75 mg, 46 %), m.p. 117-119°C, (Found $\mathbf{MH^+}$: 429.1040. Calc for $C_{22}H_{21}O_3N_2SCl$, *M*: 428.0961); ν_{max} KBr)/cm-^{1} 3300-3394 (OH and NH), 2379 (CN) and 1684 (C=O); δ_H (400 MHz; $CDCl_3$) 2.65 (2H, m, 6'- CH_2), 2.83 (1H, m, 2'-H), 3.20 (2H, m, 5'- CH_2), 3.26 (1H, br s, NH), 3.58 (2H, dd, J=12.7 and 3.6 Hz, 3'-CH_2), 3.75 (2H, s, 8'-H), 4.99 (1H, d, J=10.5 Hz, 1'-H), 6.97 (1H, dd, J=8.8 and 3.5 Hz, 8-H), 7.14 (1H, s, 2-H), 7.20-7.23 (5H, m, Ar-H), 7.41 (1H, m, 7-H), 7.51 (1H, d, J=5.7 Hz, 5-H), and 10.86 (1H, br s,-OH); δ_C (100MHz; $CDCl_3$) 30.1 (C-6'), 30.2 (C-2'), 36.7 (C-8'), 43.2 (C-3'), 55.9 (C-5'), 61.6 (C-1'), 107.9 (CN), 117.6 (C-3), 120.5 (C-8), 122.0 (C-4a), 124.8 (C-6), 128.7 (C- 11' and C-13'), 128.8 (C-12'), 128.9 (C-10' and C-14'), 129.0 (C-5), 133.8 (C-7), 138.0 (C-9'), 151.2 (C-2), 158.7 (C-8'a) and 195.2 (C=O); *m/z* 429 ($\mathbf{M^+}$, 35%) and 154 (100%).

Note:

(i) When the reaction was run for 6 weeks using 6-chloro-3-(2-cyano-3-hydroxy-1-propen-3-yl)-4*H*-1-benzopyran-4-one **213** (100 mg, 0.382 mmol), (*S*)-benzylcysteamine

(64 mg, 0.38 mmol) as free amine, and sodium acetate (63 mg, 0.76 mmol) in EtOH (4 ml), work-up and purification afforded *1-(6-chloro-4*H*-1-benzopyran-4-on-3-yl)-2-cyano-8-phenyl-4-aza-7-thiaoctanol* **259** as brown solid (66 mg, 40 %).

(ii) When the reaction was run for 5 days using 6-chloro-3-(2-cyano-3-hydroxy-1-propen-3-yl)-4*H*-1-benzopyran-4-one **213** (100 mg, 0.382 mmol), (*S*)-benzylcysteamine hydrochloride (128 mg, 0.76 mmol) as free amine, TBAB (246 mg, 0.764 mmol) as the catalyst and sodium acetate (63.1 mg, 0.764 mmol) in EtOH (4 ml), work-up and purification afforded *1-(6-chloro-4*H*-1-benzopyran-4-on-3-yl)-2-cyano-8-phenyl-4-aza-7-thiaoctanol* **259** as brown solid (79 mg, 48%).

(iii) When the reaction was run for 5 days using 6-chloro-3-(2-cyano-3-hydroxy-1-propen-3-yl)-4*H*-1-benzopyran-4-one **213** (100 mg, 0.382 mmol), (*S*)-benzylcysteamine hydrochloride (127 mg, 0.764 mmol) as free amine, and $BmimBF_4$ (2.0 mL) as the catalyst in EtOH (4 ml), work-up and purification afforded *1-(6-chloro-4*H*-1-benzopyran-4-on-3-yl)-2-cyano-8-phenyl-4-aza-7-thiaoctanol* **259** as brown solid (105 mg, 64%).

*1-(6-bromo- 4*H*-1-benzopyran-4-on-3-yl)-2-cyano-8-phenyl-4-aza-7-thiaoctanol* **260**

The experimental procedure employed for the synthesis of *1-(4*H*-1-benzopyran-4-on-3-yl)-2-cyano-8-phenyl-4-aza-7-thiaoctanol* **258** was followed, using 6-bromo-3-(2-cyano-3-hydroxy-1-propen-3-yl)-4H-1-benzopyran-4-one **214** (100 mg, 0.40 mmol), (*S*)-benzylcysteamine hydrochloride (163 mg, 0.80 mmol), sodium acetate (66 mg, 0.80 mmol) in EtOH (4ml). Work-up afforded *1-(6-bromo- 4*H*-1-benzopyran-4-on-3-yl)-2-cyano-8-phenyl-4-aza-7-thiaoctanol* **260** as brown solid oil (80 mg, 42%); (Found **MH**$^+$: 473.0535. Calc. for $C_{22}H_{21}O_3N_2SBr$, *M*: 472.0456); ν_{max} (KBr)/cm^{-1} 3300-3394 (OH and NH), 2360 (CN) and 1685(C=O); δ_H (400 MHz; $CDCl_3$) 2.67 (2H, m, 6'- CH_2), 2.82 (1H, m, 2'-H), 3.20 (2H, m, 5'-CH_2), 3.47 (1H, br s, NH), 3.59 (2H, m, 3'-CH_2),

3.80 (2H, s, 8'- CH_2), 4.99 (1H, d, J=2.4 Hz, 1'-H), 6.92 (1H, d, J=8.8 Hz, 8-H), 7.14 (1H, s, 2-H), 7.20-7.32 (5H, m, Ar-H), 7.50 (1H, m, 7-H), 7.64 (1H, dd, J=12.3 and 2.5 Hz, 5-H), and 10.02 (1H, br s, OH); δ_C (100MHz; $CDCl_3$) 30.1 (C-6'), 30.2 (C-2'), 36.7 (C-8'), 43.2 (C-3'), 55.9 (C-5'), 62.8 (C-1'), 107.1 (CN), 117.5 (C-6), 117.8 (C-3), 119.0 (C-4a), 122.2 (C-8), 128.7 (C- 11' and C-13'), 128.8 (C-12'), 128.9 (C-10' and C-14'), 133.7 (C-5), 137.1 (C-7), 138.5 (C-9'), 151.4 (C-2), 158.6 (C-8a) and 195.3 (C=O); *m/z* 473 ($\mathbf{M}^+$, 5%) and 136 (100).

Note:

(i) When the reaction was run for 6 weeks using 6-bromo-3-(2-cyano-3-hydroxy-1-propen-3-yl)-4H-1-benzopyran-4-one **214** (100 mg, 0.40 mmol), (*S*)-benzylcysteamine (135 mg, 0.80 mmol) as free amine, and sodium acetate (66 mg, 0.80 mmol) in EtOH (4 ml), work-up and purification afforded *1-(6-bromo-4*H*-1-benzopyran-4-on-3-yl)-2-cyano-8-phenyl-4-aza-7-thiaoctanol* **260** as a brown solid (63 mg, 33%).

(ii) When the reaction was run for 5 days using 6-bromo-3-(2-cyano-3-hydroxy-1-propen-3-yl)-4*H*-1-benzopyran-4-one **214** (100 mg, 0.40 mmol), (*S*)-benzylcysteamine hydrochloride (163 mg, 0.80 mmol), TBAB (258 mg, 0.80 mmol) as the catalyst and sodium acetate (66 mg, 0.80 mmol) in EtOH (4 ml), work-up and purification afforded *1-(6-bromo-4*H*-1-benzopyran-4-on-3-yl)-2-cyano-8-phenyl-4-aza-7-thiaoctanol* **260** as a brown solid (82 mg, 43%).

(iii) When the reaction was run for 5 days using 6-bromo-3-(2-cyano-3-hydroxy-1-propen-3-yl)-4*H*-1-benzopyran-4-one **214** (100 mg, 0.40 mmol), (*S*)-benzylcysteamine hydrochloride (163 mg, 0.80 mmol), and $BmimBF_4$ (2.0 mL) as the catalyst in EtOH (4 ml), work-up and purification afforded *1-(6-bromo-4*H*-1-benzopyran-4-on-3-yl)-2-cyano-8-phenyl-4-aza-7-thiaoctanol* **260** as a brown solid (107 mg, 56%).

*1- (6-fluoro-4*H*-1-benzopyran-4-on-3-yl)- -2-cyano-8-phenyl-4-aza-7-thiaoctanol* **261**

The experimental procedure employed for the synthesis of *1-[4H-1-benzopyran-4-on-3-yl)-2-cyano-8-phenyl-(4-aza-7-thiaoctanol)* **258** was followed, using 6-fluoro-3-(2-cyano-3-hydroxy-1-propen-3-yl)-4*H*-1-benzopyran-4-one **215** (100 mg, 0.52 mmol), (*S*)-benzyl cysteamine hydrochloride (211.9 mg, 1.04 mmol), and sodium acetate (85.9 mg, 1.04 mmol) in EtOH (4ml). Work-up afforded *1- (6-fluoro-4*H*-1-benzopyran-4-on-3-yl)-2-cyano-8-phenyl-4-aza-7-thiaoctanol* **261** as brown solid oil (75 mg, 35%); Found **MH**$^+$: 413.1335. Calc. for $C_{22}H_{21}O_3N_2SF$ *M*: 412.1257); ν_{max} (KBr)/cm^{-1} 3300-3394 (OH and NH), 2360 (CN) and 1653(C=O); δ_H (400 MHz; $CDCl_3$) 2.64 (2H, m, 6'-CH_2), 2.85 (1H, m, 2'-H), 3.02 (2H, m, 5'-CH_2), 3.42 (1H, br s, NH), 3.45-3.63 (2H,m, 3'-CH_2), 3.72 (2H, s, 8'-CH_2), 4.99 (1H, d, J=2.0 Hz, 1'-H), 7.01 (1H, d, J=8.3 Hz, 8-H), 7.24 (1H, s, 2-H), 7.41 (1H, t, J=3.7 Hz, 7-H), 7.50 (1H, d, J=5.7 Hz, 7-H), 7.23-7.28 (5H, m, Ar-H), and 10.27 (1H, br s, OH); δ_C (100MHz; $CDCl_3$) 30.5 (C-6'), 30.3 (C-2'), 36.5 (C-8'), 43.5 (C-3'), 56.0 (C-5'), 61.3 (C-1'), 108.1 (CN), 117.2 (C-3), 17.6 (C-5), 121.3 (C-8), 120.7 (C-4a), 121.9.8 (C-7), 128.6 (C- 11' and C-13'), 128.8 (C-12'), 129.0 (C-10' and C-14'), 138.0 (C-9'), 151.3 (C-2), 155.8 (C-6), 158.9 (C-8'a) and 195.1 (C=O); *m/z* 413 (**M**$^+$, 12%) and 154 (100%).

Note:

(i) When the reaction was run for 6 weeks using 6-fluoro-3-(2-cyano-3-hydroxy-1-propen-3-yl)-4*H*-1-benzopyran-4-one **215** (100 mg, 0.52 mmol), (*S*)-benzylcysteamine (175 mg, 1.0 mmol), and sodium acetate (86 mg, 1.0 mmol) in EtOH (4 ml), work-up and purification gave *1-(6-fluoro-4*H*-1-benzopyran-4-on-3-yl)-2-cyano-8-phenyl-4-aza-7-thiaoctanol* **261** as a brown solid (32 mg, 15%).

(ii) When the reaction was run for 5 days using 6-fluoro-3-(2-cyano-3-hydroxy-1-propen-3-yl)-4*H*-1-benzopyran-4-one **215** (100 mg, 0.52 mmol), (*S*)-benzylcysteamine hydrochloride (212 mg, 1.0 mmol), TBAB (335 mg, 1.0 mmol) as the catalyst and

sodium acetate (86 mg, 1.0 mmol) in EtOH (4 ml), work-up and purification afforded *1-(6-fluoro-4*H*-1-benzopyran-4-on-3-yl)-2-cyano-8-phenyl-4-aza-7-thiaoctanol* **261** as brown solid (85.3 mg, 40%).

(iii) When this reaction was run for 5 days using 6-fluoro-3-(2-cyano-3-hydroxy-1-propen-3-yl)-4*H*-1-benzopyran-4-one **215** (100 mg, 0.52 mmol), (*S*)-benzylcysteamine hydrochloride (211.9 mg, 1.04 mmol), and $BmimBF_4$ (2.0 mL) as the catalyst in EtOH (4 ml), work-up and purification afforded *1-(6-fluoro-4*H*-1-benzopyran-4-on-3-yl)-2-cyano-8-phenyl-4-aza-7-thiaoctanol* **261** as a brown solid (106.7 mg, 50%).

1-[6-methoxy-4H-1-benzopyran-4-on-3-yl)-2-cyano-8-phenyl-4-aza-7-thiaoctanol **262**

The experimental procedure employed for the synthesis of *1-(4H-1-benzopyran-4-on-3-yl)-2-cyano-8-phenyl-4-aza-7-thiaoctanol* **258** was followed, using 3-(2-cyano-3-hydroxy-1-propen-3-yl)-6-methoxy-4H-1-benzopyran-4-one **216** (100 mg, 0.35 mmol), *S*-benzylcysteamine hydrochloride (143 mg, 0.70 mmol), and sodium acetate (58 mg, 0.70 mmol) in EtOH (4ml). Work-up afforded *1-[6-methoxy-4H-1-benzopyran-4-on-3-yl)-2-cyano-8-phenyl-4-aza-7-thiaoctanol* **262** as brown solid oil (70 mg, 47 %); Found: $\mathbf{MH}^+$: 391.1539. Calc. for $C_{23}H_{24}O_4N_2S$, *M*: 390.1579); ν_{max} (KBr)/cm-1 3300-3394 (OH and NH), 2360 (CN) and 1623(C=O); δ_H (400 MHz; $CDCl_3$) 2.64 (2H, t, *J*=6.8 Hz, 6'-CH_2), 3.15 (1H, m, 2'-H), 3.18 (2H, m, 5'- CH_2), 3.44 (1H, br s, NH), 3.57 (2H, dd, *J*=12.9 and 3.6 Hz, 3'-CH_2), 3.73 (2H, s, 6'-CH_2), 3.75 (3H, s, OCH_3), 4.99 (1H, d, J=2.7 Hz, 1'-H), 7.01 (1H, d, *J*=8.3 Hz, 8-H), 7.24 (1H, s, 2-H), 7.41 (1H, t, *J*=3.7 Hz, 7-H), 7.50 (1H, d, J=5.7 Hz, 7-H), 7.23-7.28 (5H, m, Ar-H), and 10.27 (1H, br s, OH); δ_C (100MHz; $CDCl_3$) 29.9 (C-6'), 30.1 (C-2'), 36.4 (C-8'), 43.2 (C-3'), 58.7 (6-OCH_3), 60.0 (C-5'), 61.2 (C-1'), 107.2 (CN), 117.6 (C-3), 117.8 (C-5), 118.2 (C-4a), 122.5 (C-8), 128.7 (C- 11' and C-13'), 128.8 (C-12'), 128.9 (C-10' and C-14'), 131.2 (C-7), 135.2 (C-9), 140.3 (C-6), 146.8 (C-2), 158.6 (C-8a) and 195.3 (C=O); *m/z* 391 ($\mathbf{M}^+$, 10%) and 154 (100).

Note:

(i) When the reaction was run for 6 weeks using 3-(2-cyano-3-hydroxy-1-propen-3-yl)-6-methoxy-4H-1-benzopyran-4-one **216** (100 mg, 0.35 mmol), *S*-benzylcysteamine (118 mg, 0.70 mmol), and sodium acetate (58 mg, 0.70 mmol) in EtOH (4 ml), work-up and purification *1-[6-methoxy-4H-1-benzopyran-4-on-3-yl)-2-cyano-8-phenyl-4-aza-7-thiaoctanol* **262** as a brown solid (40 mg, 27 %).

(ii) When this reaction was run for 5 days using 3-(2-cyano-3-hydroxy-1-propen-3-yl)-6-methoxy-4H-1-benzopyran-4-one **216** (100 mg, 0.52 mmol), *S*-benzylcysteamine hydrochloride (143 mg, 0.70 mmol), TBAB (226 mg, 0.70 mmol) as the catalyst and sodium acetate (58 mg, 0.70 mmol) in EtOH (4 ml), work-up and purification afforded *1-[6-methoxy-4H-1-benzopyran-4-on-3-yl)-2-cyano-8-phenyl-4-aza-7-thiaoctanol* **262** as a brown solid (89 mg, 60%).

(iii) When this reaction was run for 5 days using 3-(2-cyano-3-hydroxy-1-propen-3-yl)-6-methoxy-4H-1-benzopyran-4-one **216** (100 mg, 0.52 mmol), *S*-benzylcysteamine hydrochloride (143 mg, 0.70 mmol), and $BmimBF_4$ (2.0 mL) as the catalyst in EtOH (4 ml), work-up and purification afforded *1-[6-methoxy-4H-1-benzopyran-4-on-3-yl)-2-cyano-8-phenyl-4-aza-7-thiaoctanol* **262** as a brown solid (99 mg, 66%).

3.5.2 Reactions of Baylis-Hillman products with ethyl glycine hydrochloride

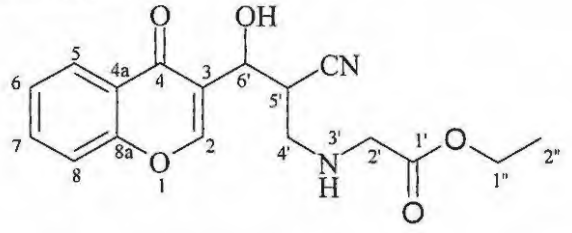

*Ethyl 5-cyano-6-(4*H*-1-benzopyran-4-on-3-yl)-6-hydroxy-3-azahexanoate* **263**

3-(2-Cyano-3-hydroxy-1-propen-3-yl)-4*H*-1-benzopyran-4-one **212** (100 mg, 0.44 mmol) was added to a stirred solution of ethyl glycine hydrochloride (124 mg, 0.88 mmol) and sodium acetate (73 mg, 0.88 mmol) in EtOH (4 ml). The resulting mixture was stirred at room temperature for 48 hours. Evaporation of the solvent *in vacuo* gave a brown oily residue which was purified by flash chromatography [on silica; elution with hexane: EtOAc (1:2)] to afford *ethyl 5-cyano-6-(4*H*-1-benzopyran-4-on-3-yl)-6-hydroxy-3-azahexanoate* **263** as brown crystalline solid (79.9 mg, 55%), m.p. 70-76°C, (Found $\mathbf{M}^+$: 330.13007. Calc. for $C_{17}H_{18}O_5N_2$, *M*: 330.12157); ν_{max} (KBr)/cm^{-1} 3200-3500 (OH and NH), 2346 (C≡N), and 1700 and 1658 (2x C=O); δ_H (400 MHz; $CDCl_3$) 1.29 (3H, t, *J*=7.1 Hz, 2''CH_3), 3.21 (1H, m, 5'-H), 3.38 (1H, dd, *J*=12.6 and 1.7 Hz, 4'-CH_2), 3.61 (1H, br s, NH), 3.79 (1H, dd, *J*=12.5 and 3.8 Hz, 4'- CH_2), 4.02 (2H, q, *J*=17.7 Hz, 2'- CH_2), 4.24 (2H, q, *J*=7.2 Hz, 1''- CH_2), 4.99 (1H, s, 6'-H), 6.85 (1H, t, *J*=7.6 Hz, 6-H), 6.98 (1H, d, *J*=8.3 Hz, 8-H), 7.24 (1H, s, 2-H), 7.39 (1H, t, *J*=7.8 Hz, 7-H), 7.52 (1H, d, *J*=7.8 Hz, 5-H), and 10.92 (1H, br s, OH); δ_C (100MHz; $CDCl_3$) 14.2 (C-2''), 30.3 (C-5'), 44.2 (C-4'), 57.12 (C-2'), 61.0(C-6'), 62.2 (C-1''), 108.9 (C-4a), 117.7 (C≡N), 118.1 (C-8), 118.5 (C-6), 119.8 (C-3), 130.9 (C-5), 134.2 (C-7), 156.2 (C-8a), 160.6 (C-2), 167.9 (1'-C=O) and 195.9 (4'-C=O); *m/z* 330 ($\mathbf{M}^+$, 4%) and 225 (100).

Note:

(i) When the reaction was run for 6 weeks using 3-(2-cyano-3-hydroxy-1-propen-3-yl)-4*H*-1-benzopyran-4-one **212** (100mg, 0.44 mmol), ethyl glycine (57 mg, 0.88 mmol),

and sodium acetate (73mg, 0.88 mmol) in EtOH (4 ml), work-up and purification afforded *ethyl 5-cyano-6-(4*H*-1-benzopyran-4-on-3-yl)-6-hydroxy-3-azahexanoate* **263** as a brown crystalline solid as (69.7 mg, 48%).

(ii) When the reaction was run for 5 days using 3-(2-cyano-3-hydroxy-1-propen-3-yl)-4*H*-1-benzopyran-4-one **212** (100.0 mg, 0.44 mmol), ethyl glycine hydrochloride (124 mg, 0.88 mmol), TBAB (367 mg, 1.1 mmol) as the catalyst and sodium acetate (73 mg, 0.88 mmol) in EtOH (4 ml), work-up and purification afforded *ethyl 5-cyano-6-(4*H*-1-benzopyran-4-on-3-yl)-6-hydroxy-3-azahexanoate* **263** as a brown crystalline solid as (84.2 mg, 58%).

(iii) When the reaction was run for 5 days using 3-(2-cyano-3-hydroxy-1-propen-3-yl)-4*H*-1-benzopyran-4-one **212** (100 mg, 0.44 mmol), ethyl glycine ester hydrochloride (124 mg, 0.88 mmol), and $BmimBF_4$ (2.0 mL) as the catalyst in EtOH (4 ml), work-up and purification afforded *ethyl 5-cyano-6-(4*H*-1-benzopyran-4-on-3-yl)-6-hydroxy-3-azahexanoate* **263** as a brown crystalline solid as (99 mg, 68%).

*Ethyl 5-cyano-6-(6-chloro-4*H*-1-benzopyran-4-on-3-yl) -6-hydroxy-3-azahexanoate* **264**

The experimental procedure employed for the synthesis of *ethyl-6-(4H-1-benzopyran-4-on-3-yl)-5-cyano-6-hydroxy-3-azahexanoate* **263** was followed, using 6-chloro-3-(2-cyano-3-hydroxy-1-propen-3-yl)-4*H*-1-benzopyran-4-one **213** (100 mg, 0.38 mmol), sodium acetate (62.7 mg, 0.76 mmol) and ethyl glycine ester hydrochloride (107.0 mg, 0.76 mmol) in EtOH (4ml). Work-up afforded *ethyl 5-cyano-6-(6-chloro-4*H*-1-benzopyran-4-on-3-yl)- 6-hydroxy-3-azahexanoate* **264** as brown solid (51.3 mg, 37%), (Found $\mathbf{MH^+}$: 365.0902, $C_{17}H_{17}O_5N_2Cl$, *M*: 364.0826); ν_{max} (KBr)/cm-1 3200-3500 (OH and NH), 2348 (C≡N), 1654 (2x C=O); 1.34 (3H, t, *J*= 8.8 Hz, 2''-CH_3), 3.08 (2H, m, 2'- CH_2), 3.24 (1H, br s, NH), 3.71 (1H, m, 5'-H), 4.12 (2H, dd, *J*=9.0 and 3.8 Hz, 4'-H), 5.07 (1H, d, *J*=7.1 Hz, 6'-H), 6.94 (1H, t, *J*=9.4 Hz, 7-H), 6.98 (1H, d, J=8.7 Hz, 8-

H), 7.49 (1H, d, *J*=2.5 Hz, 5-H), 7.53 (1H, s, 2-H) and 10.74 (1H, br s, OH); δ_C (100MHz; $CDCl_3$) 14.1 (C-2''), 30.5 (C-5'), 44.6 (C-4'), 57.4 (C-2'), 61.3 (C-6'), 62.6 (C-7'), 110.6 (C-4a), 117.7 (C≡N), 119.8 (C-3), 120.5 (C-8), 129.1 (C-5), 131.5 (C-6), 134.0 (C-7), 153.7 (C-8a), 160.7 (C-2), 167.9 (1'-C=O) and 195.7 (4'-C=O); *m/z* 365 ($\mathbf{M}^+$, 18%) and 147 (100).

Note:

(i) When the reaction was run for 6 weeks using 6-chloro-3-(2-cyano-3-hydroxy-1-propen-3-yl)-4*H*-1-benzopyran-4-one **213** (100 mg, 0.38 mmol), ethyl glycine ester (49 mg, 0.76 mmol), as free amine, and sodium acetate (63 mg, 0.76 mmol) in EtOH (4 ml), work-up and purification afforded *ethyl 5-cyano-6-(6-chloro-4*H*-1-benzopyran-4-on-3-yl)- 6-hydroxy-3-azahexanoate* **264** as a brown crystalline solid (74.9 mg, 54%).

(ii) When the reaction was run for 5 days using 6-chloro-3-(2-cyano-3-hydroxy-1-propen-3-yl)-4*H*-1-benzopyran-4-one **213** (100 mg, 0.38 mmol), ethylglycine hydrochloride (107 mg, 0.76 mmol), TBAB (245 mg, 0.76 mmol) as the catalyst and sodium acetate (63 mg, 0.76 mmol) in EtOH (4 ml), work-up and purification afforded

*ethyl 5-cyano-6-(6-chloro-4*H*-1-benzopyran-4-on-3-yl)- 6-hydroxy-3-azahexanoate* **264** as a brown crystalline solid (90.2 mg, 65%).

(iii) When the reaction was run for 5 days using 6-chloro-3-(2-cyano-3-hydroxy-1-propen-3-yl)-4*H*-1-benzopyran-4-one **213** (100 mg, 0.38 mmol), ethylglycine hydrochloride (107 mg, 0.76 mmol), and $BmimBF_4$ (2.0 mL) as the catalyst in EtOH (4 ml), work-up and purification afforded *ethyl 5-cyano-6-(6-chloro-4*H*-1-benzopyran-4-on-3-yl)- 6-hydroxy-3-azahexanoate* **264** as a brown crystalline solid (89 mg, 64%).

*Ethyl 5-cyano-6-(6-fluoro-4*H*-1-benzopyran-4-on-3-yl)-6-hydroxy-3-azahexanoate* **265**

The experimental procedure employed for the synthesis of ethyl *6-(4H-1-benzopyran-4-on-3-yl)-5-cyano-6-hydroxy-3-azahexanoate* **263** was followed, using 6-fluoro-3-(2-cyano-3-hydroxy-1-propen-3-yl)-4H-1-benzopyran-4-one **215** (100 mg, 0.41 mmol), ethylglycine ester hydrochloride (1.5 mg, 0.82 mmol), TBAB (264 mg, 0.82 mmol)and sodium acetate (68 mg, 0.82 mmol) in EtOH (4ml). Work-up afforded *ethyl 5-cyano-6-(6-fluoro-4*H*-1-benzopyran-4-on-3-yl)-6-hydroxy-3-azahexanoate* **265** as a brown oil (21.4 mg, 15%), (Found $\mathbf{M}^+$: 34 , $C_{17}H_{17}O_5N_2F$, *M*: 348.1121); ν_{max} (KBr)/cm^{-1} 3200-3500 (OH and NH), 2348 (C≡N) and 1658 (2x C=O); 1.34 (3H, t, J=8.9 Hz, 1''-CH_3), 3.08 (2H, m, 2'-CH_2), 3.24 (1H, br s, NH), 3.71 (1H, m, 5'-H), 4.12 (2H, dd, J= 9.0 and 1.7 Hz, 4'- CH_2), 5.07 (1H, d, J=7.1, 6'-H), 6.94 (1H, t, J=9.4 Hz, 7-H), 6.98 (1H, d, J=8.7 Hz, 8-H), 7.49 (1H, d, J=2.5 Hz, 5-H), 7.53 (1H, s, 2-H) and 10.74 (1H, br s, OH); δ_C (100MHz; $CDCl_3$) 14.3 (C-2''), 30.7 (C-5'), 44.7 (C-4'), 57.7 (C-2'), 61.0 (C-6'), 62.4 (C-1''), 109.4 (C-4a), 117.6 (C≡N), 117.7 (C-5), 119.8 (C-3), 121.3 (C-8), 131.5 (C-6), 149.8 (C-8a), 160.6 (C-2), 161.9 (C-7), 167.8 (1'-C=O) and 195.6 (4'-C=O); *m/z* 344 ($\mathbf{M}^+$, 30%) and 303 (100).

Note:

(i) When the reaction was run for 6 week using 6-fluoro-3-(2-cyano-3-hydroxy-1-propen-3-yl)-4H-1-benzopyran-4-one **215** (100 mg, 0.41 mmol), ethyl glycine (53 mg, 0.82 mmol), as free amine, and sodium acetate (68 mg, 0.82 mmol) in EtOH (4 ml), work-up and purification afforded *ethyl 5-cyano-6-(6-fluoro-4*H*-1-benzopyran-4-on-3-yl)-6-hydroxy-3-azahexanoate* **265** as a brown crystals (59 mg, 41%).

(ii) When the reaction was run for 5 days using 6-fluoro-3-(2-cyano-3-hydroxy-1-propen-3-yl)-4H-1-benzopyran-4-one **215** (100 mg, 0.41 mmol) ethyl glycine hydrochloride (1.5 mg, 0.82 mmol), TBAB (367 mg, 1.1 mmol) as the catalyst and sodium acetate (68 mg, 0.82 mmol) in EtOH (4 ml), work-up and purification afforded

*ethyl 5-cyano-6-(6-fluoro-4*H*-1-benzopyran-4-on-3-yl)-6-hydroxy-3-azahexanoate* **265** as a brown crystals (71.3 mg, 50%).

(iii) When the reaction was run for 5 days using 6-fluoro-3-(2-cyano-3-hydroxy-1-propen-3-yl)-4H-1-benzopyran-4-one **215** (100 mg, 0.41 mmol), ethyl glycine ester hydrochloride (1.5 mg, 0.82 mmol), and $BmimBF_4$ (2.0 mL) as the catalyst in EtOH (4 ml), work-up and purification afforded *ethyl 5-cyano-6-(6-fluoro-4*H*-1-benzopyran-4-on-3-yl)-6-hydroxy-3-azahexanoate* **265** as a brown crystals (80.0 mg, 56%).

3.5.3 Reactions of Baylis-Hillman products with D-serine methyl ester hydrochloride

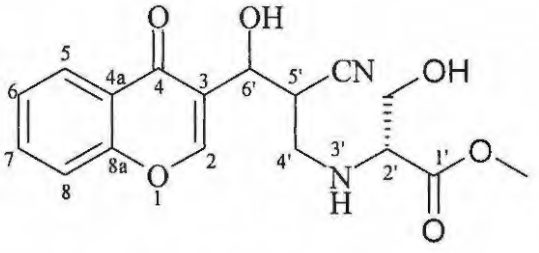

*Methyl 5-cyano-6-(4*H*-1-benzopyran-4-on-3-yl)-6-hydroxy-3-azahexanoate* **266**

3-(3-Hydroxy-2-cyanopropen-3-yl)-4*H*-1-benzopyran-4-one **212** (100 mg, 0.44 mmol) was added to a stirred solution of D-serine methyl ester hydrochloride (137 mg, 0.88mmol), and sodium acetate (73 mg, 0.88 mmol) in EtOH (4 ml). The resulting mixture was stirred at room temperature for 6 weeks. Evaporation *in vacuo* gave a brown oily residue which was purified by flash chromatography [on silica gel and elution with hexane: EtOAc (3:2)] to afford *methyl 5-cyano-6-(4*H*-1-benzopyran-4-on-3-yl)-6-hydroxy-3-azahexanoate* **266** as yellow solid (47.2 mg, 31%), (Found $\mathbf{M}^+$:345.1045. Calc for $C_{17}H_{18}O_6N_2$, *M*: 346.1164); ν_{max} (KBr)/cm^{-1} 3420 (OH and NH), 2349 (CN), 1653 and 1652 (2xC=O); δ_H (400 MHz; $CDCl_3$) 2.21 (1H, m, CH_2OH), 2.64 (1H, t, *J*=7.0 Hz, 4'-H), 3.02 (1H, t, *J*=7.5 Hz, 4'-H), 3.16 (1H, br s, 3'-NH), 3.21 (1H, m, 5'-H), 3.31-3.45 (3H, m, 2'-H and CH_2OH), 3.72 (3H, m, OCH_3), 4.98 (1H, br s, 6'-H),

6.84 (1H, t, *J*=8.5 Hz, 6-H), 7.01 (1H, d, *J*=8.5 Hz, 8-H), 7.13(1H, s, 2-H), 7.41 (1H, t, 7.5 Hz, 7-H), 7.50 (1H, d, *J*=7.8 Hz, 5-H), and 10.98 (1H, br s, 1'-OH); δ_C (100MHz; $CDCl_3$) 31.3 (C-5'), 43.1 (C-4'), 45.0 (C-2'), 55.5 (CH_2OH-8'), 59.8 (C-2' and 7'-OCH_3), 118.1 (C-8), 118.4 (CN), 127.7 (C-3), 128.8 (C-6), 128.9 (C-7), 130.6 (C-8), 133.9 (C-4a), 151.1 (C-2), 160.7 (C-8a), 172.0 (1'-C=O) and 189.7 (4-C=O); *m/z* 345($\mathbf{M^+}$, 14%) and 121 (100).

Note:

(i) When the reaction was run for 5 days using 3-(3-hdroxy-2-cyanopropen-3-yl)-4*H*-1-benzopyran-4-one **212** (100 mg, 0.44 mmol), D-serine methyl ester hydrochloride (137 mg, 0.88mmol), TBAB (284 mg, 0.88 mmol) as the catalyst and sodium acetate (73 mg, 0.88 mmol) in EtOH (4 ml), work-up and purification afforded *methyl 5-cyano-6-(4*H*-1-benzopyran-4-on-3-yl)-6-hydroxy-2-(hydroxymethyl)-3-azahexanoate* **266** as yellow solid oil (61 mg, 40%).

*Methyl 5-cyano-6-(6-chloro-4*H*-1-benzopyran-4-on-3-yl)-6-hydroxy-3-azahexanoate* **267**

The experimental procedure employed for the synthesis of *methyl 5-cyano-6-(4H-1-benzopyran-4-on-3-yl)- 6-hydroxy-2-(hydroxymethyl)-3-zahexanoate* **266** was followed, using 6-chloro-3-(3-hydroxy-2-cyanopropen-3-yl)-4*H*-1-benzopyran-4-one **213** (100 mg, 0.38 mmol), sodium acetate (63 mg, 0.76 mmol) and D-serine methyl ester hydrochloride (118 mg, 0.76 mmol) in EtOH (4ml). Work-up afforded *methyl 5-cyano-6-(6-chloro-4*H*-1-benzopyran-4-on-3-yl)-6-hydroxy-3-azahexanoate* **267** as brown oil (22 mg, 15%), (Found: $\mathbf{MH^+}$, 381.0859, $C_{17}H_{17}O_6N_2Cl$ requires *M*: 380.7751); ν_{max} (KBr)/cm^{-1} 3421 (OH and NH), 2353 (CN), 1654 and 1653 (2xC=O); δ_H (400 MHz; $CDCl_3$) 3.09 (1H, m, 5'-H), 3.57 (2H, dd, *J*= 3.36 and 12.83 Hz, 4'-H), 3.65 (2H, dd, *J*= 3.81 and 12.42 Hz, 8'-H), 3.75 (1H, m, 5'-H), 3.79 (1H, br s, 3'-NH), 3.81 (1H, br s, 8'-

OH), 3.85 (1H, m, 2'-H), 4.13 (3H, s, 7'-OCH_3), 5.15 (1H, m, 6'-H), 6.92 and 6.93 (2 x 1H, d, *J*= 8.82 Hz, 8-H), 7.32 and 7.35 (2 x 1H, t, 7-H), 7.36 (1H, s, 5-H), 7.44 and 7.48 (2 x 1H, d, *J*= 2.61 Hz, 7-H), 7.51 (1H, s, 5-H), and 10.8 (1H, br s,6'-OH); δ_C (100MHz; $CDCl_3$) 31.4 (C-5'), 43.2 (C-4'), 45.3 (C-2'), 55.8 (C-8'), 60.0 (7'-O*C*H_3), 61.3 (C-2'), 118.5 (CN), 127.1 (C-5), 127.9 (CN), 131.4 (C-8), 135.7 (C-6), 137.2 (C-4a), 145.9 (C-7), 151.1 (C-2), 158.2 (C-8a), 172.2 (1'-C=O) and 189.8 (4-C=O); *m/z* 381 ($\mathbf{M}^+$, 10%) and 149 (100).

Note:

(i) When the reaction was run for 5 days using 6-chloro-3-(2-cyano-3-hydroxy-1-propen-3-yl)-4*H*-1-benzopyran-4-one **213** (100 mg, 0.38 mmol), D-serine methyl ester hydrochloride(118.2 mg, 0.76 mmol), TBAB (284 mg, 0.76mmol) as the catalyst and sodium acetate (63 mg, 0.76 mmol) in EtOH (4 ml), work-up and purification afforded *methyl 5-cyano-6-(6-chloro-4*H*-1-benzopyran-4-on-3-yl)-6-hydroxy-3-azahexanoate* **267** as a yellow solid oil (29 mg, 20%).

*Methyl 5-cyano-6-(6-methoxy-4*H*-1-benzopyran-4-on-3-yl)-6-hydroxy-3-azahexanoate* **268**

The experimental procedure employed for the synthesis of *methyl 6-(4*H*-1-benzopyran-4-on-3-yl)-5-cyano-6-hydroxy-2-(hydroxymethyl)-3-azahexanoate* **266** was followed, using 6-methoxy-3-(3-hydroxy-2-cyanopropen-3-yl)-4*H*-1-benzopyran-4-one **216** (100 mg, 0.39 mmol), sodium acetate (64 mg, 0.78 mmol) and D-serine methyl ester hydrochloride (121 mg, 0.78 mmol) in EtOH (4ml). Work-up afforded *methyl 5-cyano-6-(6-methoxy-4*H*-1-benzopyran-4-on-3-yl)-6-hydroxy-3-azahexanoate* **268** as brown oil (40 mg, 27%), (Found: $\mathbf{M}^+$:376.0967. Calc for $C_{18}H_{20}O_7N_2$, *M*: 376.1271); ν_{max} (KBr)/cm^{-1} 3200-3421 (OH and NH), 2350(CN), 1654 and 1653 (2xC=O); δ_H (400 MHz; $CDCl_3$) 2.73 (1H, m, 5'-H), 3.53 (2H, dd, *J*=12.83 and 3.36 Hz, 4'-H), 3.64 (2H, dd, *J*=12.4 and 3.8 Hz, 8'-H), 3.75 (1H, m, 5'-H), 3.79 (1H, br s, 3'-NH), 3.81 (1H, br s, 8'-OH), 3.85 (1H, m, 2'-H), 3.76 (3H, s, 7'-OCH_3), 3.87 (3H, s, 6-OCH_3), 4.96 (1H, m,

6'-H), 6.97 and 6.99 (2 x 1H, d, *J*=8.8 Hz, 8-H), 7.38 and 7.43 (2 x 1H, t, 7-H), 8.07 and 8.27(2x1H, s, 5-H), and 10.23 (1H, br s, 6'-OH); δ_C (100MHz; $CDCl_3$) 31.2 (C-5'), 43.0 (C-4'), 45.2 (C-2'), 55.6 (C-8'), 59.8 (7'-O*C*H$_3$), 61.1 (C-2'), 107.8 (CN), 111.8 (C-5), 131.1 (C-8), 137.0 (C-4a), 139.5 (C-7), 161.9 (C-6), 162.1 (C-2), 164.2 (C-8a), 171.8 (1'-C=O) and 189.1 (4-C=O); *m/z* 376 ($\mathbf{M}^+$, 15%) and 151 (100).

Note:

(i) When the reaction was run for 5 days using 6-methoxy-3-(3-hydroxy-2-cyanopropen-3-yl)-4*H*-1-benzopyran-4-one **216** (100 mg, 0.39 mmol), D-serine methyl ester hydrochloride (121 mg, 0.78 mmol), TBAB (291 mg, 0.78 mmol) as the catalyst and sodium acetate (64 mg, 0.78 mmol) in EtOH (4 ml), work-up and purification afforded *methyl 5-cyano-6-(6-methoxy-4*H*-1-benzopyran-4-on-3-yl)-6-hydroxy-3-azahexanoate* **268** as yellow solid oil (48 mg, 33%).

3.5.4 Reaction of Baylis-Hillman products with L-Serine ethyl ester hydrochloride

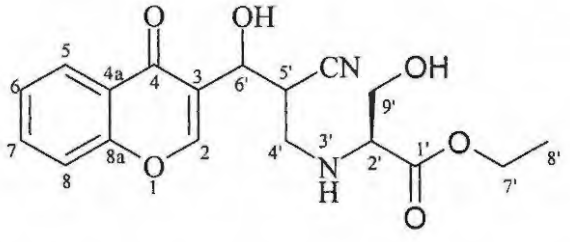

*Ethyl 5-cyano-6-(4*H*-1-benzopyran-4-on-3-yl)-6-hydroxy-2-hydroxymethyl-3-azahexanoate* **269**

3-(2-cyano-3-hydroxy-1-propen-3-yl)-4*H*-1-benzopyran-4-one **212** (100 mg, 0.44 mmol) was added to a stirred solution of L-serine ethyl ester hydrochloride (149 mg, 0.88mmol), and sodium acetate (73 mg, 0.88 mmol) in EtOH (4 ml). The resulting

mixture was stirred at room temperature for 6 weeks. Evaporation *in vacuo* gave a brown oily residue which was purified by flash chromatography [on silica gel and elution with hexane: EtOAc (3:2)] to afford *ethyl 5-cyano-6-(4*H*-1-benzopyran-4-on-3-yl)-6-hydroxy-2-hydroxymethyl-3-azahexanoate* **269** as yellow solid oil (41 mg, 26%), (Found **MH^+**:

391.14606, $C_{18}H_{20}O_6N_2$, Calc for *M*: 390.1427); ν_{max} (KBr)/cm^{-1} 3200-3421 (OH and NH), 2355 (CN), 1676 and 1654 (2xC=O); δ_H (400 MHz; $CDCl_3$) 2.73 (3H, t, *J*= 7.2 Hz, 8'-CH_3), 3.81 (1H, br s, 3'-NH), 3.57 (2H, m, 4'-H), 3.72 (2H, m, 8'-H), 3.80 (1H, m, 5'-H), 4.06 (1H, br s, 9'-OH), 4.08 (1H, m, 2'-H), 4.28 (1H, q, 7'-H), 5.03 (1H, d, *J*=7.0 Hz, 6'-H), 6.85 (1H, m, 8-H), 6.90 (1H, m, 8-H), 7.04 (1H, m, 7-H), 7.38 (1H, d, *J*=8.4 Hz, 5-H), 8.25 (1H, s, 2-H) and 10.87 (1H, br s, 6'-OH); δ_C (100MHz; $CDCl_3$) 14.2 (C-8'), 47.4 (C-5'), 53.4 (C-4'), 60.4 (C-7'), 62.8 (C-9'), 68.3 (C-2'), 68.4 (C-6'), 108.5 (CN), 118.1 (C-3), 118.2 (C-8), 118.4 (C-6), 119.7 (C-4a), 130.4 (C-5), 138.5 (C-7), 153.8 (C-2), 161.3 (C-8a), 167.2 (1'-C=O) and 191.6 (4-C=O); *m/z* 391 (**M^+**, 51%) and 149 (100).

Note:

(i) When the reaction was run for 5 days using 3-(2-cyano-3-hydroxy-1-propen-3-yl)-4*H*-1-benzopyran-4-one **212** (100 mg, 0.44 mmol), L-serine ethyl ester hydrochloride (149.3 mg, 0.88mmol), TBAB (283.6 mg, 0.88 mmol) as the catalyst and sodium acetate (72.7 mg, 0.88 mmol) in EtOH (4 ml). The workup and purification afforded *ethyl 5-cyano-6-(4*H*-1-benzopyran-4-on-3-yl)-6-hydroxy-2-hydroxymethyl-3-azahexanoate* **269** as yellow solid crystals (47.5 mg, 30%).

*Ethyl 5-cyano-6-(-6-chloro-4*H*-1-benzopyran-4-on-3-yl)-6-hydroxy-2-hydroxymethyl-3-azahexanoate* **270**

The experimental procedure employed for the synthesis of ethyl-2-methanol-6-(4H-1-benzopyran-4-on-3-yl)-5-cyano-6-hydroxy-3-azahexanoate **269** was followed, using 6-

chloro-3-(2-cyano-3-hydroxy-1-propen-3-yl)-4*H*-1-benzopyran-4-one **213** (100 mg, 0.38 mmol), sodium acetate (63 mg, 0.76 mmol) and L-serine ethyl ester hydrochloride

(129mg, 0.76 mmol) in EtOH (4ml). Work-up afforded *ethyl 5-cyano-6-(-6-chloro-4*H*-1-benzopyran-4-on-3-yl)-6-hydroxy-2-hydroxymethyl-3-azahexanoate* **270** as brown oil (44 mg, 29%). ν_{max} (KBr)/cm^{-1} 3200-3421 (OH and NH), 2926 (CN), 1676 and 1654 (2xC=O); δ_H (400 MHz; $CDCl_3$) 1.31 (3H, t, *J*=7.15 Hz, 8'-CH_3), 3.23 (1H, m, 5'-H), 3.38 (1H, br s, 3'-NH), 3.41 (1H, br s, 9'-OH), 3.81 (2H, dd, *J*=12.7 and 3.6 Hz, 4'-H), 4.08 (1H, m, 2'-H), 4.25 (2H, m, 9'-H), 5.01 (1H, d, *J*=2.7 Hz, 9'-H), 6.93 (1H, d, *J*=8.8 Hz, 8-H), 7.19 (1H, m, 7-H), 7.42 (1H, d, *J*=2.4 Hz, 5-H), 8.42 (1H, s, 2-H) and 10.7 (1H, br s, 6'-OH); δ_C (100MHz; $CDCl_3$) 14.3 (C-8'), 47.5 (C-5'), 53.7 (C-4'), 60.6 (C-7'), 62.9 (C-9'), 68.5 (C-2'), 68.7 (C-6'), 108.8 (CN), 118.6 (C-3), 120.6 (C-8), 124.6 (C-4a), 128.6 (C-5), 129.2 (C-6), 138.7 (C-7), 153.9 (C-2), 163.5 (C-8a), 167.0 (1'-C=O) and 191.4 (4-C=O); *m/z* 395(**M**$^+$,15%) and 149(100).

Note:

(i) When this reaction was run for 5 days using 6-chloro-3-(2-cyano-3-hydroxy-1-propen-3-yl)-4*H*-1-benzopyran-4-one **213**, L-serine ethyl ester hydrochloride (129 mg, 0.76 mmol)), TBAB (245 mg, 0.76 mmol) as the catalyst and sodium acetate (63 mg, 0.76 mmol) in EtOH (4 ml). The workup and purification afforded *ethyl 5-cyano-6-(-6-chloro-4*H*-1-benzopyran-4-on-3-yl)-6-hydroxy-2-hydroxymethyl-3-azahexanoate* **270** as yellow solid crystals (68 mg, 45%).

*Ethyl 5-cyano-6-(6-methoxy-4*H*-1-benzopyran-4-on-3-yl)-6-hydroxy-2-hydroxymethyl-3-azahexanoate* **271**

The experimental procedure employed for the synthesis of ethyl-2-methanol-6-(4H-1-benzopyran-4-on-3-yl)-5-cyano-6-hydroxy-3-azahexanoate **269** was followed, using 6-methoxy-3-(3-hydroxy-2-cyanopropen-3-yl)-4*H*-1-benzopyran-4-one **216** (100 mg, 0.39

mmol), sodium acetate (64 mg, 0.78 mmol) and L-serine ethyl ester hydrochloride (132 mg, 0.78 mmol) in EtOH (4ml). Work-up afforded *ethyl 5-cyano-6-(-6-methoxy-4H-1-benzopyran-4-on-3-yl)-6-hydroxy-2-hydroxymethyl-3-azahexanoate* **271** as brown oil (40 mg, 27%); ν_{max} (KBr)/cm^{-1} 3200-3421 (OH and NH), 2355 (CN), 1645 and 1636 (2xC=O); δ_H (400 MHz; $CDCl_3$) 1.32 (3H, t, *J*=7.2 Hz, 8'-CH_3), 3.01 (1H, m, 5'-H), 3.96 (1H, br s, 3'-NH), 4.00 (3H, s, 6-OCH_3), 4.02 (2H, m, 4'-H), 4.11 (1H, m, 2'-H), 4.26 (2H, m, 9'-H), 4.28 (2H, q, 9'-H), 4.81 (1H, br s, 6'-H), 5.04 (2H, br s, 9' and 6'-OH), 6.95 (1H, d, *J*=8.8 Hz, 8-H), 7.21 (1H, m, 7-H), 7.42 (1H, d, *J*=2.4 Hz, 5-H), and 8.48 (1H, s, 2-H) δ_C (100MHz; $CDCl_3$) 14.1 (C-8'), 47.2 (C-5'), 53.5 (C-4'), 60.3 (C-7'), 62.5 (C-9'), 68.8 (C-2'), 68.9 (C-6'), 108.9 (CN), 113.1 (C-5), 118.9 (C-3), 120.9 (C-8), 124.8 (C-4a), 132.7 (C-7), 154.1 (C-6), 154.3 (C-2), 158.7 (C-8a), 167.0 (1'-C=O) and 191.4 (4-C=O); *m/z* 376 ($\mathbf{M}^+$,12 %) and 155 (100).

Note:

(i) When this reaction was run for 5 days using 3-(2-cyano-3-hydroxy-1-propen-3-yl)-6-methoxy-4*H*-1-benzopyran-4-one **216**, L-serine ethyl ester hydrochloride (128.9 mg, 0.76 mmol)), TBAB (244.9 mg, 0.76 mmol) as the catalyst and sodium acetate (132.3 mg, 0.78 mmol) in EtOH (4 ml). The workup and purification afforded *ethyl 5-cyano-6-(6-methoxy-4H-1-benzopyran-4-on-3-yl)-6-hydroxy-2-hydroxymethyl-3-azahexanoate* **271** as yellow solid crystals (49 mg, 33%).

3.5.5 Reaction of Baylis-Hillman products with L-Threonine methyl ester hydrochloride

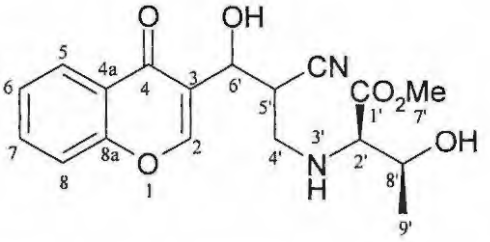

*Methyl 5-cyano-6-(4*H*-1-benzopyran-4-on-3-yl)-6-hydroxy-2-hydroxyethyl-3-azahexanoate* **272**

3-(3-Hydroxy-2-cyanopropen-3-yl)-4*H*-1-benzopyran-4-one **212** (100 mg, 0.44 mmol) was added to a stirred solution of L-threonine methyl ester hydrochloride (149 mg, 0.88mmol), and sodium acetate (72.7 mg, 0.88 mmol) in EtOH (4 ml). The resulting mixture was stirred at room temperature for 6 weeks. Evaporation *in vacuo* gave a brown oily residue which was purified by flash chromatography [on silica gel and elution with hexane: EtOAc (3:2)] to afford 7-methyl-2-methanol-(8-methyl)-6-{4H-1-benzopyran-4-on-3-yl}-5-cyano-6-hydroxy-3-azahexanoate **272** as yellow oil (41.2 mg, 25%); ν_{max} (KBr)/cm^{-1} 3200-3421 (OH and NH), 2956 (CN), 1653 and 1712 (2xC=O); δ_H (400 MHz; $CDCl_3$) 1.27 (9H, m, 9'-CH_3), 2.78 (2H, br peak, OH), 3.21 (1H, br s, 3'-NH), 3.58 (1H, m, 4'-H), 3.65 (2H, m, 4'-H and 5'-H), 3.79 (3H, s, 7'-OCH_3), 4.24 (2H, m, 8'-H), 4.44 (1H, m, 2'-H), 5.11(2H, m, 6'-H), 6.70 (4H, m, 6-H and 8-H), 7.34 (2H, m, 7-H), 7.89 (2H, 2xs, 2-H), 8.02 (2H, *J*=8.2 and 1.4 Hz, 5-H) and δ_C (100MHz; $CDCl_3$) 15.3 and 18.5 (2xC-9'), 29.1 (C-8'), 31.3 (C-5'), 53.2 (C-2'), 62.0 (C-6'), 63.3 (C-4'), 68.4 (C-7'), 108.8 (CN), 118.5 (C-8), 126.6 (C-6), 126.9 (C-3), 127.1 (C-4a), 127.4 (C-5), 129.7 (C-7), 133.2 (C-2), 158.9 (C-8a), 167.3 (1'-C=O) and 173.4 (4-C=O);

The ^{1}H NMR (Figure 75) of a new aza-Michael product **256** reveals a multiplet at 1.29 ppm which correspond to 9'–methyl diastereotopic protons three isomers, a broad peak at 2.99 ppm which correspond to OH, a multiplet at 3.21 ppm which correspond to 5'-

methine proton, a broad singlet at 2.63 ppm which correspond to 3'-amine proton, a multiplet at 3.64 ppm which correspond to one proton of 4'-methylene diastereotopic protons, a multiplet of 2'-methine proton (overlapping to another proton of 4'-methylene diastereotopic protons) at 3.76 ppm, a singlet at 3.82 ppm which correspond to 7'-methoxy protons, a multiplet at 4.29 ppm which correspond to 8'-methine proton of three isomers, a multiplet at 4.44 which correspond to 2'-methine proton, a broad peak which correspond to 6'-methine proton.

Note:

(i) When this reaction was run for 5 days using 3-(3-Hydroxy-2-cyanopropen-3-yl)-4*H*-1-benzopyran-4-one **212** (100 mg, 0.44 mmol), L-threonine methyl ester hydrochloride (149 mg, 0.88mmol), TBAB (284 mg, 0.88 mmol) as the catalyst and sodium acetate (73 mg, 0.88 mmol) in EtOH (4 ml). The workup and purification afforded 7-methyl-2-methanol-(8-methyl)-6-{4H-1-benzopyran-4-on-3-yl}-5-cyano-6-hydroxy-3-azahexanoate **272** as yellow solid crystals (61 mg, 37%).

*7-Methyl-2-methanol-(8-methyl)-6-{4*H*-1-benzopyran-4-on-3-yl-6-chloro}-5-cyano-6-hydroxy-3-azahexanoate* **273**

The experimental procedure employed for the synthesis of ethyl-2-methanol-6-(4H-1-benzopyran-4-on-3-yl)-5-cyano-6-hydroxy-3-azahexanoate **272** was followed, using 6-chloro-3-(3-hydroxy-2-cyanopropen-3-yl)-4*H*-1-benzopyran-4-one **213** (100 mg, 0.38 mmol), sodium acetate (63 mg, 0.76 mmol) and L-threonine methyl ester hydrochloride (129 mg, 0.76 mmol) in EtOH (4ml). Work-up afforded 7-methyl-2-methanol-(8-methyl)-6-{4H-1-benzopyran-4-on-3-yl-6-chloro}-5-cyano-6-hydroxy-3-azahexanoate **272** as brown oil (48.2 mg, 31%), m.p., (Found: $\mathbf{MH^+}$:395.0928 $C_{18}H_{19}O_6N_2Cl$ requires *M*: 394.0931); ν_{max} (KBr)/cm^{-1} 3200-3421 (OH and NH), 2956 (CN), 1653 and 1712 (2xC=O); δ_H (400 MHz; $CDCl_3$) 1.29 (9H, m, 9'-CH_3), 2.99 (2H, br peak, OH), 3.21 (1H, br s, 3'-NH), 3.64 (1H, m, 4'-H), 3.76 (2H, m, 4'-H and 5'-H), 3.82 (3H, s, 7'-

OCH_3), 4.29 (2H, m, 8'-H), 4.44 (1H, m, 2'-H), 6.82 (2H, m, 6-H), 6.97 (2H, dd, *J*=8.8 and 1.0 Hz, 8-H), 7.48 (2H, m, 7-H), 8.07 (2H, 2xs, 2-H), 8.18 (2H, m, 5-H) and δ_C (100MHz; $CDCl_3$) 15.5 and 19.8 (2xC-9'), 29.2 (C-8'), 31.2 (C-5'), 53.5 (C-2'), 62.0 (C-6'), 63.3 (C-4'), 68.3 (C-7'), 109.2 (CN), 118.9 (C-3), 120.5 (C-8), 124.5 (C-5), 124.8 (C-4a), 129.6 (C-7), 133.6 (C-6), 133.9 (C-2), 158.3 (C-8a), 167.3 (1'-C=O) and 173.4 (4-C=O); *m/z* 395 ($\mathbf{M}^+$,10 %) and 149 (100).

Note:

When the reaction was run for 5 days using 6-chloro-3-(3-hydroxy-2-cyanopropen-3-yl)-4*H*-1-benzopyran-4-one **213** (100 mg, 0.38 mmol), L-threonine methyl ester hydrochloride (129 mg, 0.76 mmol), TBAB (245 mg, 0.76 mmol) as the catalyst and sodium acetate (63 mg, 0.76 mmol) in EtOH (4 ml), work-up and purification afforded 7-methyl-2-methanol-(8-methyl)-6-{4H-1-benzopyran-4-on-3-yl-6-chloro}-5-cyano-6-hydroxy-3-azahexanoate **272** as a brown oil (70 mg, 45%).

3.6 HIV-1 Protease Inhibition Kinetics

Enzyme inhibition studies were conducted using a Perkin Elmer Lambda 35 UV/Vis Spectrometer with HIV-1 protease and HIV protease Substrate III having the sequence:- H-His-Lys-Ala-Arg-Val-Leu-Nitroph-Glu-Ala-Nli-Ser-NH_2. The enzyme and substrate were purchased from Bachem AG and Biosciences (Philadelphia, USA), respectively, and were used without further purification. Glacial acetic acid, sodium acetate trihydrate, NaCl and glycerol were purchased from Saarchem or Merck, while 1,4-dithiothreitol (DTT) was obtained from Roche.

3.6.1 HIV-1 Protease Linearity Assays

A certain volume of assay buffer [50mM NaOAc, 200mM NaCl, 10% (v/v) glycerol, pH 4.9, 5mM DTT] was added to a solution of HIV substrate III (10μL, 760μM) in a UV cuvette, followed by the addition of aliquots (0 to 10μL) of an aqueous solution of HIV-

1 protease (3.8μM) which started the reaction. The assay buffer volumes were adjusted to give a constant total assay volume (411μL). The spectrophotometer was set to measure the decrease in absorbance at 300nm, at 5 min intervals, at 25°C. All of the HIV-1 protease linearity assays were carried out in duplicate.

3.6.2 HIV Protease Substrate III Dependence Assays

An aqueous solution of HIV protease substrate III (0 to 40μL, 760μM) was added to a certain volume of assay buffer in a UV cuvette, followed by the addition of protease (4 μL, 3.8μM) which started the reaction. The assay buffer volumes were adjusted to give a constant total assay volume (411μL). The spectrophotometer was set to measure the decrease in absorbance at 300nm, at 5 min. intervals, at 25°C. All of the HIV-1 protease substrate dependence assays were carried out in triplicate.

3.6.3 Inhibition Assay using Chromone Derivatives

An aqueous solution of HIV protease substrate III (10μL, 760μM) was mixed with varying volumes of a 254 μM stock solution of the chromone derivative **258** in DMSO. Aliquots (16 μL, 32 μL, 35 μL and 41 μL) were added to a certain volume of assay buffer (adjusted to give a constant total assay volume of 411μL) in a UV cuvette, followed by an aqueous solution of HIV-1 protease (4 μL, 3.8μM) to start the reaction. The buffer solution (411μL) was used as the blank and DMSO (40μL) was used as the control. The spectrophotometer was set to measure the decrease in absorbance at 300nm, at 5 min. intervals, at 25°C. Each assay was carried out in triplicate. Inhibition assays were also carried out using the same method for the chromone derivative **263** (0 - 40 μL, 303 μM) and the chromone derivative **266** (10μL, 20μLand 30μL, 289μM).

3.6.4 Evaluation of K_m, V_{max} and K_i

The kinetic data obtained from the HIV-1 protease inhibition assays for the chromone derivatives **258**, **263** and **266** were processed using the UV Kinlab software and the Grafit 5 programme was used to plot all the graphs. Lineweaver-Burk plots were constructed from the data to obtain the Michaelis constant (K_m) and maximum initial velocity (V_{max}) as well as to determine type of inhibition occurring in each case. Dixon plots were also constructed to determine the inhibition constants (K_i) of the specific inhibitors.

The experimental data obtained from the above assays and used to plot the graphs in Figures 66 – are tabulated in the pages which follow.

Data used for **Figure 66**. Linearity dependence Plot.

Volume µL	[HIV-1 PR] µM	v_0 units/minute
0	0	0
0	0	0
2	0.018491	84.53164776
2	0.018491	101.9501186
4	0.036983	236.1262102
4	0.036983	202.7072705
6	0.055474	264.6157509
6	0.055474	259.1745169
8	0.073966	207.3544017
8	0.073966	340.8836437
10	0.092457	191.7226177
10	0.092457	340.3877679

Data used for **Figure 67a**. Michaelis-Menten Plot

Volume μL	[HIV-1 PR] μM	v_0 units/minute
0	0	0
0	0	0
0	0	0
5	9.245742	76.62
5	9.245742	94.68
5	9.245742	86.76
10	18.49148	124.62
10	18.49148	124.62
10	18.49148	126.48
15	27.73723	155.34
15	27.73723	142.26
15	27.73723	160.38
20	36.98297	195.3
20	36.98297	178.26
20	36.98297	192.54
40	73.96594	225.06
40	73.96594	226.08
40	73.96594	256.44

Data used for **Figure 67b**. Lineweaver-Burk Plot

Volume μL	[HIV-1 PR] μM	1/ [HIV-1 PR] μM^{-1}	v_0 units/minute	$1/v_0$ minute/ units
0	0	-	0	2.229654
0	0	-	0	1.80538
0	0	-	0	217.3913
5	9.245742	0.108158	76.62	7.830854
5	9.245742	0.108158	94.68	6.337136
5	9.245742	0.108158	86.76	6.915629
10	18.49148	0.054079	124.62	4.814636
10	18.49148	0.054079	124.62	4.814636
10	18.49148	0.054079	126.48	4.743833
15	27.73723	0.036053	155.34	3.862495
15	27.73723	0.036053	142.26	4.21763
15	27.73723	0.036053	160.38	3.741115
20	36.98297	0.027039	195.3	3.072197
20	36.98297	0.027039	178.26	3.36587
20	36.98297	0.027039	192.54	3.116236
40	73.96594	0.01352	225.06	2.665956
40	73.96594	0.01352	226.08	2.653928
40	73.96594	0.01352	256.44	2.339729

Data used for **Figure 67c**. Hanes-Woolf Plot

Volume μL	[HIV-1 PR] μM	v_0 units/minute	[HIV-1 PR] / v_0 μM.minute.units^{-1}
0	0	0	-
0	0	0	-
0	0	0	-
5	9.245742	76.62	0.12067
5	9.245742	94.68	0.097653
5	9.245742	86.76	0.106567
10	18.49148	124.62	0.148383
10	18.49148	124.62	0.148383
10	18.49148	126.48	0.146201
15	27.73723	155.34	0.178558
15	27.73723	142.26	0.194976
15	27.73723	160.38	0.172947
20	36.98297	195.3	0.189365
20	36.98297	178.26	0.207466
20	36.98297	192.54	0.192079
40	73.96594	225.06	0.32865
40	73.96594	226.08	0.327167
40	73.96594	256.44	0.288434

Data used for **Figures 68 a and b**

[Compound **252**] μM	Enzyme Activity units/min.	Enzyme Activity (%)	[Compound **260**] μM	Enzyme Activity units/min.	Enzyme Activity (%)
0	0.0027	100	0	0.0015	100
0	0.0022	100	0	0.0015	100
0	0.0025	100	0	0.0016	100
19.78	0.0016	59.26	3.52	0.0013	83.85
19.78	0.0016	59.26	3.52	0.0013	84.21
19.78	0.0014	51.85	3.52	0.0014	88.15
22.25	0.0013	48.15	7.03	0.0014	73.48
22.25	0.0011	40.74	7.03	0.0010	68.15
24.72	0.0013	48.15	7.03	0.0011	69.38
24.72	0.0016	59.26	10.88	0.0012	79.25
24.72	0.0013	48.15	10.88	0.0011	70.43
25.96	0.0009	33.33	10.88	0.0010	65.09
25.96	0.0013	48.15	14.50	0.0010	64.20
25.96	0.0013	48.15	14.50	0.0008	52.08
29.05	0.0009	33.33	14.50	0.0008	51.89
29.05	0.0006	33.33	18.13	0.0007	47.60
29.05	0.0013	22.22	18.13	0.0007	47.45
32.75	0.0009	48.15	18.13	0.0009	58.36
32.75	0.0007	33.33	21.75	0.0008	52.53
32.75	0.0007	25.93	21.75	0.0007	48.19
37.08	0.0008	25.93	21.75	0.0007	47.09
37.08	0.0011	40.74	29.00	0.00038	25.16

					Experimental
37.08	0.00012	4.44	29.00 29.00 36.25 36.25	0.0002 0.0002 0.0009	13.44 11.47 57.26 62.43

Data used for Figure 69a. Lineweaver-Burk plot when [chromone derivative **252**] is 0μM

1/ [HIV-1 PR substrate III] μM^{-1}	v_0 units/minute	$1/v_0$ minute/units
0.00	8.1291142	0.1230146
0.108158	85.374339	0.0117131
0.054079	125.23389	0.0079851
0.036053	152.26829	0.0065674
0.027039	188.3968	0.0053079
0.01352	234.99884	0.0042553

Data used for Figure 69a. Lineweaver-Burk plot when [chromone derivative **252**] is 10μM

1/ [HIV-1 PR substrate III] μM^{-1}	v_0 units/minute	$1/v_0$ minute/units
0.00	3.723309	0.268578
0.108158	66.1032	0.015128
0.054079	116.1418	0.00861
0.036053	108.1852	0.009243
0.027039	167.236	0.00598
0.01352	186.0281	0.005376

Data used for **Figure 69a.** Lineweaver-Burk plot when [chromone derivative **252**] is 22μM

1/ [HIV-1 PR substrate III] μM^{-1}	v_0 units/minute	$1/v_0$ minute/units
0.00	40.80228	0.024508
0.108158	42.36827	0.023603
0.054079	64.65627	0.015466
0.036053	129.7364	0.007708
0.027039	107.1587	0.010835
0.01352	92.29456	0.009332

Data used for **Figure 69b.** Dixon plot

[chromone derivative **252**] μM^{-1}	$1/v_0$ minute/units when [substrate] is 9.25μM	$1/v_0$ minute/units when [substrate] is 18.25μM
0.00	0.01	0.01
10.00	0.15	0.09
20.00	0.16	0.09
22.00	0.24	0.15
25.00	0.25	0.15

Data used for **Figure 70a.** Lineweaver-Burk plot when [chromone derivative **260**] is 0μM

1/ [HIV-1 PR substrate III] μM^{-1}	v_0 units/minute	$1/v_0$ minute/units
0.00	8.1291142	0.1230146
0.108158	85.374339	0.0117131
0.054079	125.23389	0.0079851
0.036053	152.26829	0.0065674
0.027039	188.3968	0.0053079
0.01352	234.99884	0.0042553

Data used for **Figure 70a.** Lineweaver-Burk plot when [chromone derivative **260**] is 7.03μM

1/ [HIV-1 PR substrate III] μM^{-1}	v_0 units/minute	$1/v_0$ minute/units
0.00	2.478043	0.403544
0.108158	42.15914	0.02372
0.054079	71.93778	0.013901
0.036053	88.91899	0.011246
0.027039	101.1136	0.00989
0.01352	128.7195	0.007769

Data used for **Figure 70a.** Lineweaver-Burk plot when [chromone derivative **260**] is 14.5μM

1/ [HIV-1 PR substrate III] μM^{-1}	v_0 units/minute	$1/v_0$ minute/units
0.00	7.40171	0.135104
0.108158	49.96784	0.020013
0.054079	101.4901	0.009853
0.036053	95.60087	0.01046
0.027039	110.0482	0.009087
0.01352		

Data used for **Figure 70b.** Dixon plot

[chromone derivative **260**] μM^{-1}	$1/v_0$ minute/units when [substrate] is 18.49μM	$1/v_0$ minute/units when [substrate] is 27.73μM
0.00	0.010347	0.006009
7.03	0.013901	0.011246
14.5	0.009853	0.01046
21.75	0.036977	0.017709

3.7 Computer Modelling

Molecular modelling was performed on a Silicon Graphics O^2 work-station using the CERIUS^2 version 4.5 modelling platform; the Drieding force field was used for energy minimization and the LigandFit module was used to explore the interactions between the HIV-1 protease receptor cavity and the synthetic inhibitors during docking.

The binding energies (kcal.mol^{-1}) for each of the twenty conformers of compounds **2**, **222**, **222**, **241**, **258**, **260**, **266**, **269**, **272** and **274** that were scored in the HIV-1 protease receptor cavity, are tabulated below.

No. of score	Comp. **222**	Comp. **245**	Comp. **263**	Comp. **266**	Comp. **269**	Comp. **272**	Comp. **274**
1	252.2	204.7	156.4	155.2	160.3	139.9	156.1
2	243.8	203.2	154.8	140.4	133.0	108.1	154.4
3	241.9	197.5	119.7	114.3	117.8	83.3	153.0
4	240.8	193.3	116.2	103.1	104.1	81.9	152.7
5	234.3	191.3	114.9	97.9	103.0	70.0	152.4
6	222.6	188.9	109.3	90.4	88.3	69.7	149.7
7	222.3	186.0	108.7	89.6	84.2	60.0	145.6
8	218.4	179.1	108.0	87.6	83.7	57.5	141.6
9	213.2	174.7	107.6	83.2	79.7	57.3	140.5
10	198.1	163.9	105.3	76.8	78.4	54.9	140.1
11	195.9	160.7	105.0	74.1	78.1	48.3	139.8
12	190.9	150.2	103.8	71.6	77.4	45.1	137.0
13	184.2	141.8	101.9	71.1	69.6	40.5	135.2
14	181.0	136.3	101.8	70.8	67.5	36.6	133.9
15	169.1	131.3	99.4	69.9	60.2	36.4	133.7
16	165.8	115.1	97.3	69.7	58.6	34.9	133.5
17	149.3	106.3	93.4	66.7	55.1	32.4	132.3
18	128.3	88.8	93.0	65.1	53.9	31.3	131.4
19	127.4	76.5	90.2	64.1	48.8	29.6	131.3
20	97.2	61.6	87.8	60.9	46.7	29.5	129.4

3.8 CHEMICAL KINETIC STUDIES

^{1}H-NMR spectroscopic data, obtained on a Bruker Avance 400MHz spectrometer, at 298K, were used for the kinetic studies. Reactants were weighed and then transferred into 1ml graduated NMR tube in the order: 3-methoxy-2-nitrobenzaldehyde, trimethoxybenzene (TMB), DABCO and, finally, $CDCl_3$. The resulting mixture was allowed to dissolve completely which normally takes about 5min, and the methyl vinyl ketone (MVK) was then added to increase the volume of the solution to *1.0* mL. The resulting sample was then placed in the NMR spectrometer to run the first spectrum; subsequent spectra were run at 10min intervals for a period of 14 hours.

The experimental procedures for each of these four aryl aldehydes examined reaction mixtures were as follows:

1. Methyl vinyl ketone (0.370 mL, 4.44 mmol) was added to a solution of 3-methoxy-2-nitrobenzaldehyde (0.119 g, 0.657 mmol), trimethoxybenzene (0.0172 g, 0.105 mmol), DABCO (0.0353 g, 0.315 mmol) and $CDCl_3$ (0.53mL,). The reaction mixture was placed in the NMR and allowed to run for 14hours. The data obtained was converted into concentration using the trimethoxybenzene (TMB) as the standard. The results obtained gave linear first-order plot with respect to 3-methoxy-2-nitrobenzaldehyde and second-order plot with respect to MVK, the entire reaction was found to be pseudo second-order.

2. The procedure used in experiment 1 was followed using: 3-methoxy-2-nitrobenzaldehyde (0.238 g, 1.11 mmol), trimethoxybenzene (0.014g, 0.0832mmol), DABCO (0.0366g, 0.326mmol), $CDCl_3$ (0.53mL) and MVK (0.37mL, 4.44 mmol) to make the total volume of 1 mL. The results obtained gave linear first-order plot with respect to 3-methoxy-2-nitrobenzaldehyde and second-order plot with respect to MVK, the entire reaction was found to be pseudo second-order.

3. The procedure used in experiment 1 was followed using: 3-methoxy-2-nitrobenzaldehyde (0.119g, 0.657 mmol), trimethoxybenzene (0.014g, 0.0832mmol), DABCO (0.0366g, 0.326mmol), $CDCl_3$ (0.16mL) and MVK (0.74mL, 8.89 mmol) to make the total volume of 1 mL. The results obtained gave linear first-order plot with respect to 3-methoxy-2-nitrobenzaldehyde and second-order plot with respect to MVK, the entire reaction was found to be pseudo second-order.

4. The procedure used in experiment 1 was followed using: 2-chloro-6-nitrobenzaldehyde (0.101g, 0.544mmol), trimethoxybenzene (0.0126g, 0.0749mmol), DABCO (0.0316g, 0.282mmol), $CDCl_3$ (0.53mL) and MVK (0.37mL, 4.44 mmol) to make the total volume of 1 mL. The results obtained gave linear first-order plot with respect to 3-methoxy-2-nitrobenzaldehyde and second-order plot with respect to MVK, the entire reaction was found to be pseudo second-order.

5. The procedure used in experiment 1 was followed using: 5-chloro-6-nitrobenzaldehyde (0.101g, 0.545mmol), trimethoxybenzene (0.0126g, 0.0749mmol), DABCO (0.0320g, 0.285mmol), $CDCl_3$ (0.53mL) and MVK (0.37mL, 4.44 mmol) to make the total volume of 1 mL. The results obtained gave linear first-order plot with respect to 3-methoxy-2-nitrobenzaldehyde and second-order plot with respect to MVK, the entire reaction was found to be pseudo second-order.

6. The procedure used in experiment 1 was followed using: 4-nitrobenzaldehyde (0.102g, 0.672mmol), trimethoxybenzene (0.0193g, 0.0115mmol), DABCO (0.0375g, 0.334mmol), $CDCl_3$ (0.53mL) and MVK (0.37mL, 4.44 mmol) to make the total volume of 1 mL. The results obtained gave linear first-order plot with respect to 3-methoxy-2-nitrobenzaldehyde and second-order plot with respect to MVK, the entire reaction was found to be pseudo second-order.

The experimenta data obtained from NMR studies and used to plot the graphs in Figures 106 – 116 and for the determination of rate constants for compounds 275a, 275f, 280 and 281 are tabulated below.

Data used for Figures 108, 110 and 112

time sec.	[A] M	[B] M	[E] M	$[F]_{syn}$ M	$[F]_{anti}$ M	[H] M	[R] + [P] M
0	0.7305	4.9387	0.0000	0.0000	0.0000	0.0000	0.7305
420	0.4814	3.7800	0.0469	0.0574	0.0969	0.0174	0.7831
1051	0.3930	3.6672	0.0682	0.0969	0.1043	0.0343	0.7970
1684	0.3104	3.5765	0.0973	0.1209	0.0984	0.0375	0.7854
2316	0.2360	3.3521	0.1085	0.1399	0.1008	0.0497	0.7598
2953	0.1942	3.4102	0.1267	0.1593	0.1070	0.0718	0.7837
3584	0.1546	3.3707	0.1337	0.1701	0.1085	0.0727	0.7732
4217	0.1174	3.3358	0.1310	0.1856	0.1136	0.0826	0.7627
4848	0.0872	3.2765	0.1500	0.1949	0.1163	0.0921	0.7790
5481	0.0674	3.3544	0.1546	0.1973	0.1112	0.1064	0.7622
6113	0.0535	3.1288	0.1546	0.2015	0.1174	0.1148	0.7639
6746	0.0233	3.1602	0.1546	0.2019	0.1263	0.1256	0.7476
7378	0.0233	3.0835	0.1543	0.2093	0.1333	0.1267	0.7685
8010	0.0105	3.0719	0.1554	0.2035	0.1260	0.1401	0.7377
8644	0.0000	2.8556	0.1581	0.2147	0.1325	0.1503	0.7581
9277	0.0000	2.9254	0.1597	0.2182	0.1368	0.1692	0.7720
9910	0.0000	2.9137	0.1608	0.2136	0.1364	0.1686	0.7662
10543	0.0000	2.9544	0.1570	0.2147	0.1457	0.1866	0.7761
11176	0.0000	2.7963	0.1558	0.2136	0.1411	0.1886	0.7656
11809	0.0000	2.9230	0.1535	0.2147	0.1422	0.1916	0.7656
12442	0.0000	2.9463	0.1597	0.2174	0.1411	0.2093	0.7773
13076	0.0000	2.9219	0.1543	0.2190	0.1453	0.2154	0.7779
13709	0.0000	2.8242	0.1492	0.2104	0.1535	0.2244	0.7697
14343	0.0000	2.8033	0.1496	0.2186	0.1481	0.2317	0.7744
14974	0.0000	2.8265	0.1438	0.2070	0.1558	0.2357	0.7598
15607	0.0000	2.7742	0.1461	0.2112	0.1593	0.2453	0.7749
16240	0.0000	2.7742	0.1422	0.2104	0.1601	0.2535	0.7691
16873	0.0000	2.7184	0.1446	0.2136	0.1647	0.2610	0.7842
17505	0.0000	2.7033	0.1395	0.2101	0.1659	0.2651	0.7732
18138	0.0000	2.7754	0.1384	0.2120	0.1744	0.2793	0.7872
18772	0.0000	2.6928	0.1426	0.2093	0.1709	0.2825	0.7842
19406	0.0000	2.6859	0.1349	0.2108	0.1732	0.2892	0.7784
20039	0.0000	2.6138	0.1302	0.2116	0.1806	0.3003	0.7837
	0.0000						

Experimental

20672	0.0000	2.5766	0.1353	0.2042	0.1756	0.3035	0.7726
21305	0.0000	2.7149	0.1329	0.2089	0.1802	0.3119	0.7831
21937	0.0000	2.6103	0.1298	0.2035	0.1818	0.3200	0.7726
22571	0.0000	2.5963	0.1298	0.2062	0.1845	0.3293	0.7808
23204	0.0000	2.5905	0.1287	0.2066	0.1829	0.3282	0.7773
23836	0.0000	2.5940	0.1267	0.1996	0.1899	0.3535	0.7744
24470	0.0000	2.5731	0.1178	0.2062	0.1907	0.3471	0.7720
25103	0.0000	2.5638	0.1205	0.2073	0.1887	0.3622	0.7749
25737	0.0000	2.5417	0.1186	0.1957	0.1934	0.3712	0.7616
26370	0.0000	2.5091	0.1201	0.2031	0.1977	0.3741	0.7813
27003	0.0000	2.5126	0.1232	0.2062	0.2000	0.3628	0.7941
27635	0.0000	2.4894	0.1186	0.2019	0.1980	0.3817	0.7779
28267	0.0000	2.4463	0.1163	0.2054	0.1992	0.3901	0.7813
28867	0.0000	2.4545	0.1085	0.2031	0.2097	0.3982	0.7819
29533	0.0000	2.4173	0.1167	0.2027	0.2077	0.4043	0.7906
30167	0.0000	2.4266	0.1136	0.2035	0.2066	0.4084	0.7854
30799	0.0000	2.3394	0.1132	0.2035	0.2128	0.4194	0.7941
31434	0.0000	2.4138	0.1139	0.2019	0.2124	0.4200	0.7924
32066	0.0000	2.4115	0.1105	0.2023	0.2201	0.4264	0.7994
32700	0.0000	2.3812	0.1116	0.2004	0.2186	0.4276	0.7959
33333	0.0000	2.3975	0.1112	0.2015	0.2198	0.4357	0.7988
33966	0.0000	2.3417	0.1039	0.2042	0.2170	0.4427	0.7877
34599	0.0000	2.3696	0.1046	0.2008	0.2236	0.4442	0.7935
35231	0.0000	2.2975	0.1008	0.1988	0.2178	0.4549	0.7761
35865	0.0000	2.3231	0.1050	0.1992	0.2182	0.4587	0.7837
36497	0.0000	2.2754	0.1050	0.1969	0.2244	0.4662	0.7895
37131	0.0000	2.2696	0.1015	0.1980	0.2248	0.4535	0.7866
37764	0.0000	2.2696	0.1043	0.2050	0.2314	0.4753	0.8110
38397	0.0000	2.2545	0.1039	0.1922	0.2314	0.4808	0.7912
39030	0.0000	2.2557	0.0992	0.1949	0.2302	0.4715	0.7866
39662	0.0000	2.1998	0.0992	0.1996	0.2376	0.4933	0.8046
40295	0.0000	2.1894	0.0973	0.2011	0.2372	0.5005	0.8034
40929	0.0000	2.2301	0.0853	0.1996	0.2418	0.4988	0.7901
41563	0.0000	2.1638	0.0969	0.1973	0.2380	0.5020	0.7982
42197	0.0000	2.1010	0.0942	0.1957	0.2395	0.5066	0.7941
42831	0.0000	2.1487	0.0942	0.1965	0.2407	0.4982	0.7970
43465	0.0000	2.0998	0.0915	0.1973	0.2426	0.5017	0.7970
44099	0.0000	2.1138	0.0903	0.1938	0.2426	0.5035	0.7901
44733	0.0000	2.1150	0.0934	0.1980	0.2446	0.5142	0.8040
45367	0.0000	2.0405	0.0810	0.1965	0.2442	0.5235	0.7825
46001	0.0000	2.0743	0.0868	0.1930	0.2477	0.5255	0.7912
46635	0.0000	2.0650	0.0857	0.1965	0.2511	0.5409	0.7999
47269	0.0000	2.0394	0.0868	0.1946	0.2477	0.5284	0.7935
47903	0.0000	2.0533	0.0895	0.1922	0.2496	0.5296	0.7970
48537	0.0000	2.0603	0.0864	0.2008	0.2577	0.5459	0.8174

						Experimental	
49171	0.0000	2.0405	0.0864	0.1949	0.2542	0.5337	0.8034
49805	0.0000	2.0068	0.0868	0.1930	0.2573	0.5607	0.8058
50439	0.0000	1.9975	0.0822	0.1806	0.2558	0.5505	0.7779
51073	0.0000	2.1801	0.0814	0.2004	0.2554	0.5636	0.8058
51707	0.0000	1.9929	0.0779	0.1946	0.2612	0.5572	0.8005
52341	0.0000	1.9092	0.0826	0.1810	0.2608	0.5700	0.7866
52975		1.9557	0.0818	0.1926	0.2581	0.5689	0.7988

Data used for Figure 106 and 107

Uncorrected time (s)	Corrected time (s)	[A] (M)	-ln[A] Exp.	-ln[A] Calc.
0	0	0.7305	0.3140	0.3138
631	420	0.4814	0.7311	0.5130
1051	1051	0.3930	0.9340	0.8123
1684	1684	0.3104	1.1698	1.1126
2316	2316	0.2360	1.4438	1.4123
2953	2953	0.1942	1.6390	1.7145
3584	3584	0.1546	1.8667	2.0138
4217	4217	0.1174	2.1419	2.3141
4848	4848	0.0872	2.4395	2.6134
5481	5481	0.0674	2.6966	2.9136
6113	6113	0.0535	2.9284	3.2134
6746	6746	0.0233	3.7613	3.5137
7378	7378	0.0233	3.7613	3.8134
8010	8010	0.0105	4.5598	4.1132

Data used for Figure 109

time (s)	[E] (M)	[Ecorr] (M)	$[E] - [E]_{mod}$ (M)
0	0.0000	0.2570	0.0000
420	0.0469	0.2559	0.0715
1051	0.0682	0.2542	0.1052
1684	0.0973	0.2524	0.1505
2316	0.1085	0.2507	0.1691
2953	0.1267	0.2490	0.1982
3584	0.1337	0.2472	0.2104
4217	0.1310	0.2455	0.2080
4848	0.1500	0.2438	0.2382
5481	0.1546	0.2421	0.2469
6113	0.1546	0.2403	0.2487
6746	0.1546	0.2386	0.2504
7378	0.1543	0.2369	0.2515

Experimental

8010	0.1554	0.2352	0.2550
8644	0.1581	0.2334	0.2608
9277	0.1597	0.2317	0.2649
9910	0.1608	0.2300	0.2683
10543	0.1570	0.2282	0.2643
11176	0.1558	0.2265	0.2642
11809	0.1535	0.2248	0.2625
12442	0.1597	0.2230	0.2735
13076	0.1543	0.2213	0.2671
13709	0.1492	0.2196	0.2613
14343	0.1496	0.2179	0.2636
14974	0.1438	0.2161	0.2566
15607	0.1461	0.2144	0.2618
16240	0.1422	0.2127	0.2577
16873	0.1446	0.2109	0.2629
17505	0.1395	0.2092	0.2571
18138	0.1384	0.2075	0.2571
18772	0.1426	0.2058	0.2652
19406	0.1349	0.2040	0.2553
20039	0.1302	0.2023	0.2501
20672	0.1353	0.2006	0.2594
21305	0.1329	0.1988	0.2576
21937	0.1298	0.1971	0.2547
22571	0.1298	0.1954	0.2564
23204	0.1287	0.1936	0.2564
23836	0.1267	0.1919	0.2552
24470	0.1178	0.1902	0.2436
25103	0.1205	0.1885	0.2494
25737	0.1186	0.1867	0.2482
26370	0.1201	0.1850	0.2523
27003	0.1232	0.1833	0.2586
27635	0.1186	0.1815	0.2534
28267	0.1163	0.1798	0.2516
28867	0.1085	0.1782	0.2416
29533	0.1167	0.1764	0.2557
30167	0.1136	0.1746	0.2528
30799	0.1132	0.1729	0.2539
31434	0.1139	0.1712	0.2568
32066	0.1105	0.1694	0.2533
32700	0.1116	0.1677	0.2568
33333	0.1112	0.1660	0.2579
33966	0.1039	0.1642	0.2486
34599	0.1046	0.1625	0.2515
35231	0.1008	0.1608	0.2474
35865	0.1050	0.1591	0.2555

Experimental

36497	0.1050	0.1573	0.2573
37131	0.1015	0.1556	0.2538
37764	0.1043	0.1539	0.2596
38397	0.1039	0.1521	0.2607
39030	0.0992	0.1504	0.2555
39662	0.0992	0.1487	0.2572
40295	0.0973	0.1469	0.2560
40929	0.0853	0.1452	0.2397
41563	0.0969	0.1435	0.2589
42197	0.0942	0.1418	0.2566
42831	0.0942	0.1400	0.2583
43465	0.0915	0.1383	0.2560
44099	0.0903	0.1366	0.2559
44733	0.0934	0.1348	0.2623
45367	0.0810	0.1331	0.2455
46001	0.0868	0.1314	0.2559
46635	0.0857	0.1296	0.2559
47269	0.0868	0.1279	0.2594
47903	0.0895	0.1262	0.2652
48537	0.0864	0.1244	0.2623
49171	0.0864	0.1227	0.2640
49805	0.0868	0.1210	0.2663
50439	0.0822	0.1192	0.2611
51073	0.0814	0.1175	0.2616
51707	0.0779	0.1158	0.2581
52341	0.0826	0.1140	0.2668
52975	0.0818	0.1123	0.2674

$E = [Ecorr]_{initial} - [Ecorr]_{final}$

Data used for Figures 113 and 114

time sec.	[E] (M)	$[F]_{syn}$ (M)	$[F]_{anti}$ (M)	$[F]_{tot}$ (M)	$[F]_{tot} - [E]$ (M)
0	0.0000	0.0000	0.0000	0.0000	0.0000
420	0.0469	0.0574	0.0969	0.2314	0.1610
1051	0.0682	0.0969	0.1043	0.3017	0.1994
1684	0.0973	0.1209	0.0984	0.3290	0.1831
2316	0.1085	0.1399	0.1008	0.3610	0.1982
2953	0.1267	0.1593	0.1070	0.3994	0.2093
3584	0.1337	0.1701	0.1085	0.4180	0.2174
4217	0.1310	0.1856	0.1136	0.4488	0.2523
4848	0.1500	0.1949	0.1163	0.4668	0.2418
5481	0.1546	0.1973	0.1112	0.4628	0.2308
6113	0.1546	0.2015	0.1174	0.4785	0.2465
6746	0.1546	0.2019	0.1263	0.4924	0.2604
7378	0.1543	0.2093	0.1333	0.5139	0.2825

Experimental

8010	0.1554	0.2035	0.1260	0.4942	0.2610
8644	0.1581	0.2147	0.1325	0.5209	0.2837
9277	0.1597	0.2182	0.1368	0.5325	0.2930
9910	0.1608	0.2136	0.1364	0.5250	0.2837
10543	0.1570	0.2147	0.1457	0.5407	0.3052
11176	0.1558	0.2136	0.1411	0.5319	0.2982
11809	0.1535	0.2147	0.1422	0.5354	0.3052
12442	0.1597	0.2174	0.1411	0.5378	0.2982
13076	0.1543	0.2190	0.1453	0.5465	0.3151
13709	0.1492	0.2104	0.1535	0.5459	0.3221
14343	0.1496	0.2186	0.1481	0.5500	0.3256
14974	0.1438	0.2070	0.1558	0.5441	0.3285
15607	0.1461	0.2112	0.1593	0.5558	0.3366
16240	0.1422	0.2104	0.1601	0.5558	0.3424
16873	0.1446	0.2136	0.1647	0.5674	0.3506
17505	0.1395	0.2101	0.1659	0.5639	0.3546
18138	0.1384	0.2120	0.1744	0.5796	0.3721
18772	0.1426	0.2093	0.1709	0.5703	0.3564
19406	0.1349	0.2108	0.1732	0.5761	0.3738
20039	0.1302	0.2116	0.1806	0.5883	0.3930
20672	0.1353	0.2042	0.1756	0.5697	0.3668
21305	0.1329	0.2089	0.1802	0.5837	0.3843
21937	0.1298	0.2035	0.1818	0.5779	0.3831
22571	0.1298	0.2062	0.1845	0.5860	0.3913
23204	0.1287	0.2066	0.1829	0.5843	0.3913
23836	0.1267	0.1996	0.1899	0.5843	0.3942
24470	0.1178	0.2062	0.1907	0.5953	0.4186
25103	0.1205	0.2073	0.1887	0.5941	0.4133
25737	0.1186	0.1957	0.1934	0.5837	0.4058
26370	0.1201	0.2031	0.1977	0.6011	0.4209
27003	0.1232	0.2062	0.2000	0.6093	0.4244
27635	0.1186	0.2019	0.1980	0.6000	0.4221
28267	0.1163	0.2054	0.1992	0.6069	0.4325
28867	0.1085	0.2031	0.2097	0.6191	0.4564
29533	0.1167	0.2027	0.2077	0.6157	0.4407
30167	0.1136	0.2035	0.2066	0.6151	0.4447
30799	0.1132	0.2035	0.2128	0.6244	0.4546
31434	0.1139	0.2019	0.2124	0.6215	0.4505
32066	0.1105	0.2023	0.2201	0.6337	0.4680
32700	0.1116	0.2004	0.2186	0.6284	0.4610
33333	0.1112	0.2015	0.2198	0.6319	0.4651
33966	0.1039	0.2042	0.2170	0.6319	0.4761
34599	0.1046	0.2008	0.2236	0.6366	0.4796
35231	0.1008	0.1988	0.2178	0.6250	0.4738
35865	0.1050	0.1992	0.2182	0.6261	0.4686

36497	0.1050	0.1969	0.2244	0.6319	0.4744
37131	0.1015	0.1980	0.2248	0.6343	0.4819
37764	0.1043	0.2050	0.2314	0.6546	0.4982
38397	0.1039	0.1922	0.2314	0.6354	0.4796
39030	0.0992	0.1949	0.2302	0.6377	0.4889
39662	0.0992	0.1996	0.2376	0.6558	0.5069
40295	0.0973	0.2011	0.2372	0.6575	0.5116
40929	0.0853	0.1996	0.2418	0.6622	0.5343
41563	0.0969	0.1973	0.2380	0.6529	0.5075
42197	0.0942	0.1957	0.2395	0.6529	0.5116
42831	0.0942	0.1965	0.2407	0.6558	0.5145
43465	0.0915	0.1973	0.2426	0.6598	0.5226
44099	0.0903	0.1938	0.2426	0.6546	0.5191
44733	0.0934	0.1980	0.2446	0.6639	0.5238
45367	0.0810	0.1965	0.2442	0.6610	0.5395
46001	0.0868	0.1930	0.2477	0.6610	0.5308
46635	0.0857	0.1965	0.2511	0.6715	0.5430
47269	0.0868	0.1946	0.2477	0.6633	0.5331
47903	0.0895	0.1922	0.2496	0.6627	0.5284
48537	0.0864	0.2008	0.2577	0.6877	0.5581
49171	0.0864	0.1949	0.2542	0.6738	0.5441
49805	0.0868	0.1930	0.2573	0.6755	0.5453
50439	0.0822	0.1806	0.2558	0.6546	0.5314
51073	0.0814	0.2004	0.2554	0.6837	0.5616
51707	0.0779	0.1946	0.2612	0.6837	0.5668
52341	0.0826	0.1810	0.2608	0.6627	0.5389
52975	0.0818	0.1926	0.2581	0.6761	0.5534

Data used for Figure 115

time sec.	[B] (M)	1/[B] (M^{-1})
0	4.9387	0.2025
420	3.7800	0.2646
1051	3.6672	0.2727
1684	3.5765	0.2796
2316	3.3521	0.2983
2953	3.4102	0.2932
3584	3.3707	0.2967
4217	3.3358	0.2998
4848	3.2765	0.3052
5481	3.3544	0.2981
6113	3.1288	0.3196
6746	3.1602	0.3164

7378	3.0835	0.3243
8010	3.0719	0.3255
8644	2.8556	0.3502
9277	2.9254	0.3418
9910	2.9137	0.3432
10543	2.9544	0.3385
11176	2.7963	0.3576
11809	2.9230	0.3421
12442	2.9463	0.3394
13076	2.9219	0.3422
13709	2.8242	0.3541
14343	2.8033	0.3567
14974	2.8265	0.3538
15607	2.7742	0.3605
16240	2.7742	0.3605
16873	2.7184	0.3679
17505	2.7033	0.3699
18138	2.7754	0.3603
18772	2.6928	0.3714
19406	2.6859	0.3723
20039	2.6138	0.3826
20672	2.5766	0.3881
21305	2.7149	0.3683
21937	2.6103	0.3831
22571	2.5963	0.3852
23204	2.5905	0.3860
23836	2.5940	0.3855
24470	2.5731	0.3886
25103	2.5638	0.3901
25737	2.5417	0.3934
26370	2.5091	0.3985
27003	2.5126	0.3980
27635	2.4894	0.4017
28267	2.4463	0.4088
28867	2.4545	0.4074
29533	2.4173	0.4137
30167	2.4266	0.4121
30799	2.3394	0.4275
31434	2.4138	0.4143
32066	2.4115	0.4147
32700	2.3812	0.4200
33333	2.3975	0.4171
33966	2.3417	0.4270
34599	2.3696	0.4220
35231	2.2975	0.4353

35865	2.3231	0.4305
36497	2.2754	0.4395
37131	2.2696	0.4406
37764	2.2696	0.4406
38397	2.2545	0.4436
39030	2.2557	0.4433
39662	2.1998	0.4546
40295	2.1894	0.4568
40929	2.2301	0.4484
41563	2.1638	0.4622
42197	2.1010	0.4760
42831	2.1487	0.4654
43465	2.0998	0.4762
44099	2.1138	0.4731
44733	2.1150	0.4728
45367	2.0405	0.4901
46001	2.0743	0.4821
46635	2.0650	0.4843
47269	2.0394	0.4903
47903	2.0533	0.4870
48537	2.0603	0.4854
49171	2.0405	0.4901
49805	2.0068	0.4983
50439	1.9975	0.5006
51073	2.1801	0.4587
51707	1.9929	0.5018
52341	1.9092	0.5238
52975	1.9557	0.5113

Data for the reaction of 4-nitrobenzaldehyde **275a**.

time sec.	[A] (M)	$[F]_{anti}$ (M)	[B] (M)	$[F]_{syn}$ (M)	[E] (M)	[H] (M)	ln[A]
0	0.7470	0.0000	4.8052	0.0000	0.0000	0.0000	0.2916
420	0.3066	0.1526	4.3652	0.0122	0.1004	0.0008	1.1821
636	0.1934	0.1532	4.2344	0.0111	0.1371	0.0028	1.6428
1273	0.1273	0.1607	4.2392	0.0180	0.1620	0.0033	2.0610
1910	0.0834	0.1649	4.1046	0.0183	0.1768	0.0150	2.4836
2546	0.0561	0.1687	4.0148	0.0153	0.1860	0.0239	2.8797
3181	0.0386	0.1683	3.9369	0.0081	0.1888	0.0204	3.2537
3817	0.0270	0.1737	3.8916	0.0178	0.1960	0.0378	3.6112
4453	0.0194	0.1784	3.8465	0.0164	0.2016	0.0436	3.9448
5089	0.0139	0.1851	3.8090	0.0209	0.2055	0.0579	4.2772
5725	0.0099	0.1888	3.7016	0.0208	0.2069	0.0660	4.6122
6361	0.0076	0.1925	3.7047	0.0304	0.2081	0.0826	4.8759
6996	0.0059	0.1996	3.6622	0.0305	0.2106	0.0922	5.1363

Experimental

7633	0.0044	0.2036	3.5787	0.0374	0.2087	0.1045	5.4306
8269	0.0038	0.2053	3.5363	0.0414	0.2068	0.1124	5.5655
8905	0.0034	0.2103	3.4978	0.0475	0.2050	0.1233	5.6937
9540	0.0028	0.2187	3.5029	0.0539	0.2078	0.1316	5.8623
10177	0.0026	0.2201	3.4548	0.0621	0.2030	0.1459	5.9369
10813	0.0024	0.2313	3.4902	0.0688	0.2072	0.1589	6.0348
11450	0.0023	0.2305	3.3960	0.0741	0.2016	0.1639	6.0790
12085	0.0021	0.2332	3.3360	0.0795	0.1995	0.1720	6.1750
12721	0.0018	0.2419	3.3355	0.0879	0.2042	0.1876	6.3238
13357	0.0020	0.2452	3.3309	0.0915	0.2002	0.1957	6.1914
13992	0.0021	0.2507	3.3076	0.0955	0.1993	0.2068	6.1821
14628	0.0020	0.2517	3.2388	0.1020	0.1947	0.2168	6.2013
15264	0.0016	0.2597	3.2390	0.1086	0.2008	0.2265	6.4449
15899	0.0019	0.2633	3.2314	0.1136	0.1951	0.2404	6.2522
16536	0.0015	0.2725	3.2234	0.1177	0.2007	0.2501	6.4736
17173	0.0016	0.2748	3.1823	0.1218	0.1972	0.2578	6.4502
17810	0.0015	0.2817	3.1897	0.1292	0.2002	0.2698	6.5012
18446	0.0016	0.2836	3.1704	0.1295	0.1969	0.2760	6.4341
19085	0.0019	0.2864	3.1390	0.1332	0.1911	0.2860	6.2614
19721	0.0015	0.2915	3.1000	0.1405	0.1942	0.2979	6.4997
20358	0.0018	0.2932	3.0623	0.1399	0.1899	0.2957	6.3114
20993	0.0015	0.2993	3.0578	0.1456	0.1918	0.3118	6.5092
21630	0.0014	0.3025	3.0382	0.1504	0.1914	0.3204	6.5641
22266	0.0014	0.3012	2.9598	0.1528	0.1877	0.3227	6.5690
22922	0.0020	0.3069	2.9856	0.1563	0.1833	0.3398	6.2322
23559	0.0013	0.3118	2.9492	0.1655	0.1889	0.3493	6.6838
24196	0.0014	0.3172	2.9479	0.1669	0.1870	0.3590	6.5881
24833	0.0019	0.3173	2.9152	0.1659	0.1805	0.3613	6.2536
25468	0.0014	0.3243	2.8973	0.1760	0.1856	0.3740	6.5830
26105	0.0013	0.3297	2.9127	0.1791	0.1878	0.3813	6.6389
26748	0.0013	0.3320	2.8722	0.1832	0.1855	0.3897	6.6170
27385	0.0015	0.3379	2.8777	0.1864	0.1861	0.4004	6.4923
28022	0.0013	0.3370	2.8268	0.1888	0.1826	0.4050	6.6373
28658	0.0020	0.3364	2.7859	0.1859	0.1740	0.4087	6.2092
29294	0.0019	0.3414	2.7804	0.1915	0.1779	0.4100	6.2432
29929	0.0019	0.3422	2.7373	0.1907	0.1717	0.4243	6.2535
30566	0.0018	0.3483	2.7440	0.1969	0.1738	0.4343	6.2967
31210	0.0019	0.3514	2.7440	0.1991	0.1758	0.4362	6.2687
31848	0.0014	0.3594	2.7375	0.2091	0.1802	0.4498	6.5719
32484	0.0020	0.3591	2.7135	0.2040	0.1714	0.4571	6.1900
33121	0.0019	0.3575	2.6538	0.2046	0.1687	0.4587	6.2454
33757	0.0018	0.3615	2.6407	0.2091	0.1698	0.4643	6.3139
34426	0.0018	0.3677	2.6391	0.2140	0.1723	0.4734	6.3313
35108	0.0019	0.3690	2.6130	0.2126	0.1686	0.4802	6.2923
35768	0.0017	0.3700	2.5828	0.2160	0.1694	0.4786	6.3521
36409	0.0018	0.3761	2.5944	0.2197	0.1681	0.4951	6.3236
37045	0.0016	0.3768	2.5588	0.2227	0.1684	0.4958	6.4144
37682	0.0014	0.3826	2.5646	0.2281	0.1725	0.5071	6.6057
38319	0.0016	0.3818	2.5176	0.2261	0.1664	0.5143	6.4419
38956	0.0016	0.3919	2.5557	0.2329	0.1725	0.5213	6.4165
39594	0.0019	0.3885	2.5046	0.2291	0.1639	0.5263	6.2906
40229	0.0020	0.3947	2.5137	0.2317	0.1655	0.5364	6.2228
40867	0.0018	0.4003	2.5127	0.2340	0.1663	0.5503	6.3418
41504	0.0018	0.4010	2.4841	0.2350	0.1640	0.5527	6.2983

Experimental

42141	0.0019	0.3993	2.4463	0.2345	0.1628	0.5509	6.2867
42777	0.0019	0.4031	2.4398	0.2345	0.1625	0.5584	6.2438
43420	0.0018	0.4108	2.4420	0.2428	0.1645	0.5730	6.2962
44057	0.0019	0.4130	2.4318	0.2404	0.1624	0.5806	6.2825
44693	0.0016	0.4214	2.4413	0.2505	0.1703	0.5926	6.4527
45075	0.0018	0.4154	2.3827	0.2428	0.1619	0.5863	6.3336

Data for the reaction of 5-chloro-6-nitrobenzaldehyde **280**.

time sec.	[A] (M)	[E] (M)	$[F]_{anti}$ (M)	[B] (M)	$[F]_{syn}$ (M)	[H] (M)	ln[A]
0	0.6053	0.0000	0.0000	4.8053	0.0000	0.0000	0.5020
420	0.2758	0.0022	0.0125	4.4088	0.0140	0.0000.2	1.2880
636	0.2058	0.0079	0.0130	4.3938	0.0166	0.0000.8	1.5806
1273	0.1584	0.0100	0.0124	4.3623	0.0194	0.00029	1.8427
1910	0.1245	0.0105	0.0117	4.3364	0.0213	0.00093	2.0835
2546	0.0986	0.0118	0.0111	4.2909	0.0214	0.00292	2.3168
3181	0.0792	0.0119	0.0115	4.2666	0.0225	0.00338	2.5352
3817	0.0631	0.0141	0.0118	4.2007	0.0234	0.00448	2.7637
4453	0.0501	0.0147	0.0132	4.1548	0.0262	0.00290	2.9945
5089	0.0392	0.0148	0.0137	4.0990	0.0263	0.00852	3.2394
5725	0.0316	0.0149	0.0153	4.0553	0.0266	0.01110	3.4532
6361	0.0255	0.0176	0.0169	4.0221	0.0305	0.01958	3.6683
6996	0.0200	0.0185	0.0181	3.9727	0.0278	0.02730	3.9145
7633	0.0159	0.0168	0.0182	3.9383	0.0280	0.02957	4.1420
8269	0.0124	0.0154	0.0190	3.9213	0.0294	0.02981	4.3940
8905	0.0096	0.0159	0.0192	3.9010	0.0319	0.03623	4.6509
9540	0.0075	0.0159	0.0203	3.8981	0.0355	0.04010	4.8987
10177	0.0054	0.0209	0.0223	3.9026	0.0367	0.07092	5.2178
10813	0.0045	0.0164	0.0216	3.8577	0.0374	0.07610	5.4021
11450	0.0031	0.0231	0.0238	3.8804	0.0374	0.08183	5.7887
12085	0.0028	0.0175	0.0232	3.8449	0.0293	0.06871	5.8819
12721	0.0016	0.0205	0.0245	3.8405	0.0336	0.09169	6.4663
13357	0.0008	0.0224	0.0257	3.8354	0.0356	0.09363	7.1063
13992	0.0013	0.0173	0.0250	3.8064	0.0291	0.08635	6.6505
14628	0.0009	0.0200	0.0264	3.8021	0.0320	0.09777	7.0597
15264	0.0005	0.0222	0.0275	3.7999	0.0350	0.10980	7.5416
15899	0.0001	0.0208	0.0280	3.7814	0.0327	0.11093	9.0000
16536	0.0000	0.0199	0.0278	3.7649	0.0318	0.10984	10.3776
17173	0.0000	0.0215	0.0289	3.7606	0.0344	0.12534	
17810	0.0000	0.0216	0.0293	3.7453	0.0337	0.12986	
18446	0.0000	0.0220	0.0298	3.7311	0.0344	0.13394	
19085	0.0000	0.0183	0.0297	3.7005	0.0283	0.13482	
19721	0.0000	0.0203	0.0310	3.7083	0.0312	0.13523	
20358	0.0000	0.0185	0.0309	3.6721	0.0278	0.13116	
20993	0.0000	0.0202	0.0320	3.6792	0.0319	0.14821	
21630	0.0000	0.0200	0.0321	3.6622	0.0304	0.15058	
22266	0.0000	0.0213	0.0331	3.6538	0.0335	0.15839	
22922	0.0000	0.0200	0.0329	3.6383	0.0308	0.15890	
23559	0.0000	0.0196	0.0336	3.6251	0.0304	0.16296	
24196	0.0000	0.0208	0.0344	3.6207	0.0318	0.16753	

Experimental

24833	0.0000	0.0205	0.0348	3.6002	0.0308	0.17279	
25468	0.0000	0.0233	0.0362	3.6135	0.0353	0.17559	
26105	0.0000	0.0206	0.0360	3.5874	0.0299	0.17864	
26748	0.0000	0.0205	0.0363	3.5830	0.0300	0.18287	
27385	0.0000	0.0204	0.0370	3.5719	0.0297	0.18715	
28022	0.0000	0.0197	0.0369	3.5651	0.0295	0.19029	
28658	0.0000	0.0205	0.0376	3.5439	0.0299	0.19435	
29294	0.0000	0.0205	0.0383	3.5463	0.0299	0.20032	
29929	0.0000	0.0202	0.0388	3.5291	0.0296	0.20416	
30566	0.0000	0.0206	0.0390	3.5235	0.0301	0.20785	
31210	0.0000	0.0209	0.0399	3.5105	0.0297	0.21245	
31848	0.0000	0.0201	0.0400	3.5031	0.0298	0.21599	
32484	0.0000	0.0202	0.0405	3.4894	0.0299	0.21979	
33121	0.0000	0.0204	0.0407	3.4846	0.0292	0.22515	
33757	0.0000	0.0198	0.0413	3.4708	0.0295	0.22741	
34426	0.0000	0.0212	0.0421	3.4677	0.0310	0.23075	
35108	0.0000	0.0208	0.0423	3.4504	0.0297	0.23573	
35768	0.0000	0.0227	0.0432	3.4598	0.0331	0.24553	
36409	0.0000	0.0205	0.0428	3.4383	0.0294	0.24684	
37045	0.0000	0.0219	0.0438	3.4354	0.0305	0.24718	
37682	0.0000	0.0212	0.0439	3.4202	0.0306	0.24863	
38319	0.0000	0.0227	0.0446	3.4287	0.0338	0.26050	
38956	0.0000	0.0213	0.0448	3.4047	0.0303	0.25748	
39594	0.0000	0.0215	0.0455	3.4020	0.0304	0.26206	
40229	0.0000	0.0217	0.0458	3.3884	0.0308	0.26552	
40867	0.0000	0.0230	0.0463	3.3788	0.0331	0.27568	
41504	0.0000	0.0219	0.0461	3.3650	0.0308	0.27250	
42141	0.0000	0.0218	0.0470	3.3562	0.0309	0.27487	
42777	0.0000	0.0221	0.0473	3.3559	0.0316	0.28138	
43420	0.0000	0.0230	0.0474	3.3465	0.0325	0.28893	
44057	0.0000	0.0226	0.0486	3.3467	0.0325	0.29384	
44693	0.0000	0.0216	0.0480	3.3210	0.0303	0.29559	
45352	0.0000	0.0218	0.0492	3.3111	0.0310	0.29877	
46000	0.0000	0.0224	0.0490	3.3020	0.0315	0.30089	
46638	0.0000	0.0215	0.0493	3.2786	0.0303	0.29830	
47274	0.0000	0.0231	0.0496	3.2797	0.0329	0.31019	
47912	0.0000	0.0221	0.0491	3.2656	0.0322	0.31084	
48549	0.0000	0.0222	0.0505	3.2519	0.0308	0.31168	
49185	0.0000	0.0222	0.0507	3.2585	0.0309	0.31462	
49822	0.0000	0.0222	0.0508	3.2513	0.0320	0.32226	
50459	0.0000	0.0221	0.0514	3.2418	0.0307	0.32752	
51096	0.0000	0.0227	0.0519	3.2287	0.0319	0.32789	
51738	0.0000	0.0226	0.0521	3.2200	0.0316	0.33016	
52376	0.0000	0.0222	0.0523	3.2094	0.0315	0.33371	

Data for the reaction of 2-chloro-6-nitrobenzaldehyde **281**.

time sec.	[A] (M)	[E] (M)	$[F]_{anti}$ (M)	[B] (M)	$[F]_{syn}$ (M)	[H] (M)	ln[A]
0	0.6047	0.0000	0.0000	4.8053	0.0000	0.0000	0.5030
420	0.5298	0.1112	0.0464	2.1026	0.0030	0.0007	0.6352
636	0.5164	0.1280	0.0473	2.1499	0.0045	0.0064	0.6609
1273	0.4913	0.1353	0.0432	2.1319	0.0070	0.0132	0.7108
1910	0.4687	0.1418	0.0430	2.1066	0.0081	0.0202	0.7578
2546	0.4534	0.1476	0.0448	2.1046	0.0081	0.0266	0.7910
3181	0.4243	0.1498	0.0558	2.0431	0.0133	0.0465	0.8573
3817	0.4041	0.1492	0.0549	2.0168	0.0159	0.0486	0.9062
4453	0.3768	0.1470	0.0640	1.9524	0.0178	0.0576	0.9761
5089	0.3603	0.1478	0.0644	1.9342	0.0192	0.0651	1.0208
5725	0.3417	0.1484	0.0727	1.9032	0.0219	0.0762	1.0738
6361	0.3205	0.1485	0.0779	1.8454	0.0238	0.0875	1.1378
6996	0.3095	0.1498	0.0837	1.8413	0.0292	0.0959	1.1728
7633	0.2965	0.1502	0.0841	1.8123	0.0302	0.0989	1.2156
8269	0.2891	0.1519	0.0885	1.8116	0.0348	0.1099	1.2410
8905	0.2804	0.1515	0.0944	1.7941	0.0339	0.1162	1.2716
9540	0.2749	0.1527	0.0962	1.7952	0.0362	0.1223	1.2913
10177	0.2668	0.1515	0.1004	1.7724	0.0367	0.1266	1.3211
10813	0.2620	0.1538	0.1119	1.7790	0.0375	0.1414	1.3395
11450	0.2520	0.1507	0.1096	1.7404	0.0376	0.1431	1.3782
12085	0.2470	0.1486	0.1191	1.7389	0.0381	0.1545	1.3984
12721	0.2408	0.1459	0.1217	1.7315	0.0383	0.1592	1.4237
13357	0.2356	0.1437	0.1261	1.7227	0.0403	0.1638	1.4456
13992	0.2314	0.1409	0.1304	1.7249	0.0397	0.1707	1.4634
14628	0.2265	0.1394	0.1372	1.7166	0.0399	0.1766	1.4850
15264	0.2186	0.1352	0.1431	1.6834	0.0412	0.1842	1.5204
15899	0.2177	0.1361	0.1462	1.7115	0.0434	0.1885	1.5248
16536	0.2124	0.1339	0.1490	1.6958	0.0429	0.1946	1.5492
17173	0.2049	0.1290	0.1614	1.6686	0.0420	0.2071	1.5854
17810	0.2018	0.1287	0.1644	1.6684	0.0459	0.2103	1.6006
18446	0.1959	0.1255	0.1723	1.6439	0.0455	0.2177	1.6304
19085	0.1931	0.1242	0.1761	1.6493	0.0459	0.2264	1.6445
19721	0.1875	0.1198	0.1789	1.6276	0.0431	0.2289	1.6741
20358	0.1819	0.1139	0.1941	1.6033	0.0470	0.2424	1.7046
20993	0.1788	0.1083	0.1997	1.5998	0.0470	0.2473	1.7213
21630	0.1751	0.1035	0.2077	1.5901	0.0489	0.2533	1.7425
22266	0.1705	0.0964	0.2182	1.5755	0.0477	0.2624	1.7691
22922	0.1688	0.0948	0.2267	1.5858	0.0495	0.2724	1.7789
23559	0.1643	0.0920	0.2362	1.5674	0.0509	0.2798	1.8059
24196	0.1594	0.0878	0.2438	1.5442	0.0508	0.2865	1.8366
24833	0.1581	0.0870	0.2406	1.5534	0.0493	0.2879	1.8447
25468	0.1528	0.0806	0.2584	1.5272	0.0497	0.3029	1.8789
26105	0.1497	0.0803	0.2623	1.5167	0.0523	0.3103	1.8992
26748	0.1475	0.0801	0.2574	1.5111	0.0518	0.3088	1.9138
27385	0.1422	0.0780	0.2680	1.4827	0.0497	0.3217	1.9502
28022	0.1402	0.0759	0.2714	1.4782	0.0561	0.3266	1.9649
28658	0.1396	0.0763	0.2774	1.4863	0.0577	0.3400	1.9689

Experimental

29294	0.1366	0.0742	0.2835	1.4764	0.0584	0.3437	1.9907
29929	0.1322	0.0733	0.2814	1.4462	0.0568	0.3455	2.0232
30566	0.1301	0.0710	0.2947	1.4474	0.0616	0.3638	2.0393
31210	0.1200	0.0643	0.2851	1.3883	0.0360	0.3281	2.1201
31848	0.1249	0.0669	0.3060	1.4289	0.0605	0.3784	2.0805
32484	0.1207	0.0646	0.3070	1.4037	0.0552	0.3749	2.1141
33121	0.1178	0.0643	0.3073	1.3883	0.0553	0.3768	2.1386
33757	0.1107	0.0582	0.3113	1.3616	0.0378	0.3651	2.2006
34426	0.1076	0.0565	0.3119	1.3398	0.0377	0.3652	2.2293
35108	0.1066	0.0575	0.3140	1.3472	0.0371	0.3734	2.2383
35768	0.1024	0.0552	0.3190	1.3145	0.0373	0.3758	2.2792
36409	0.1007	0.0549	0.3222	1.3076	0.0360	0.3827	2.2958
37045	0.0982	0.0536	0.3302	1.2981	0.0342	0.3944	2.3204
37682	0.0951	0.0522	0.3337	1.2746	0.0364	0.3989	2.3532
38319	0.0927	0.0525	0.3309	1.2629	0.0303	0.3966	2.3785
38956	0.0922	0.0530	0.3396	1.2676	0.0371	0.4114	2.3841
39594	0.0915	0.0554	0.3396	1.2687	0.0461	0.4145	2.3911
40229	0.0875	0.0525	0.3464	1.2445	0.0356	0.4190	2.4360
40867	0.0844	0.0510	0.3438	1.2235	0.0278	0.4174	2.4722
41504	0.0894	0.0584	0.3511	1.2700	0.0608	0.4475	2.4148
42141	0.0877	0.0588	0.3615	1.2673	0.0688	0.4748	2.4336
42777	0.0849	0.0571	0.3646	1.2489	0.0669	0.4790	2.4662
43420	0.0839	0.0594	0.3654	1.2523	0.0678	0.4846	2.4779
44057	0.0811	0.0574	0.3681	1.2324	0.0676	0.4881	2.5126
44693	0.0796	0.0568	0.3704	1.2152	0.0602	0.4848	2.5303
45352	0.0772	0.0565	0.3670	1.1975	0.0595	0.4802	2.5610
46000	0.0756	0.0571	0.3696	1.1858	0.0593	0.4887	2.5824
46638	0.0753	0.0575	0.3794	1.1937	0.0630	0.4976	2.5861
47274	0.0724	0.0562	0.3813	1.1628	0.0614	0.4986	2.6261
47912	0.0707	0.0561	0.3792	1.1581	0.0610	0.4999	2.6486
48549	0.0682	0.0538	0.3829	1.1354	0.0599	0.5031	2.6855
49185	0.0676	0.0557	0.3822	1.1281	0.0606	0.5060	2.6941
49822	0.0656	0.0556	0.3880	1.1144	0.0608	0.5143	2.7242
50459	0.0639	0.0544	0.3977	1.1049	0.0626	0.5251	2.7499
51096	0.0627	0.0555	0.3957	1.0948	0.0616	0.5243	2.7696
51738	0.0617	0.0576	0.3904	1.0939	0.0618	0.5265	2.7861
52376	0.0603	0.0582	0.3970	1.0887	0.0607	0.5319	2.8083

4. REFERENCES

1. M.E. Klotman and F. Wong-Staal, in *The Human Retroviruses*, R.C. Gallo and G. Jay Academic Press, London, 1991, pp. 35, 36.
2. E. P. Peçanha, L. J. O. Figueiredo, R. M.Brindeiro, A. Tanuri, A. R. Calazans and O.A.C. Antunes, *II FARMACO*, 2003, **58**, 149.
3. J. H. Strauss and E. G. Strauss, *Viruses and Human Disease*, Academic Press, London, 2002, pp. 196,197.
4. S. Scarlata and C. Cater, *Biochimica et Biophysica Acta*, 2003, **1614**, 62-64.
5. F. Gao, E. Bailes, D. L. Robertson, Y. Chen, C. M. Rodenburg, S. F. Michael, L. B. Cummins, L. O. Arthur, M. Peeters, G. M. Shaw, P. M. Sharp and B. H. Hahn, *Nature*, 1999, **397**, 436-441.
6. Ref. 3, pp. 204, 205.
7. F. Barré-Sinoussi, J. C. Chermann, M. Rey, M.T. Nugeyre, S. Chamaret, J. Gruest, C. Dauguet, C. Axler-Blin, F. Vézinet-Brun, C. Rouzioux, W. Rozenbaum and L. Montagnier, *Science*, 1983, **220**, 868.
8. R.C. Gallo, S.Z. Salahuddin, M. Popovic, G.M. Shearer, M. Kaplan, B.F. Haynes, T.J. Palker, R. Redfield, J. Oleske, B. Safai, G. White, P. Foster and P.D. Markham, *Science*, 1984, **224**, 501.
9. J. L. Marx, *Science*, 1986, **232**, 699.
10. J. Coffin, A. Haase, J.A. Levy, L. Montagnier, S. Oroszlan, N. Teich, H. Temin, K. Toyoshima, H. Varmus, P. Vogt and R. Weiss, *Science*, 1986, **232**, 697.
11. J. A. Levy, A. D. Hoffman, S. M. Kramer, J. A. Landis, J.M. Shimabukuro and L.S. Oshiro, *Science*, 1984, **225**, 840-841.
12. F. Clavel, D. Guétard, F. Brun-Vézinet, S. Chamaret, M. Rey, M. O. Santos-Ferreira, A.G. Laurent, C. Dauguet, C. Katlama, C. Rouzioux, D. Klatzamann, J.L. Champalimaud and L. Montagnier, *Science*, 1986, **233**, 343.
13. J. Erickson, D. J. Neidhart, J. VanDrie, D. J. Kempf, X. C. Wang, D. W. Norbeck, J. J. Plattner, J. W. Rittenhouse, M. Turon, N. Wideburg, W. E.

Kohlbrenner, R. Simmer, R. Helfrich, D. A. Paul, M. Knigge, *Science*, 1990, **249**, 527.

14. D. O. White and F. Fenner, *Medical Virology*, **3**, Academic Press, London, 1986, pp 31, 32.
15. Ref 14, p. 210.
16. J. P. Vacca and J. H. Condra, *Drug Des. Discov.*, 1997, **2**(7), 261-262.
17. M. P. Sherman and W.C. Greene, *Microbes and Infection*, 2002, **4**, 67-69.
18. Ref. 1, pp. 337, 338.
19. Ref. 3, p. 174-187.
20. J. Jacque, K. Triques, M. Stevenson, *Nature*, 2002, **418**, 435.
21. M. Ottman, C. Gabus and J. Darlix, *J. Virol.*, 1995, **69**(3), 1778 -1779.
22. C. A. Bewley and S. Otero-Quintero, *J. Am. Chem. Soc.*, 2001, **123(17)**, 3892.
23. Ref. 3, p. 49.
24. K. Wiegers, G. Rutter, H. Kottler, U. Tessmer, H. Hohenberg, and H. G. Kräusslich, *J. Virol.*, 1998, **72**(4), 2846.
25. R. Welker, H. Hohenberg, U. Tessmer, C. Huckhagel and H. Kräusslich, *J. Virol.*, 2000, **74**(3), 1168-1169.
26. M. Shehu-Xhigala, H.G. Kraeusslich, S. Pettit, R. Swanstrom, J. Y. Lee, J.A. Marshall, S.M. Crowe and J. Mak, *J. Virol.*, 2001, **75**(19), 9156.
27. J. Lanman, T. T. Lam, M. R. Emmett, A. G. Marshall, M. Sakalian and Jnr P.E. Prevelige, *Nat. Struct. Mol. Biol.*, 2004, **11**(7), 676.
28. A. K. Debnath, *J. Med. Chem.*, 2003, **46**, 4501.
29. Ref. 17, p. 70.
30. F. Romanelli, *Am. J. Pharm. Educ.*, 2001, **65**, 186-187.
31. H. M. Abdel-Rahman, G. S. Al-karamany, N. A. El-Koussi, A. F. Youssef and Y. Kiso, *Curr. Med. Chem.*, 2002, **9**, 1905-1907.
32. C. Tang, Y. Ndassa, and M. F. Summers, *Nat. Struct. Biol.*, 2002, **9**(7), 537.
33. D.A. Davis, K. Yusa, L. A. Gillim, F. M. Newcomb, H. Mitsuya and R. Yarchoan, *J. Virol.*, 1999, **73**(2), 1156.

34. J. Jiang and C. Aiken, *Virology*, 2006, **346**, 460.

35. T. Sperka, J. Pitlik, P. Bagossi, J. Tözser, *Bioorg. Med. Chem. Lett.*, 2005, **15**, 3086.

36. G. F. Short III, M. Lodder, A. L. Laikhter, T. Arslan and S. M. Hetch, *J. Am. Chem. Soc.*, 1999, **121**, 478.

37. E. J. Rodriguez, T. S. Angeles and T. D. Meek, *Biochemistry*, 1993, **32**, 12380.

38. S. D. Young, L. S. Payne, W. J. Thompson, N. Graffin, T. A. Lyle, S.F. Britcher, S.L. Graham, T. H. Schultz, A. A. Deana, P.L. Darke, J. Zugay, W. A. Schleif, J. C. Quintero, E. A. Emini, P. S. Anderson and J. R. Huff, *J. Med. Chem.*, 1992, **35**, 1702.

39. R. Zutshi and J. Chmielewski, *Bioorg. Med. Chem. Lett.*, 2000, **10**, 1901.

40. G. L. Marcorin, T. Da Ros, S. Castellano, G. Stefancich, *Org. Lett.*, 2000, **25**(2), 3955.

41. I. T. Weber, M. Miller, M. Jaskólski, J. Leis, A. M. Skalka, A. Wlodawer, *Science*, 1989, **243**, 928.

42. R. Lapatto, T. Blundell, A. Hemmings, J. Overington, A. Wilderspin, S. Wood, J.R. Merson, P.J. Whittle, D. E. Danley, K. F. Geoghegan, S. J. Hawrylik, S. E. Lee, K. G. Scheld and P. M. Hobart, *Nature*, 1999, **342**, 229.

43. L. H. Pearl and W. R. Taylor, *Nature*, 1999, **397**, 436-441.

44. A. Friedler, I. Blumenzweig, L. Baraz, M. Steinitz, M. Kotler and C. Gilon, *J. Mol. Biol.*, 1999, **287**, 94.

45. N. Kurt, W. R. P. Scott, C. A. Schiffer and T. Haliloglu, *Proteins: Struct., Funct. Genet.*, 2003, **51**, 409.

46. J. Wu, J. M. Adomat, T. W. Ridky, J. M. Louis, J. Leis, R. W. Harrison, I. T. Weber, *Biochemistry*, 1998, **37**, 4518.

47. A. Brik and C. Wong, *Org. Biomol. Chem.*, 2003, **1**, 5-6.

48. P.L. Darke, C.T. Leu, L.J. Davis, J.C. Heimbach, R.E. Diehl, W.S. Hill, R.A. Dixon and I. S. Sigal, *J. Biol. Chem.*, 1989, **264**, 2307.

49. E. Jenwitheesuk and R. Samudrala, *BMC Struct. Biol.*, 2003, **3**(2), 1

50. M. Miller, J. Scheneider, B. K. Sathyanarayana, M. V. Toth, G. R. Marshall, L. Clawson, L. Selk, S. B. H. Kent and A. Wlodawer, *Science*, 1989, **246**, 1149.
51. J. V. N. V. Prasad, E. A. Lunney, D. Ferguson, P. J. Tummino, J. R. Rubin, E. L. Reyner, B. H. Stewart, R. J. Guttendorf, J. M. Domagala, L. I. Suvorov, S. V. Gulnik, I. A. Topol, T. N. Bhat and J. W. Erickson, *J. Am. Chem. Soc.*, 1995, **117**(45), 11070.
52. Ref. 14, p. 585.
53. T. Zhu, B. T. Korber, A. J. Nahmias, E. Hooper, P.M. Sharp and D. D. Ho, *Nature*, 1998, **391**, 594.
54. Z. Lu, S. Raghavan, J. Bohn, M. Charest, M. Charest, M. W. Stahlhut, C. A. Rutkowski, A. L. Simcoe, D. B. Olsen, W. A. Schleif, A. Carella, L. Gabryelski, L. Jin, J. H. Lin, E. Emini, K. Chapman and J. R. Tata, *Bioorg. Med. Chem. Lett.*, 2003, **13**, 1821.
55. http://www.avert.org/worldstats.htm
56. A. C. Nair, I. Bonin, A. Tossi, W. J. Welsh and S. Miertus, *J. Mol. Graph. Model.*, 2002, **21**, 172.
57. B. L. King, S. Vajda and C. DeLisi, *FEBS Lett.*,1996, **384**, 87.
58. R. Wolfenden, *Bioorg. Med. Chem. Lett.*, 1999, **7**, 647.
59. J.E. House, *Principles of Chemical Kinetics*, Wm. C. Brown Publishers, London, 1997, pp. 185.
60. Ref. 16, p. 262.
61. J. L. Duffy, T. A. Rano, N. J. Kevin, K. T. Chapman, W. A. Schleif, D. B. Olsen, M. Stahlhut, C. A. Rutkowski, L.C. Kuo, L. Jin, J. H. Lin, E. A. Emini and J. R. Tata, *Bioorg. Med. Chem. Lett.*, 2003, **13**, 2569.
62. A. H. Corbett, M. L. Lim and A. D. M. Kashuba, *Annals Pharmacother.*, 2002, **36**, 193-194.
63. E. De Clercq, *The International Journal of Biochemistry & Cell Biology*, 2004, **36**, 1814-1815.
64. J. T. Randolph and D.A. DeGoey, *Curr. Top. Med. Chem.*, 2004, **4**, 1079-1095.

65. U. S. Justesen, C. Perdesen, N.A. Klitgaard, *J. Chromatogr. B*, 2003, **783**, 491-493.

66. Z. Xu, J. Singh, M.D. Schwinden, B. Zheng, T.P. Kissick, B. Patel, M.J. Humora, F. Quiroz, L. Dong, D. Hsieh, J. E. Heikes, M. Pudipeddi, M. D. Lindrud, S. K. Srivastava, D. R. Kronenthal and R. H. Mueller, *Org. Proc. Res & Dev.*, 2002, **6**, 323.

67. F. Zhang, K. T. Chapman, W. A. Schleif, D. B. Olsen, M. Stahlhut, C. A. Rutkowski, L. C. Kuo, L. Jin, J. H. Lin, E. A. Emini and J. R. Tata, *Bioorg. Med. Chem. Lett.*, 2003, **13**, 2573-2576.

68. E. De Clercq, *J. Clin. Virol.*, 2004, **30**, 118-122.

69. J. F. Miller, C. W. Andrews, M. Brieger, E. S. Furfine, M. R. Hale, M. H. Hanlon, R. J. Hazen, I. Kaldor, Ed W. Mclean, D. Reynolds, D. M. Sammond, A. Spaltenstein, R. Tung, E. M. Turner, R. X. Xu, and R. G. Sherrill, *Bioorg. Med. Chem. Lett.*, 2006, **16**, 1788-1789.

70. http://www.fda.gov/oashi/aids/virals.html

71. A. K. Gosh and S. Fidanze, *J. Org. Chem.*, 1998, **63**, 6146

72. A. K. Gosh, S.P. Mckee, W. J. Thompson, P. L. Darke and J. C. Zugay, *J. Org. Chem.*, 1993, **58**, 1027.

73. A.K. Gosh, W. J. Thompson, S.P. McKee, T.T. Duong, T. A. Lyle, J. C. Chen, P. L. Darke, J.A. Zugay, E. A. Emini, W. A. Schleif, J. R. Huff and P. S. Anderson, *J. Med. Chem.*, 1993, **36**, 292-293.

74. T. J. McQuade, A. G. Tomasselli, L. Liu, V. Karacostas, B. Moss, T. K. Sawyer, R. L. Heinrickson, W. G. Tarpley, *Science*, 1990, **447**, 454.

75. M.L Vazquez, M. L. Bryant, M. Clare, G. A. DeCrescenzo, E. M. Doherty, J. N. Freskos, D. P. Getman, K. A. Houseman, J. A. Julien, G. P. Kocan, R. A. Mueller, H. Shieh, W. C. Stallings, R. A. Stegeman, and J. J. Talley, *J. Med. Chem.*, 1995, **38**(4), 582.

76. K. M. Dawood and T. Fuchigami, *J. Org. Chem.*, 2001, **66**, 7691.

77. J. T. Wong, *Kinetics of Enzyme Mechanisms*, Academic Press Inc., London, 1975, p1.

78. H.U. Bergmeyer, K. Gawehn, *Principles of Enzymatic Analysis*, Verlag Chemie, Weinheim, and Academic Press, New York, 1978.

79. C.H. Wynn, *The Structure and Function of Enzymes*, 2nd edition, Edward Anorld Ltd, London, 1979, pp .

80. Ref. 59, pp. 190-193.

81. J. M. Zhou, C. Liu and C. L. Tsou, *Biochemistry*, 1989, **28**, 1070-1076.

82. D. Voet, J.G. Voet and C. W. Pratt, *Fundamentals of Biochemistry, Life at the Molecular Level*, 2nd edition, John Wiley and Sons, Inc., New York, 2006, pp. 357-379.

83. Bachem catalogue, 2003.

84. T. Walenzyk, C. Carola, H. Buchholz and B. König, *Tetrahedron*, 2005, **61**, 7366-7369.

85. Á. Somogyi, I. Komáromi and Z. Dinya, *Acta Chim. Hung.*, 1987, **124**, 857-862.

86. J. Staunton, in *Comprehensive Organic Chemistry*, (D.H. Barton and W.D. Ollis eds.), Pergamon Press, Oxford, 1979, **4**, p. 677.

87. P.J. Brogden, C.D. Gabbut and J.D. Hepworth, in *Comprehensive Heterocyclic Chemistry,* A.R. Katritzky and C.W. Rees, Eds., Pergamon Press, Oxford, 1984, Vol. **3**, pp. 574, 575.

88. P. Kumar and M. S. Bodas, *Org. Lett.*, 2000, **2**(24), 3821.

89. H.M. Ishiki, P.M. Donate and S.E. Galembeck, *J. Mol. Str. (Theochem)*, 1998, **423**, 235.

90. Ref. 87, p. 613.

91. Ref. 87, p. 637.

92. Ref. 87, pp. 670-78.

93. R. Polly and P.R. Taylor, *J. Phys. Chem. A*, 1999, **103**, 10343-10346.

94. T. Eicher and S. Hauptmann, *The Chemistry of Heterocycles*, Gutmann, New York, pp. 262, 263.

96. Ref. 87, pp. 593-600.

97. M. Hesse, H. Meier, B. Zeeh, A. Linden and M. Murray, *Spectroscopic Methods in Organic Chemistry*, Georg Thieme Verlag, Stuttgart, 1997, pp. 48, 49.

98. Ref. 93, p. 10343.

99. S. Ghoshal, S. Singh, M. P. Bhagat and Y. Kumar, *Phytochemistry*, 1982, **21**(12), 2944.

100. M. C. Nicklaus, N. Neamati, H. Hong, A. Mazumder, S. Sunder, J. Chen, G. W. A. Milne and Y. Pommier, *J. Med. Chem.*, 1997, **40**, 926.

101. L. W. McGarry and M. R. Detty, *J. Org. Chem.* 1990, **55**(14), 4349-52.

102. M. Morito, K. Tanimoto, S. Nakano, T. Ozaki, A. Nakano and K. Komai, *J. Agric. Food Chem.*, 2003, **51**, 389.

103. M. R. Fesen, Y. Pommier, F. Leteurtre, S. Hiroguchi, J. Yung, K.W. Kohn, *Biochem. Pharmacol.*, 1994, **48**, 596.

104. D. Yu, C. Chen, A. Brossi and K. Lee, *J. Med. Chem.*, 2004, **47**, 4073-4076.

105. J. Ungwitayatorn, W. Samee and J. Pimthon, *J. Mol. Struct.*, 2004, **689**, 100-105.

106. S.K. Wrigley, M. A. Latif, T. M. Gibson, M. I. Chicarelli-Robinson and D. H. Williams, *Pur. Appl. Chem.*,1994, **66**(11), 2383.

107. S. Ghoshal, Y. Kumar , S. Singh and K. Ahad, *Phytochemistry*, 1983, **21**(11), 2592.

108. T. Satake, K. Kamiya, Y. Saiki, T. Hama, Y. Fujimoto, H. Endang and M. Umar, *Phytochemistry*, 1999, **50**, 303-4.

109. P. P. Mebe, *Phytochemistry*, 1987, **26**(29), 2646.

110. P. Tane, J.F. Ayafor, B. Luc Sondengam and J. D. Connolly, *Phytochemistry*, 1990, **29**(3), 1004-1005.

111. C. Sun, W. Syu, Y. Huang, C. Chen and J. Ou, *J. Nat. Prod.*, 1997, **60**, 382.

112. Ref. 87, p 692.

113. J.S.G. Cox, *Adv. Drug Res.*, 1970, **5**, 155.

114. L. Lin, Y. Kuo and C. Chou, *J. Nat. Prod.*, 2000, **63**, 627.

115. T. Brasseur and L. Angenot, *Phytochemistry*, 2003, **26**(12), 3331.

116. T. Yagura, M. Ito, F. Kiuchi, G. Honda and Y. Shimada, *Chem. Pharm. Bull.*, 2003, **51**(5), 560-561.

117. H. Tanaka, M. Hirata, H. Etoh, H. Shimizu, M. Sako, J. Murata, H. Murata, D. Darnaedi and T. Fukai, *Phytochemistry*, 2003, **62**, 1243-1244.

118. E. Fillion, A. M. Dumas, B. A. Kuropatwa, N. R. Malhotra and T. C. Sitler, *J. Org. Chem.* 2006, **71**, 411.

119. C. A. Gray, P.T. Kaye and A. T. Nchinda, *J. Nat. Prod.*, 2003, **66**, 1146-1147.

120. S. S. Ibrahim, *Ind. Eng. Chem. Res.*, 2001, **40**, 37-38.

121. P.T. Kaye and I.D.I Ramaite, *S. Afr. J. Chem.*, 2003, **56**, 25-26.

122. M. Mazzei, R. Dondero, B. Ledda, F. Demontis and L. Vargiu, *IL Farmaco*, 2002, **26**, 1800-1801.

123. J. C. Jaen, L. D. Wise, T.G. Heffner, T. A. Pugsley and L. T. Meltzer, *J. Med. Chem.*, 1991, **34**, 284-256.

124. A. Nishinaga, H. Ando, K. Maruyama and T. Mashino, *Synthesis*, 1992, 841.

125. A. K. Ganguly, S. Kaur, P.K. Mahata, D. Biswas, B. N. Pramanik and T. M. Chan, *Tetrahedron Lett.*, 2005, **46**, 4120.

126. G. J. P. Becket and G. W. Ellis, *Tetrahedron Lett.*, **9**, 1976, 719.

127. A. Nohara, T. Umetani and Y. Sanno, *Tetrahedron*, 1974, **30**, 3353.

128. S. G. Jagadeesh, G. L. D Krupadanam and G. Srimannarayana, *Synth. Commun.*, 1998, **28**, 3827.

129. K. M. Dawood and T. Fuchigami, *J. Org. Chem.* 2001, **66**, 7692.

130. S. G. Jagadeesh, G. L. D Krupadanam and G. Srimannarayana, *Indian J. Chem.*, 1997, **36**(B), 965.

131. L. W. McGarry and M. R. Detty, *J. Org. Chem.* 1990, **55**(14), 4349-52.

132. K. Wahala and T. A. Hase, *J. Chem. Soc. Perkin Trans. 1*, 1991, 3005-3008.

133. Ref. 89, p 239.

134. G. Singh, R. Singh, N. K. Girdhar and M. P. S. Ishar, *Tetrahedron*, 2002, **58**, 2471-2472.

135. C. K. Gosh and S. Khan, *Synthesis*, 1981, 719-720.

136. J. Quiroga, A. Rengifo, B. Insuasty, R. Abonia, M. Nogueras and A. Sánchez, *Tetrahedron Lett.*, 2002, **43**, 9062.

137. G. Singh, R. Singh and M. P. S. Ishar, *Tetrahedron*, 2002, **58**, 7884

138. P. Langer and B. Appel, *Tetrahedron Lett.*, 2002, **44**, 7921.

139. J. Kóňa, W. M. F. Fabian and P. Zahradník, *J. Chem. Soc., Perkin Trans. 2,* 2001, 423.

140. Ref. 87, p. 704.

141. A. Nohara, H. Kuriki, T. Saijo, K. Ukawa, T. Murata and Y. Sanno, *J. Med. Chem.*, 1975, **18**(1), 34.

142. Ref. 87, pp. 697-700.

143. K. Gosh and K. K. Mukhopadhyay, *J. Indian Chem. Soc.*, 1978, **55**, 386.

144. K. Kumar, R. Kapoor, A. Kapur and M. P. S. Ishar, *Org. Lett.*, 2000, **2**(14), 2024.

145. V. D. Sevenard, V. Y. Sosnovskikh, A. A. Kolomeitsev, M. H. Königsmann and G. Röschenthaler, *Tetrahedron Lett.*, 2003, **44**, 7625.

146. M. Malecka, W. Massa, K. Harms and E. Budzisz, *J. Mol. Struc.*, 2005, **737**, 260.

147. U. Albrecht, M. Lalk and P. Langer, *Bioorg. Med. Chem. Lett.*, 2005, **13**, 1532.

148. E. Sottofattori, M. Anzaldi, M. Mazzei, M. Miele, A. Balbi, D. S. Pyshnyi, O.D. Zakharova and T.V. Abramova, *Bioorg. Med. Chem. Lett., 2003*, **13**, 1516.

149. A. Sandulache, A. M. S. Silva and J. A. S. Cavaleiro, *Tetrahedron.* 2002, **58**, 107.

150. C. Gosh and N. Tewari, *J. Org. Chem.*, 1980, 4(10), 1966.

151. G. E. Daia, C. D. Gabbutt, J. D. Hepworth, B. M. Heron, D. E. Hibbs and M. B. Hursthouse, *Tetrahedron Lett.*, 2002, **43**, 4507.

152. J. H. Drewes and P. T. Kaye, *S. Afr. J. Chem.*, 1987, **40**, 165.

153. D.N. Davidson and P.T. Kaye, *Synth. Commun.*, 1990, **20**, 727.

154. D.N. Davidson and P.T. Kaye, *J. Chem. Soc., Perkin Trans. 2*, 1991, 927.

155. D.N. Davidson and R.B. English and P.T. Kaye, *J. Chem. Soc., Perkin Trans. 2*, 1991,1181.

156. D.N. Davidson and P.T. Kaye, *J. Chem. Soc., Perkin Trans. 2*, 1991,1509.

157. P.T. Kaye and I.D.I. Ramaite, *J. Chem. Res. (S)*, 1994, 482.

158. P.T. Kaye and I.D.I. Ramaite, *J. Chem. Res. (S)*, 1995, 78.

159. P.T. Kaye and I.D.I. Ramaite, *J. Chem. Res. (S)*, 1997, 414.

160. D.N. Davidson, P.T. Kaye and I.D.I Ramaite, *J. Chem. Res. (S)*, 1993, 462.

161. M. L. Bode and P.T. Kaye, *J. Chem. Soc., Perkin Trans. 1*, 1993, 1809.

162. O. B. Familoni, P.T. Kaye and P. J. Klaas, *J. Chem. Soc., Chem. Commun.*, 1998, 2563.

163. P.T. Kaye and X. W. Nocanda, *Synthesis*, 2003, 531-534.

164. P.T. Kaye and X. W. Nocanda, *J. Chem. Soc., Perkin Trans. 1*, 2000, 1331.

165. P.T. Kaye and X. W. Nocanda, *Synthesis*, 2001, 2389-2392.

166. P.T. Kaye, A. T. Nchinda, L. V. Sabbagh, J. Bacsa, *J. Chem. Res. (S)*, 2003, **3**, 111.

167. P.T. Kaye, D. M. Molefe, A. T. Nchinda, L. V. Sabbagh, *J. Chem. Res.* 2004, **4**, 303.

168. S. Koeller and J. Lellouche, *Tetrahedron*, 1999, **40**, 7043.

169. B. S. Furniss, A. J. Hannaford, P. W. G. Smith and A. R. Tatchell, *Vogel's Texbook of Practical Organic Chemistry*, Longman Scientific and Technical, United States, 1989, 5th Edn., p. 992.

170. D. Arigoni, A. Vasella, K.B. Sharpless and H. P. Jensen, *J. Amer. Chem. Soc.*, 1973, **95**(23), 7917.

171. H. P. Jensen and K. B. Sharpless, *J. Org. Chem.*, 1975, **40**(2), 264.

172. Ref. 169, p. 628.

173. I. J. S. Fairlamb, J. M. Dickinson and M. Pegg, *Tetrahedron Lett.*, 2001, **42**, 2206.

174. C.S. Ra and G. Park, *Tetrahedron Lett.*, 2003, **44**, 1099.

175. K. B. Sharpless and R. F. Lauer, *J. Amer. Chem. Soc.*, 1972, **94**, 7154.

176. J. E. Remias and A. Sen, *J. Mol. Cat. A Chem.*, 2003, **201**, 65.

177. S. E. Drewes, N. D. Emslie, J. S. Field, A. A. Khan and N. S. Ramesar, *Tetrahedron Lett.*, 1993, **34**(7), 1205.

178. T. Kataoka, T. Iwama, S. Tsujiyama, T. Iwamura and S. Watanabe, *Tetrahedron*, 1998, **54**, 11813.

179. C. Yu, B. Liu and L. Hu, *J. Org. Chem.*, 2001, **66**, 5413.

180. J. N. Kim, K. Y. Lee, H. Ham, H. R. Kim and E. K. Ryu, *Bull. Korean Chem. Soc.*, 2001, **22**(2), 135.

181. S. Luo, X. Mi, H. Xu, P. G. Wang and J. Cheng, *J. Org. Chem.*, 2004, **69**, 8413.

182. K. E. Price, S. J. Broadwater, B. J. Walker and D. T. McQuade, *J. Org. Chem.*, 2005, **70**, 3980.

183. F. Ameer, S. E. Drewes, S. Freese and P. T. Kaye, *Synth. Commun.*, 1988, **18**, 495.

184. Y. Hayashi, K. Okado, I. Ashimine and M. Shoji, *Tetrahedron Lett.*, 2002, **43**, 8683-8685.

185. V. K. Aggarwal and A. Mereu, *J. Chem Soc., Chem. Commun.*, 1999, 2311-2112.

186. M. L. Bode and P. T. Kaye, *Tetrahedron Lett.*, 1991, **32**(40), 5611-5613.

187. L. J. Brzezinski, S. Rafel and J. W. Leahy, *Tetrahedron*, **53**(48), 16425-16426.

188. Y. Iwabuchi, M. Nakatani, N. Yokoyama and S. Hatakeyama, *J. Am. Chem. Soc.*, 1999, **121**, 10219-10220.

189. L. Xu and C. Xia, *Tetrahedron Lett.*, 2004, **45**, 4507.

190. L. Xu, C. Xia and X. Hu, *J. Chem Soc., Chem. Commun.*, 2003, 2570.

191 B.C. Ranu, S.S. Dey and A. Hajra, *Arkivoc*, 2002, **viii**, 76.

192. L. Xu, J. Li, S. Zhou and C. Xia, *New. J. Chem.*, 2004, **28**, 183.

193. L. Xu, L. Li, C. Xia, S. Zhou, J. Li and X. Hu, *Synlett*, 2003, **15**, 2337.

194. A. Arcadi, P. A. Attanasi, L. Crescentini and E. Rossi, *Tetrahedron Lett.*, 1997, **38**(13), 2329.

195. D.J. Kempf, K.C. Marsh, J.F. Denissen, E. McDonald, S. Vasavononda, C. A. Flentge, B.E. Green, L. Fino, C.H. Park and X.P. Kong, *Proc. Nat. Acad. Sci.*, 1995, **92**, 2484.

196. G.V. De Lucca, S. E. Viitanen and P.Y.S. Lam, *Drug Disc. Today*, 1997, **2**, 6.

197. G. L. Marcorin, T. Da Ros, S. Castellano, G. Stefancich, *Org. Lett.*, 2000, **25**(2), 3955.

198. A. T. Nchinda, PhD Thesis, Rhodes University, 2001.

199. M. Shi, C. Li and J. Jiang, *Molecules*, 2002, **7**, 721-726.

200. M. Shi, C. Li and J. Jiang, *Tetrahedron*, 2003, **59**, 1180-1185.

201. M. Shi, C. Li and J. Jiang, *Chem.Commun.*, 2001, 833-834.

202. D. Basavaiah, A. J. Rao and T. Satyanarayana, *Chem. Rev.*, 2003, **103**, 828-829.

203. Ref. 202, p. 813.

204. D. Basavaiah, P.D. Rao and R.S. Hyderabad, *Tetrahedron*, 1996, **52**(24), 8005-8006.

205. H. Hu, Q. N. Van, V. A. Mandelshtam and A. J. Shaka, *J. Magn. Reson.*, 1998, **134**, 76-87.

206. NMR Textbook for T_1half-life reaction.

207. S. Klutchko, M.P. Cohen, J. Sharel Jr. and M. von Strandtmann, *J. Heterocycl. Chem.*, 1974, **11**, 183.

208. W. Baker, *J. Chem. Soc.*, 1933, 1381.

209. I. Hirao, M. Yamaguchi and M. Hamada, *Synthesis*, 1984, 1076.

210. F.M.E. Abdel-Megeld, M.A.F. El-Kaschef ans A.A.G. Ghattas, *Egypt J. Chem.*, 1977, **20**, 453.

211. H. Nakazumi, T. Ueyama and T. Kitao, *J. Heterocycl. Chem.*,1984, **21**, 193.

212. A. T. Nchinda, unpublished work.

213. L.V. Sabbagh, unpublished work.